Title

Synthesis and biological activity of analogs of the neurotoxin 1-methyl-4-phenyl-1,2,3,6-tetrahydrophyridine (MPTP) and its monoamine oxidase derived metabolites

Author

Johnson, Elizabeth Anne

Publication Date

1989

Peer reviewed|Thesis/dissertation

SYNTHESIS AND BIOLOGICAL ACTIVITY OF ANALOGS OF THE NEUROTOXIN 1-METHYL-4-PHENYL-1,2,3,6-TETRAHYDROPYRIDINE (MPTP) AND ITS MONOAMINE OXIDASE DERIVED METABOLITES

by

ELIZABETH ANNE JOHNSON
B.S., UNIVERSITY OF MICHIGAN, 1980
M.S., UNIVERSITY OF MICHIGAN, 1984

DISSERTATION

Submitted in partial satisfaction of the requirements for the degree of

DOCTOR OF PHILOSOPHY

in

PHARMACEUTICAL CHEMISTRY

in the

GRADUATE DIVISION

of the

UNIVERSITY OF CALIFORNIA

San Francisco

ABSTRACT

The structure-activity relationship (SAR) of substituted tetrahydropyridines as substrates for Monoamine Oxidase (MAO) was examined through the synthesis and evaluation of two methyl substituted analogs of the neurotoxic tertiary amine 1-methyl-4-phenyl-1,2,3,6-tetrahydropyridine (MPTP). Neither the 1,2-dimethyl-4-phenyl-1,2,3,6-tetrahydropyridine (**17**) nor the 1,6-dimethyl-4-phenyl-1,2,3,6-tetrahydropyridine (**18**) are substrates for either the A or B forms of MAO. It was also demonstrated that neither tetrahydropyridine analog shares the neurotoxic effect of MPTP. However, the chemically synthesized 2-electron and 4-electron oxidation products, 1,2-dimethyl-4-phenyl-1,2-dihydropyridinium ion (**15**) and 1,2-dimethyl-4-phenylpyridinium ion (**60**), respectively, which are methyl analogs of the MAO derived metabolites of MPTP, share the toxic properties associated with these metabolites, $MPDP^+$ and MPP^+, respectively For example, both the dihydropyridinium **15** and pyridinium species **60** are cytotoxic in the freshly isolated rat hepatocyte preparation. Furthermore, the pyridinium ion is an effective inhibitor of mitochondrial respiration. Finally, the 1,2-dimethyl-4-phenylpyridinium species **60** is demonstrated to be an inhibitor of mouse striatal synaptosomal uptake of both [^{3}H] dopamine and [^{3}H] MPP^+. These findings indicate that while the SAR which governs

MAO substrate activity in substituted tetrahydropyridines is very restrictive, the SAR which dictates the toxic properties of the dihydropyridinium ion and pyridinium ion products of MAO-catalysed bioactivation is much less restrictive.

DEDICATION

This dissertation is dedicated with love and thanks to my husband

Bob

whose patience, understanding and many long hours of Katie-sitting made the writing possible; and to my daughter

Katie

who has waited many hours for her momma to come out and play.

ACKNOWLEDGEMENTS

I wish to express my gratitude and appreciation to Professor Neal Castagnoli, Jr. for his guidance during the course of these studies and for his expert editorial advice; to Professor Anthony Trevor for many helpful discussions; to my parents for their continuing confidence and encouragement; and to my good friends Beth Castro, Meg Phillips, Ellen Wu and many others who shared with me the unique experience of UC-San Francisco

This work was supported in part by a National Institutes of Health Training Grant; this support is gratefully acknowledged

TABLE OF CONTENTS

LIST OF FIGURES

LIST OF SCHEMES

LIST OF TABLES

CHAPTER 1 Introduction

PARKINSONS DISEASE ETIOLOGY, INCIDENCE, CURRENT TREATMENTS, LIMITATIONS OF CURRENT TREATMENTS.

Parkinson's disease is a progressive disease of the elderly characterized by tremor, akinesia, muscle rigidity, loss of facial expression, and gait and postural disturbances. The disease, first described by James Parkinson in 1817, now afflicts between 200,000 and 400,000 persons in the United States alone. An estimated 40,000 new cases are diagnosed each year.

The current treatment is aimed at amelioration of the primary biochemical defect responsible for the symptoms of the disease, i.e. decreased neurotransmitter release by the inhibitory dopaminergic neurons of the substantia nigra with resulting increased influence of the stimulatory acetyl choline releasing neurons in the basal ganglia. Other neurotransmitters such as norepinephrine, GABA, histamine and serotonin may have some modifying effects on the primary transmitter defect, but these effects are not yet well understood.

The most common treatment, dopamine replacement therapy, is accomplished by administration of levodopa [S-(-)-3-(3,4-dihydroxyphenyl)-L-alanine, **1**] an amino acid which is the biochemical precursor of dopamine. This compound is often given in conjuction with the peripherally acting dopa decarboxylase inhibitor

carbidopa (2) in order to reduce the severity of the side effects associated with dopamine replacement therapy. Carbidopa prevents the decarboxylation of levodopa in the periphery and helps to preserve its action for the central nervous system.

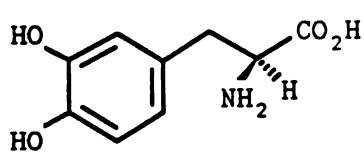

1

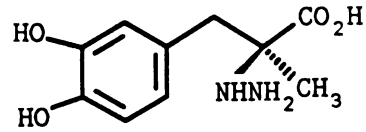

2

Although the initial response to dopamine replacement therapy is positive for about 75% of parkinsonian patients, with time this favorable response seems to diminish. After 5 years of treatment, one third of those patients with an initial favorable response still benefit from levodopa treatment. However, another third of the patients have lost some of the initial response and the remaining third have lost all initial benefits and are worse after 5 years of treatment than they were prior to treatment.[1]

This loss of response to dopamine replacement therapy as well as the side effects associated with the therapy (nausea, vomiting, hallucinations, "on-off effect") require that new forms of treatment for Parkinson's disease be found. Dopamine receptor agonists such as bromocriptine have so far proved no more effective than levodopa.[152] Treatment with amantidine, a

dopamine releasing agent, produces moderate improvement in some parkinsonian patients but is also associated with adverse side effects including unusual skin pigmentation.[152]

ROLE OF MPTP IN PARKINSON'S DISEASE RESEARCH

A better understanding of the complex brain lesion underlying Parkinson's disease could contribute greatly to the discovery of better treatments for the disease. Prior to 1983, research on the pathology of Parkinson's disease relied heavily on the use of 6-hydroxydopamine (3) to induce a biochemical brain lesion in research animals similar to that observed in idiopathic Parkinson's disease. This compound is selectively taken up by catecholaminergic neurons and then, because of its extreme susceptibility to oxidation, it is able to cause the selective destruction of sympathetic neurons. Chemical sympathectomy induced by 6-hydroxydopamine treatment is, unfortunately, not the optimal model of idiopathic Parkinsons disease since it affects norepinephrine neurons as well as dopamine neurons. The lesion observed in Parkinson's disease is almost totally restricted to the dopaminergic neurons in the zona compacta of the substantia nigra. In 1983, however, with the discovery of the parkinsonism producing neurotoxin MPTP (1-methyl-4-phenyl-1,2,3,6-tetrahydropyridine, 4), a new and very powerful research tool became available.

Langston has discussed the striking similarity of the parkinsonian syndrome induced in human drug addicts (after inadvertant self administration) with the syndrome observed in idiopathic Parkinson's disease.[2] MPTP appears to cause a pure parkinsonian state in humans which is clearly permanent, distinguishing it from the many forms of reversible drug-induced parkinsonism. MPTP has also been effective in producing a non-human primate model of the disease in which selective nerve cell loss in the substantia nigra compacta, irreversible decreased dopamine levels in the striatum, and chronic impairment of extrapyramidal motor function are observed.[3]

The five years since MPTP was discovered have produced an explosion in knowledge as hundreds of researchers have raced to investigate the mechanism of action of this neurotoxin, its metabolism, and to exploit its potential as a model of Parkinson's disease. A great deal of progress has been made in these endeavors but there is still a great deal left to learn. Furthermore much controversy has arisen over the interpretation of the existing knowledge. One of the questions that remain unanswered is whether MPTP itself or some closely related endogenous or exogenous neurotoxin might be responsible for idiopathic Parkinson's disease. Prior to the discovery of MPTP, this possibility had not been given much weight by the medical community.

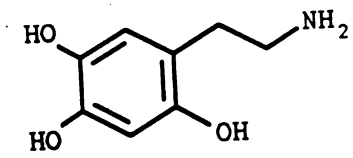

3

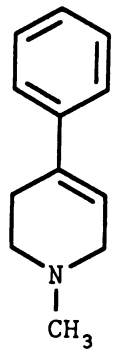

4

MECHANISM OF ACTION OF MPTP

Chiba et al. reported in 1984 that MPTP was metabolized by brain mitochondrial fractions and that the metabolism was blocked by specific inhibitors of monoamine oxidase B (MAO B).[4] Salach et al. then showed, using purified MAO A and B, that MPTP was rapidly oxidized especially by the B form.[5] Although MPTP is oxidized by both forms of MAO, only specific inhibition of the B form was shown to prevent the in vivo neurotoxicity observed with MPTP.[6,7,8] These findings have led to the conclusion that metabolism of MPTP by MAO B is required for expression of it's neurotoxic effects.

Chiba et al. demonstrated that the metabolism of MPTP by MAO B (Scheme 1-1) proceeds first through a two electron oxidation to yield $MPDP^+$ (5), an unstable dihydropyridinium species.[9] The dihydropyridinium species is further oxidized by two electrons to the more stable pyridinium compound MPP^+ (6) in a step which may be spontaneous or enzyme catalyzed.

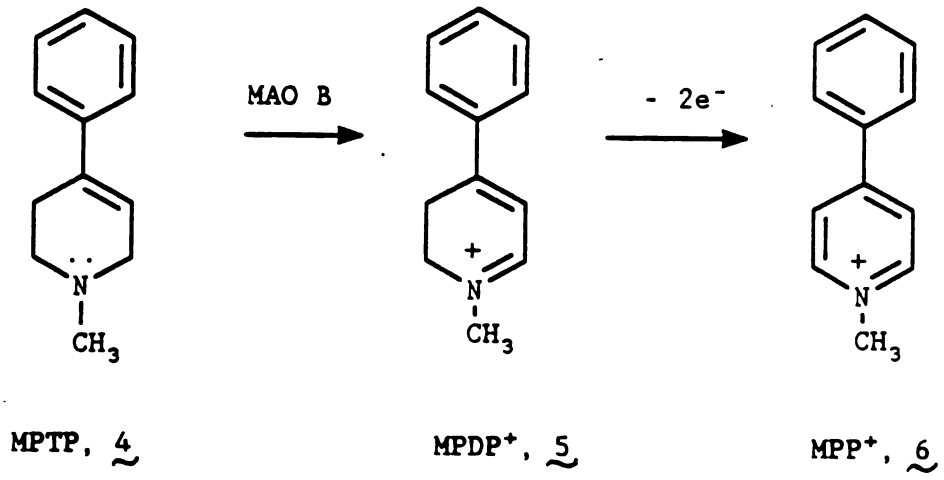

MPTP, 4 MPDP+, 5 MPP+, 6

Scheme 1-1. Bioactivation of MPTP by MAO B

The study of the toxic properties of the metabolites $MPDP^+$ and MPP^+ has subsequently become the main focus in the search for the molecular mechanism of MPTP neurotoxicity.

MPTP is also known to be metabolized by Cytochrome P450 which yields the N-demethylated tetrahydropyridine 7 (Weissman et al.[10]) and by flavin monooxygenase which produces the N-oxide 8 (Cashman and Zeigler[11]). However, neither of these metabolites has been shown to have neurotoxic potential.

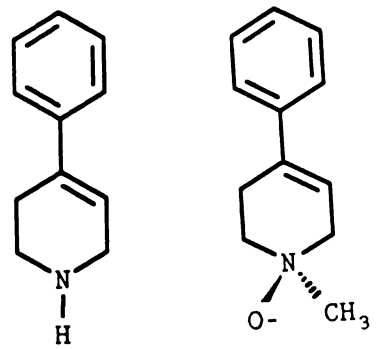

7 8

PROPERTIES OF $MPDP^+$

$MPDP^+$ is an unstable species which undergoes oxidation and disproportionation. These chemical properties render the compound difficult to study in most biological systems. For example, Caldera et al. have shown that a 5 mM solution of $MPDP^+$ in phosphate buffer at pH 7.4 undergoes disproportionation (Scheme 1-2) to form MPTP and MPP^+ with a half life of only 20 minutes.[12]

$MPDP^+$ solutions of much lower concentration, such as 50 uM, do not undergo disproportionation but instead suffer auto-oxidation to form MPP^+ quantitatively with a half-life of about 10 hours. The rate of the oxidation process is accelerated by the addition of MAO B, even when the MAO B has been inactivated by Deprenyl (**10**).[9] This result is consistant with the view that non-enzymatic formation of MPP^+ may be an important intraneuronal mechanism of MPP^+ formation.

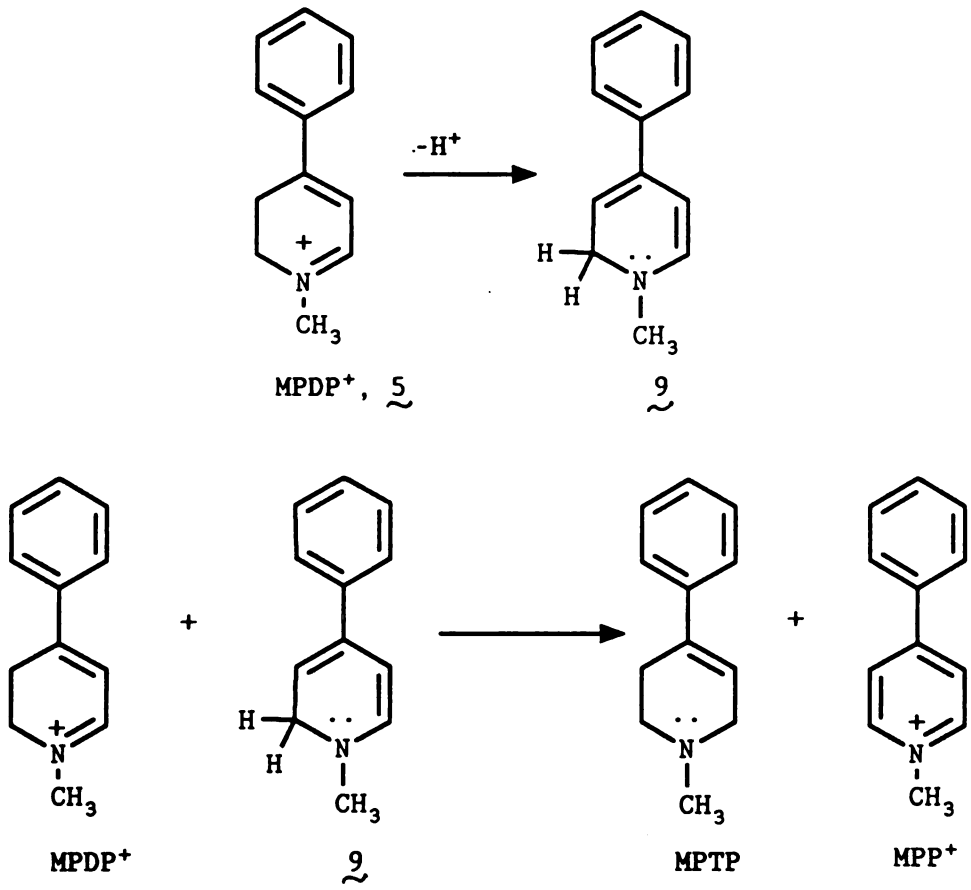

Scheme 1-2 Disproportionation reaction of $MPDP^+$

The disproportionation and auto-oxidation reactions make assessment of $MPDP^+$ effects in biological systems difficult since one may be observing the effects of all 3 species (MPTP, $MPDP^+$, and MPP^+) rather than the effect of $MPDP^+$ itself whenever an initial concentration of 50 uM $MPDP^+$ or greater is used. Perhaps because of its inherent instability, few studies of $MPDP^+$ toxicity have been made, even though it is an obligate intermediate in the oxidation of MPTP by MAO B. It has been shown that $MPDP^+$ is cytotoxic to freshly isolated rat hepatocytes.[13] At equimolar concentrations $MPDP^+$ was sufficiently toxic to kill 100% of the cells more rapidly than either MPTP or MPP^+.[13] The more rapid cytotoxic action of $MPDP^+$ has been attributed to two factors. $MPDP^+$ may be an intrinsically more potent cytotoxin due to its electrophilic nature which may allow alkylation of critical cellular proteins. Neither MPTP or MPP^+ share this potential characteristic. The other factor may be an access effect. $MPDP^+$ can deprotonate to form the uncharged dienamine **9** which can readily cross a cell membrane. In contrast the quaternary pyridinium species MPP^+ cannot easily cross a cell membrane. In the absence of activation by MAO, MPTP is not toxic to hepatocytes.

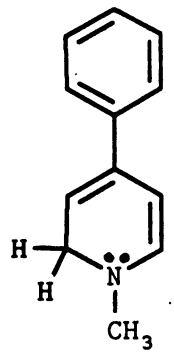

9

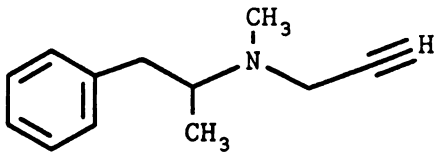

10

PROPERTIES OF MPP^+

MPP^+ (6), the terminal MAO B derived metabolite of MPTP (Scheme 1-1), is chemically much more stable than $MPDP^+$. The aromaticity of the pyridinium ring renders MPP^+ stable with respect to the disproportionation and auto-oxidation observed with $MPDP^+$. MPP^+ is a quaternary pyridinium salt which is highly polar. Given systemically, MPP^+ will not easily cross a membrane barrier such as the blood brain barrier, a factor which limits the biological testing that can be accomplished with this compound. In order to establish the identity of the neurotoxic metabolite of MPTP it would be useful to be able to observe the same types of toxicity observed with MPTP following systemic administration of the candidate toxin. However, since both MPP^+ and $MPDP^+$ are physically unsuited for systemic administration or cannot be expected to gain access to the central nervous system, this experiment cannot be performed. MPP^+ was known to be a toxic compound before it was discovered to be a

metabolite of MPTP. Its potential as an herbicide was explored because of its structural similarity to paraquat, **11**.[32]

MPP^+ when directly administered to dopaminergic neurons of the substantia nigra caused potent but relatively nonspecific tissue damage (Jonsson [14]).

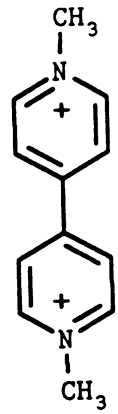

11

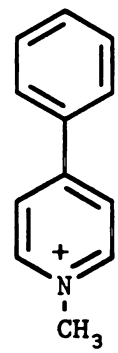

6

PROPOSAL FOR SYNTHESIS AND STUDY OF 1,2,2-TRIMETHYL-4-PHENYL-1,2-DIHYDROPYRIDINE (12), A STABILIZED FORM OF $MPDP^+$

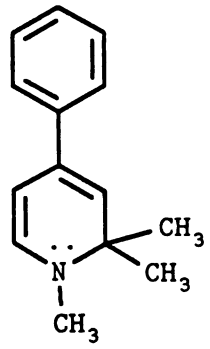

12

To examine the mechanism of MPTP induced neurotoxicity more closely, we wished to more thouroughly examine the properties of $MPDP^+$ in biological systems. In order to remove the chemical and physical obstacles to the study of this compound, we proposed the synthesis of a stabilized $MPDP^+$ analog, 1,2,2-trimethyl-4-phenyl-1,2-dihydropyridine (**12**). The presence of the geminal dimethyl moiety at the 2 position was designed to block the auto-oxidation and disproportionation processes observed with $MPTP^+$ since loss of a methyl group from the 2 position (required for oxidation) would be a much slower process than the hydride loss observed in oxidation and disproportionation of MPDP+. Furthermore, the trimethyl compound, an uncharged species, was expected to exhibit much more favorable bioavailability characteristics including the ability to cross biological

membranes. The pKa of the nitrogen in compound **12** was estimated to be close to 8 due to the pKa lowering influence of the congugated benzyl diene system.[129] Thus **12** was expected to be able to adopt a protonated, charged form (**13**) at physiological pH, similar to the charged form of $MPDP^+$, yet be able to gain access to the CNS system by crossing membranes as the uncharged form. The electrophilic C_6 carbon atom of the charged form (**13**) was expected to exhibit similar reactivity to $MPDP^+$ which would allow the assessment of the role that electrophilic alkylation of critical cellular proteins plays in the toxic properties of $MPDP^+$.

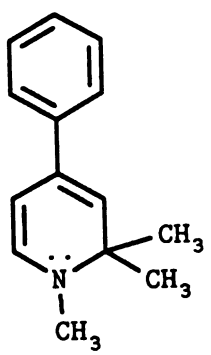

12

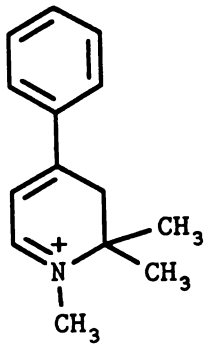

13

Our first proposed synthetic route to **12** (Scheme 1-3) was designed take advantage of the susceptibility of MPP^+ to attack by a Grignard reagent, methyl magnesium bromide. Subsequent formation of dihydropyridine **14** was to be followed by protonation to form **15** and **16** followed by reduction to form tetrahydropyridines **17** and **18** in a synthetic scheme discussed in more detail in Chapter 2 of this dissertation. The dimethyl tetrahydropyridines **17**

and **18** were also interesting compounds, and we proposed to characterize their interactions with monoamine oxidase (MAO). After purification, it was expected, compound **18** could be oxidized via the Polonovski rearrangement chemistry reported by Portoghese et al[53] to give the dihydropyridinium ion **19**. It was envisioned that the second geminal methyl group could then be introduced by treatment with methyl magnesium bromide to give the 1,2,2-trimethyl-tetrahydropyridine **20** which could be oxidized by a second round of the Polonovski rearrangement to yield **21** and its tautomer, the desired product **12**.

Difficulties were encountered with this synthetic scheme which are described more fully in Chapter 2. Briefly, **17** and **18** were not the only products of reaction of MPP^+ with methyl magnesium bromide and compound **18** could not be easily purified, thus synthetic scheme 1-3 was temporarily abandoned in favor of scheme 1-4.

Scheme 1-4 was modeled after a sequence reported by Casey and McEarlane whose objective had been the synthesis of a related compound 1,2-dimethyl-4-phenylpiperidin-4-ol **33**.[54] In their experience, unintentional dehydration of the piperidinol led to formation of a mixture of **17** and **18** in poor yield. Although this route did not appear to be an efficient synthesis of **17** and **18**, it did appear suitable for adaptation to provide **12**.

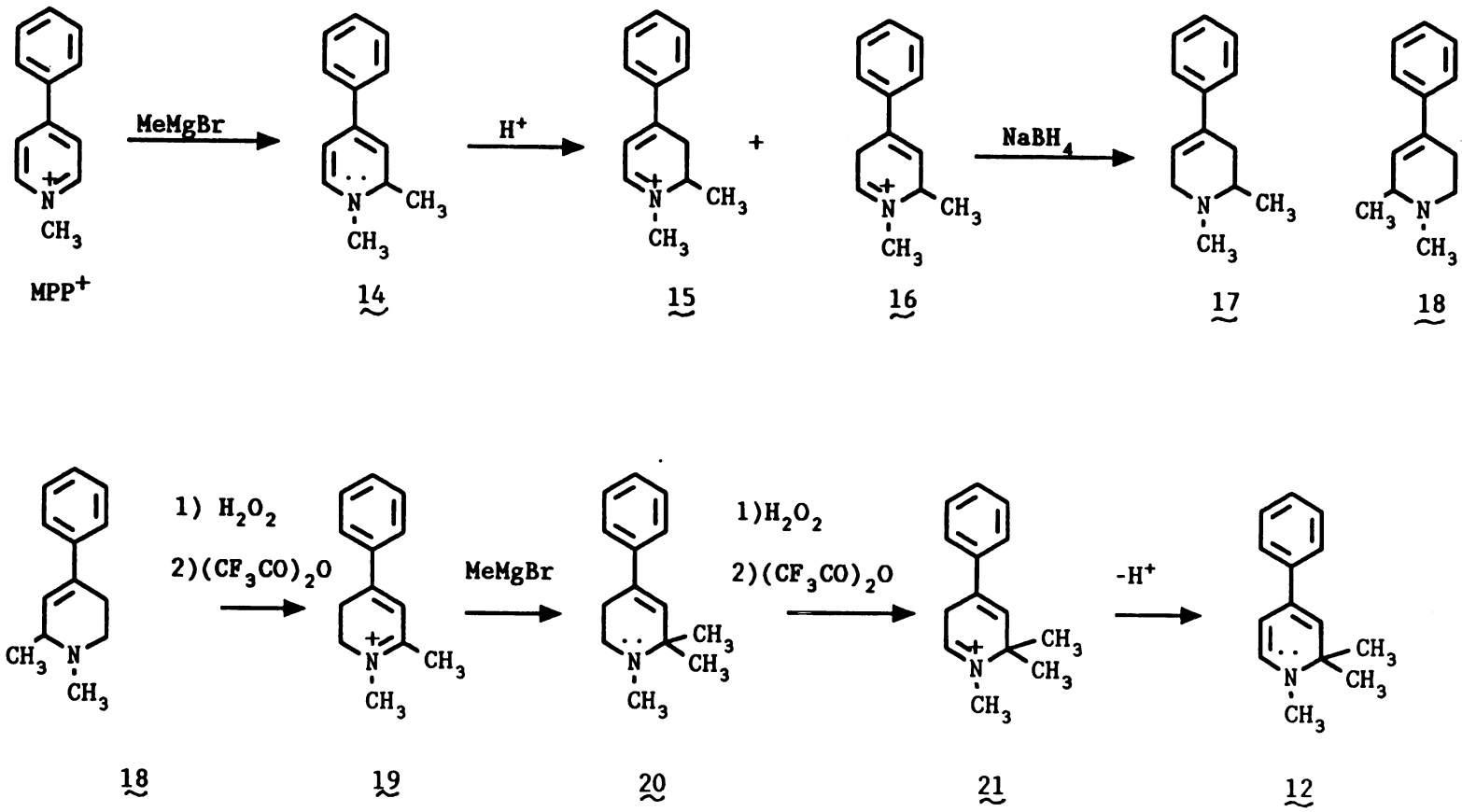

Scheme 1-3. Proposed synthetic route to 1,2,2-trimethyl-4-phenyl--1,2-dihydropyridine (12)

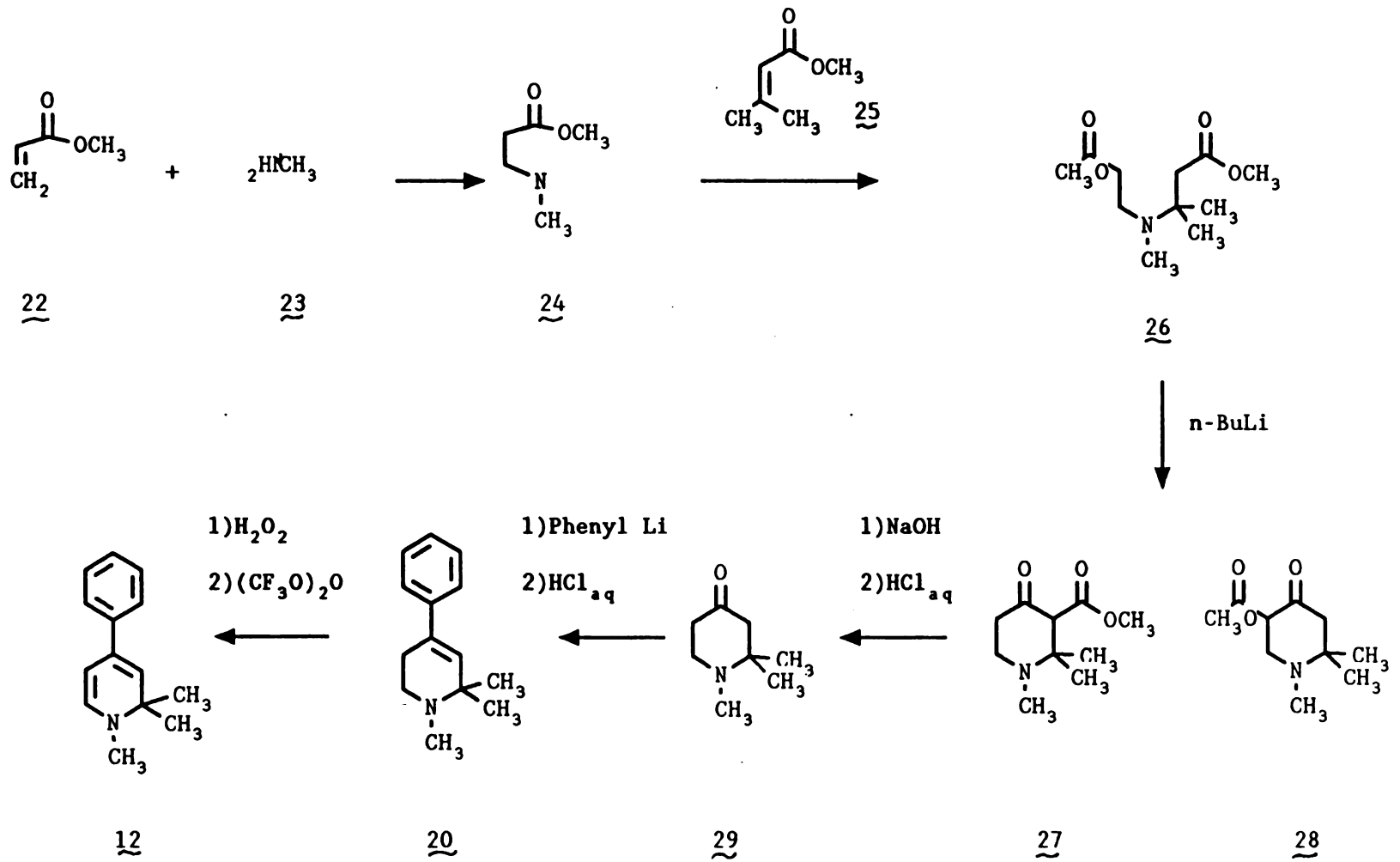

Scheme 1-4. Proposed synthetic route to 1,2,2-trimethyl-4-phenyl-1,2-dihyropyridine (12)

It was envisioned that methyl 3-aminopropionate (**24**) would be synthesized by Micheal reaction of methyl acrylate (**22**) with methyl amine (**23**) according to the method of Lindsay and Cheldelin.[97] Then, following the method of Casey and McEarlane,[54] amine **24** would be reacted with the geminal dimethyl acrylate derivative **25** in Micheal fashion to yield the diester **26**. An intramolecular Dieckman condensation would then yield a mixture of ketoesters **27** and **28**. Saponifiction of the mixture followed by decarboxylation was expected to lead to the 1,2,2-trimethyl substituted 4-pyridione **29**. Attack by phenyllithium on the ketone functionality of **29** would yield a piperidinol which would be dehydrated with aqueous HCl to yield the 1,2,2-trimethyl-4-phenyl-1,2,5,6-tetrahydropyridine **30**. Subsequent oxidation of **30** using Polonovski type conditions was expected to lead to the desired product 1,2,2-trimethyl-4-pheny-1,2-dihydropyridine (**12**). However, slow progress was made as difficulties in the Micheal addition of methylamine (**23**) to methyl acrylate (**22**) were encountered. The desired monoadduct **24** proved to be only a minor component (14%) of a product mixture consisting chiefly of the diadduct **32**. The monoadduct **24** was purified by distillation and identified by GC-MS giving the expected molecular ion at m/e 117. The 80 MHz ^{1}H NMR (CD_3CN) of **24** exhibited a characteristic singlet at 1.34 ppm corresponding to the secondary amine proton which dissappeared on D_2O

exchange. Furthermore, the signals corresponding to the methylene protons (2.48-2.74 ppm) integrated for a total of 4 protons as expected for **24** while the signal corresponding to the ester methyl group (3.61 ppm) integrated for the necessary 3 protons. The 80 MHz ^1H NMR of the diadduct **32**, in contrast, lacked a signal corresponding to a secondary amine proton. Instead the tertiary character of this amine was confirmed by the appearance of a singlet at 2.24 ppm (3H, N-methyl) as well as a multiplet at 2.5-2.7 ppm which integrated for 8 protons and corresponded to the 4 methylene protons on each of 2 N-propionyl side chains. The integration of the methyl ester proton signal (6H) also confirmed the assignment of this structure. The GC-MS of the diadduct exhibited a molecular ion at m/e 203 and a base peak of m/e 130 corresponding to a loss of methyl acetate. Despite this difficulty, the other required starting material, ester **25** was prepared by esterification of the corresponding acid chloride with methanol. It's identity was confirmed by it's 80 MHz ^1H NMR (CD_3CN) which exhibited a singlet corresponding to the 3 methyl ester protons at 3.61 ppm, doublets at 1.88 ppm and at 2.13 ppm corresponding to the geminal vinylic methyl groups, and a multiplet at 5.15 ppm which arose from the vinylic proton.

Small amounts of each of **24** and **25** had been prepared and purified, ready for condensation to form the diester

26 when the results of an elegant study by Sayre et al. were published. Sayre had already successfully synthesized the 1,3,3-trimethyl-4-phenyl-2,3-dihydropyridinium salt (31) via a route similar to our own.[55] He then showed that on intranigral administration in the rat, this alternative stabilized $MPDP^+$ analogue is 2 to 3 orders of magnitude less toxic than MPP^+.[56] Furthermore, Sayre demonstrated that although the adducts of benzylthiol, benzylamine, and imidazole with 31 could by demonstrated by NMR, no stable adducts could be isolated. These findings were interpreted to mean that alkylation of critical cellular proteins by $MPDP^+$ was not likely toplay a role in the neurotoxicity observed with MPTP. Sayre also addressed the possibility (earlier suggested by Castagnoli et al. [57]) that $MPDP^+$ might exert a neurotoxic effect via a redox interaction with dopamine. It had been postulated that dopamine might be oxidized to the cytotoxic dopamine quinone 33 with the concommittant reduction of $MPDP^+$ to MPTP. Such an interaction might well result in a redox cycle since $MPDP^+$ would be regenerated by MAO catalyzed oxidation. The production of toxic dopamine oxidation products had been proposed very early in the unraveling MPTP scenario as a possible mechanism of MPTP induced neurotoxicity. Sayre, however, demonstrated the lack of redox reactivity between dopamine and $MPDP^+$.[56]

Altogether, these studies appeared to indicate that the neurotoxicity of $MPDP^+$ was minor compared to that of MPP^+. We therefore redirected the scope of this dissertation research effort.

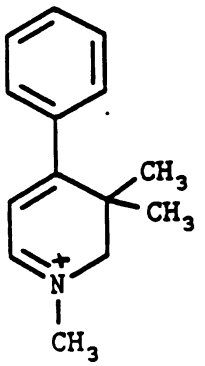

31

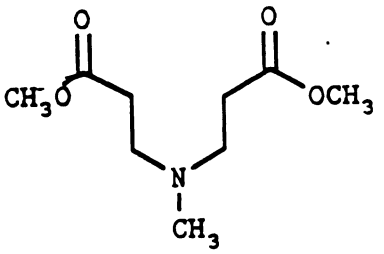

32

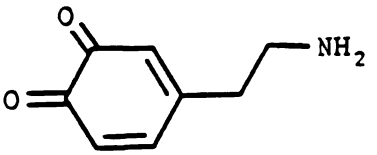

33

BACKGROUND OF TETRAHYDROPYRIDINES IN PHARMACEUTICALS. OUR NEED TO LEARN MORE ABOUT SUBSTRATE PROPERTIES OF TETRAHYDROPYRIDINES AND MAO.

Substituted tetrahydropyridines have long been of interest in the pharmaceutical industry. In the 1940's, tetrahydropyridines were examined for activity as narcotic analgesics.[15] Their usefulness as cough suppressants, mydriactic agents, hypnotics, and barbiturate potentiators has also been explored.[16] More recently MPTP itself was utilized as a synthetic intermediate in benzomorphan synthesis. One of the chemists involved in the synthesis developed irreversible parkinsonism by age 37 probably due to accidental inhalation or skin contact with MPTP.[16a] This incident points out the need for a better understanding of the

structure-activity relationship of tetrahydropyridines as substrates for MAO. If these compounds are to be used safely as pharmaceuticals or as synthetic intermediates we must be able to predict their metabolic fate. In addition we must develop a better understanding of the toxicological properties of potential metabolic products.

CHAPTER 2 Synthesis and biological activity of methyl substituted analogs of the neurotoxin MPTP and its monoamine oxidase derived metabolites, $MPDP^+$ and MPP^+

A study of the structure-activity relationship of substituted tetrahydropyridines as substrates for monoamine oxidase should take several factors into account. The electronic, steric, and lipophilic characteristics of the tetrahydropyridine will affect binding to the enzyme active site and may affect the catalytic competence of the enzyme. Substitution at one site on the molecule may have more impact on substrate activity than at another site depending on the enzyme mechanism. In fact the enzyme mechanism is so important to SAR that the mechanism is often examined by a carefully conducted structure-activity study. In the case of monoamine oxidase, a large amount of information about the enzyme and its mechanism are available from work with other substrate classes. A brief review of this information is warranted.

MONOAMINE OXIDASE; CHARACTERISTICS, MECHANISM AND SUBSTRATE SPECIFICITY

Monoamine oxidase (MAO) [monoamine; O_2 oxidoreductase, EC 1.4.3.4] plays an important role in regulating the levels of the biogenic amines and neurotransmitters, catalyzing their oxidative deamination

to form the corresponding aldehydes.[109] MAO is a flavin containing protein with a molecular weight of approximately 120,000 daltons,containing two subunits of 60,000 to 63,000 daltons each.[121,122] The enzyme is located primarily in the outer mitochondrial membrane.[110] MAO occurs in both neuronal and nonneuronal tissue, e.g. platelets, placenta, liver, heart and lung.[111] It occurs in two immunologically[74] and catalytically distinct forms, MAO A and MAO B.[112] In some tissues a single form is present e.g. MAO A in human placenta and MAO B in human platelets and in bovine liver.[113] More commonly both forms are present in a given tissue although the ratio of the forms may vary with tissue source.[115] Monoclonal antibodies specific for each of the forms have shown that MAO A is located in catecholaminergic cells, including those present in the substantia nigra, while MAO B is located in serotonergic regions.[74] MAO B was also found in astrocytes, a neuronal helper cell population found in all parts of the brain.[74] MAO A preferentially deaminates 5-hydroxytryptamine and is susceptible to the selective suicide inactivator chlorgyline (**34**).[112] MAO B preferentially deaminates phenethylamine and benzylamine and is more sensitive to suicide inactivation by deprenyl (**10**).[116]

Prior to the discovery of the MAO substrate properties of MPTP, very few tertiary amine substrates of MAO were known. The few examples consisted primarily of

N,N-dimethyl-N-benzyl and N,N-dimethyl-N-phenethyl compounds which were analogs of the biogenic amine substrates of MAO.[114] Other tertiary amines whose oxidation is catalysed by monoamine oxidase include the propargyl amine suicide inactivators of MAO such as deprenyl (**10**) and chlorgyline (**34**), however, these compounds are not commonly considered "substrates" of the enzyme. Thus MPTP became the first known example of a new class of tertiary amine substrates of monoamine oxidase. Other endogenous primary amines (Table 2-1) have been characterized as specific substrates for MAO A or MAO B or as nonspecific substrates of both.[153]

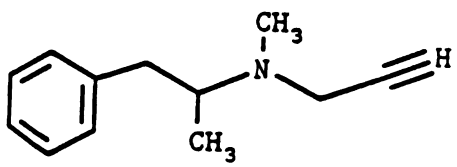

10

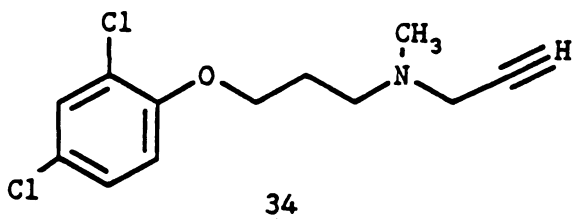

34

TABLE 2-1. Characterization of Biogenic Monoamines as Substrates for Type A and Type B MAO using Rat Brain or Liver Mitochondria

Type A	Type A and Type B	Type B
5-hydroxytryptamine	p-tyramine	2-Phenylethylamine
5-methoxytryptamine	m-tyramine	(low conc.)
epinephrine	dopamine	2-phenylethanolamine
norepinephrine	tryptamine	(low conc.)
metanephrine	p-octopamine	o-tyramine
normetanephrine	m-octopamine	1,4-dimethyl-histamine
	p-synephrine	
	2-phenylethylamine (high conc.)	
	2-phenylethanolamine (high concentration)	

Reference 153

MAO is a flavoenzyme containing the cofactor flavin adenine dinucleotide (FAD). Unlike most other flavoenzymes the FAD of MAO is covalently linked to the protein via a thioether bond between a cysteine residue and the C_8-methyl substituent of the flavin moiety (Fig. 2-1).[18] With most other flavin enzymes the flavin moiety is free to dissociate from the protein. Little is known about the active site of MAO other than the structure of a pentapeptide containing the cysteine to which the flavin moiety is bound. In 1971 Walker et al. isolated the pentapeptide from beef liver mitochondrial MAO B with the sequence shown in Figure 2-1.[18] This sequence was

confirmed for MAO B by Yu in 1980 who also reported the same sequence for MAO A.[19]

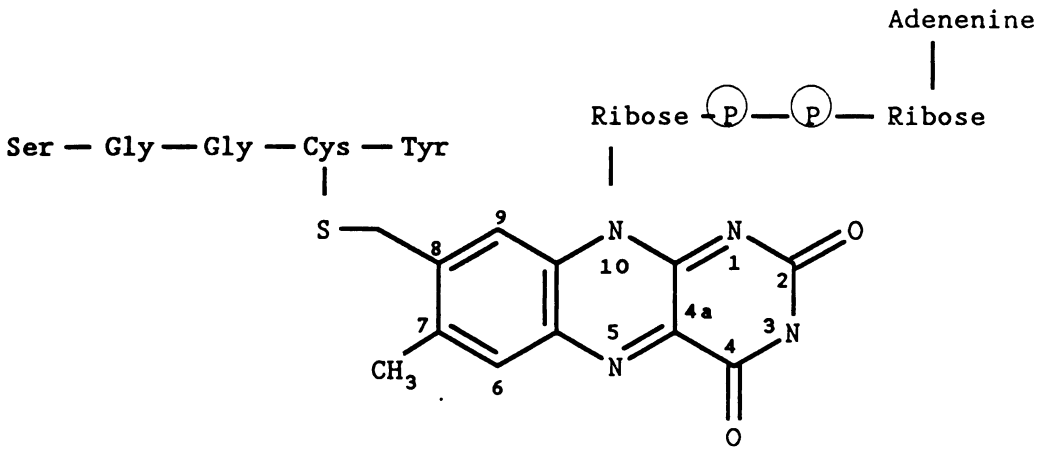

Figure 2-1. Partial amino acid sequence of MAOB containing the flavin moiety.

The complete peptide sequence or x-ray structure of MAO A or B has not yet been reported. However, in a study by Cawthon et al. (1981) limited proteolysis followed by polyacrylamide gel electrophoresis was used to demonstrate that the two formes of MAO have distinctly different peptide sequences and may therefore arise from different gene loci.[21] Yasunobu et al. have given evidence that cysteines are at the active site and are essential for activity from a study of the effects of specific thiol alkylating reagents on MAO activity.[20]

On the basis of studies of the mechanism of inactivation of MAO by various cyclopropylamine analogs[22,119,127,154-157], a one electron mechanism for

the MAO catalyzed oxidation of amines was proposed by Silverman. The mechanism is illustrated in Scheme 2-1 for benzylamine oxidation as proposed by Silverman et al.[22]

The flavin starts the cycle in the oxidized form (35) which accepts the first electron from the nitrogen lone pair of the amine (36). The transfer of the first electron results in formation of the flavin semiquinone (37) and an aminium radical cation of benzylamine (38).[22] The aminium radical cation is a short lived species which rapidly gives up a proton to form the carbon centered radical species 39.[22] A second electron is then transferred from 39 to the flavin coenzyme with the resultant formation of the fully reduced flavin coenzyme (40) and benzyliminium cation (41).[22] At this point the oxidation of the amine species is complete and the iminium species is released from the enzyme. Primary and secondary iminium species are hydrolyzed in the biological milieu to form the corresponding aldehyde and ammonia in a typical Schiff's base hydrolysis.[117] In the case of MPTP, however, the iminium species $MPDP^+$ does not undergo detectable hydrolysis but is further oxidized by 2 electrons or undergoes disproportionation as has been previously discussed. To return the enzyme to its starting state, the reduced flavin (40) must be reoxidized by 2 electrons. This oxidation is accomplished by molecular oxygen which reacts with the

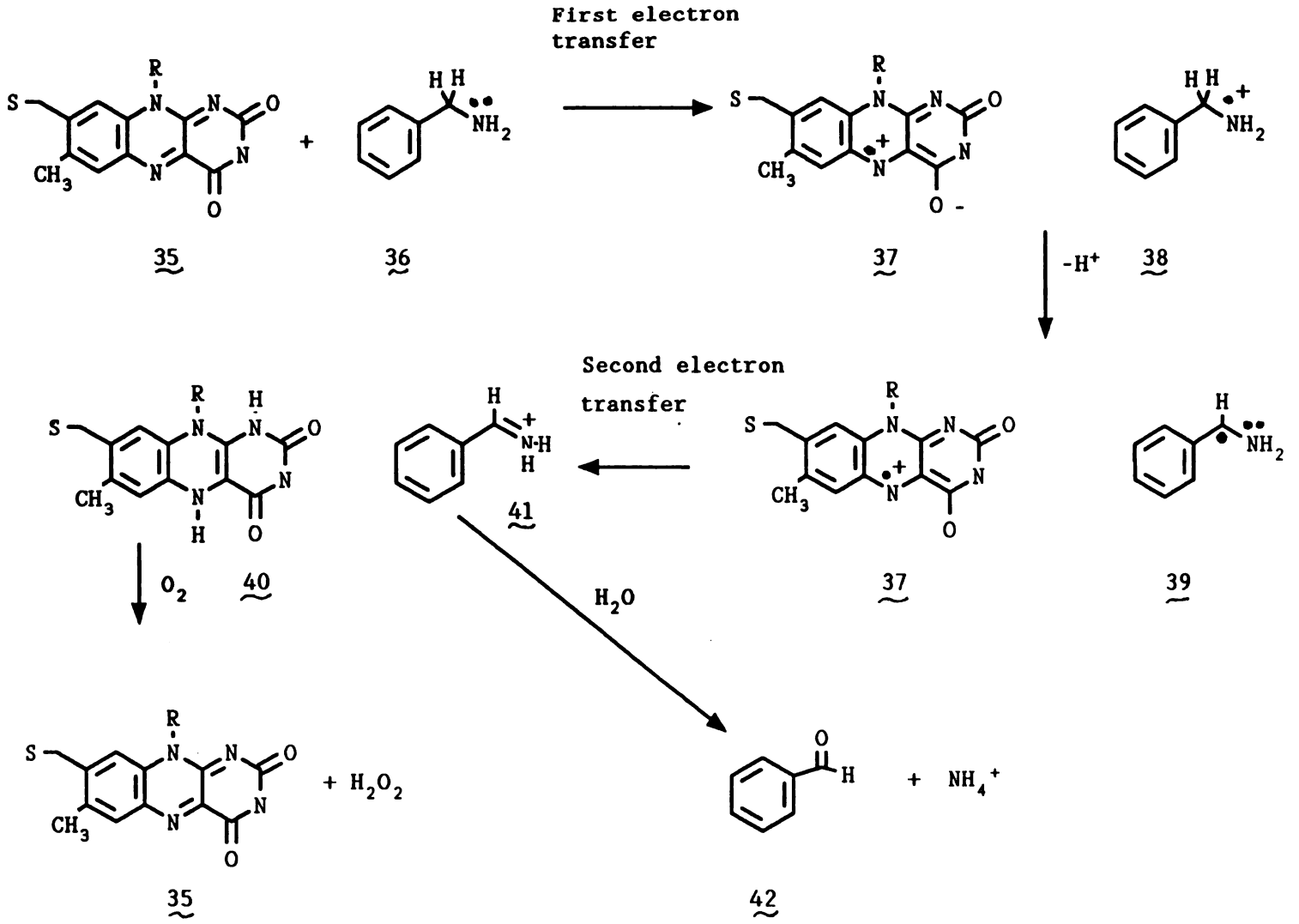

Scheme 2-1. Silverman's proposed mechanism for MAO catalysed amine oxidation

flavin in a series of 2 consecutive single electron transfers to form hydrogen peroxide and the oxidized flavin. [118]

We and others were interested in the special structural characteristics of MPTP which rendered it a good substrate for MAO, since as discussed above, tertiary amines are in general poor substrates for MAO. After the initiation of the work described here, some significant contributions were made by others to the body of knowledge about the structure-activity relationship of substituted tetrahydropyridines as substrates for MAO.

Heikkila et al., using crude mitochondrial preparations, showed that the double bond of the tetrahydropyridine ring is required for significant MAO activity since saturation of the double bond results in complete loss of activity.[23] Hekkila also showed that the methyl-substituent on the nitrogen atom of MPTP was crucial to MAO substrate activity since replacement of the methyl group with a hydrogen, ethyl or propyl group resulted in a substantial decrease in substrate activity.[23] Gessner et al. (1986) reported that purified human liver MAO B would tolerate little substitution of the phenyl ring with retention of MAO substrate activity.[24] Substitution at 4' with the electronegative chloro group or electron donating hydroxy group gave compounds **43** and **44** with 7% and 0%, respectively, of MPTP's substrate activity.[24] These data imply that the

reason for the detrimental effect on substrate activity may not be related to the electronic effects of these substituents but may instead be related to steric effects. Since both the chlorine and hydroxyl substituents are larger than the hydrogen atom present on MPTP, the presence of the larger substituent may simply interfere with proper enzyme-substrate fit, thus lowering substrate activity. These investigators also showed that the position of the phenyl group on the tetrahydropyridine ring was important since the C_2 (**45**) and C_5 (**46**) regioisomers of MPTP were devoid of MAO substrate activity.[24] (This finding was subsequently corroborated in our laboratory. Dr. Patricia Caldera synthesized analogs **45** and **46** by sodium borohydride reduction of the corresponding substituted pyridinium ions. I then assayed their activity as MAO substrates using both a UV absorbance assay and an oxygen consumption assay discussed later in this chapter. Neither compound exhibited substrate activity.) Gessner et al. also investigated the effect of placement of additional methyl groups at the 3 and 5 positions of MPTP.[123] These additional methyl groups confer increased steric bulk to the tetrahydropyridine ring. It was found that the compound with the additional methyl group at the 3 position, **47**, retained 13% of the activity observed with MPTP while the 5-methyl compound, **48**, dropped to 6% of MPTP's acitivity. Thus additional steric bulk placed

at the 3 and 5 positions of MPTP was detrimental to MAO substrate activity. These findings, however, were not available to us as we started our study of the effects of tetrahydropyridine substitution on MAO substrate activity. We were particularly interested in the effects of substitution at the 2 and 6 positions of MPTP because of the mechanism we proposed for MAO B catalysed oxidation of MPTP (Scheme 2-2).

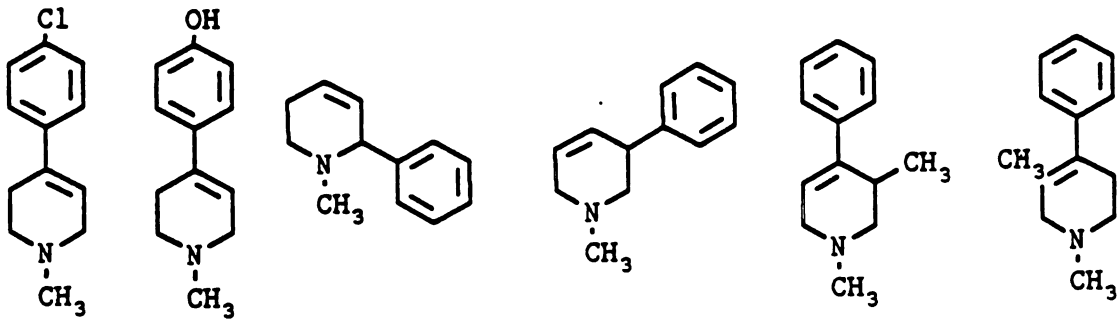

43 44 45 46 47 48

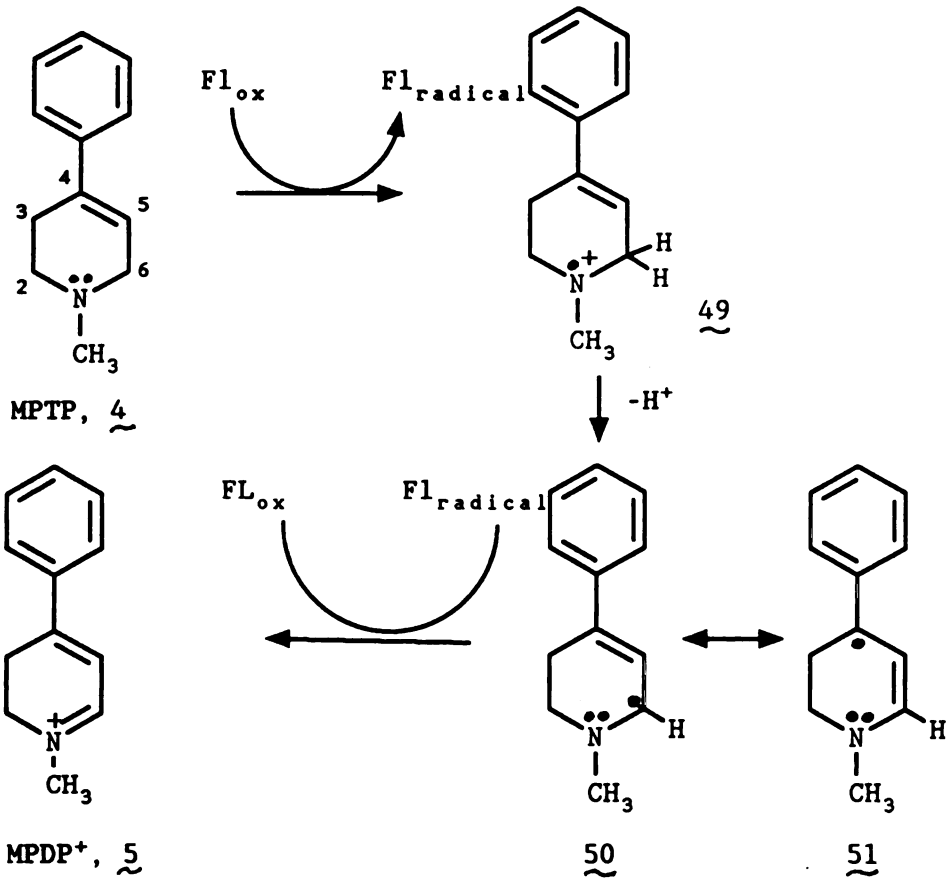

Scheme 2-2. A proposed mechamism for MAOB catalyzed MPTP oxidation

In analogy with the mechanism proposed by Silverman,[22] we proposed that MPTP underwent a series of two consecutive single electron transfers forming first the radical-cation **49** which could lose a proton at C_6 to form the allylic carbon based radical **50**. Resonance stabilization is possible for this product of the first electron transfer through the resonance form **51**. A second electron transfer to form the fully reduced flavin and $MPDP^+$ would complete the oxidation mechanism. In general tertiary amines are poor MAO substrates, yet MPTP oxidation is catalysed at a rate of 1.7 nmol/min per microgram of protein, 40% of the rate observed with benzylamine, MAO B's most rapidly oxidized substrate.[126] The resonance stabilization of the allylic radical (**50** and **51**) may explain MPTP's enhanced MAO activity relative to other tertiary amines. Formation of the allylic radical is dependent on deprotonation at position 6 and hence should be affected by the acidity of the proton at postion 6. The rate at which the H_6 proton is lost can be modified by subtitution. For example it is known that as a carbon atom becomes more alkyl substituted, the pKa of a proton attached to the central carbon atom generally increases. For example, the pKa of ethyl acetoacetate (**52**) is 10.7, but that of ethyl methylacetoacetate (**53**) is 12.7.[119,120] Thus we reasoned that alkyl substitution at position C_6 of MPTP would increase the pKa of the remaining proton on C_6 and might substantially slow the

rate of MAO catalysed oxidation. On the other hand, studies on the mechanism of electrochemical oxidation of amines, also a 2 step-1 electron mechanism, suggest that the rate limiting step of the oxidation is the first slow electron transfer from the nitrogen non-bonded pair of electrons.[127,158] Thus substitution which affects the oxidation potential of the nitrogen non-bonded pair of electrons may also significantly affect the rate of MAO catalysed oxidation of a substituted tetrahydropyridine. Measurement of the ionization potentials of alkylamines has shown that addition of an alpha methyl group to the substituent of an aliphatic amine results in a lowered ionization potential by approximately 2 Kcal/mole (Table 2-2).[128]

Table 2-2. Oxidation potentials of aliphatic alkyl amines.

Amine	Ionization potential (kcal/mole)
$MeNH_2$	222.8
$EtNH_2$	218.4
n-$PrNH_2$	216.8
i-$PrNH_2$	214.9
piperidine	199.7
N-methylpiperidine	191.2

Ionization potentials from ref.[128] Measured on a Perkin-Elmer PS-18 photoelectron spectrometer.

Thus alkyl substitution at the C_6 position of MPTP might increase the rate of MAO catalyzed oxidation due to a lowered oxidation potential for the non-bonded electrons of the nitrogen atom. We suspected that the

increased steric bulk of methyl substitution of the C_6 carbons atom might also have a negative impact on the rate of MAO catalyzed oxidation, since an additional methyl group might interfere with proper enzyme-substrate fit. Thus we were aware of a number of possible conflicting effects that methyl substitution of MPTP might have on MAO substrate activity. Furthermore, we had proposed the mechanism of MAO catalyzed MPTP oxidation where deprotonation and oxidation occur at C_6, based on the demonstrated formation of $MPDP^+$.[138] However, we were aware of the possibility that MPTP might also be oxidized at the C_2 carbon which would lead to the formation of the 2,5-dihydropyridinium ion **54**. Such a product might not be detected in a UV assay of MAO catalysed oxidation since its chromophore would be the same as that of the parent amine MPTP. Thus MPTP had the potential for oxidation at each of 2 sites though we believed that the majority of MAO catalyzed oxidation occured at the C_6 carbon atom. Silverman, in studies of methyl substitution with other MAO substrates, has demonstrated 2 phenomena of interest in this regard. First, he showed that placement of a methyl group on the site of oxidation can convert a very rapidly oxidized substrate benzylamine (**36**) to an extremely slowly oxidized substrate alpha-methy benzylamine (**55**).[25] Secondly, he showed that in a molecule with two potential sites for oxidation by MAO, which are normally oxidized

to equal extents by the enzyme, placement of a methyl group on one of the oxidizable sites will cause the enzyme to shift its focus to the other site.[127] For example, N-cyclopropylbenzylamine (**56**) is oxidized by MAO at either of two sites (Scheme 2-3). Oxidation at the benzylmethylene carbon atom (Path A) leads to the products benzaldehyde (**42**) and cyclopropylamine (**59**). Alternatively, oxidation at the cyclopropyl carbon atom (Path B) leads to cyclopropyl ring opening and inactivation of the enzyme.[127] However, when an additional methyl group is placed at the benzyl carbon atom to give N-cyclopropyl-alphamethylbenzylamine (**57**), oxidation at the benzyl methylene carbon atom (Path A) is dramatically reduced to only 1% of cyclopropyl carbon atom oxidation.[25] Thus alpha methyl substitution on substrates of MAO has a variety of effects on MAO substrate activity.

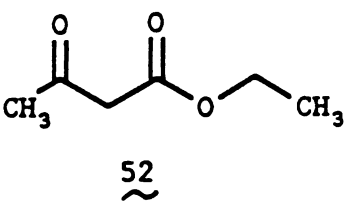

52

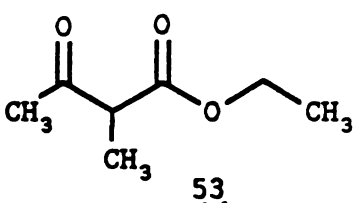

53

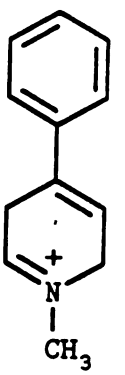

54

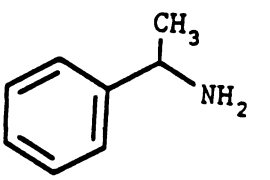

55

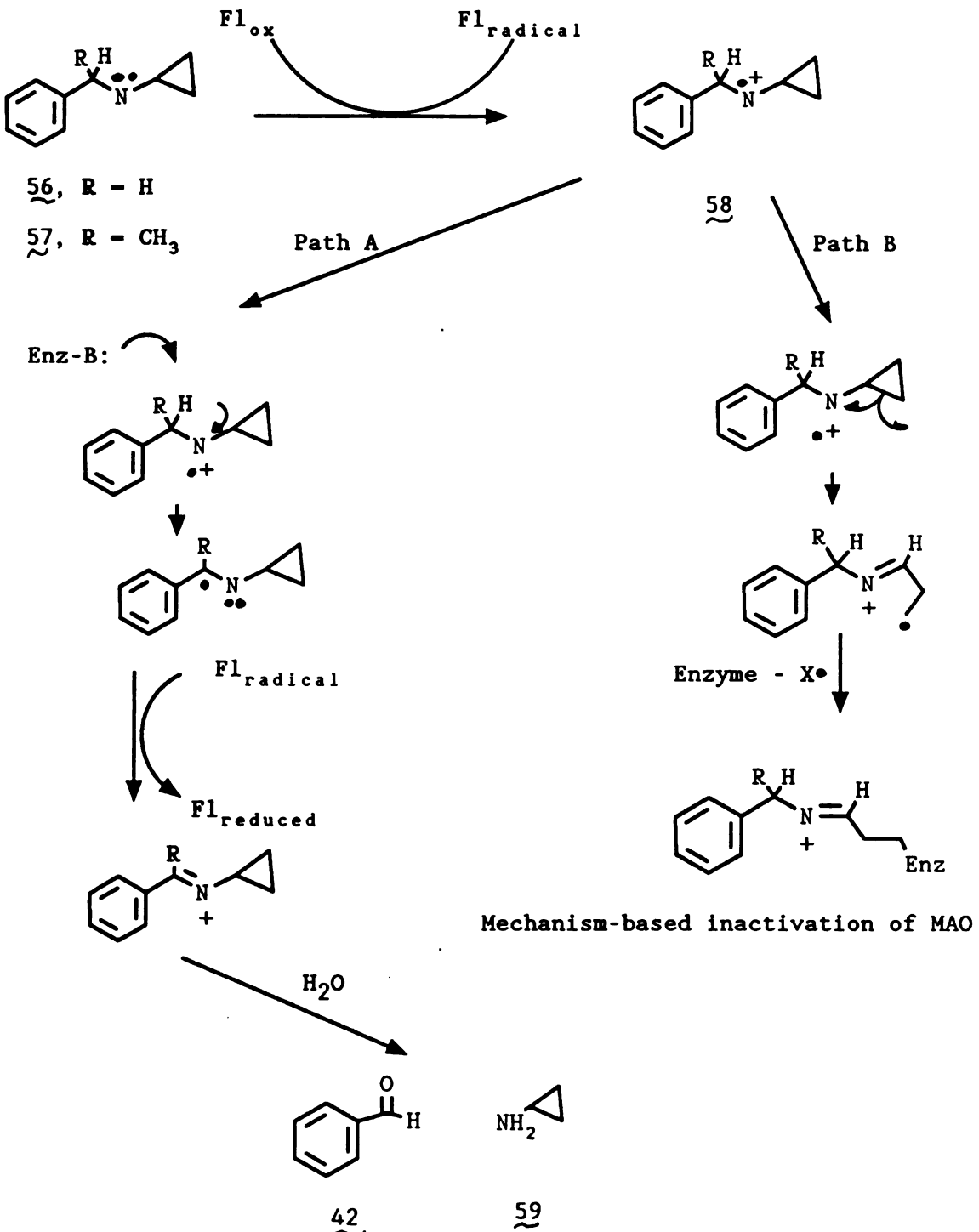

Mechanism-based inactivation of MAO

Scheme 2-3. Silvermans's proposed mechansim for Mechanism-based inactivation of MAO by N-cyclopropylbenzylamine

SPECIFIC AIMS OF CURRENT RESEARCH

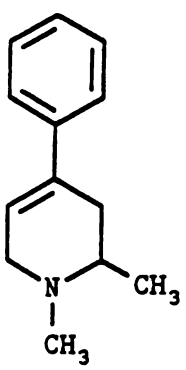

17

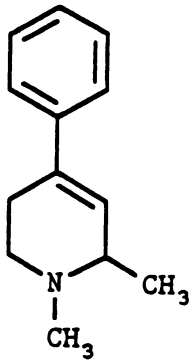

18

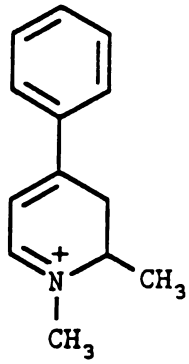

15

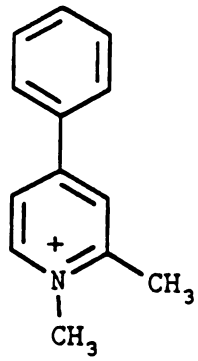

60

In order to examine the influence of alpha-methylation on the substrate activity of MPTP, we proposed to synthesize the two analogs with additional methyl groups at the 2 and 6 positions, 1,2-dimethyl-4-phenyl-1,2,3,6-tetrahydropyridine (**17**), and 1,6-dimethyl-4-phenyl-1,2,3,6-tetrahydropyridine (**18**), respectively. In analogy with the work reported by Gessner[123] and Silverman,[25] we expected that methyl substitution might result in substantially altered MAO B substrate activity (and subsequent neurotoxicity). We expected that the effect of increased steric bulk might be more pronounced in the 6-substituted compound (**18**) since the new methyl group would be placed directly on the site most likely oxidized by the enzyme. In analogy with the effects shown by Silverman [25], alpha methylation at carbon atom 6 (**18**) might result in enhanced MAO catalyzed oxidation at carbon atom 2. Likewise, alpha methylation at carbon atom 2 (**17**) might result in enhanced MAO catalyzed oxidation at carbon atom 6. On the other hand, due to

the effects of alpha methylation resulting in a lowered ionization potential of the nitrogen atom's non-bonded electrons, both **17** and **18** might exhibit enhanced substrate activity, relative to MPTP. Alternatively, increased steric hindrance due to placement of a methyl group at either position might result in decreased MAO substrate activity for both **17** and **18**, relative to MPTP. Furthermore, a fourth possible effect of alpha-methylation related to the effect of the new methyl group on the pKa of hydrogen atoms alpha to the nitrogen. A raised pKa due to alpha methylation at C_6 (**18**) might decrease the rate at which the H_6 proton was lost, resulting in a decreased substrate activity. However, methylation at C_2 (**17**) which might raise the pKa of H_2 might have little effect on the substrate activity of the tetrahydropyridine. According to the proposed mechanism of MPTP induced neurotoxicity, i.e. neurotoxic effects are dependent on MAO catalysed MPTP oxidation, alterations of MAO substrate activity due to alpha methylation should be reflected in altered neurotoxic effects. Thus synthesis of **17** and **18** and investigation of their respective MAO activities and neurotoxic potential would allow us to probe both the sensitivity of the enzyme to alpha methyl substitution in tetrahydropyridines and the strength of the connection between tetrahydropyridine MAO substrate activity and neurotoxicity. As a natural extension of our interest in

the effects of alpha methylation in tetrahydropyridines, we also wished to explore the effects of alpha methylation on the toxic properties of the potential metabolites of methyl substituted tetrahydropyridines. Synthesis of compounds **15** and **60**, the methyl substituted analogs of $MPDP^+$ and MPP^+, respectively, would afford the opportunity to begin structure-activity studies of the potentially toxic metabolites of tetrahydropyridines. Direct chemical synthesis of **15** and **60** would allow us to bypass the MAO catalysed oxidation step which would be essential for study of the toxic properties of these compounds should the MAO substrate activity of **17** and **18** prove to be significantly inhibited. Furthermore, synthesis of the potential metabolites **15** and **60** would provide the opportunity for unambiguous characterization of metabolic products.

INTRODUCTION TO SYNTHESIS OF SUBSTITUTED TETRAHYDROPYRIDINES

Tetrahydropyridines are accessible via at least three synthetic routes: 1) Grignard reaction of arylmagnesium halides with substituted pyridones followed by dehydration,[15] 2) Aminomethylation of olefins,[17] and 3) Sodium borohydride reduction of substituted pyridinium salts.[26] These routes are illustrated in Scheme 2-4 as envisioned for the synthesis of **17** and **18**.

Route 1 would have required the synthesis of 1,2-dimethyl-4-pyridone (**61**) as a precursor which would involve a multi-step synthesis rendering the route somewhat unattractive. Route 2 was also unattractive as it would have required the separation of a mixture of intermediate products including MPTP along with the desired intermediate methylaminoethylstyrene (**62**). A route was desired in which handling of known toxic compounds could be minimized, therefore a modification of route 3 (shown in Scheme 2-5) appeared to be the most attractive initial route.

Route 1) Grignard reaction of Phenyl magnesiumbromide with an appropriately substituted pyridone

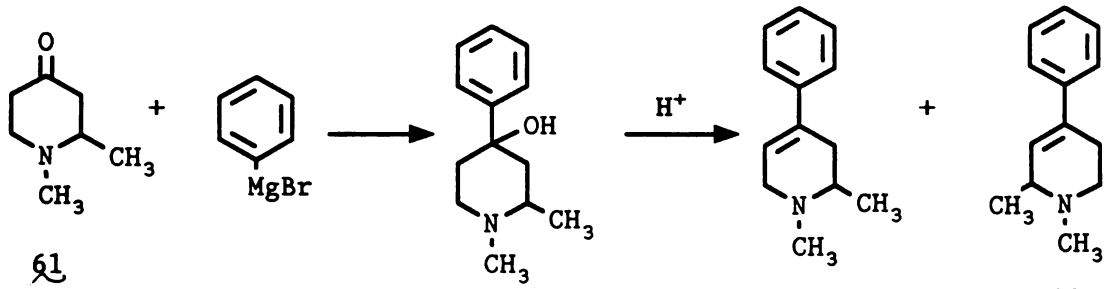

Route 2) Aminomethylation of olefins

step 1

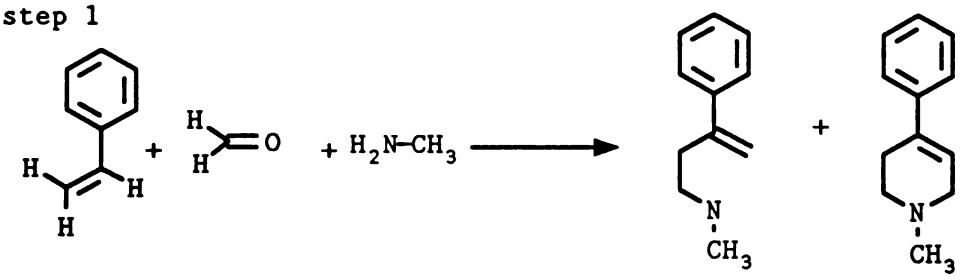

step 2

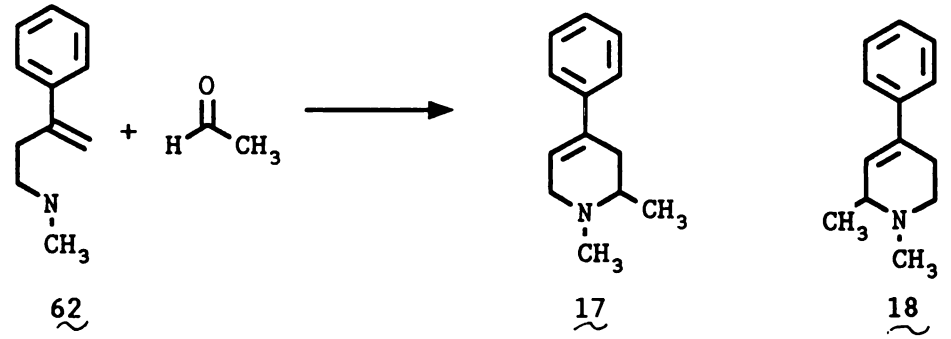

Route 3) Sodium borohydride reduction of substituted pyridinium salts

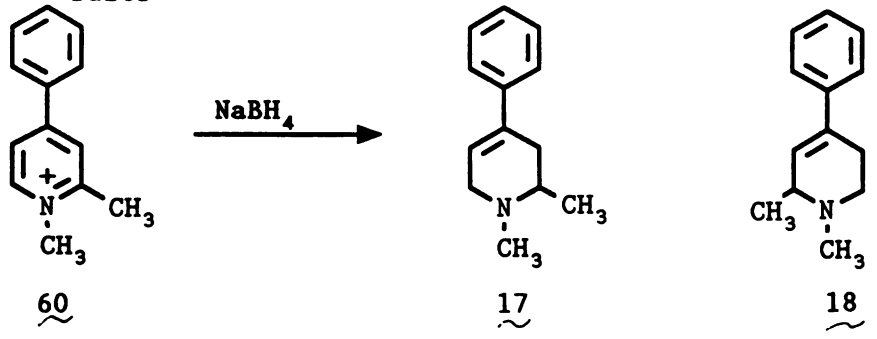

Scheme 2-4. Potential synthetic routes to the methyl-substituted tetrahydropyridines 17 and 18

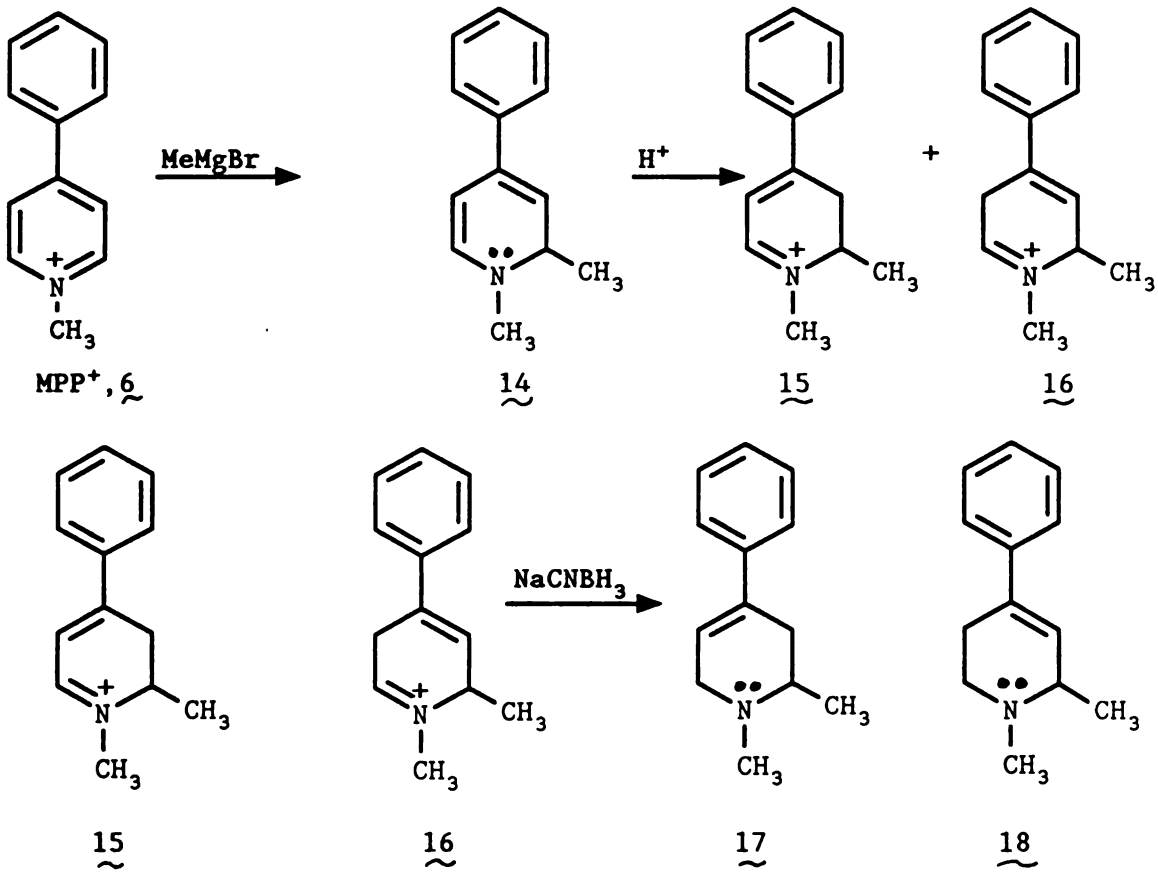

Scheme 2-5. Proposed synthetic route to methyl-substituted tetrahydropyridines 17 and 18

Thiessen et al. showed that the action of Grignard reagents on 4-alkyl substituted pyridinium salts results in formation of 1,2,4-tri-alkyl and aryl substituted 1,2-dihydropyridines.[30] By analogy, we expected that reaction of methyl magnesium bromide with MPP^+ would yield the dihydropyridine intermediate **14**. It was expected that sodium cyanoborohydride reduction of the protonated forms of **14** would yield a mixture of **17** and **18** as shown in Scheme 2-5. Since MPTP could arise as a potential side product from the reduction of unreacted MPP^+, we desired a method by which progress of the Grignard reaction could be monitored. We wished to ensure that the consumption of MPP^+ was as complete as possible before the reduction step was initiated. To accomplish this we planned to take advantage of the characteristic UV absorbance maxima displayed by MPP^+ (290 nm) and $MPDP^+$ (345 nm). Aliquots of the Grignard reaction mixture would be removed anaerobically and immediately diluted into aqueous hydrochloric acid. The resulting solutions would be immediately assayed by UV spectroscopy. The dihydropyridine product **14** of the Grignard reaction would be detected as its protonated form **15** which, due to its similarity to $MPDP^+$, was expected to exhibit a strong UV absorbance at 345 nm. This method was chosen in preference to direct detection of **14** due to the documented instability of alkyl-aryl substituted dihydropyridines with respect to air

oxidation.[136] In practice, this method of monitoring the Grignard reaction proved to be less quantitative than anticipated as will be described in the next section.

ATTEMPTED SYNTHESIS OF 1,2-DIMETHYL-4-PHENYL-1,2,3,6-TETRAHYDROPYRIDINE (17) AND 1,6-DIMETHYL-4-PHENYL-1,2,3,6-TETRAHYDROPYRIDINE (18) BY GRIGNARD REACTION ON MPP^+ FOLLOWED BY SODIUM CYANOBOROHYDRIDE REDUCTION

Large quantities of MPP^+ were prepared by methyl iodide alkylation of commercially available 4-phenyl pyridine for use as starting material in the Grignard reaction sequence. The synthetic MPP^+ was characterized by a sharp melting point at 165-166 ^oC (lit. 167-169 ^oC[35]) and the 240 MHz ^1H NMR spectrum which was fully consistant with the 1-methy-4-phenylpyridinium iodide structure (Figure 2-2).

The Grignard reaction requires use of an aprotic solvent and is usually performed in diethyl ether or tetrahydrofuran. The highly polar nature of the quaternary pyridinium salt MPP^+ led to very limited solubility in either of these solvents. Therefore to aid in dissolution, the MPP^+ was finely crushed and suspended at a dilute concentration (0.05 M) in diethyl ether. A color change from the pale yellow (associated with suspended MPP^+) to a peach color was always observed on addition of methyl magnesium bromide (5 equivalents) to the MPP^+ suspension. Since dissolution of the suspended

starting material was generally not complete until about 2 hours after addition of the Grignard reagent, the first samples for UV analysis were rarely removed before 2 hours. Typically, a 1 mL aliquot of the Grignard reaction mixture was removed anaerobically using a dry glass syringe and immediately diluted 1:1,000 in either 1 M aqueous HCl or 1 M HCl in methanol. A typical UV spectrum obtained in this manner (Figure 2-3) showed a clear UV maximum at 345 nm with minimal absorbance at 270 nm. Such a spectrum was taken as indication that MPP^+ had been consumed with subsequent formation of the dihydropyridine **14** (detected as protonated form **15**). It was our desire, however, to be able to quantitate the extent of reaction based on UV absorbance which, we discovered, is technically difficult. It was found that when the Grignard aliquot was diluted 1:1,000 with 1 M aqueous HCl, the absorbance at 345 nm, though always the UVmax of the spectrum, was low (0.15-0.18 absorbance units) relative to the theoretical absorbance expected for the dihydropyrinium species **15**. For example, Grignard reactions were always performed at 0.05 M, thus a 1:1,000 dilution should have given 50×10^{-6} M concentration. The molar absorptivity for $MPDP^+$ is 17,400, thus the absorbance for a 50×10^{-6} M solution of **15**, (signal of a theoretical 100% yield of **14**), was expected to be approximately 0.87 absorbance units.

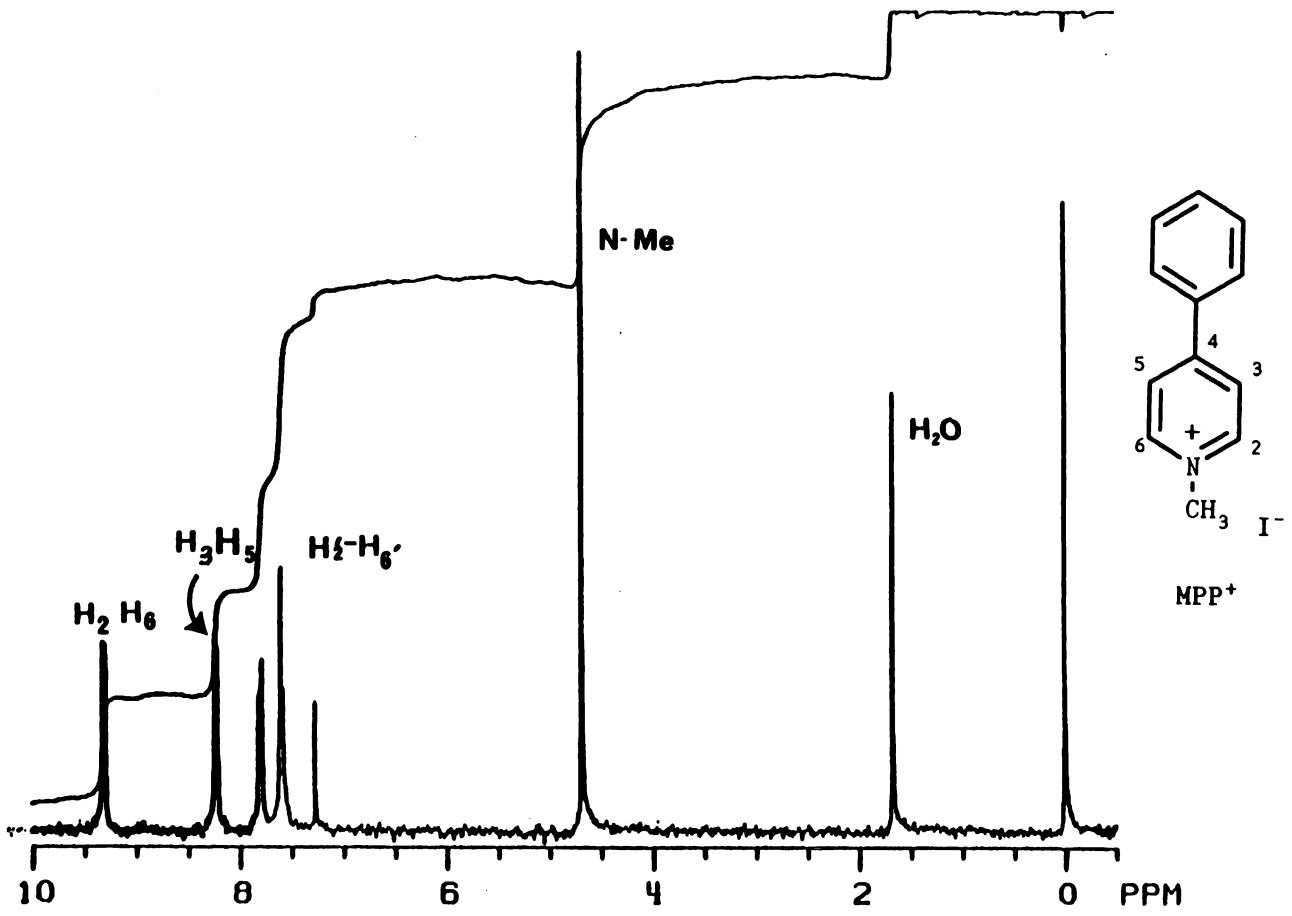

Figure 2-2. 240-MHz ^{1}H NMR ($CDCl_3$) spectrum of 1-methyl-4-phenylpyridinium iodide (**6**)

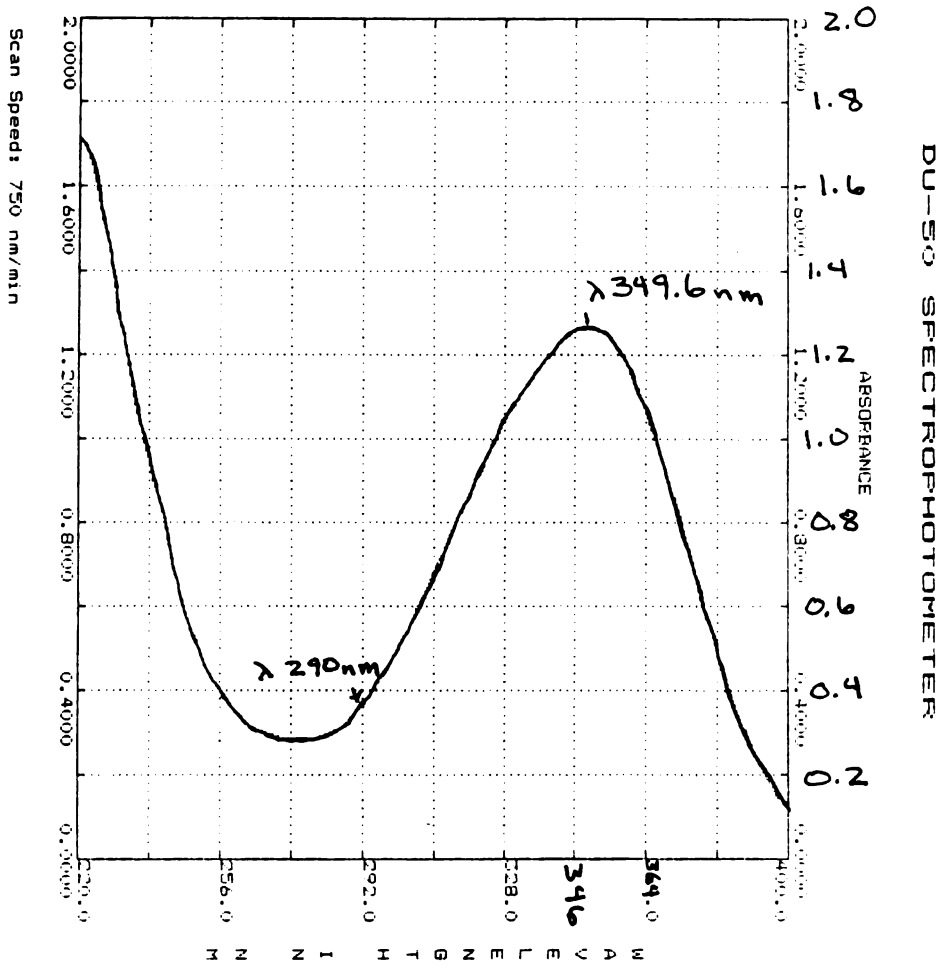

Figure 2-3. A typical UV spectrum obtained from a 1:1000 dilution of an aliquot of Grignard reaction mixture after 2 hours reaction time, showing a clear UVmax at~345 nm and minimal absorbance at 290 nm.

Thus dilutions of Grignard reaction solutions in 1 M aqueous HCl gave only about 17% of the expected optical density at 345 nm, even though absorbance at 290 nm was much lower and sometimes at baseline indicating consumption of the starting material. In contrast, solutions obtained by dilution of the Grignard reaction mixture in 1 M HCl in methanol gave higher absorbance at 345 nm. On one occasion (Figure 2-4) a UV spectrum of an aliquot taken after 2 hours reaction time and diluted 1:1,000 in 1 M HCl in methanol exhibited a UV maximum at 345 nm with absorbance of 0.90 units accounting for 100% conversion of MPP^+ to dihydropyridinium **15**. However, on other occasions spectra obtained from dilution in 1M HCl in methanol gave absorbances greater than 0.9 units, at times as high as 1.26 units (149% of theoretical). This occured despite all precautions taken to ensure the accuracy of sampling and dilution.

Furthermore, the UV spectrum of a sample diluted in 1 M aqueous HCl was unstable with time, which was discovered in the following manner. During the course of one Grignard reaction the initial UV spectrum of a sample diluted 1:1,000 in 1 M aqueous HCl was obtained on a UV spectrometer which had not been allowed its full requisite warm-up period. This spectrum (Figure 2-5) exhibited a UVmax at 345 nm consistant with formation of **15** although it, like other spectra obtained from solutions made with aqueous HCl, exhibited a low

absorbance (0.19 units) relative to the theoretical absorbance (0.87 units). In order to ascertain whether the low absorbance was due to use of the insufficiently warmed up spectrometer, the sample was capped to prevent evaporation and a new spectrum was taken 15 minutes later after the warm-up period for the instrument was complete. The new spectrum (Figure 2-6) showed an absorbance of 0.29 units at 345 nm, a dramatic change, but absorbance at 256 nm (formerly 0.4 units) had dropped to 0.36 units. Thus the increase of absorbance at 345 nm over the 15 minute period, which seemed too dramatic to be accounted for by instrument vagueries, could not be simply attributed to sample evaporation since absorbance at another wavelength had dropped. The absorbance of the capped sample was followed over the next 5.5 hours and the results of these successive UV scans are summarized in Table 2-3.

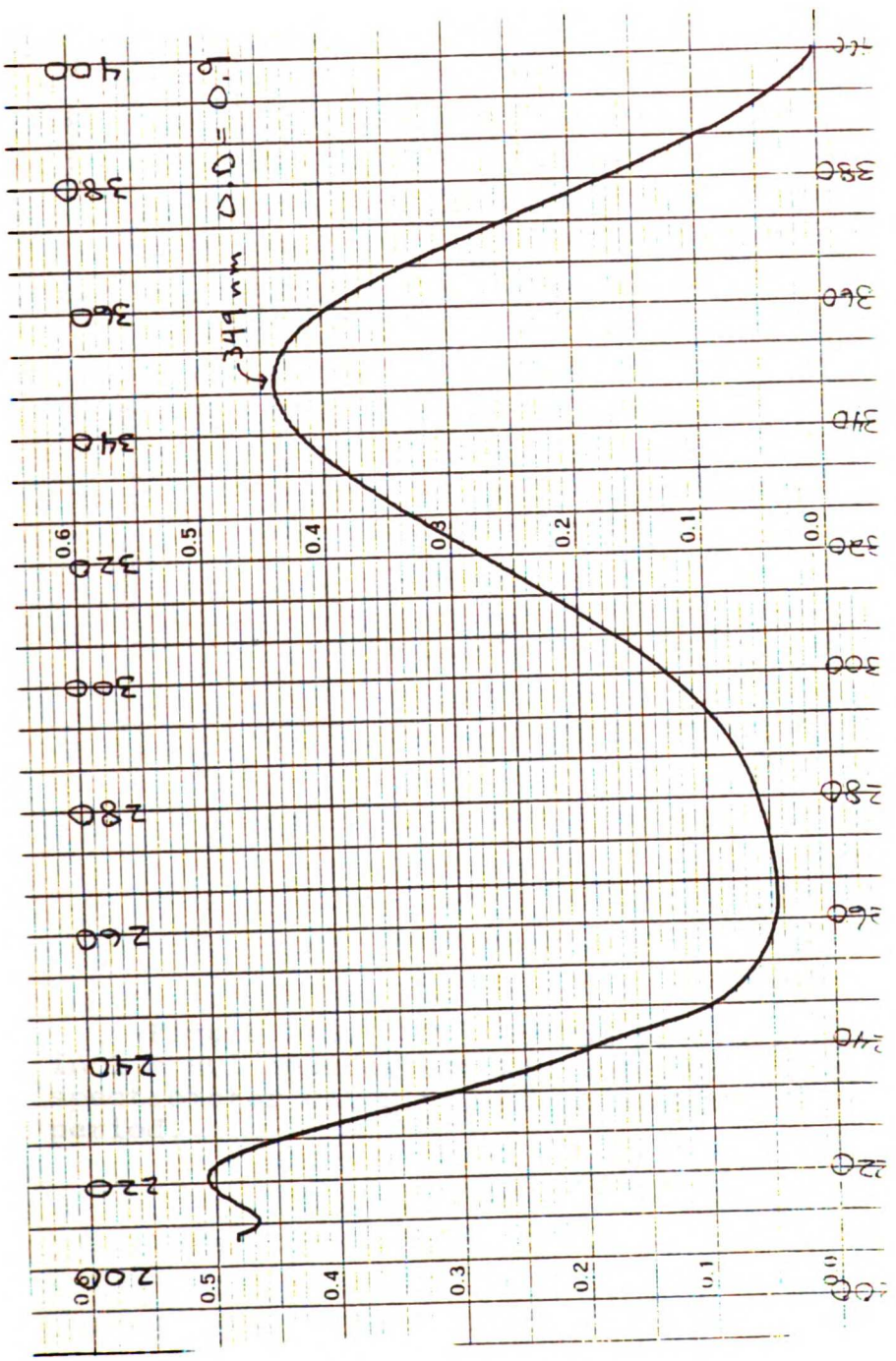

Figure 2-4. UV spectrum of a diluted aliquot (1:1000 in 1 M HCl in methanol) showing 100% conversion of MPP^+ to dihydropyridinium **15**. Full scale of the spectrum equals 2 absorbance units, thus the UVmax at 345 nm is at 0.9 absorbance units.

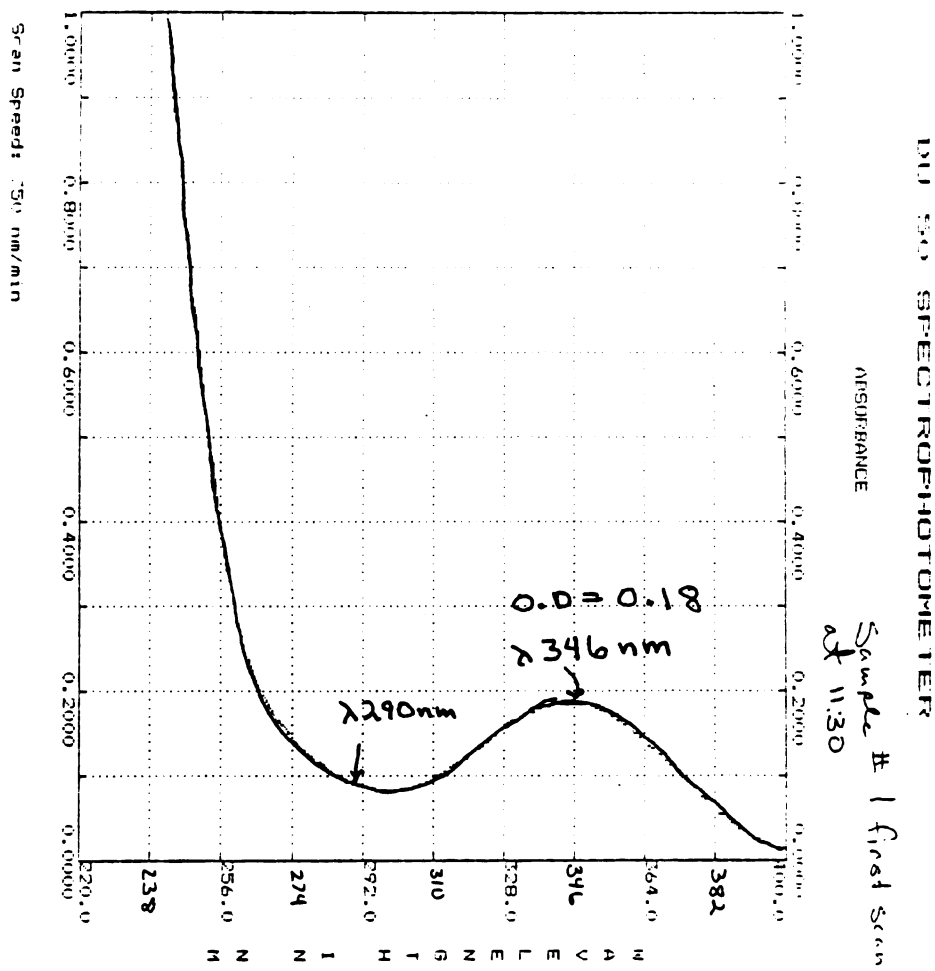

Figure 2-5. UV spectrum of a diluted aliquot (1:1000 in 1 M HCl aqueous), taken immediately after dilution on a spectrometer which had not been allowed its full warm-up period.

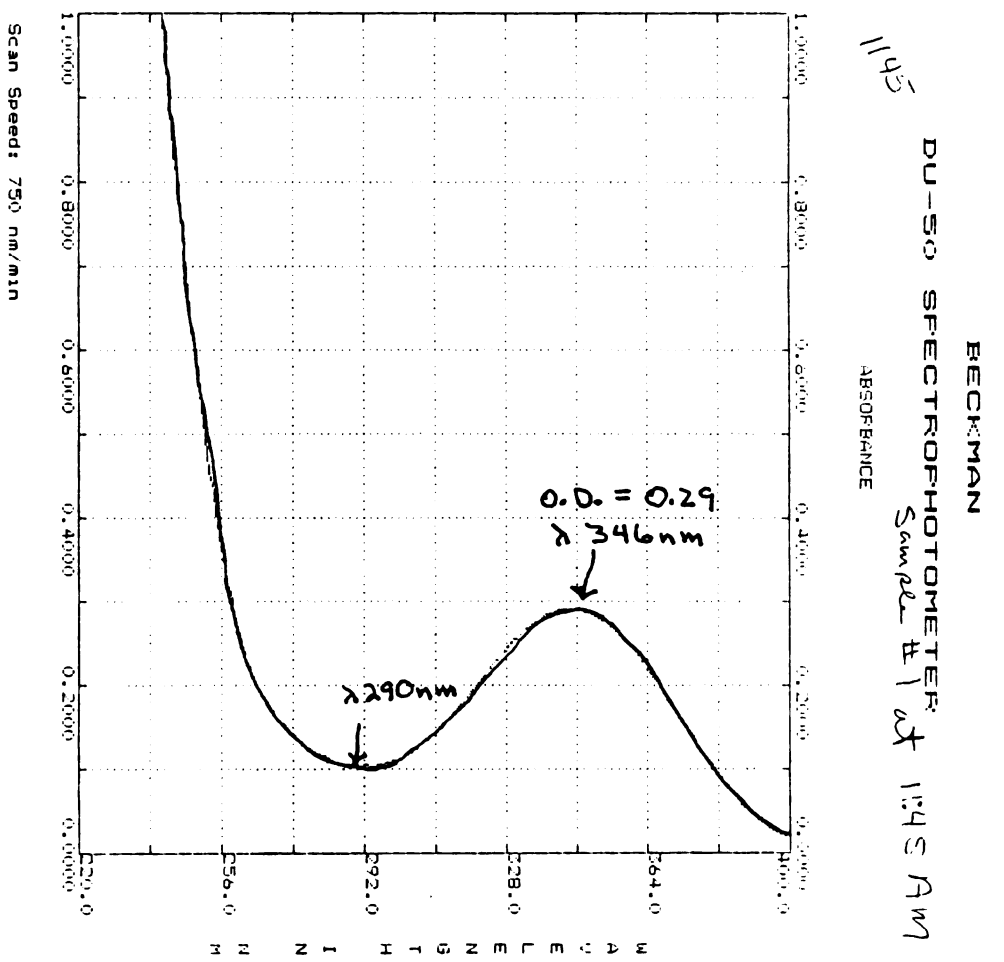

Figure 2-6. UV spectrum of the same solution as in Figure 2-5, taken 15 minutes after dilution. Spectrometer was fully warmed-up.

Table 2-3. The time-dependent Change in UV absorbance of a sample removed from a Grignard reaction and diluted 1:1,000 in 1 M aqueous HCl.

Age of sample in minutes	Absorbance at 345 nm	% Theoretical Absorbance	Absorbance at 256 nm
0	0.19	22%	0.40
15	0.29	35%	0.36
30	0.31	37%	0.35
45	0.34	41%	0.34
105	0.65	78%	0.28
165	0.93	114%	0.14
185	0.97	116%	0.20
210	1.06	127%	0.18
225	1.11	133%	0.16
340	1.32	158%	0.10

UV information extracted from successive scans of a capped sample at 220-400 nm, obtained on a Beckman DU-50 UV-VIS spectrometer.

This same information is presented in graphic form in Figure 2-7. It was found that absorbance at 345 nm continued to rise over the 5 hour period while absorbance at 256 nm continued to drop at a slower rate. Later in the reaction, a second sample was removed, diluted and its absorbance followed over time, it displayed similar behavior though it was followed for a shorter period, proving that this phenonmenon was reproducible. We can speculate that one possible source of the changing UV absorbance for a diluted Grignard sample may arise from equilibration between the protonated forms of dihydropyridine **14**.

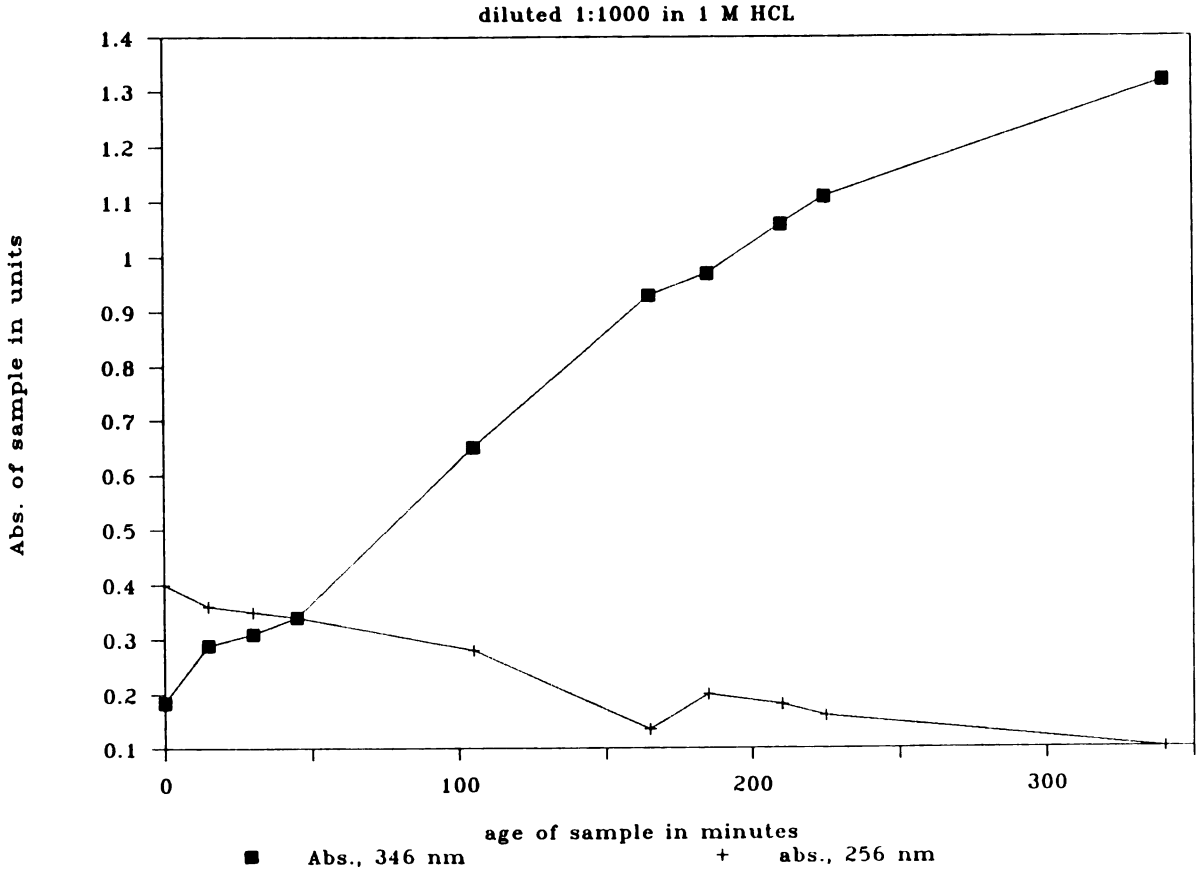

Figure 2-7. Graph of the change in UV absorbance with time of a sample of a Grignard reaction mixture, diluted 1:1000 in aqueous 1 M HCL. ■ denotes absorbance at 346 nm, + denotes absorbance at 256 nm. Data extracted from sequential UV scans from 225 to 400 nm.

As illustrated in Scheme 2-5, two protonated forms of **14** are possible including the dihydropyridium **15**, expected to have a UV max at 345 as well as the dihydropyridinium **16**. Dihydropyridinium **16** might be expected to exhibit a maximal UV absorbance at approximately 248 nm, similar to that of MPTP, since both compounds contain the same styrene type UV chromophore. Thus the changing UV absorbance of the Grignard sample diluted in aqueous HCl may be explained by initial formation of both dihydropyridinium species **15** and **16** followed by a time dependent equilibration of **16** to **15**. The greater thermodynamic stability of **15**, attributed to the conjugated diene system not shared by **16**, may provide the driving force for such an equilibration. Possibly the formation of **15** is favored by dilution into 1 M HCl in methanol which might account for the higher absorbance at 345 nm observed for those solutions. The stability of a sample diluted in acidic methanol was not determined, thus this explaination must remain speculation.

Due to the complications reported above, it was concluded that the UV absorbance at 345 nm of a diluted Grignard reaction aliquot was not a reliable indication of the progress of the Grignard reaction. Instead, the absorbance at 290 nm (the UV max of MPP^+) was used to gauge consumption of the starting pyridinium ion as an estimate of reaction progress.

As before, samples of the Grignard reaction were removed after complete dissolution of the starting material. If the spectrum of a diluted sample showed baseline or minimal absorbance at 290 nm, accompanied by a UVmax at 345 nm (indicating presence of the dihydropyridinium ion **15**), the Grignard reaction was judged complete.

As depicted in Scheme 2-5, the next step of our projected reaction sequence for synthesis of **17** and **18** required the formation of the protonated dihydropyridinium ions **15** and **16** which required aqueous conditions. To achieve this (and at the same time inactivate any unreacted methyl magnesium bromide), the Grignard reaction mixture was quenched by the slow and careful addition of aqueous HCl. The quenching reaction was exothermic and produced copious amounts of gas. After the quench reaction had subsided, sodium cyanoborohydride ($NaCNBH_3$), an acid stable borohydride reducing agent, was used in the reduction step. After several hours, work-up conditions for the resulting reaction mixture (made basic by addition of $NaCNBH_3$) were tested on several small aliquots of the reaction mixture. The first test aliquot was acidified with aqueous HCl and extracted with dichloromethane using the rationale that the expected protonated tetrahydropyridine products, **17**·HCl and **18**·HCl should remain in the aqueous phase while any unreacted pyridinium starting material should

be extracted into the dichloromethane. (We later found that this assumption was incorrect and that the relatively polar solvent dichloromethane is actually a good solvent for hydrochloride salts of **17** and **18**). According to the results obtained by UV (prior to quenching the reaction), the starting material had been consumed. It was expected that TLC of the dichloromethane extract should show only a small amount of the MPP^+, if anything. A TLC solvent system (acetonitrile:dichloromethane, 1:1) had been developed which gave good mobility for MPP^+ (Rf 0.33) so that we expected to be able to identify unreacted MPP^+. However, the results of TLC of the dichloromethane extract of the acidified aliquot gave a strong new spot with Rf 0.16 in addition to 6 other minor spots. A second test aliquot was removed from the reaction mixture and further basified with sodium carbonate. TLC of a dichloromethane extract of this aliquot gave the same TLC results as had been seen with the acidified aliquot except with less intense spots implying a lower extraction efficiency from the basified aqueous aliquot. Based on this information, the remainder of the Grignard reaction mixture was acidified and extracted with dichloromethane to yield a yellow oil. Confirmatory TLC of the oil indicated the presence of 1 major component (Rf 0.16) and 6 trace components. In order to obtain an 80 MHz ^1H NMR of this crude product, the oil was diluted with deuterated

chloroform ($CDCl_3$), however immediately on dilution, a white crystalline material began to precipitate from the diluted oil. The crystals were filtered, washed with chloroform and dried for analysis. The remaining diluted yellow oil, now a mother liquor, was evaporated to recover the oil for analysis.

The crystalline solid was first analysed by 80 MHz ^1H NMR (CD_3CN) (Figure 2-8) which identified the compound as the 1,2-dimethyl substituted pyridinium ion **60**. The key identifying signals were found at 2.79 ppm (3H) and at 4.16 ppm (3H) which corresponded to the C_2-CH_3 and N-CH_3 protons, respectively. Comparison of this spectrum with that of MPP^+ (Figure 2-9) gave evidence that the methyl substitution had occured at C_2 since one of the protons alpha to the nitrogen atom (signal at 8.9 ppm) was missing in the spectrum of **60**. The material was obtained in 7% yield (73.7 mg)

The contents of the yellow oil, (still showing multiple components by TLC), were also analysed by NMR but gave rise to a complex spectrum which remained uninterpreted at that time (Figure 2-10)

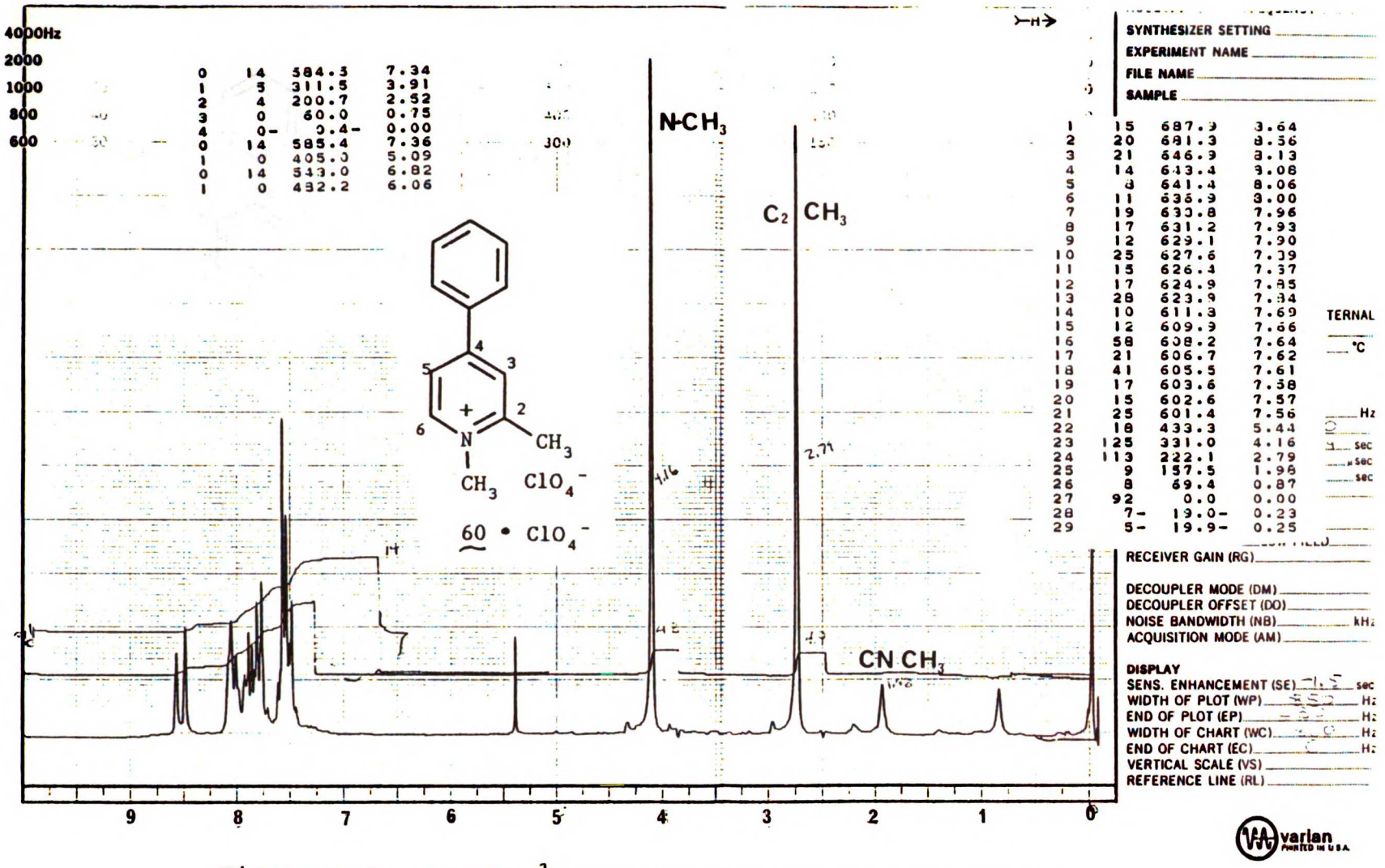

Figure 2-8. 80-MHz ^1H NMR (CD_3CN) spectrum of white crystalline solid obtained from Grignard reaction identified as 1,2-dimethyl-4-phenylpyridinium ion (**60**).

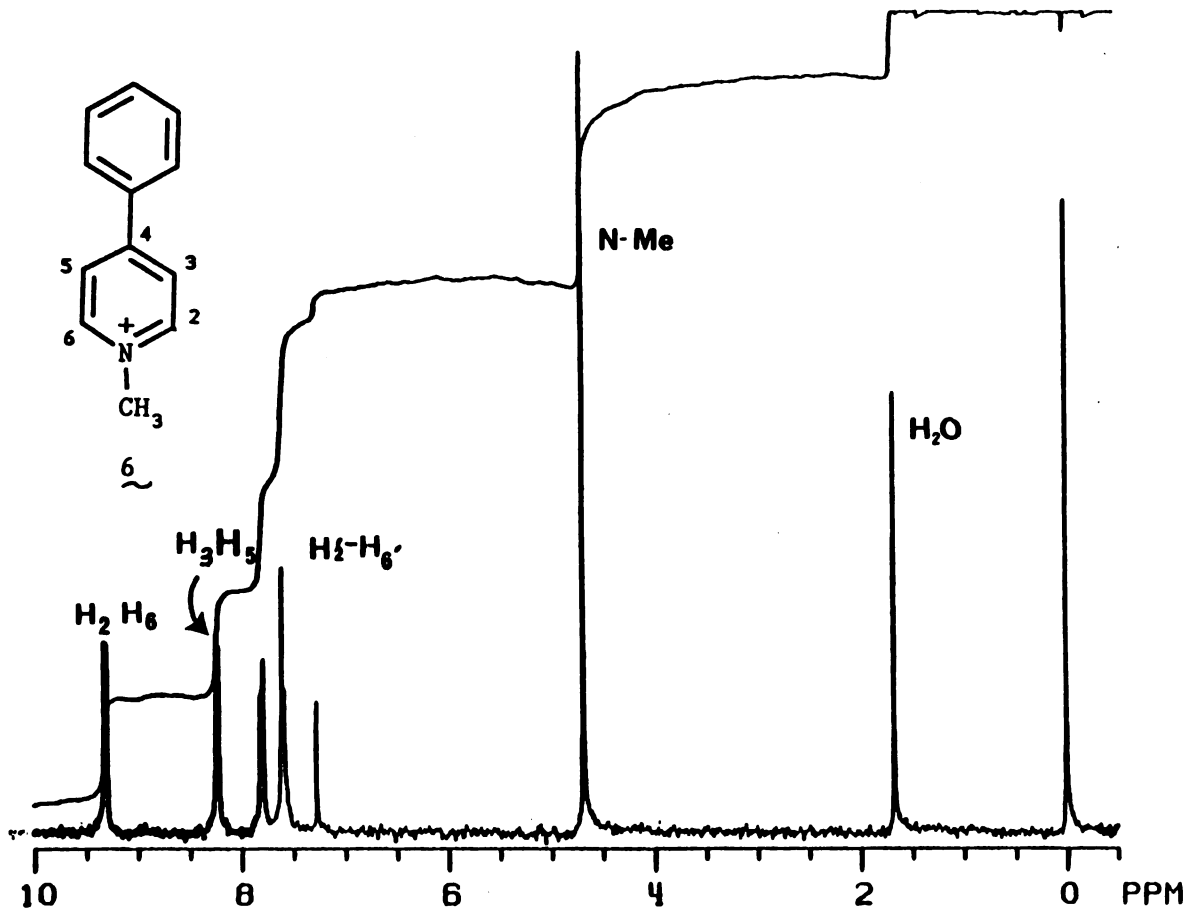

Figure 2-9. 240-MHz ^{1}H NMR ($CDCl_3$) spectrum of 1-methyl-4-phenylpyridinium iodide (**6**)

Figure 2-10. 80-MHz ^{1}H NMR ($CDCl_3$) spectrum of yellow oil remaining after crystallization of **60**.

The isolation of the methyl substituted pyridinium ion **60** was unexpected from the reaction sequence above (Grignard reaction followed by $NaCNBH_3$). It was believed that oxidation of the highly reactive dihydropyridine **14** (refer to Scheme 2-5) had occured before or during the protonation step which had preceded addition of the $NaCNBH_3$.

In order to investigate this possibility, a second Grignard reaction was performed and quenched with aqueous HCl but the reduction step was omitted. Again. TLC of the dichloromethane extract indicated formation of at least 7 products and again the 2-methyl substituted pyridinium ion **60** was isolated (~36%) from the product mixture. Recrystallization of this product from acetonitrile resulted in beautiful needle type crystals. The 240 MHz ^1H NMR ($CDCl_3$) spectrum (Figure 2-11) of the sample indicated hydration (H_2O signal at 1.50 ppm). Extended heating (65 ^oC) under high vacuum did not result in production of an anhydrous sample. However the size of the H_2O peak in the NMR spectrum of **60** could be reduced by D_2O exchange.

Further evidence for the characterization of this compound as the 1,2-dimethyl-4-phenyl-pyridinium ion **60** came from the LSI-mass spectrum (Figure 2-12) obtained using a thioglycerol matrix and a Kratos MS-50 mass spectrometer fitted with a cesium ion emitting gun. The cationic nature of **60** led to its' direct desorption and

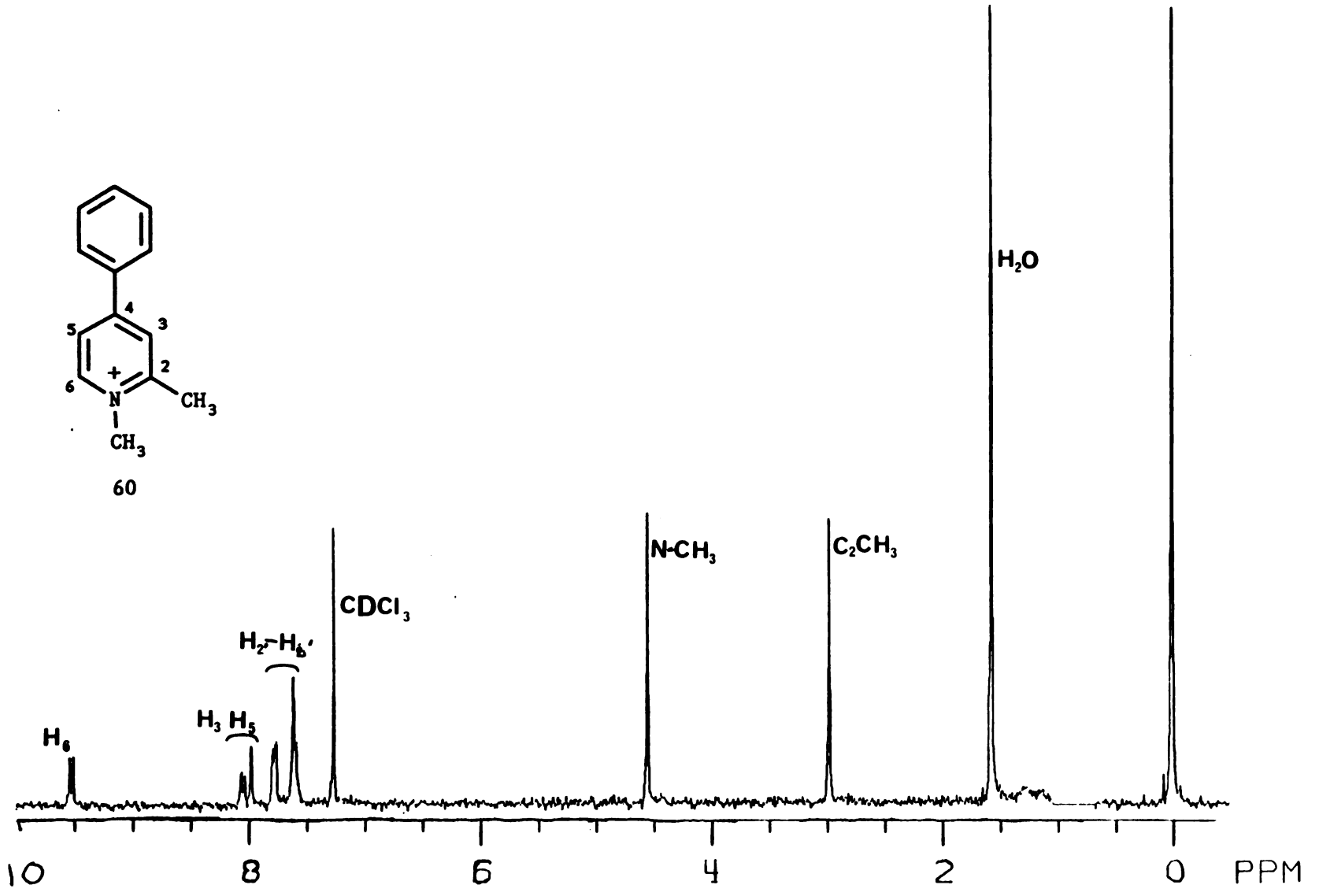

Figure 2-11. 240-MHz ^{1}H NMR ($CDCl_3$) spectrum of a hydrated sample of 1,2-dimethyl-4-phenylpyridinium ion (60).

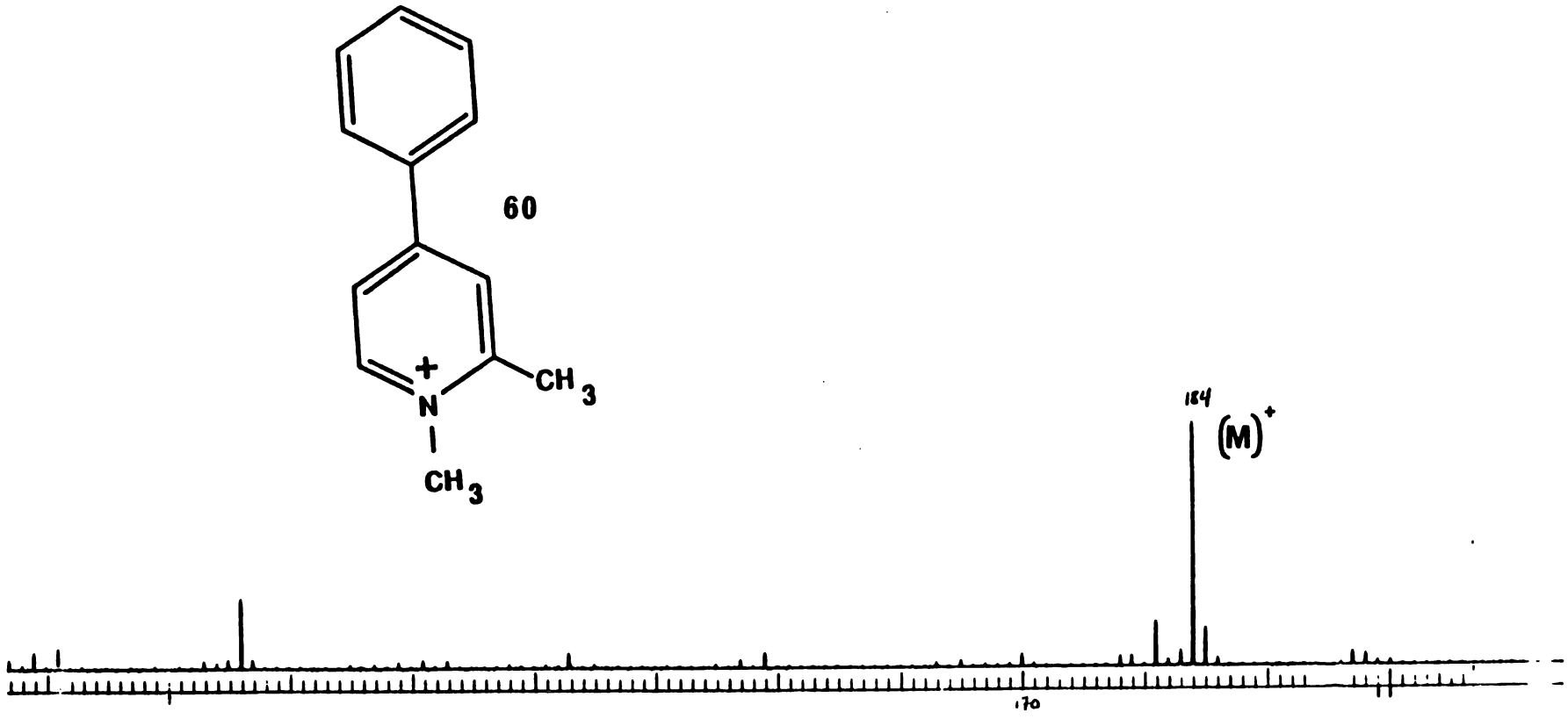

Figure 2-12. Liquid Secondary Ionization-Mass Spectrum of 1,2-dimethyl-4-phenylpyridinium ion (**60**) using thioglycerol as matrix.

eventual detection. This low energy method of vaporization causes very little fragmentation of the analyte. The major ion observed in the LS-MS spectrum of the product was at m/e 184 which corresponded to the molecular ion of this cationic species.

Finally, the maximal UV absorption for **60** was determined to be 284 nm, (extinction coefficient 17,500), which is very similar to that of MPP^+ (UVmax 290 nm, ext. coeff. 18,000), a characteristic chromophore for the 4-phenyl substituted pyridinium compounds. The possibility of hydration (indicated in the NMR spectrum discussed above) proved to be a problem when the sample was sent for microanalysis. In addition to hydration which complicates the interpretation of results from microanalysis, the identity of the counter ion for the pyridinium species **60** derived from this reaction sequence and workup was in question. The starting material MPP^+ had entered the reaction mixture as an iodide salt. It had then been treated with methyl magnesium bromide allowing the possibility of conversion to a bromide salt. The work-up of the reaction then included treatment with hydrochloric acid which allowed the possibility of formation of the chloride salt. Thus there was no way to predict which halide salt of the pyridinium species had been isolated from the reaction mixture and no guarentee that a single pure salt had been isolated as opposed to a mixture of iodide, bromide and chloride salts. A sample

of the compound was dried under high vacuum at 65 ^{o}C for twelve hours to remove as much water as possible and subjected to microanalysis. The microanalysis results (Found: C, 48.19%; H, 4.88%; N, 4.30%) were consistant with neither a simple iodide salt (calc. C, 50.18%; H, 4.53%; N, 4.50%) nor the iodide hydrate (calc. C, 47.43%; H, 4.9%; N, 4.26%). The results were even less likely to be consistant with the bromide or chloride salts of **60**, which, owing to their lower molecular weights, should have given higher percentages of carbon in the microanalysis than would the iodide salt. The unidentified halide counter-ion made calculation of the molecular weight for **60** isolated from this reaction difficult, thus yields could only be estimated. Estimates were made based on the molecular weight calculated for the iodide salt (the heaviest of the possible halides) in order to give the most conservative estimate. Yields ranged from 13% in the case discussed above to 38% in the best example. Furthermore, the halide salt isolated as discribed above was both hygroscopic and prone to air-oxidation causing the development of a red tinge due to the formation of molecular iodine after exposure to air for short periods of time. In order to overcome these problems, the mixed halide salt of **60** was converted to a perchlorate salt by treatment with aqueous silver perchlorate. The perchlorate salt formed beautiful opalescent needles (39% yield after

recrystallization from acetone) which were not hygroscopic and were analytical for $C_{13}H_{14}N \cdot ClO_4$. They gave a sharp melting point at 160-161 ^{o}C. Conversion to the perclorate salt did not change either the UV or NMR spectrum of the compound, however the perchlorate salt crystals were difficult to solubilize in aqueous media. The eventual preparation of solutions of **60**$\cdot ClO_4$ for biological testing therefore required sonication to ensure that the compound was fully in solution.

Up to this point no real effort had been made to characterize the other 4-6 products (as evidenced by TLC) of the Grignard reaction. An aborted effort at identification included the evaporation of the acetone and acetonitrile mother liquors from the recrystallizations described above to give a highly colored oil which was chromatographed over silica gel with acetonitrile/chloroform, (1:19). The 65 fractions which were collected from this process were all very highly colored ranging from red to yellow. However, despite the color, each fraction was too dilute for analysis by TLC giving no UV active spot on silica gel. The colors of each fraction darkened and changed with time indicating probable instability which further discouraged my attempt to identify the components. Thus the compounds were not identified at this time. Instead the synthesis of **17** and **18** via sodium borohydride reduction of **60** was pursued.

SYNTHESIS OF 1,2-DIMETHYL-4-PHENYL-1,2,3,6-TETRAHYDROPYRIDNE (17) AND 1,6-DIMETHYL-4-PHENYL-1,2,3,6-TETRAHYDROPYRIDNE (18) VIA SODIUM BOROHYDRIDE REDUCTION OF 60

Purified 1,2-dimethyl-4-phenylpyridinium halide (**60**) obtained from the Grignard reaction reported above was treated with excess sodium borohydride in methanol at room temperature. After decomposition of unreacted sodium borohydride by the addition of water, the products were extracted with diethyl ether. The extracts were evaporated to give an oil which, when subjected to NMR analysis (Figure 2-13), indicated the presence of both **17** and **18**, the expected tetrahydropyridine products of reduction of **60**. Formation of both **17** and **18** had been expected based on the mechanism for this reduction, shown in Scheme 2-6, as proposed by Lyle et al. for the general reduction of pyridinium salts.[26] The first step of the reduction involves hydride ion attack at the least hindered electrophilic carbon atom, C_6, to form the dihydropyridine compound **63**. The uncharged dihydropyridine undergoes protonation at each of two sites, C_3 and C_5 resulting in the formation of isomeric dihydropyridinium species **64** and **19**. A second equivalent of hydride is then delivered to the new electrophilic site located at C_2 resulting in formation of tetrahydropyridines **17** and **18**.

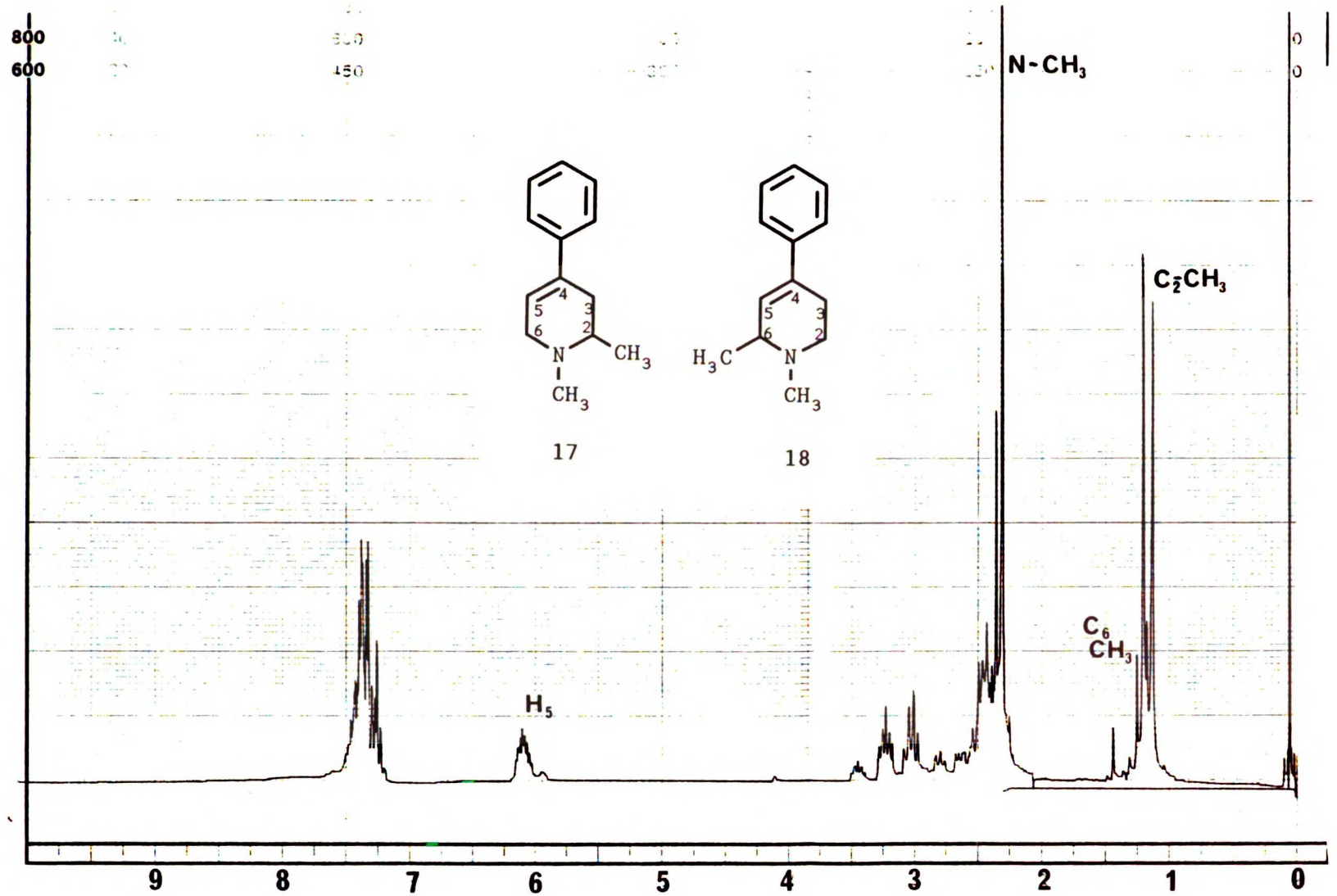

17

18

Figure 2-13. 80-MHz ^{1}H NMR (CD_3CN) spectrum of a mixture of **17** and **18**, the products of sodium borohydride reduction of **60**.

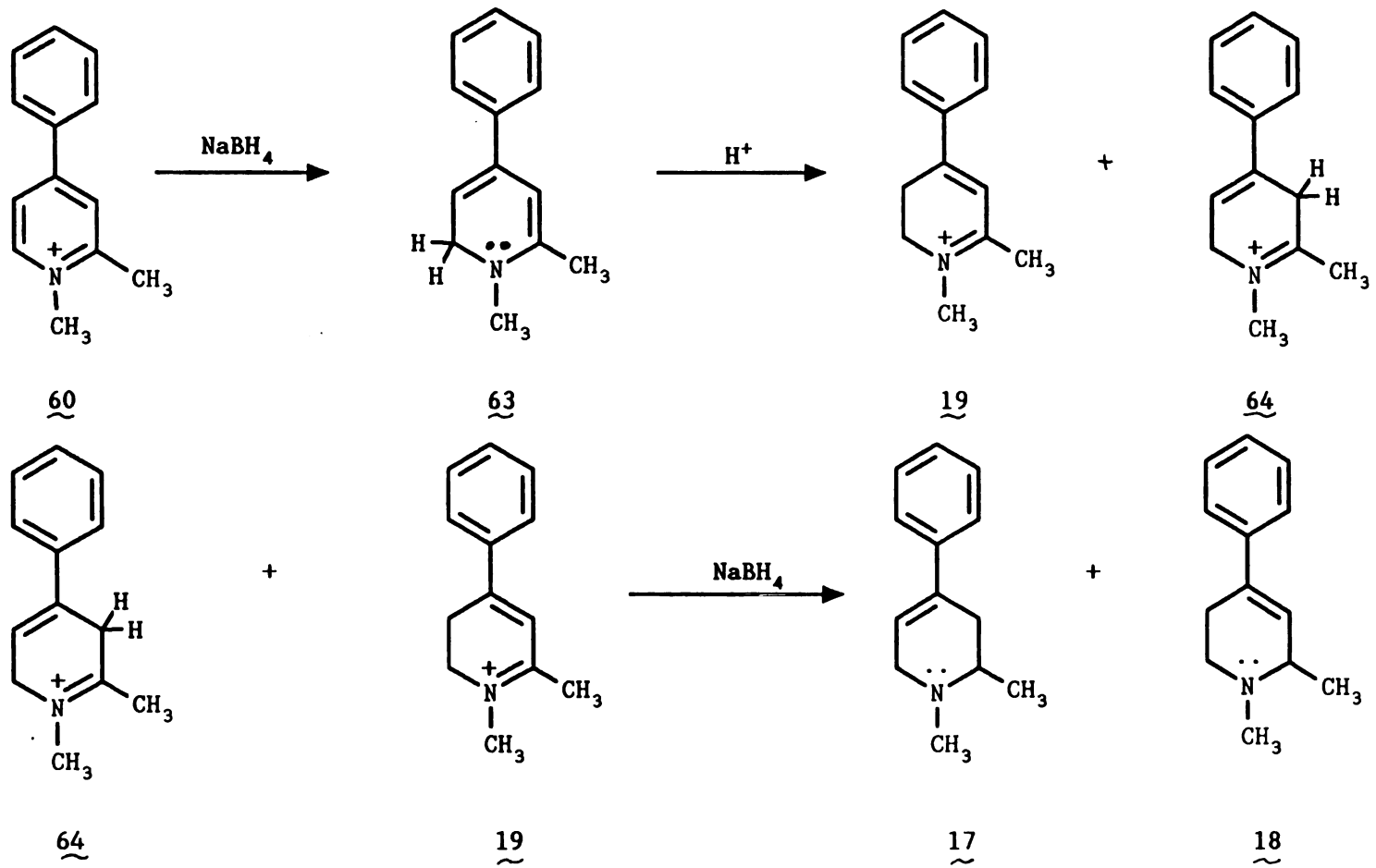

Scheme 2-6. Lyle's proposed mechanism for sodium borohydride reduction of substituted pyridinium ions, shown for reduction of 60

The spectrum shown in Figure 2-13 clearly shows both intense and weak signals corresponding to a major and minor product. The relative positions and peak heights of the signals gave an initial clue as to which of the tetrahydropyridines was the major product. One would have predicted the first order splitting pattern for a single product to give a doublet for the new C-methyl substituent. Instead an intense doublet at 1.1 ppm superimposed on a weaker doublet at 1.15 ppm was observed. The relative downfield position of the weaker doublet led to its assignment to the methyl proton signal of compound **18** since these protons will experience the deshielding effect of the allylic system.[130] Jackman has stated that an alkyl proton deshielded by a double bond in the beta position will experience a downfield shift of as much as 0.05 ppm which is consistant with the effect observed in this case.[130] Therefore, the more intense doublet at 1.15 ppm was assigned to the C-methyl signal of **17**, which was tentatively identified as the major product of the reaction. Identification of the signals produced by the H_6 and H_2 protons of compounds **18** and **17**, respectively, gave another indication of which of the two compounds was the major component of the reaction mixture. Their identification was based on the following: Similar to the effect described above, a deshielding effect is also experienced by the allylic proton H_6 proton of compound **18**. Jackman has stated that

allylic protons will experience a downfield shift of as much as 0.1 ppm compared to chemically similar but non-allylic protons.[130] Thus the signal for H_6 of compound **18** should be found at a position in the spectrum which is downfield relative to H_2 of compound **17**, which for this case represents the chemically similar but non-allylic proton. Schoolery, in his analysis of the ^1H NMR spectrum of 1-methyl-1,2,3,6-tetrahydropyridine, has shown that the combination of allylic character plus the deshielding effect of its neighboring nitrogen atom combine to make the H_6 proton of this less substituted tetrahydropyridine the most downfield signal (3.33 ppm) of the aliphatic proton signals in the spectrum (1.63-3.33 ppm).[132] The most downfield aliphatic signal of the spectrum of our putative mixture of **17** and **18**, a multiplet at 3.45 ppm, was one of the less intense signals of the spectrum. We assigned this multiplet to the H_6 proton of compound **18** based on Schoolery's work. Its small peak height again supported the concept that compound **18** was a minor component of the product mixture. The H_2 proton signal of compound **17** was positively identified using a double resonance experiment. The rationale for this experiment was based on the fact that the newly introduced C_2 methyl group of compound **17** and the non-allylic H_2 proton are vicinally coupled, and being non-allylic should, theoretically, give signals which are upfield in the NMR spectrum relative to the

corresponding vicinally coupled homoallylic C_6-methyl and allylic H_6 signals of **18**. In the double resonance experiment, the NMR sample was irradiated at a frequency corresponding to the intense doublet (1.1 ppm) to decouple the signal arising from the C_2-methyl group of **17**. Theoretically only the the signal arising from H_2 of **17** should be simplified in the resulting 80-MHz ^1H NMR spectrum (Figure 2-14). Indeed, the only change detected in the decoupled spectrum was in an intense multiplet integrating for 1 proton at 2.45 ppm which simpified and became more intense. Thus the signal for the H_2 proton was identified as the multiplet at 2.45 ppm by both its chemical shift, (the most upfield of the aliphatic protons) and by its behavior in the double resonance experiment. Its intensity, which indicated that it belonged to the major component of the product mixture gave further evidence that compound **17** was the major compound while **18** was the minor component.

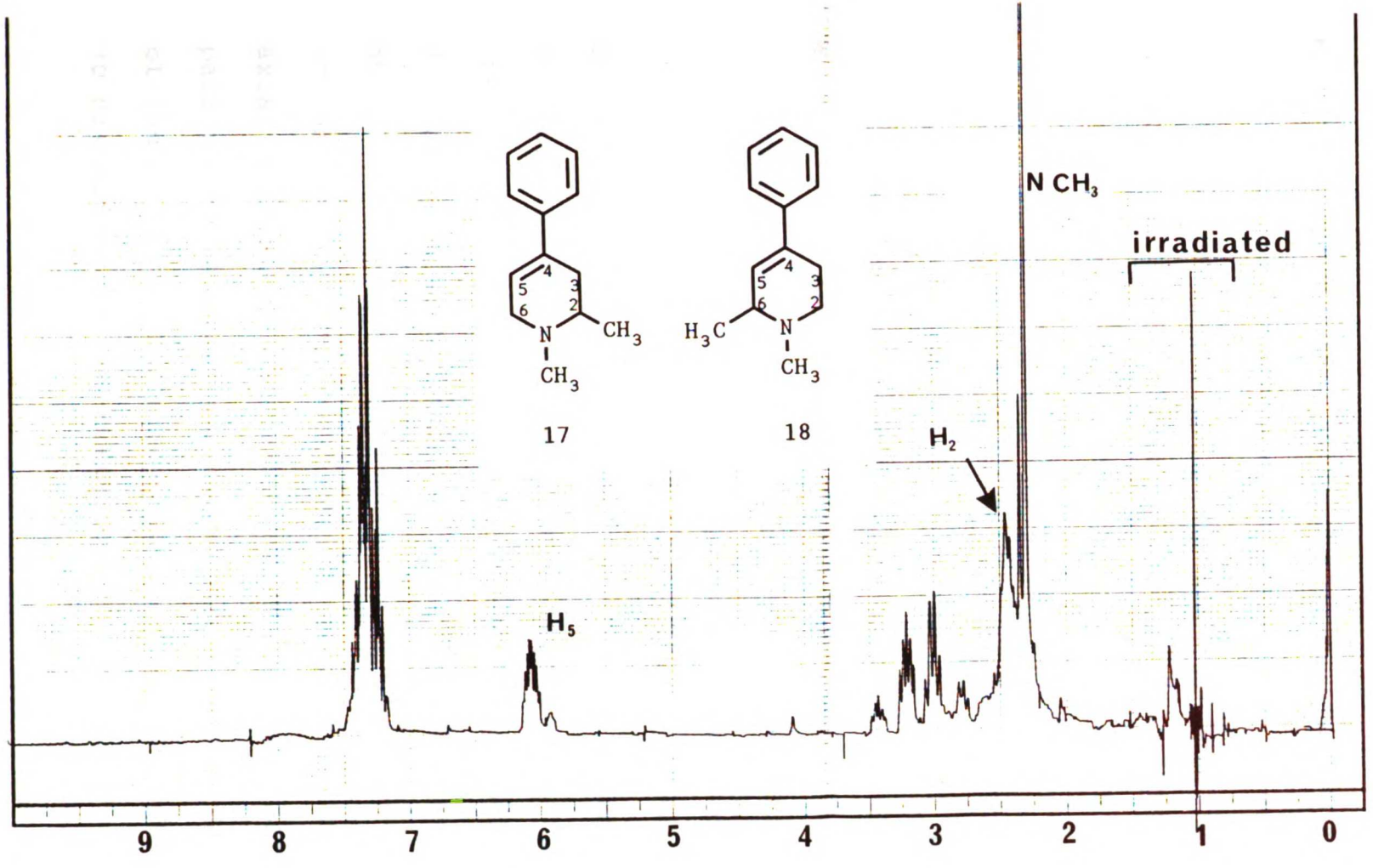

Figure 2-14. 80-MHz ^1H NMR (CD_3CN) spectrum of the same sample as in Figure 2-13, irradiated at 1.1-1.25 ppm to decouple the C_2-CH_3 and C_6-CH_3 protons.

Another indication that the products arising from sodium borohydride reduction of **60** are a mixture of tetrahydropyridines comes from the appearance of the olefinic region of the spectrum in Figure 2-13. The olefinic proton in a pure product should give one signal near 6.0 ppm. This mixture displayed two signals (5.95 ppm and 6.05 ppm) in the olefinic region. The smaller signal at 5.95 ppm was assigned tentatively to the H_5 proton of compound **18** because this vinylic proton would experience a shielding effect by the C_6-methyl and would be expected to fall at a position upfield relative to the H_5 of **17**.[131] In order to obtain more definitive ^1H NMR data we examined this sample at 240 and 500 MHz (Figs. 2-15 and 2-16, respectively). At 500 MHz field strength the signal separation is much better due to the higher **delta** v/J ratio acheived with the 500 MHz instrument. In addition the narrow band width decoupler of the 500 MHz spectrometer (General Electric GN-500) made selective decoupling of each proton easier. The features of the 500-MHz ^1H NMR ($CDCl_3$) spectrum of the product mixture are different from the 80-MHz ^1H spectrum in that the H_6 axial and equatorial protons of **17** are displayed as a pair of symmetrical doublets at 3.2 and 3.05 ppm. Each of the H_6 proton resonances are split into doublets (ca. 30 hz) due to geminal coupling.

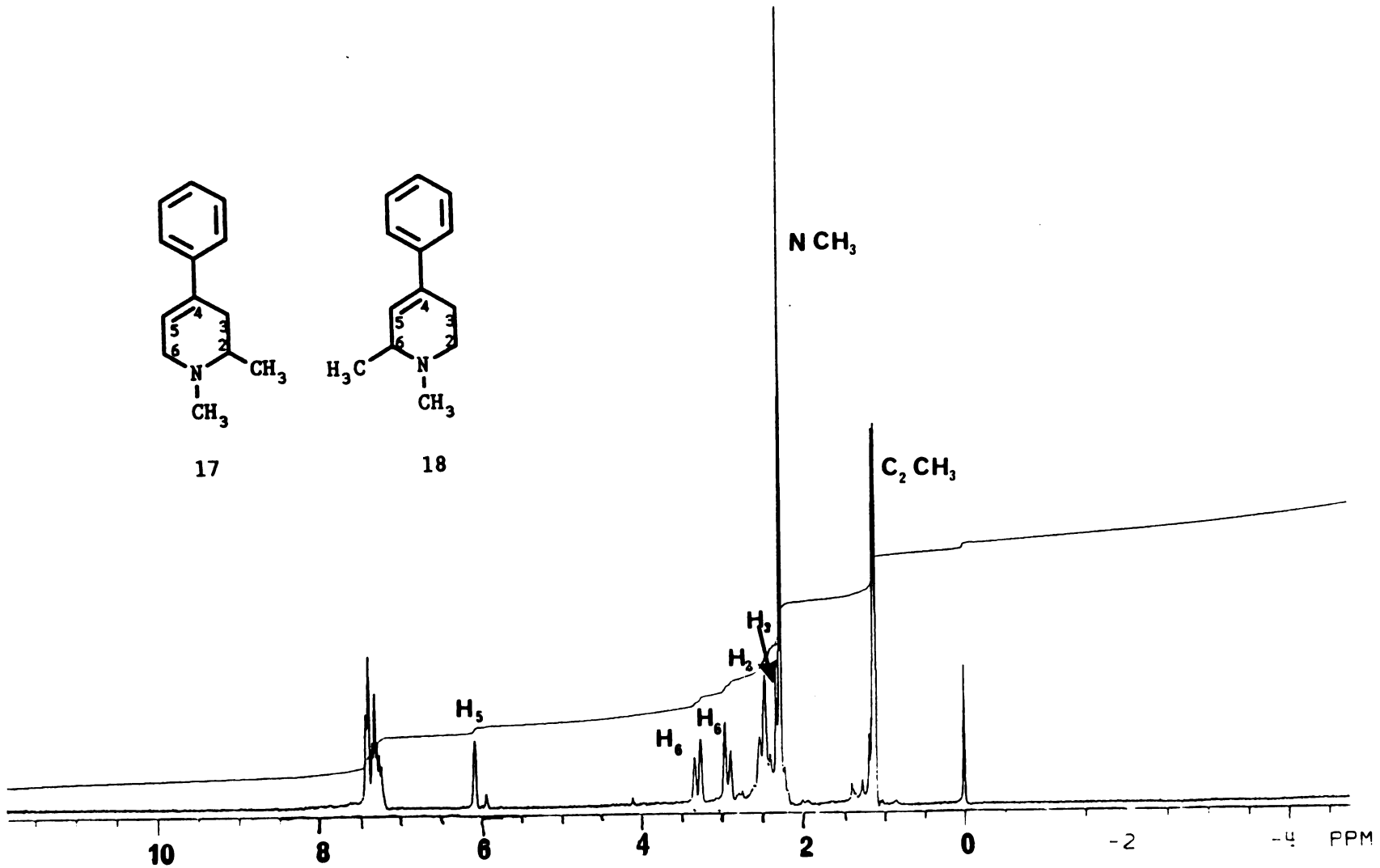

17 18

Figure 2-15. 240-MHz ^1H NMR (CD_3CN) spectrum of a mixture of **17** and **18**, the products of sodium borohydride reduction of **60**.

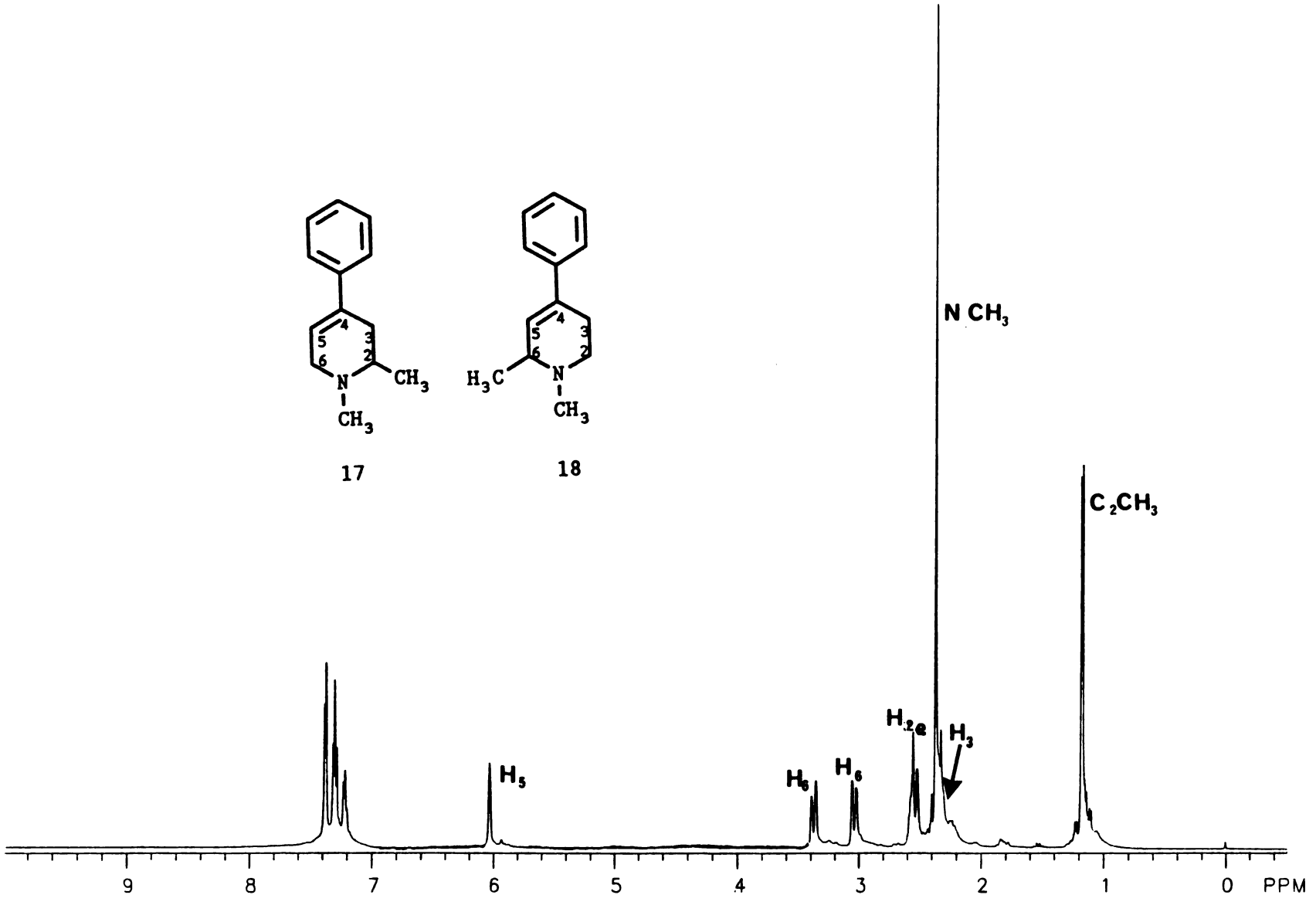

Figure 2-16. 500-MHz ^{1}H NMR ($CDCl_3$) spectrum of a mixture of **17** and **18**, the products of sodium borohydride reduction of **60**.

In double resonance experiments, irradiation of the sample with the frequency of either the H_6 axial or equatorial proton (3.4 and 3.05 ppm, respectively) results in simplification of the non-irradiated H_6 signal to a singlet. The geminal coupling of the H_6 axial proton with the H_6 equatorial proton and vice versa dominates the splitting pattern of these protons in the 500-MHz ^1H NMR spectrum.

Assignment of the multiplet at 2.55 ppm as the signal for H_2 of **17** was confirmed in another set of double irradiation experiments similar to those described earlier for the 80-MHz specta, which took advantage of the coupled relationship of the H_2 proton of **17** and C_2-methyl protons of **17**. In contrast to the case with the 80-MHz instrument, it was possible, with the 500-MHz instrument, to selectively irradiate the sample with a frequency corresponding to the H_2 proton (2.55 ppm) with minimal overlap into the H_3 and H_6 proton signal regions. The result was complete simplification of the C_2-methyl doublet for compound **17** into a singlet. Irradiation of no other aliphatic proton signal (including those at 3.4, 3.05 and 2.25 ppm) gave such a simplification. These results confirmed the identity of the signal at 2.55 ppm as that belonging to the H_2 proton of **17**. As was expected for this proton, its spectral characteristics indicated that it was strongly coupled to the C_2-methyl

protons but not allylic, consistant with the relatively upfield position for its signal in the ^{1}H NMR spectrum.

The mixture of tetrahydropyridines obtained from the reduction of **60** were not separable on TLC (silica gel plates) in either of two solvent systems [1) methanol/chloroform. 1:19; 2) ethyl acetate/hexame 1:9) or on HPLC (Ultrasil-CX caton exchange column; mobile phase acetonitrile/buffer, 2:3, where buffer was 0.1 M acetic acid, 0.05M triethylamine hydrochloride adjusted to pH 2.3 with formic acid, flow rate 1.5 mL per minute). Thus the ^{1}H NMR spectra were the best evidence that the reaction had given amixture of products as had been expected according to the work by Lyle. [26] The UV spectrum of the mixture of tetrahydropyridines was obtained during HPLC using a Hewlett-Packared 1040A diode array detection system and exhibited a UVmax at 243 nm similar to that of MPTP (240 nm) as was expected for the tetrahydropyridine chromophore. A crude estimate of the ratio of products **17** (ca. 76%) and **18** (ca. 24%), could be obtained from the ratio of NMR peak heights of the 2- and 6- methyl doublets in the original 80-MHz ^{1}H NMR spectrum (Figure 2-13).

Thus the reduction of **60** with sodium borohydride on a small scale (ca 100 mg) had given the desired products **17** and **18** in 93% overall yield. We made no further attempt at this time to separate **17** and **18** since only a small amount of the mixture had been produced, but

instead refocused our attention on the Grignard reaction to obtain large quantities of **60** (for later reduction) and to identify the other products of the Grignard reaction. Ultimately, the utility of the ^{1}H NMR spectra described above was not limited to identification of the products of sodium borohydride reduction of **60** but also gave important structural information which aided in identification of the previously unidentified products of the methyl Grignard reaction on MPP^{+}.

RE-EXAMINATION OF METHYL GRIGNARD REACTION WITH MPP^{+}, DISCOVERY OF A DISPROPORTIONATION REACTION

We refocused our attention on the reaction of methyl magnesium bromide with MPP^{+}. We had evidence that attack of methyl magnesium bromide on MPP^{+} resulted in formation of dihydropyridine **14** which was detected as the protonated form **15**. Since many reports of the instability of alkyl substituted dihydropyridines such as **14** have appeared [133-136], we tentatively explained the formation of **60** as the product of an air catalyzed oxidation of dihydropyridinium **15** during the dichloromethane extraction of products from the HCl quenched Grignard reaction mixture. At this point it seemed useful to examine the Grignard reaction more closely to determine the exact point at which the oxidation leading to **60** had occured. It also seemed worthwhile to attempt to isolate the dihydropyridinium

ion **15** (the detected protonation product of **14**) since this methyl substituted analog of $MPDP^+$ was desired for toxicity evaluation. On a large scale, MPP^+ was allowed to react with excess methyl magnesium bromide in diethyl ether until the usual color change (from yellow to peach) was observed, and UV analysis (near baseline absorbance at 290 nm) indicated that the pyridinium starting material had been consumed. As usual aqueous HCl was added by syringe to maintain anaerobic conditions. An aliquot of the ether layer of the quenched reaction mixture was removed anaerobically for UV analysis after the quench procedure. The aliquot was diluted in ether rather than aqueous HCl and displayed both a UVmax at 350 nm as well as a strong absorbance at 280 nm. The new observation of absorbance at 280 nm introduced the possibility that the pyridinium compound **60** had been formed prior to extraction or introduction of air to the reaction mixture. The strong absorbance at 350 nm was tentatively assigned to the unprotonated dihydropyridine **14** although this assignment was later discounted (Meyers and Singh have shown that the closely related dihydropyridine species **65** exhibits a weak UV absorbance at 312 nm [137]). A larger aliquot of the ether layer of the quenched Grignard reaction was removed and immediately concentrated for examination with NMR spectroscopy. The concentrate rapidly changed color from a golden yellow to a dark brown before the NMR spectrum

could be obtained. However, addition of a few drops of DCl caused the color of the concentrate to brighten and stabilize. The resulting 240-MHz ^1H NMR spectrum (CD_3CN) (Figure 2-17) was extremely similar to spectra obtained from the mixture of tetrahydropyridines obtained via sodium borohydride reduction of pyridinium **60** (Figures 2-13, 2-15, and 2-16). The two characteristic olefinic peaks at 6.05-6.1 ppm were evident, though less well resolved in Figure 2-17 compared to the spectra of the reduction products (Figures 2-13, 2-15, and 2-16). Furthermore, the 1.2-1.4 ppm region of the spectrum in Figure 2-17 contained three distintive sets of doublets with the same coupling constant (6 Hz) found in the C_2-methyl and C_6-methyl doublets of compounds **17** and **18**, respectively. Four doublets might be expected on the basis of diastereomeric pairs formed on protonation of **17** and **18**. In this spectrum, three are visible with the fourth doublet hidden under superimposed signals (see later discussion on NMR characteristics of **17** and **18**).

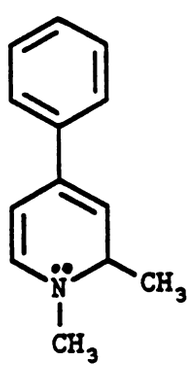

14

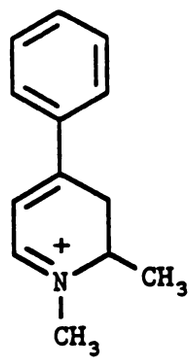

15

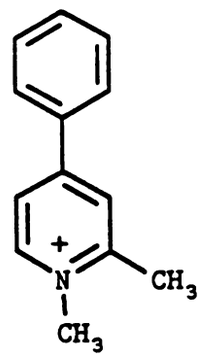

60

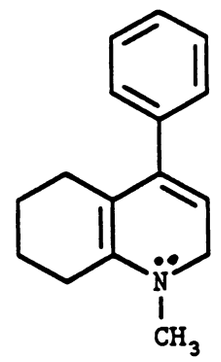

65

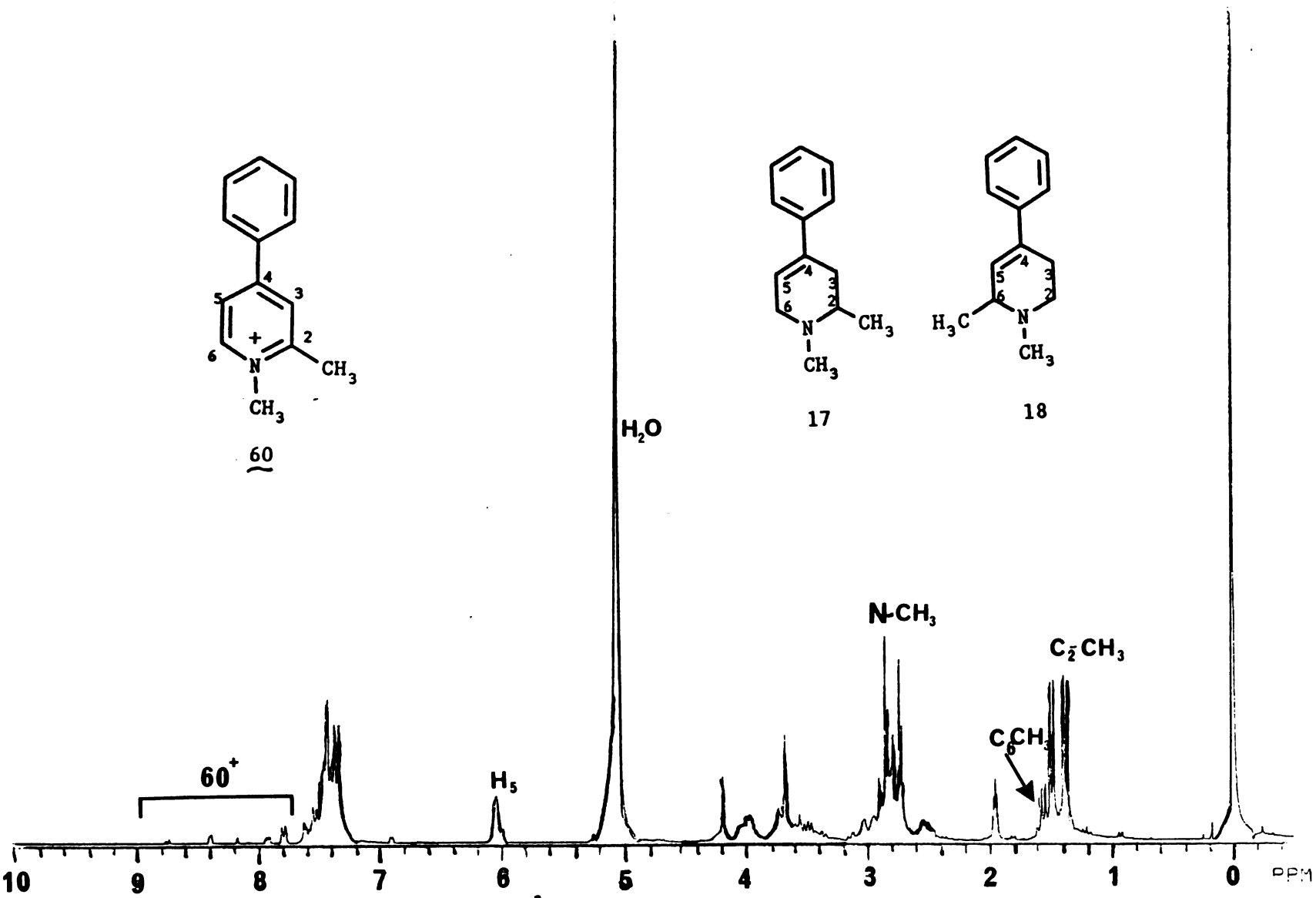

Figure 2-17. 240-MHz ^1H NMR (CD_3CN) spectrum of the ether layer from a quenched Grignard reaction showing the presence of tetrahydropyridines **17** and **18** and pyridinium ion **60**.

Thus the very important ^{1}H NMR spectrum displayed in Figure 2-17 immediately suggested the presence of tetrahydropyridine compounds.

The formation of tetrahydropyridine compounds along with the pyridinium compound **60** found on previous occasions was very strong evidence for the possibility of a disproportion reaction occuring after the formation of dihydropyridine **14**. Though at the outset we had not anticipated a disproportionation reaction of **14** we immediately recognized its high likelyhood based on the disproportionation observed with $MPDP^{+}$ and its conjugate base earlier reported by Chiba et al., [9] Peterson et al., [138] and Gessner et al [80].

In order to explore further the possibility that disproportionation of **14** and **15** had led to formation of the pyridinium **60** and tetrahydropyridines **17** and **18**, the remainder of the ether layer of the quenched Grignard reaction was separated from the aqueous layer (formed on addition of aqueous HCl) and evaporated to give a crude brown oil, the weight (5.5 g) of which accounted for approximately half of the pyridinium starting material. After dilution with anhydrous ether followed by a brief filtration over alumina to remove some highly colored contaminants, the dry ether solution was treated with gaseous HCl to precipitate the hydrochloride salts of a mixture of tetrahydropyridines **17** and **18** as a yellow powder (0.5 g, mp 180-184 ^{o}C). Due to difficulties

experienced in the NMR facility at this time only very poor quality spectra of this product were obtained (Figure 2-18). However the general features of the ^{1}H NMR spectrum corresponded to a mixture of tetrahydropyridines. Later higher quality spectra confirmed the identity of the yellow powder as a mixture of **17** and **18** HCl salts (Figure 2-19). Capillary column gas-chromatography of the free base of the mixture gave two peaks with retention times of 11.02 and 11.03 minutes, corresponding to 14% and 86%, respectively, of the mixture. GC-MS also gave two peaks in the total ion current chromatogram and mass spectra obtained from each of these peaks displayed a molecular ion at m/e 187 which corresponded to the methyl-substituted tetrahydropyridines **17** and **18** (Figures 2-20 and 2-21, respectively). The mixture of hydrochloride salts, isolated as a stable yellow powder, was stored while attention was turned to the aqueous layer of the original reaction mixture which should have contained the pyridinium ion **60** if disproportionation had occured. For a description of the final purification and characterization of pure **17** and **18** see the sections on separation of **17** and **18** and on synthesis of **18** below.

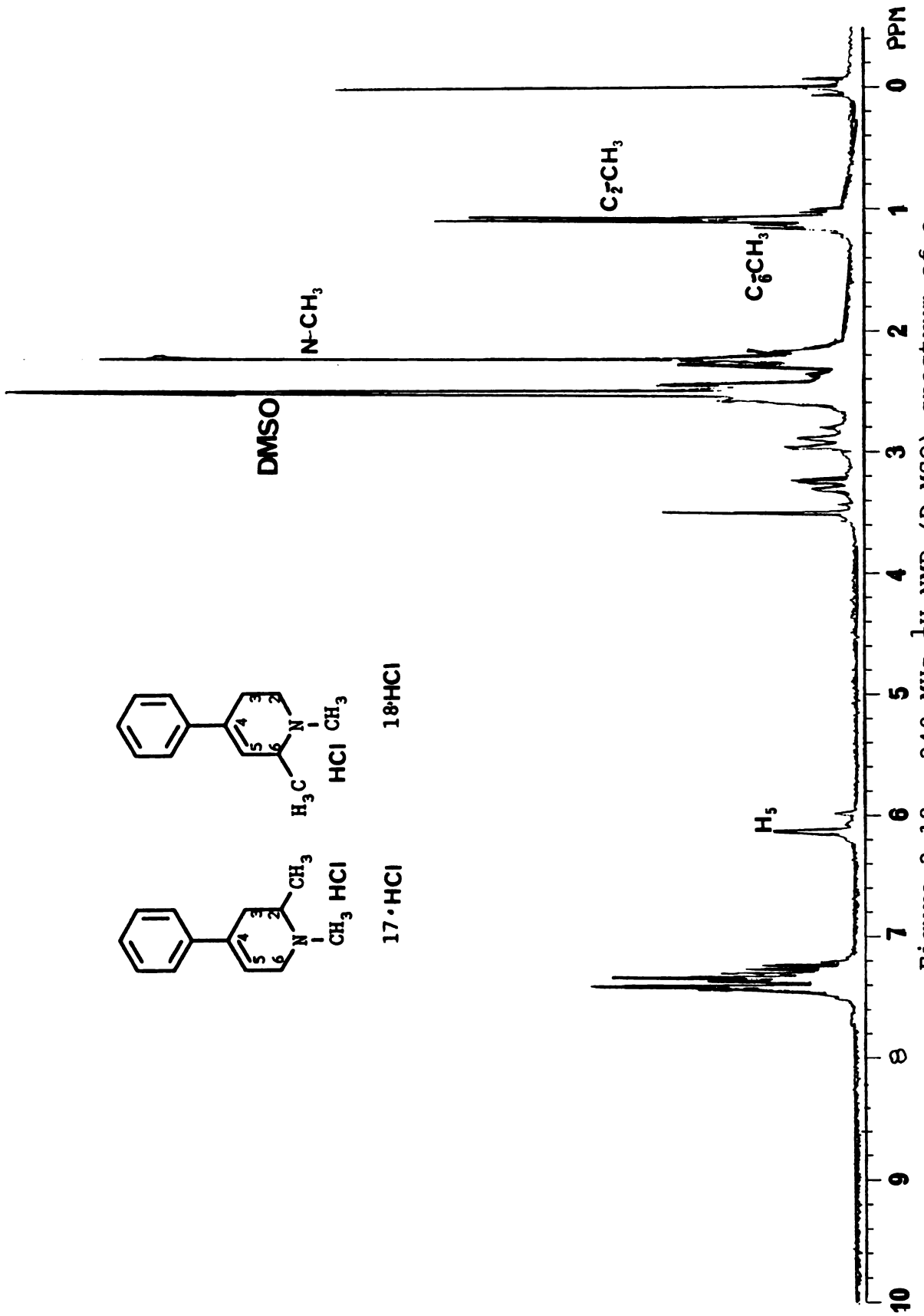

Figure 2-18. 240-MHz ^{1}H NMR (D_6MSO) spectrum of a crude mixture of tetrahydropyridines **17**·HCl and **18**·HCl obtained from disproportionation.

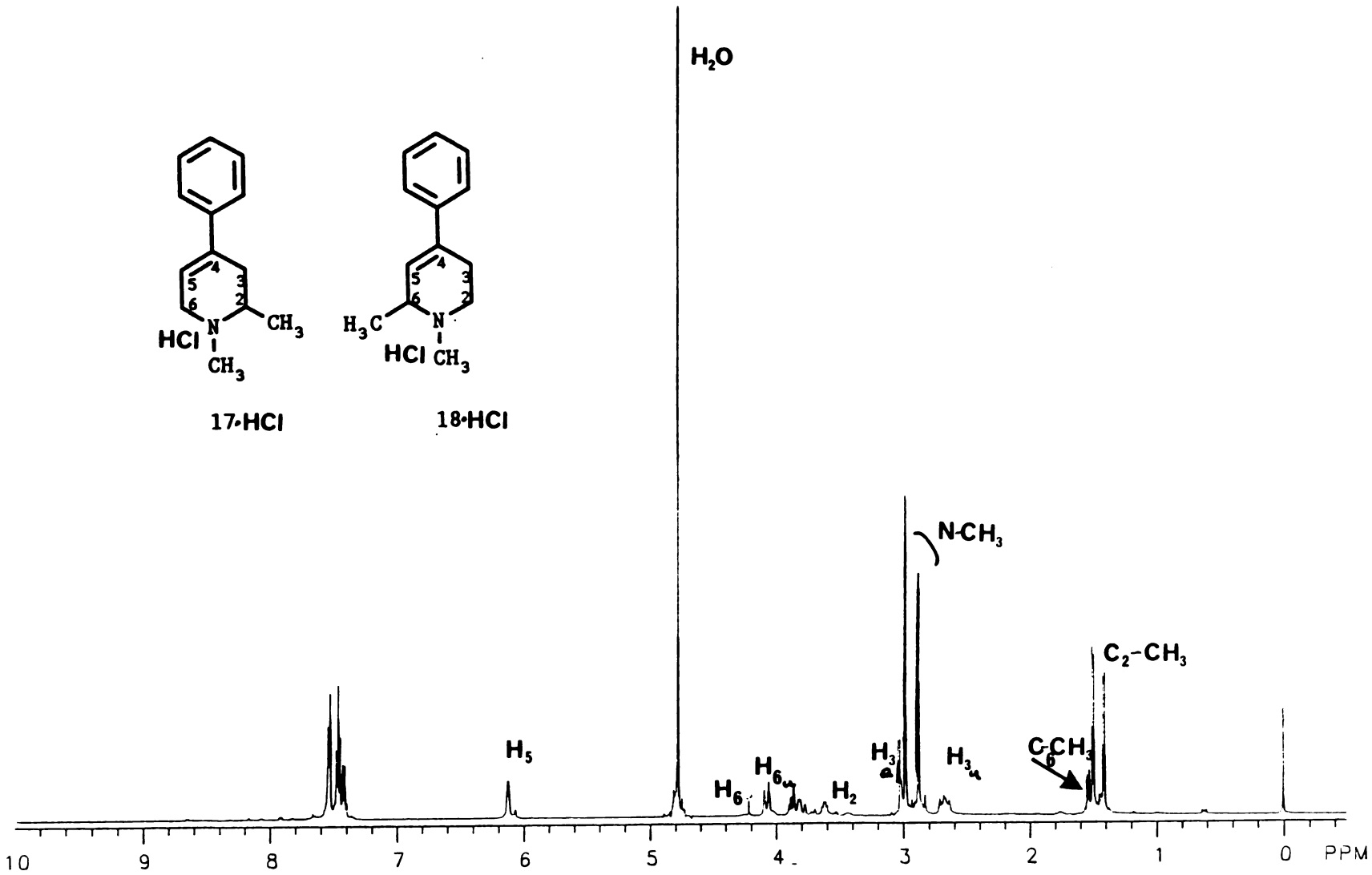

Figure 2-19. 500-MHz ^1H NMR (D_2O) spectrum of a crude mixture of tetrahydropyridines **17**·HCl and **18**·HCl obtained from disproportionation.

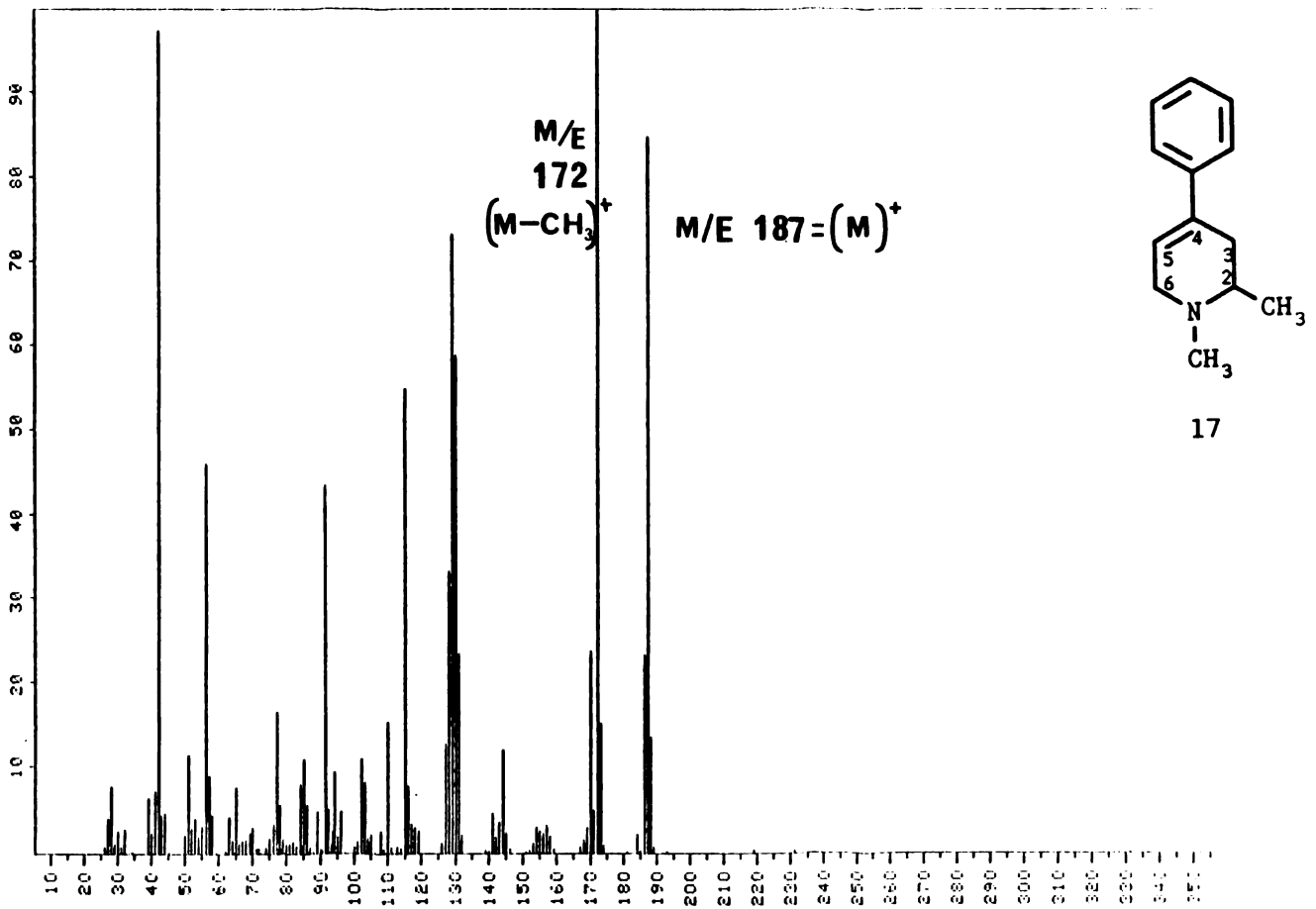

Figure 2-20. GC-EI Mass spectrum of 1,2-dimethyl-4-phenyl-1,2,3,6-tetrahydropyridine **17**.

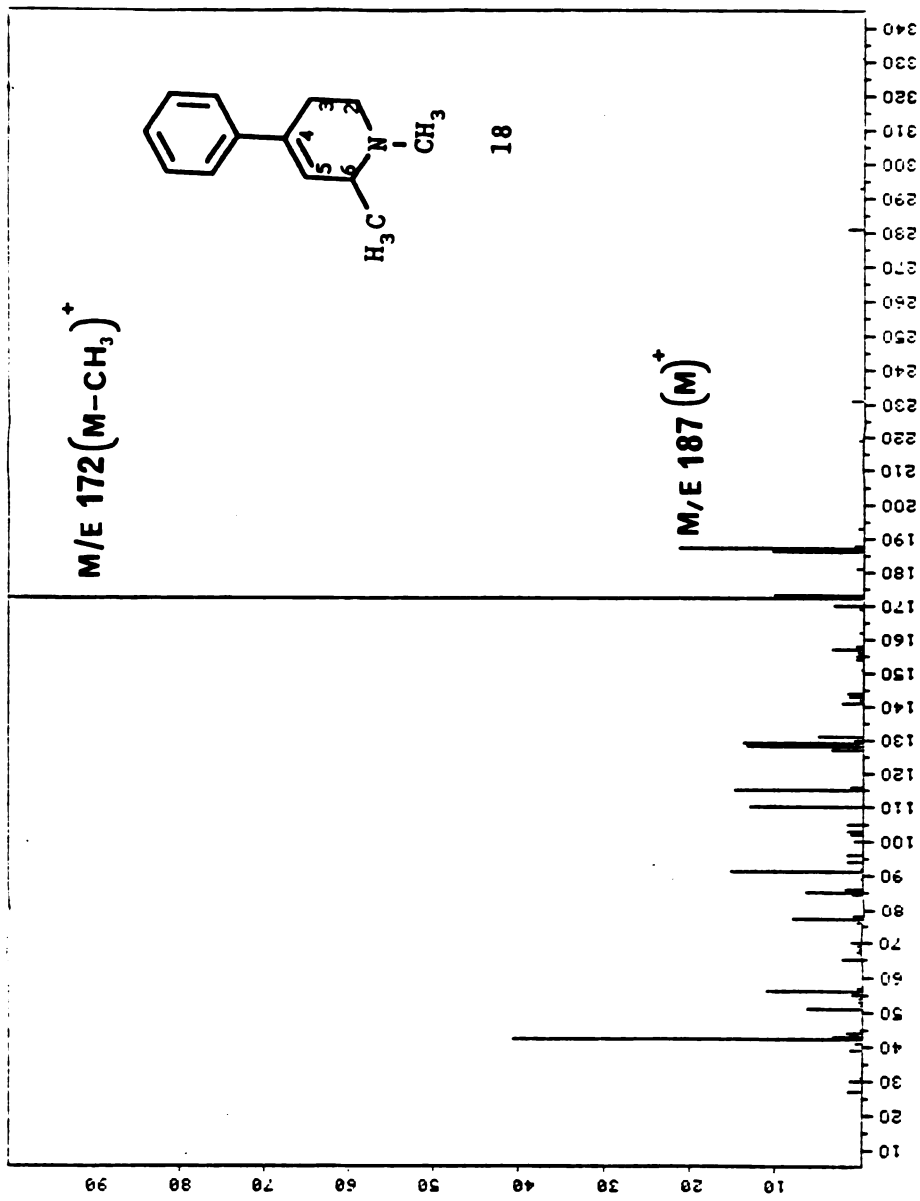

Figure 2-21. GC-EI Mass spectrum of 1,6-dimethyl-4-phenyl-1,2,3,6-tetrahydropyridine **18**.

In order to isolate **60**, the aqueous layer obtained from the quenched methyl Grignard reaction mixture above was saturated with sodium chloride to facilitate the extraction of water-soluble pyridinium salts with dichloromethane. The dichloromethane extracts were combined and evaporated to yield a yellow-orange crystalline solid (crude product 7.9 g) which accounted for approximately 60% of the original pyridinium starting material by weight. The UV spectrum of this crude product displayed a UVmax at 284 nm, the same as that of pyridinium **60** as previously characterized. After recrystallization from acetonitrile, the 240-MHz ^1H NMR ($CDCl_3$, Figure 2-22) was fully consistant with identification of the pyridinium species as **60**, displaying a peak corresponding to the C_2-methyl at 2.98 ppm.

The base peak in the CI-MS (Figure 2-23) of recrystallized **60** was at m/e 170, consistant with thermal dequaternization of **60** and subsequent protonation of the pyridine to give $(M-14)^+$ as is seen with MPP^+.[4] Thus **60** was again shown to be a product of the methyl Grignard reaction, apparently due to disproportionation.

Since the losses experienced in purification of the tetrahydropyridine and pyridinium products made estimation of the stoichiometry of the reaction difficult, an attempt was made to quantitate the crude products in a subsequent experiment.

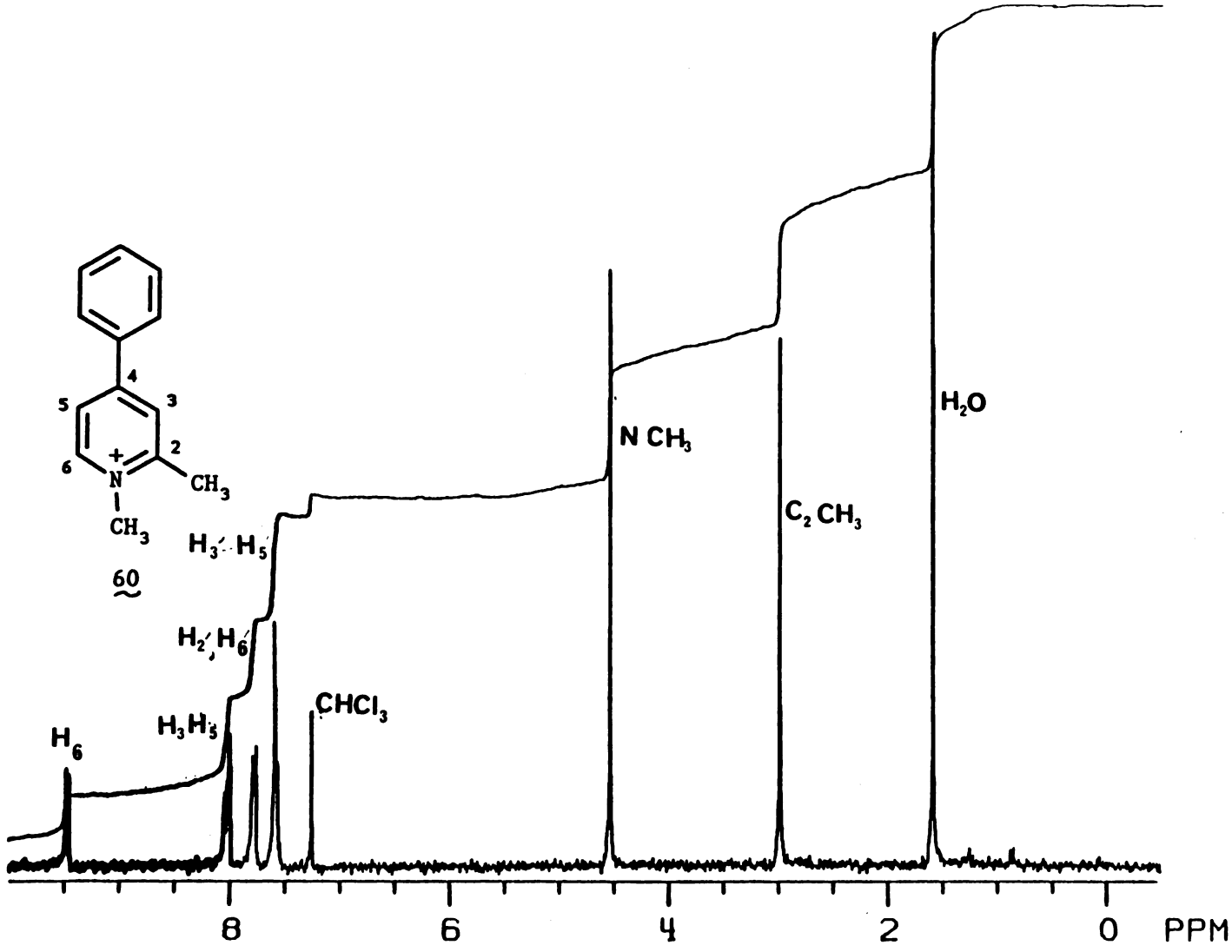

Figure 2-22. 240-MHz ^{1}H NMR ($CDCl_3$) of 1,2-dimethyl-4-phenylpyridinium ion (**60**) isolated from disproportionation and recrystalized in acetonitrile.

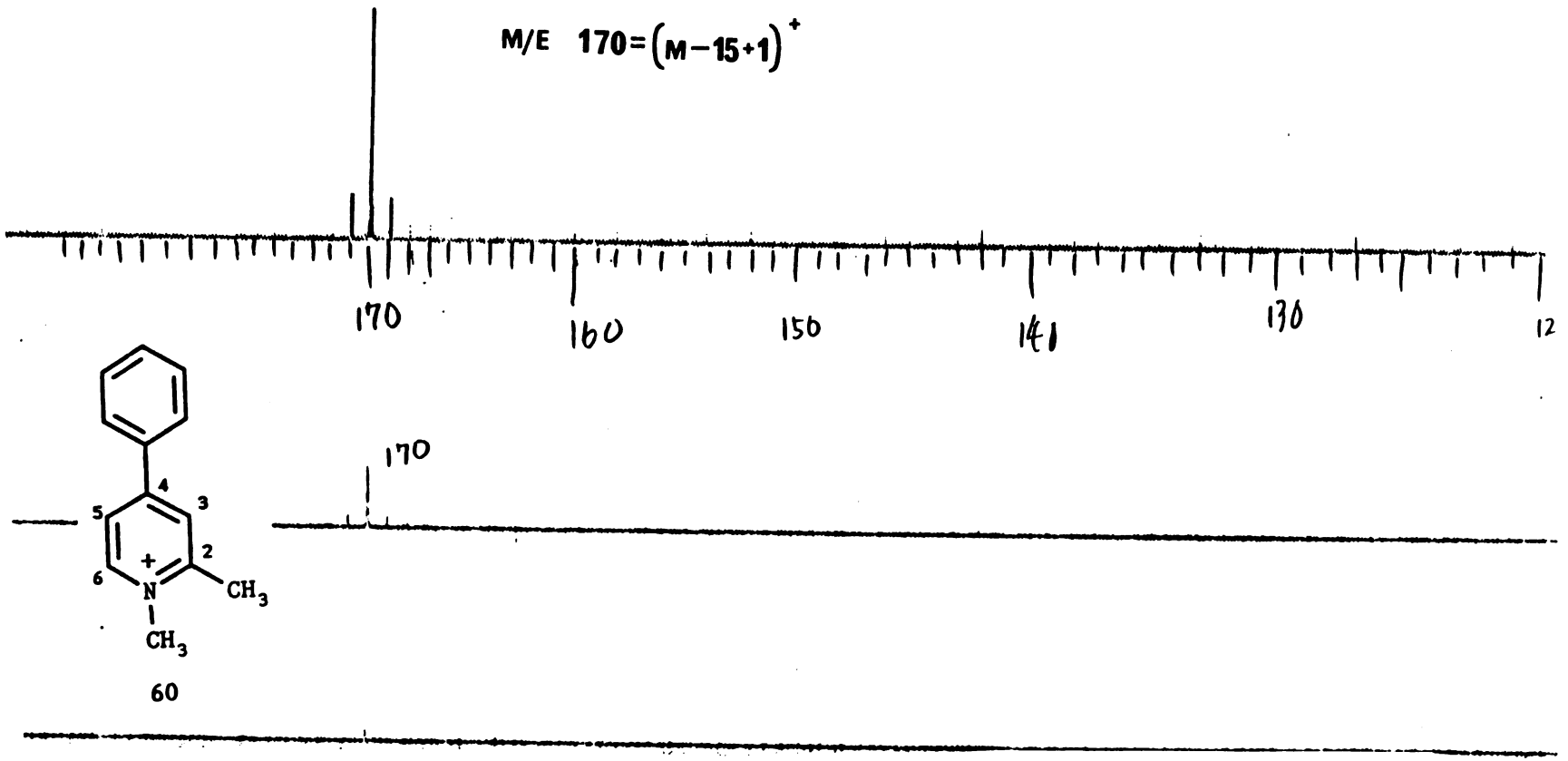

60

Figure 2-23. Chemical ionization Mass Spectrum of 1,2-dimethyl-4-phenylpyridinium ion (**60**) isolated from disproportionation.

The crude product mixture was isolated from the quenched Grignard reaction by dichloromethane extraction after the ether which served as solvent for the Grignard reaction had been removed by aspiration. The crude extract was subjected to HPLC analysis using a cation exchange column and solvent system used for separation MPP^+ and $MPDP^+$ (see legend, Figure 2-24, modified after Shinka et al.[139]). Using a Hewlett-Packard 1040A diode array UV detection system the HPLC chromatogram was simultaneously monitored at 3 different wavelengths in order to assess the presence of the dihydropyridinium ion (345 nm) as well as the tetrahydropyridines (244 nm) and the pyridinium species (295 nm). This chromatogram (Figure 2-24) displayed large peaks at 4.1 minutes (UVmax 244 nm), and at 8.1 minutes (UVmax 295 nm) indicating large quantities of the tetrahydropyridine and pyridinium compounds, respectively. To confirm the identities of the peaks at 4.1 minutes and at 8.1 minutes retention times, a sample of the partially purified hydrochloride salts of mixed tetrahydropyridines **17** and **18** obtained from a previous reaction was chromatographed under the same conditions and gave a single peak also with the same retention time of 4.1 minutes, while the perchlorate salt of **60** gave a peak with retention time 8.07 minutes. A third, small, poorly resolved peak in the chromatogram of the crude mixture (Figure 2-24), at a retention time of 6.15 minutes, was assigned to a trace of remaining

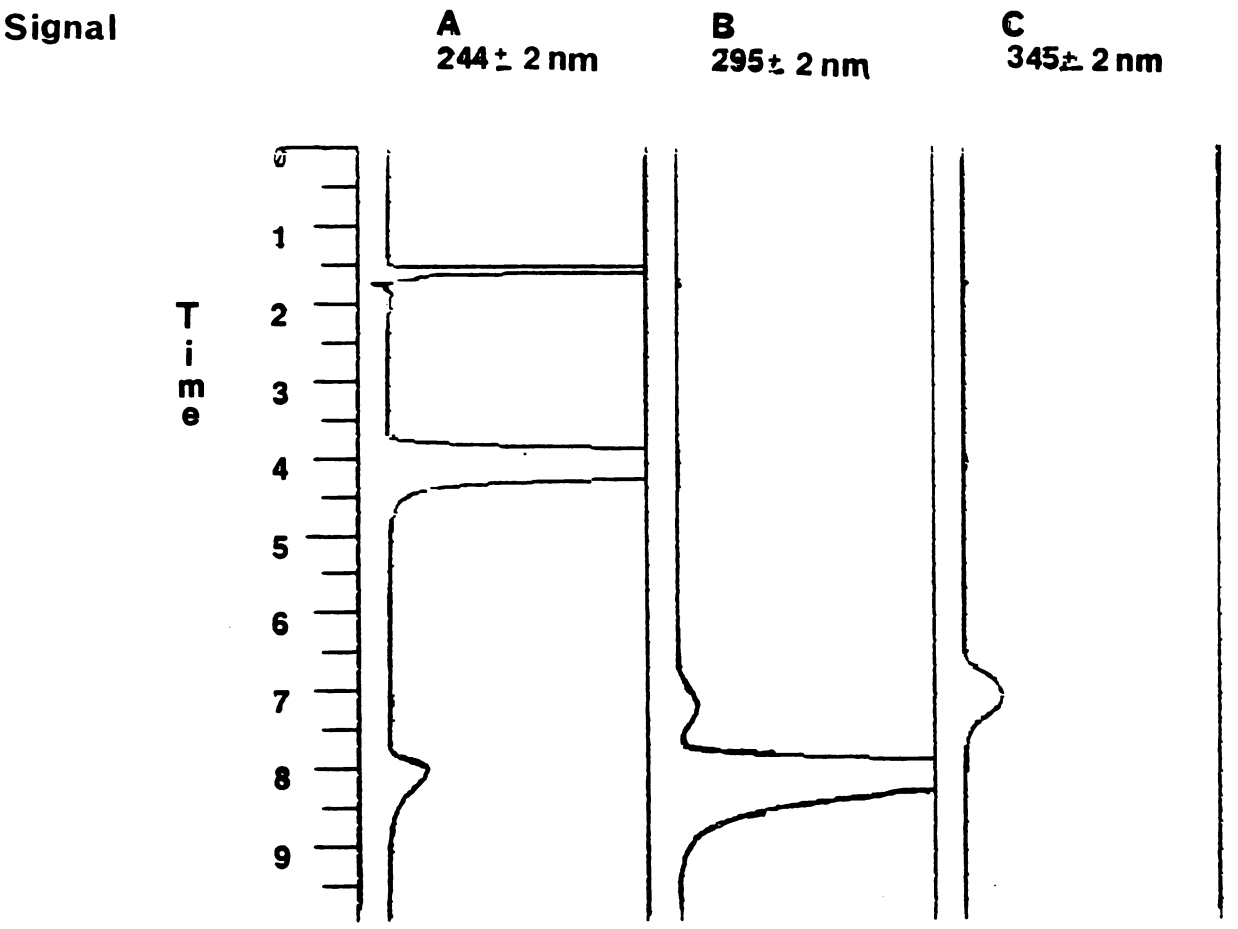

Figure 2-24. Diode array-HPLC chromatogram of crude product mixture from the disproportionation reaction. The tetrahydropyridines **17** and **18** elute as a single peak with a retention of time 4 min, while the pyridinium salt **60** elutes at a retention time of 8 min. A small amount of **15** elutes at retention time 7.5 min.

Column: Altex ultrasil-cx, 4.6 x 25 mm
Flow rate: 2 mL/min
Solvent: acetonitrile 15%, buffer 85%
Buffer: 0.1M Acetic acid, 0.05 M triethylamine hydrochlooride, adjusted to pH 2.3 with formic acid

dihydropyridinium **15** since it was detected at 343 nm. Neither the pyridinium species **60** or the tetrahydropyridines **17** and **18** exhibit significant absorbance at 343 nm.

Furthermore, the tetrahydropyridine MPTP, the pyridinium species MPP^+, and the dihydropyridinium species $MPDP^+$ give similar retention times (3.4 min, 6.0 min and 5.9 min) under these chromatographic conditons (Shinka et al., 1987 [139])

The disproportionation of **14** and **15** to form **17**, **18** and **60** was also accompanied by a change in the UV absorbance of the reaction mixture from a spectrum with predominant absorbance at 345 nm to a spectrum with maxima at both 284 and 248 nm as might be expected due to the absorbance of the pyridinium and tetrahydropyridine species, respectively. In an attempt to determine the time course of the disproportionation a Grignard reaction was carried out as usual with an initial concentration of 0.05 M MPP^+, after two hours UV analysis of the mixture showed complete conversion of the starting pyridinium species MPP^+ to dihydropyridine **14**, measured as **15**. An aliquot of 1 M HCl in methanol was then added by syringe to the Grignard reaction. Methanolic HCl was chosen over aqueous HCl to avoid the formation of a two phased system. Presumably under these conditions that aliquots removed for UV analysis after acid addition would accurately reflect the contents of a homogeneous reaction

mixture and allow the determination of the time course of disproportionation. Immediately after the addition of the methanolic HCl, an aliquot was removed for UV analysis and diluted into methanolic HCl. The UV spectrum (Figure 2-25) of this sample showed two absorbance maxima of approximately equal intensity at 280 nm and at 236 nm with a much less intense peak at 360 nm. Thus, within minutes after the addition of acid this spectrum indicated the presence of pyridinium, tetrahydropyridine and dihydropyridinium species, respectively showing that the disproportionation had occured during protonation of the Grignard reaction mixture. Even at this very early time (within minutes) the disproportionation appeared nearly complete since the peak at 360 nm, (taken as an indication of the dihydropyridinium) was the least intense peak of the spectrum. The intensity of the peaks thus observed was disturbing however. The peaks at 280 nm and at 236 nm correspond to 0.039 M pyridinium species and 0.057 M tetrahydropyridine species, respectively, in addition to the peak at 360 nm which corresponds to 0.014 M dihydropyridinium giving a total formation of 0.106 M products formed from a starting material concentration of 0.05M. Obviously, this estimate was inaccurate since it would have indicated that more moles of product were formed than had been present in the original starting material.

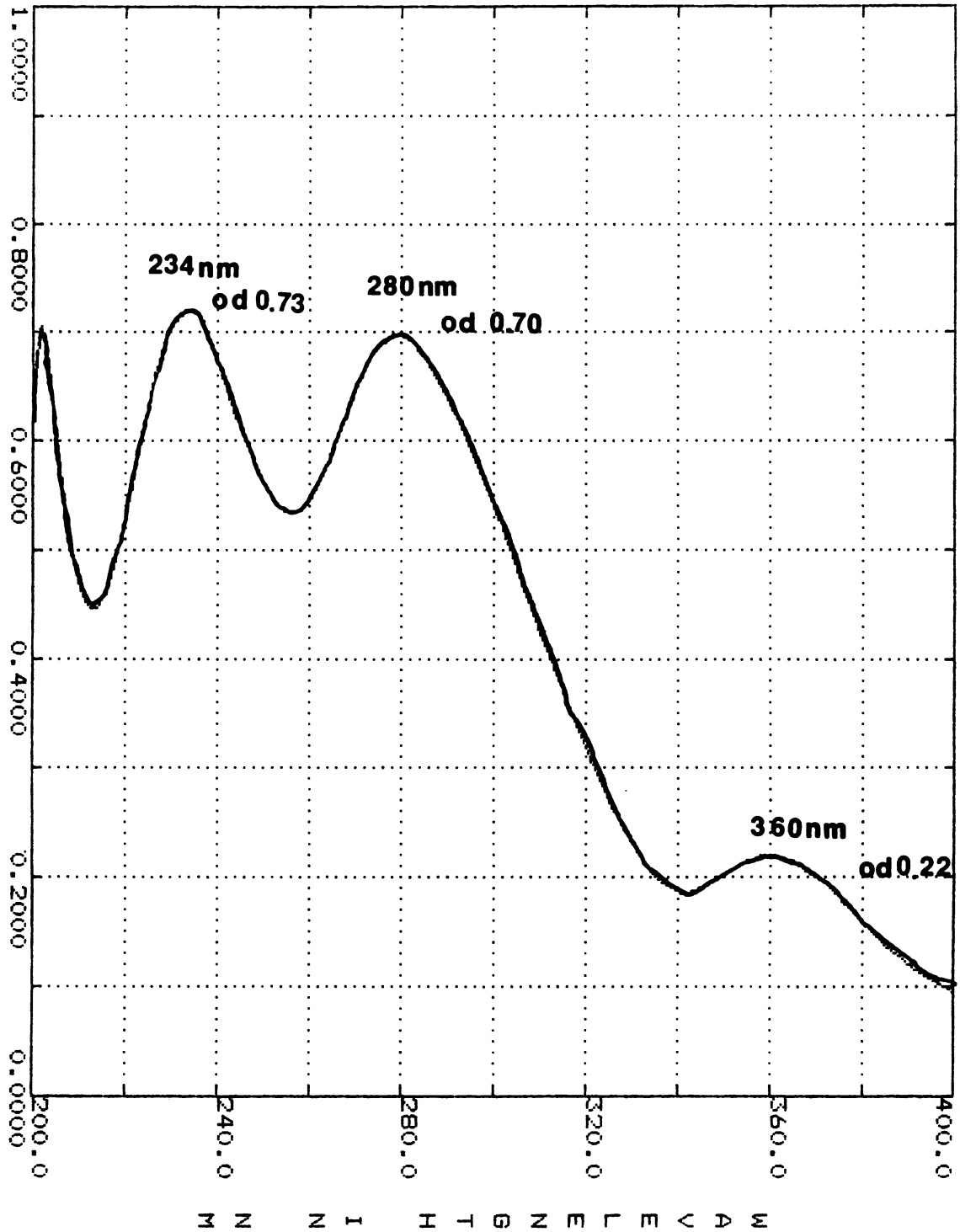

Figure 2-25. UV spectrum of a Grignard reaction mixture taken immediately after addition of methanolic HCl showing nearly complete disproportionation withing minutes of acid addition.

We felt the inaccuracy stemmed from our assumption that the molar absorptivities of the methylated species were the same as those of MPTP, $MPDP^+$ and MPP^+ which had been used to estimate the concentrations of **17**, **18**, **15** and **60** based on UV absorbance. After final purification of each compound the true molar absorptivity values were calculated, (see experimental). To examine this problem from another perspective we took advantage of the capabilities of the Hewlett-Packard 1040A diode array HPLC detector which provides both a curvilinear representation of the chromatogram as well as a digital report of the absorbance of the eluting compounds at the wavelength of interest in units derived from the "area under the curve" of the chromatogram trace. These units, which are proportional to the eluting concentration of a UV absorbant compound, can be used to estimate the relative amounts of components of a mixture. Monitored at 244 nm the tetrahydropyridine peak at 4.1 minutes gave an absorbance of 4344 mAUs, while the peak at 8.1 minutes, monitored at 295 nm gave an absor-bance of 3017 mAUs. The ratio of absorbance of the two peaks give a ratio of tetrahydropyridine/pyridinium species detected in the crude mixture as 4344/3017 or 1.44. This evidence would indicate that roughly one tetrahydropyridine molecule was formed for every pyridinium molecule formed. This crude estimate of stoichiometry is consistant with the mechanism proposed in Scheme 2-7.

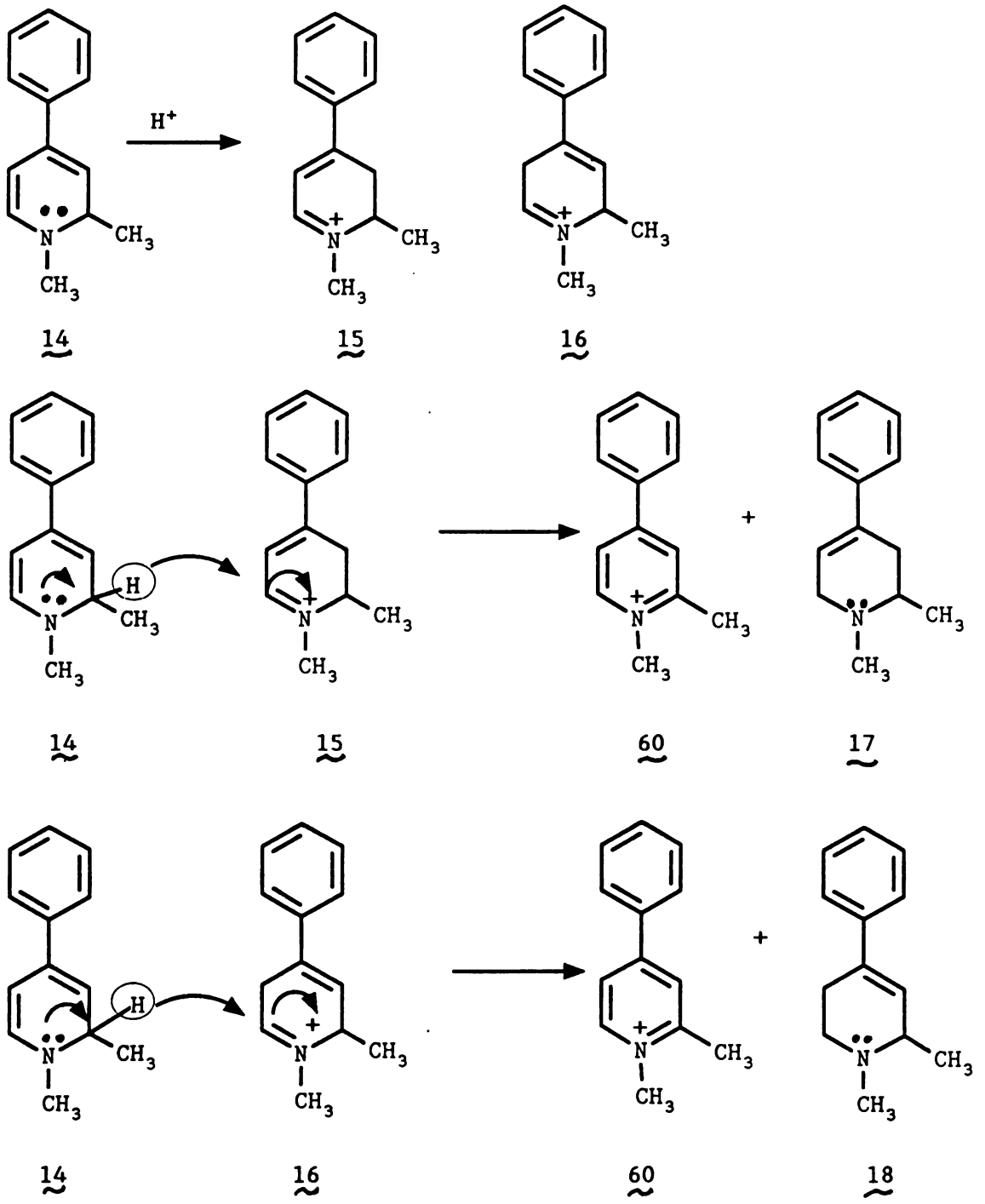

Scheme 2-7. A proposed mechanism for the disproportionation of 1,2-dimethyl-4-phenyl-1,2-dihydropyridine (14) with its protonated forms 15 and 16 to yeild 1,2-dimethyl-4-phenyl-pyridinium ion (60) and the 1,2- and 1,6-dimethyl-4-phenyl-1,2,3,6-tetrahydropyridines (17) and (18), respectively.

According to this suggested mechanism, the first step of the reaction involves protonation of the weakly basic dienamine **14**. The protonation can occur at either of 2 positions. Protonation at the terminal carbon atom of the dienamine C_3 yields dihydropyridinium species **15** in which the positive charge on the nitrogen atom is stabilized by resonance with the aromatic system of the phenyl ring. Because of this resonance stabilization, conjugated species such as **15** are thought to be more stable than the alternative unconjugated product **16** which is formed by protonation at the central dienamine carbon atom C_5. Opitz and Mertz made a detailed study of the rates of protonation at the central and terminal carbon atoms of dienamine systems in the reduction of dienamines derived from crotonaldehyde.[140] They and others [141,142] showed that the predominant protonation site is determined by the conditions of the reaction. Lyle [142] has summarized their findings as follows: Weak acids lead to the kinetically-controled product by proton attack at the central position of the enamine and strong acids give the product of thermodynamic control by attack of the proton at the terminal position. This rule was also formulated by Ingold[143] and is sometimes referred to as "Ingold's rule". Thus in our case, the strong acid conditions which led to disproportionation were likely to favor formation of **15** as the initial protonation product. The second step of the disproportionation reaction

involves transfer of a hydride equivalent from the unprotonated dihydropyridine **14** to the electrophilic carbon atoms (C_6) of each of the protonated forms **15** and **16**. The final result is formation of equivalent amounts of pyridinium ion (**60**) and tetrahydropyridine (**17** + **18**). NMR and, later, reversed-phase HPLC studies showed that **17** was the major tetrahydropyridine isomer formed, possibly reflecting the greater stability and favored formation of the protonated dihydropyridinium ion **15** in step 1 of the disproportionation.

The disproportionation process is favored by slow quenching of the Grignard reaction since this allows formation of **15** and **16** to occur in the presence of **14**. Later, in the synthesis of the dihydropyridinium ion **15**, it was found that reversal of the addition, i.e., addition of the Grignard reaction mixture to strong acid, leads to isolation of a stable, relatively pure dihydropyridinium salt. Formation of undesired products in the disproportionation reaction could be minimized by performing the Grigard reaction in dilute conditions (0.05 M).

The disproportionation reaction was unexpected but yielded three of the desired methyl substituted products. Pyridinium **60** could be obtained in good yield and it was believed that **17**, which was also obtained in good yield, could be separated from **18** by recrystallization of the hydrochloride salts. Therefore, we decided to

capitalize on the disproportionation reaction. Large scale reactions were performed to obtain the quantities of products needed.

Repeated recrystallizations of the mixture of hydrochloride salts of **17** and **18** in isopropanol/diethyl ether gave a product with a sharp melting point. This product gave one spot after TLC in several solvent systems and its 240-MHz ^{1}H NMR appeared to be that of pure **17**·HCl (Figure 2-26).

Preliminary data on the MAO substrate and inhibitory properties as well as mouse dopaminergic neurotoxicity and isolated rat hepatocyte cytotoxicity of this product were obtained (to be described in a later section) before a 500-MHz 1H NMR (Figure 2-27) revealed that the product was still a mixture of the two tetrahydropyridines 17 and 18. The higher field strength instrument combined with better adjustment of the instruments magnetic field (shimming) allowed resolution of the dual olefinic proton signals and three distinct doublets for the C6-methyl protons of 18 and the C2-methyl protons of 17.
Later, reversed phase-HPLC studies would indicate that recrystallization had succeeded in changing the ratio of **17**:**18** from 64:36% in the crude product to 85:15% after 3 recrystallizations.

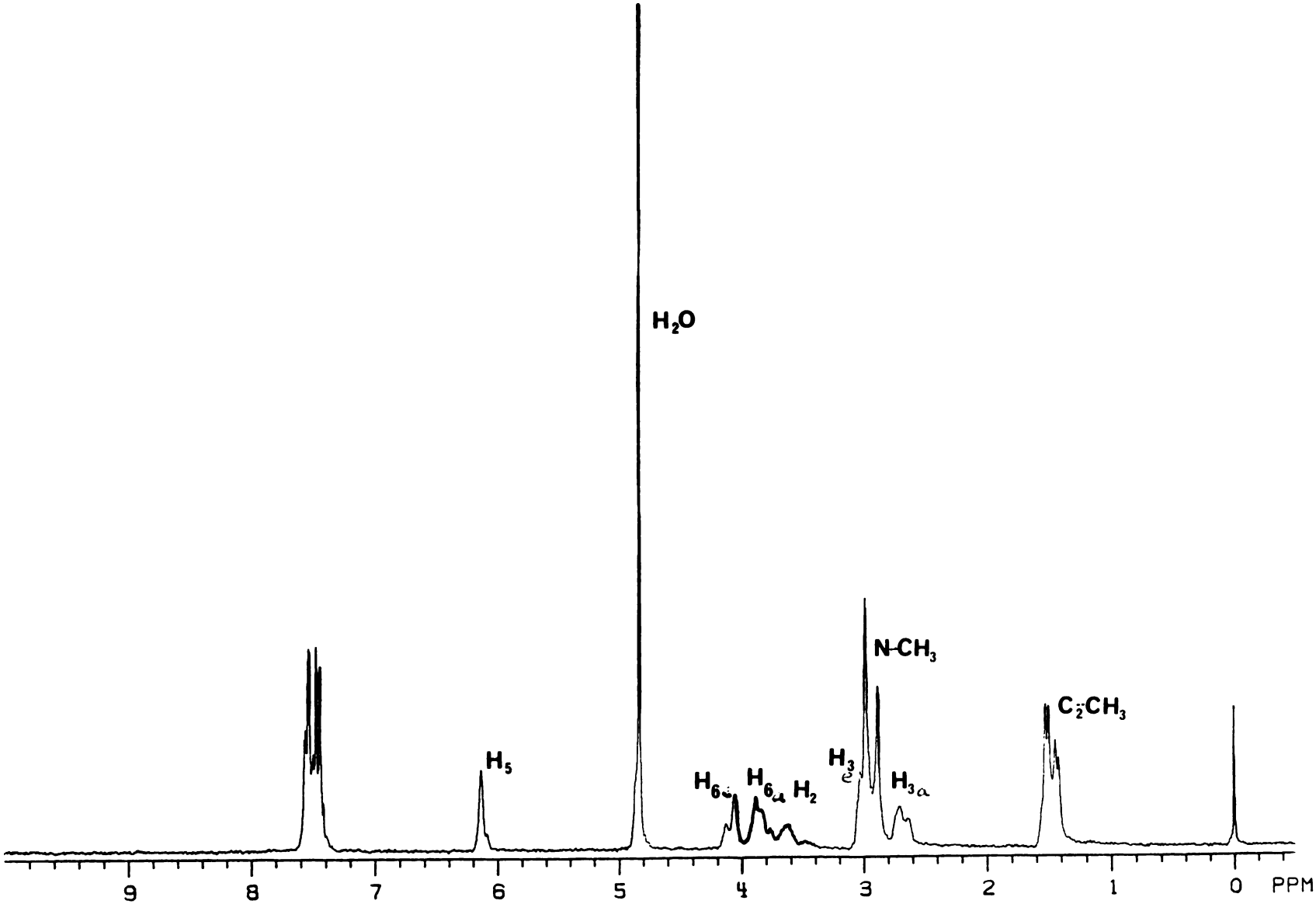

Figure 2-26. 240-MHz ^{1}H NMR (D_2O) spectrum of a mixture of tetrahydropyridines **17**·HCl and **18**·HCl obtained after 3 recrystalizations from isopropanol/diether ether.

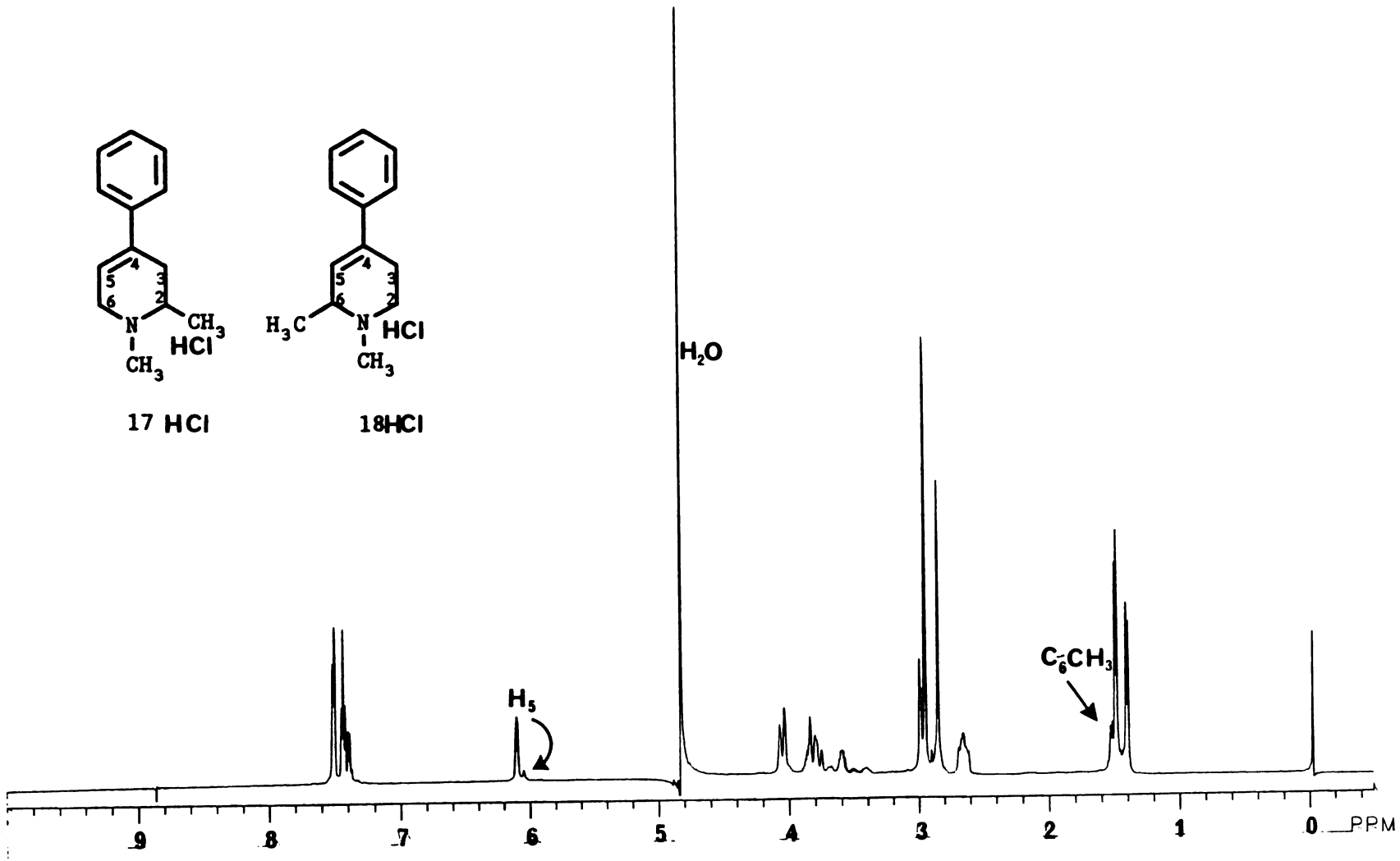

Figure 2-27. 500-MHz ^{1}H NMR (D_2O) spectrum of the same mixture of **17**·HCl and **18**·HCl as in Figure 2-26, obtained after 3 recrystalizations from isopropanol/diether ether.

SEPARATION OF **17** AND **18**

It became clear from this experience that TLC was not a reliable indicator of the isomeric purity of these tetrahydropyridines. Methods were required for both the analytical and preparative scale separation of the olefin isomers **17** and **18**. Attempts to separate the compounds on alumina as well as silver nitrate impregnated silica gel plates (often useful in separation of olefin isomers[28]) were also unsuccessful. High performance liquid chromatography (HPLC) using a cation exchange type column was also unsuccessful. A successful separation was achieved on an analytical scale using a Pirkle type column. This is a 5 micron particle sized column which has a chiral stationary phase consisting of d-(N-3,5-dinitrobenzoyl)phenylglycine covalently bonded to aminopropyl residues on a silica gel base. The chiral stationary phase forms three-point interactions with components of the sample and has been used to separate enantiomeric and diastereomeric mixtures.[27] Using slow solvent flow rates, the two olefin isomers showed as much as a two minute separation in retention times (Figure 2-28). This system appeared to be an attractive method for separation of the olefin isomers on a preparative scale.

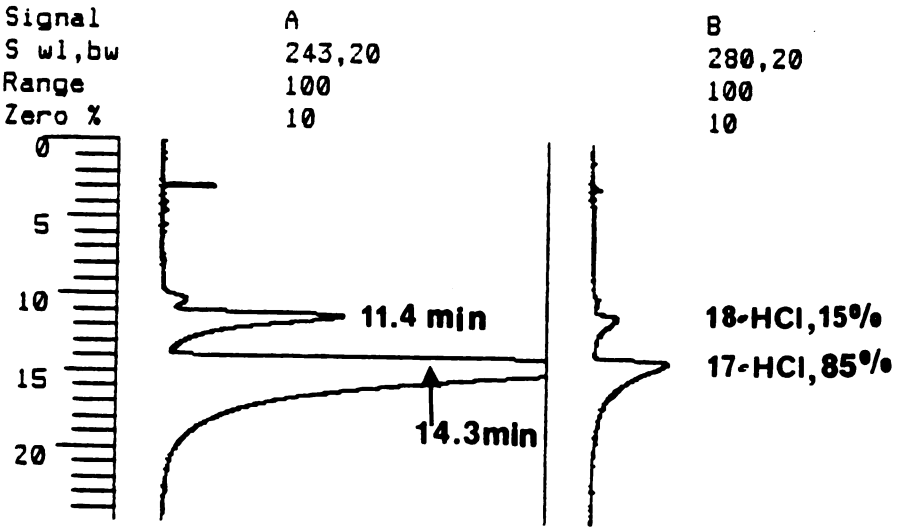

Figure 2-28. Chiral column HPCL chromatogram of a mixture of **17**·HCl and **18**·HCl. Column: 5 um d-(N-3,5-dinitrobenzoyl)-phenyl glycine, 4.6 X 250 mm. Solvent: 5% Isopropanol in Hexane. Flowrate: 1 mL per min.

The preparative Pirkle column, however, is made with a larger 10 micron size particle which is less uniformly coated than is the 5 micron analytical column. The preparative column, with its poorer resolution characteristics, was unable to achieve a satisfactory separation of mixtures of **17** and **18**. Unfortunately, degradation of the resolution of the Pirkle analytical scale HPLC system developed after several weeks of use, and this approach was abandoned. Since recrystallization of the hydrochloride salts of **17** and **18** had resulted in some enrichment of the mixture in **17**, attention was turned to finding another salt of **17** and **18** which might on recrystallization improve the separation. The separation of enantiomeric pairs of basic compounds has been achieved by formation and recrystallization of their (-)-di-p-toluoyl-l-tartrate salts. This approach was however not successful for the separation of **17** and **18**.

A second HPLC system was developed using a reversed phase C_{18} column and an acetonitrile/buffer mobile phase. This system gave consistantly reproducible baseline separation of the olefin isomers and was used for all subsequent analyses. Figure 2-29 shows examples of the separation achieved with this system.

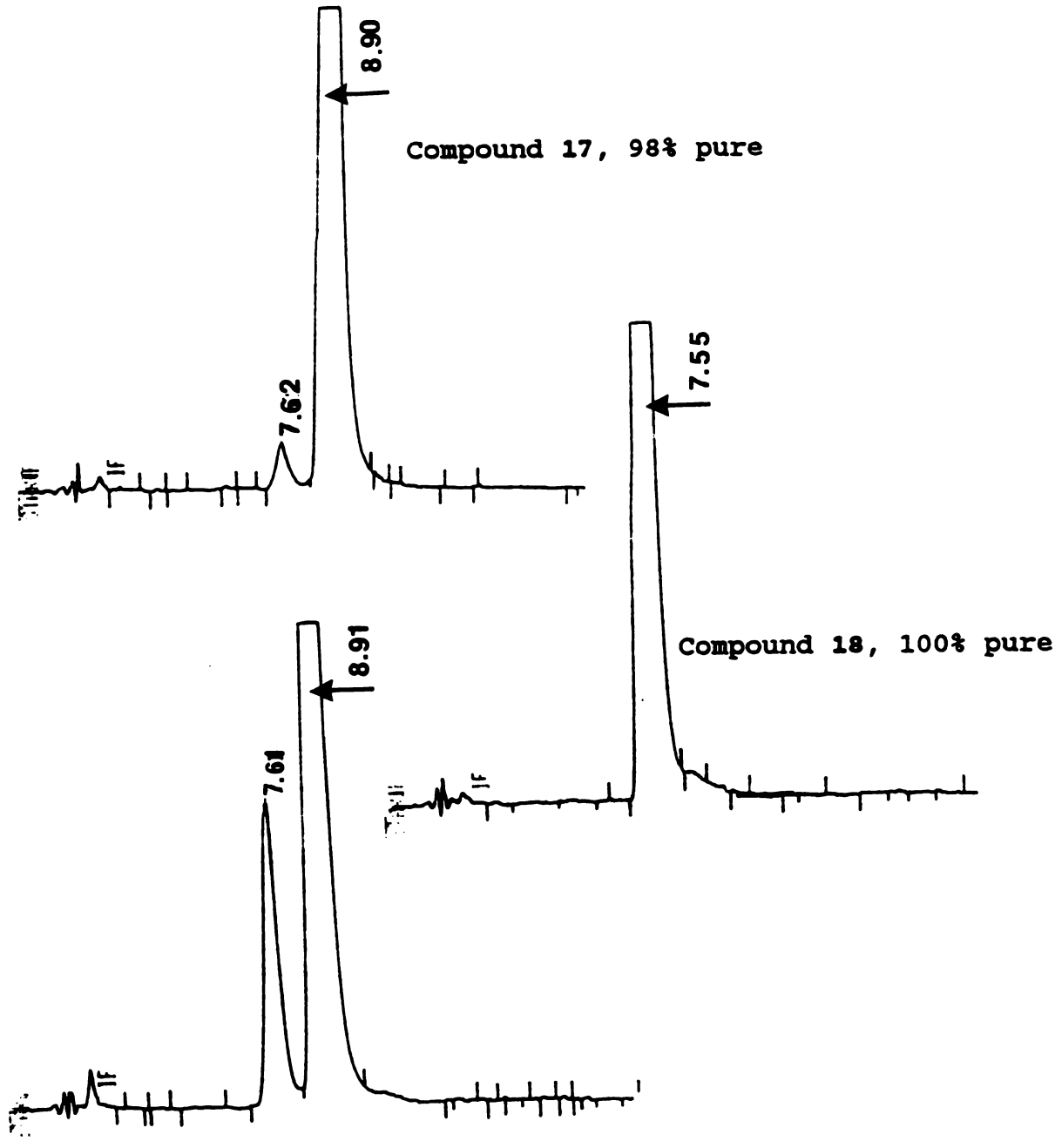

Figure 2-29. Reversed phase HPLC chromatograms of 17 (Fig. 4a), 18 (Fig. 4b), and a mixture of 17 and 18 (Fig 4c). Compounds 17 and 18 elute at retention times of 8.9 min and 7.6 min respectively.

The problem of preparative scale separation was finally solved when a Chromatotron centrifugal separation apparatus was acquired by our laboratory. This device consists of a spinning plate which is coated with very fine grade silica gel and a mechanism for application of sample and solvent. The spinning plate separates compounds more efficiently than traditional column chromatography due to the finer grade of silica. Centrifugal force speeds the flow of solvent through the silica gel bed to allow rapid separations. The system combines the resolution of thin layer chromatography with speed, scale and ease of use of HPLC or MPLC systems.

A solvent mixture ($CHCl_3$:MeOH, 9:1) was developed which gave an elongated spot for the tetrahydropyridines on silica TLC. Though not fully resolved on TLC the mixture of tetrahydropyridines could be separated with this solvent system on the Chromatotron by careful fraction collection. The purity of each fraction was then determined by reversed phase HPLC. Using this method compound **17** was obtained in 98% purity. For storage the compound was converted to its HCl salt. Recrystallization from ethanol/diethyl ether gave the analytical compound. The UV characteristics of **17**·HCl were similar but not identical to those of MPTP. MPTP has a maximal UV absorbance at 240 nm (ext. coeff. 12,000). Tetrahydropyridine **17** has the same UV chromophore as MPTP but its maximal absorption occurs at

242 nm (ext. coeff. 9,800). The EI-mass spectrum (Figure 2-30) which displayed a molecular ion at m/e 187 and a base peak corresponding to the loss of methyl (m/e 172) confirmed the structure. The 500-MHz ^1H NMR characteristics of pure **17**·HCl further confirm the structure (Figure 2-31). A single peak appears for the olefinic proton at 6.1 ppm. Since in compound **17**, the olefin proton is distant from the C_2-methyl group, which exerts a slight shielding effect, the chemical shift of the H_5 proton in **17** is shifted downfield of the olefin proton signal in **18**. In contrast to the triplet of doublets observed for the C_2 and C_6 methyl groups for the mixture of **17** and **18**, only a pair of doublets is observed with pure **17**·HCl. The pair arises from the diastereotopic nature of the C_2 carbon atom on protonation of the nitrogen atom in **17** and is further discussed below in the section on NMR characterization of **17** and **18**. An important aspect of these doublets was noted in the characterization of pure **17**·HCl; on irradiation of the C_2-methyl doublets only the peaks at 3.6 and 3.85 ppm were altered. This observation resulted in assignment of these peaks to the H_2 axial and H_2 equatorial protons, respectively. Since these protons gave signals <u>upfield</u> of the other aliphatic proton signals, this compound was further positively identified as **17**.

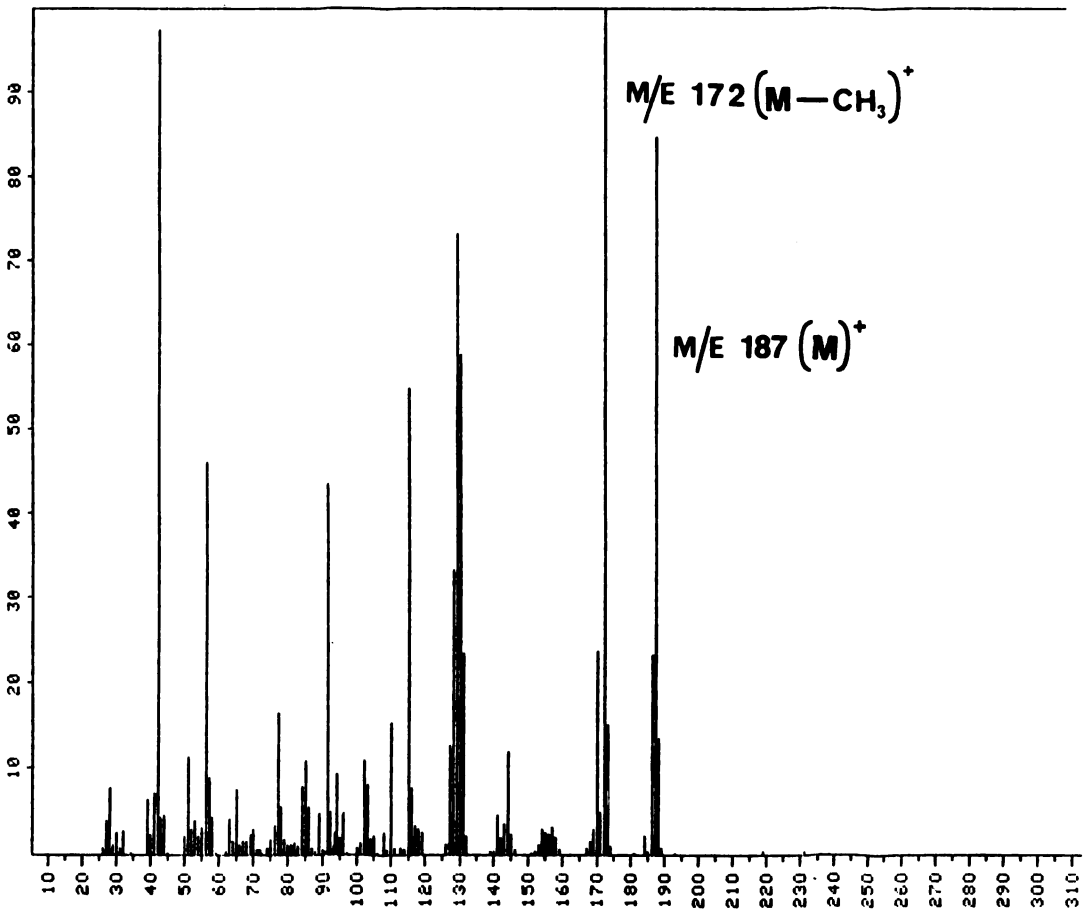

Figure 2-30. GC-EI Mass spectrum of pure **17**.

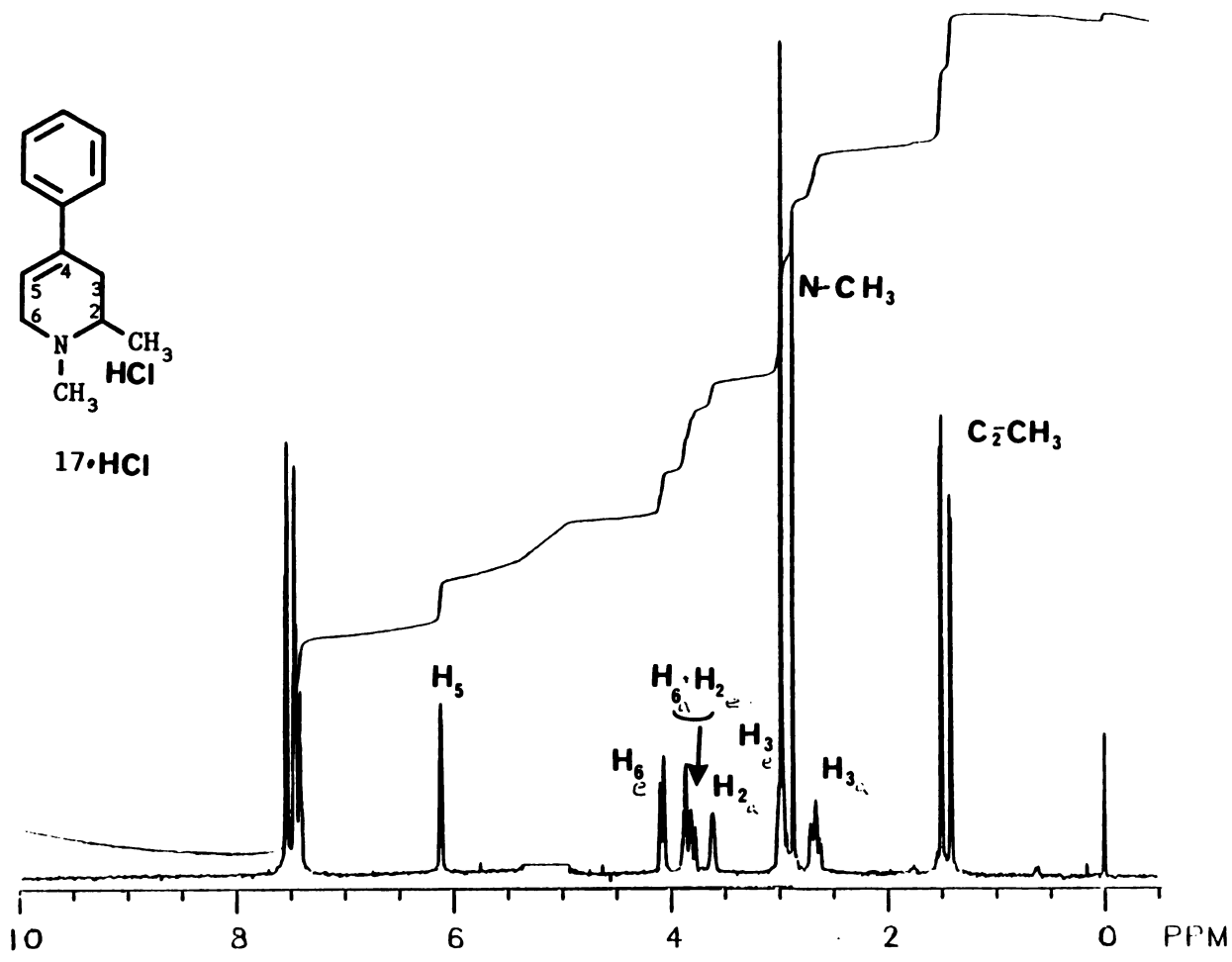

Figure 2-31. 500-MHz ^{1}H NMR (D_2O) spectrum of pure 1,2-dimethyl-4-phenyl-1,2,3,6-tetrahydropyridine **17**·HCl assayed 98% isomeric purity by reversed-phase HPLC. DCl added to sharpen signals.

Finally, reversed-phase HPLC of the purified compound indicated 98% purity of **17** exhibited by a large peak eluting at 8.9 minutes (Figure 2-29). The accompanying peak with retention time of 7.6 minutes is due to a 2% contamination by **18**. In light of the difficulty with separation, this small contaminant was judged acceptable.

SYNTHESIS OF PURE **18**

Compound **18** had been detected as a minor product from the sodium borohydride reduction of pyridinium salt **60** using methanol as solvent. Inspection of the mechanism proposed for the sodium borohydride reduction (Scheme 2-6) (as well as experience with the disproportionation discussed above and the precedent of Lyle [142]) led to the conclusion that the product ratio might be controlled by the ratio of protonated products in step 2 where the solvent, (in this case methanol) is the proton source. We reasoned that the product ratio might be changed if more acidic conditions could be found for sodium borohydride reduction of **60** which would favor the formation of dihydropyridinium isomer **19**. Then tetrahydropyridine **18** might result as the major product of the reduction. Therefore the initial synthetic approach to **18** was to try more acidic conditions for the reduction of **60** to **18**. In the first attempt a solvent of 1 M HCl in methanol was used as the medium for the

reaction. Furthermore sodium cyanoborohydride was chosen as the reducing agent due to its improved stability in acidic conditions. However, under these conditions the reducing agent, decomposed and no tetrahydropyridine was formed at all. Subsequently, the acidity of the reaction was more carefully titrated using methyl orange as an internal pH indicator. Methanolic HCl was added dropwise to maintain the pH at 3, the lowest pH at which sodium cyanoborohydride could be used. Again starting material was recovered, and HPLC of the crude reaction mixture indicated no tetrahydropyridine was formed although a large excess of reducing agent had been used. We reasoned that the inability of cyanoborohydride to carry out the reduction of **60** might be related to the cyano substituent. The stability of sodium cyanoborohydride in acidic conditions is thought to be due to the electron withdrawing characteristics of the cyano substituent which reduce the susceptibility of the boron-hydride complex to hydrolysis. Unfortunately this effect also reduces its ability to deliver a hydride equivalent to the desired target. To test this hypothesis we carried out a reaction of sodium cyanoborohydride and **60** in methanol with no acid present which indicated that cyanoborohydride is too weak a reducing agent to attack the pyridinium salt. Although a very small amount of tetrahydropyridine was formed after 100 fold excess sodium cyanoborohydride and 29 hours reaction time, the

reaction was too slow to be synthetically useful even under neutral conditions. We then demonstrated that sodium borohydride is capable of reduction of **60** in the presence of glacial acetic acid. The reaction proceeded rapidly to give a mixture of **17** and **18** as well as another product. The additional product, which had very non-polar chromatographic properties (Rf 0.8 on silica gel TLC) was separated from the tetrahydropyridines by column chromatography. Its 80 MHz ^{1}H NMR ($CDCl_3$) spectrum (Figure 2-32) was nearly identical to that of mixtures of **17** and **18**. Amine-borane complexes analogous to **66** and **67** with similarly non-polar chromatographic characteristics have been reported as products of the sodium borohydride reduction of the 3- and 5-phenyl-substituted pyridinium methiodides by Gessner and Brossi (1985).[29] Gessner used thermospray mass-spectrometry to unambiguously characterize the amine-borane complex. Since we did not have this particular method of mass-spectrometry available, we could only make a tentative identification of the non-polar material as a mixture of amine-borane complexes **66** and **67** based on the NMR and chromatographic properties. These marginal results led us to pursue the preparation of pure **18** by yet another route.

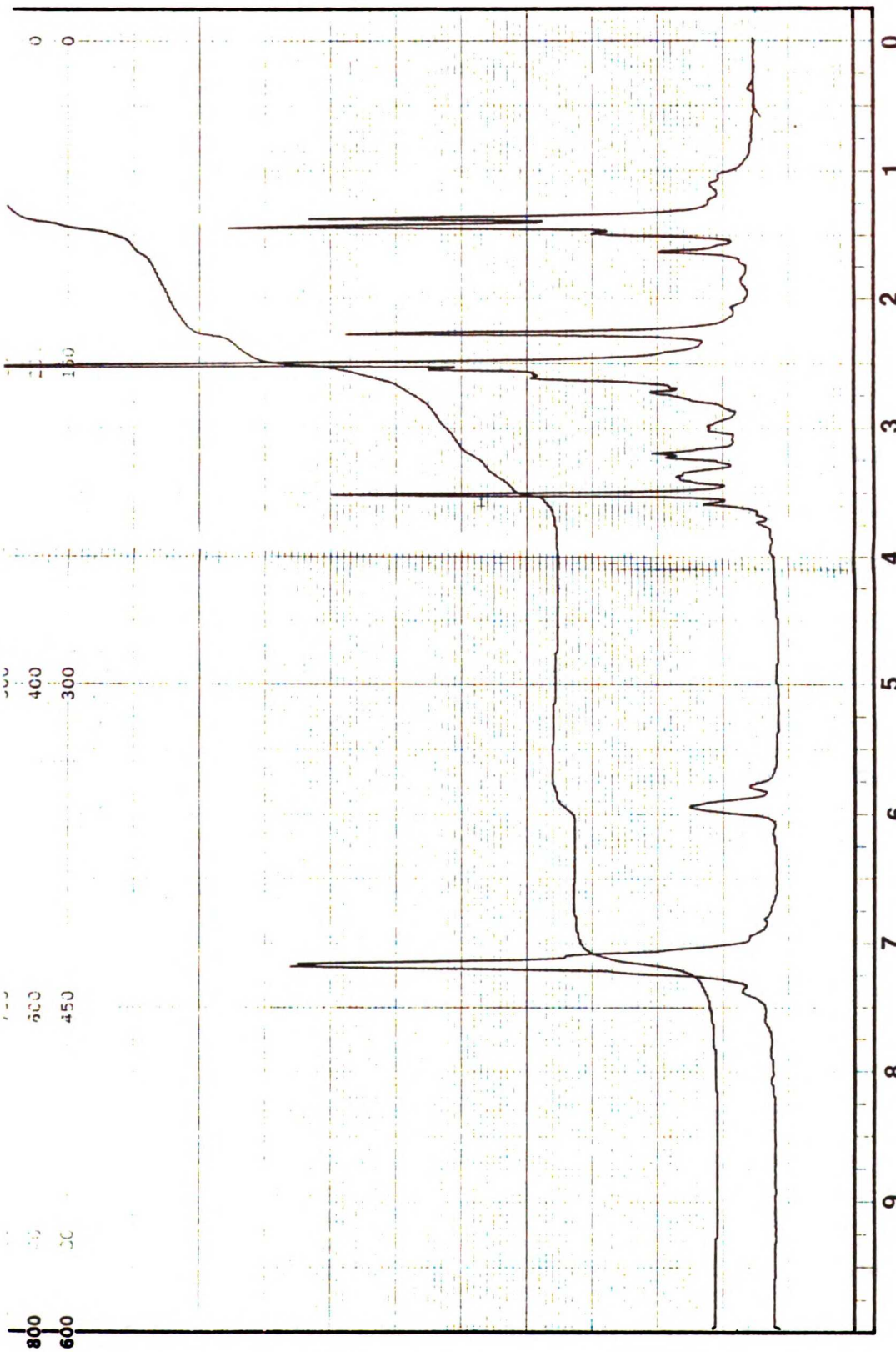

Figure 2-32. 80-MHz ^{1}H NMR ($CDCl_3$) spectrum of the non-polar product of sodium borohydride reduction of 1,2-dimethyl-4-phenylpyridinium ion (**60**) in the presence of acetic acid.

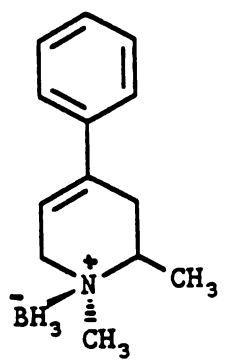

66

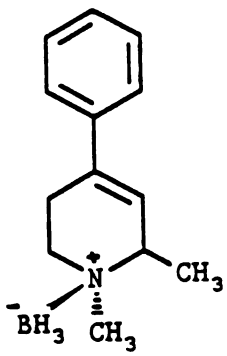

67

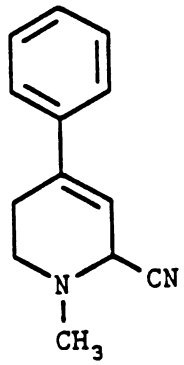

69

The susceptibility of 2-cyano-1-methyl-1,2,3,6-tetrahydropyridine (**69**) to Grignard attack has been well documented.[31] The alpha-aminonitrile can undergo substitution of the cyano group by Grignard reagents such as benzyl, thenyl, or benzo[b]thienylmethylmagnesium halides.[31] Since **69** was readily available, we examined this reaction as a potential avenue to **18**. A Grignard reaction of **69** with methylmagnesium bromide in diethyl ether gave an acceptable yield (55%) of pure **18** (analyzed by reversed phase HPLC, Figure 2-29). The compound was converted to its hydrochloride salt by treatment with methanolic HCl and characterized by NMR and microanalysis. The 500 MHz ^1H NMR (D_2O) spectrum (Figure 2-33) of this compound confirmed its structure as **18**·HCl exhibiting a pair of doublets for the C_6-methyl protons at 1.5 ppm and 1.48 ppm. The olefinic H_5 proton of **18**·HCl exhibited a double peak at 6.25 ppm.

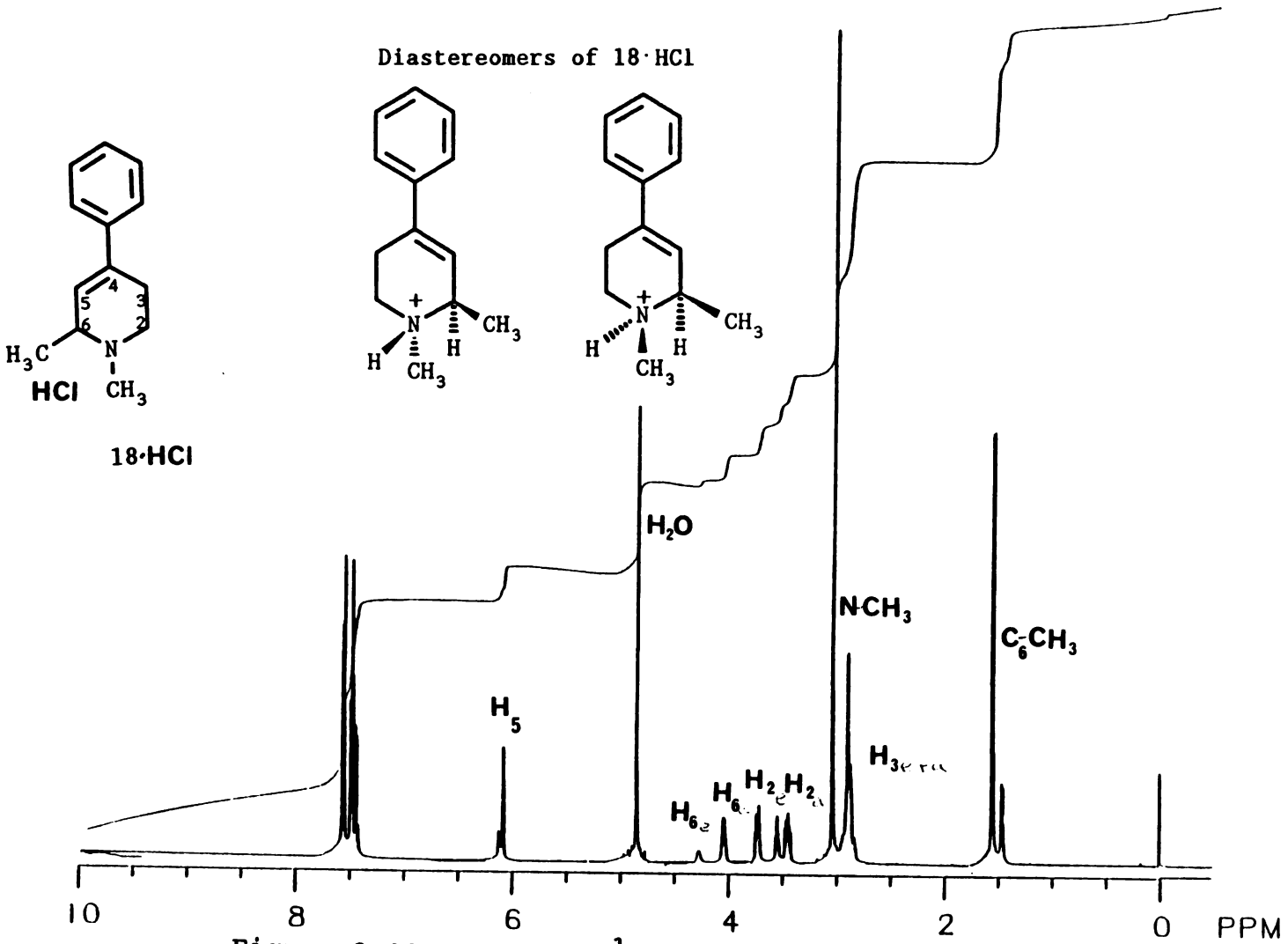

Figure 2-33. 500-MHz ^{1}H NMR (D_2O) spectrum of pure 1,6-dimethyl-4-phenyl-1,2,3,6-tetrahydropyridine hydrochloride (**18**·HCl) assayed 100 % isomeric purity by reversed-phase HPCL.

These results are attibuted to the diastereotopic nature of the hydrochloride salt of **18** and will be further discussed in the next section.

NMR CHARACTERIZATION OF 17 AND 18

The NMR experiments described above for the characterization of the mixture of tetrahydropyridine products obtained from the reduction of **60** so closely resembled those obtained from the products of the Grignard/disproportionation reaction that they were also the first important clue as to the identity of the mixture of tetrahydropyridines thus obtained. However, the products of the disproportionation reaction had been isolated as hydrochloride salts for improved stability. The appearance of the NMR spectra of the mixed salts of **17** and **18** (Figure 2-27) is made more complex by the diastereomers formed on protonation.

THE EFFECT OF DIASTEREOMERS ON THE NMR EXPERIMENT

Figure 2-34 illustrates the diastereomers obtained from protonation of **17** and **18**. The pure (assayed by HPLC, see chromatogram in Figure 2-29b) sample of **18**·HCl still gave 2 peaks in the olefinic region of the NMR spectrum (Figure 2-33) as well as two peaks for the N-methyl protons at 2.85 ppm and at 3.0 ppm. The two peaks are observed here as a result of the diastereomers formed

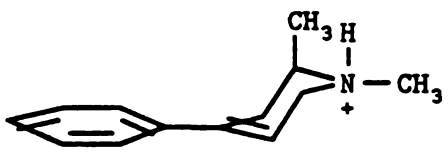

17, Diastereomer A

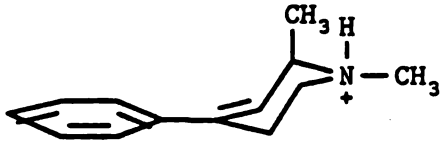

18, Diastereomer A

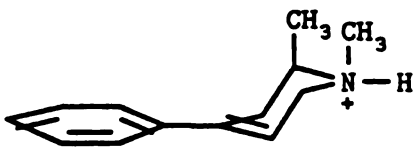

17, Diastereomer B

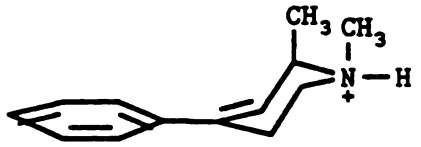

18, Diastereomer B

Figure 2-34. Stereo-drawing of diastereomers of **17**·HCl and **18**·HCl

on protonation. The proton may experience different magnetic environments in the two diastereomers leading to a different chemical shift for the H_5 protons in each diastereomer. Similarly, 2 sharp singlet signals are observed for the diasterotopic N-CH_3 protons in the NMR spectra of each of the pure tetrahydropyridine (Figures 2-31 and 2-33).

The diastereomers formed on protonation of the tetrahydropyridine nitrogen atom are not distinctly separate chemical entities but instead are interchangeable through inversion of the pyramidal nitrogen atom. The inversion, which occurs at room temperature, is slow enough that the NMR experiment is capable of distinguishing the different diastereomeric forms, resulting in multiple signal peaks for each proton. However, the peaks which represent the tetrahydropyridine ring protons are often quite broad in a spectrum obtained from a sample dissolved in D_2O (e.g. protons H_2-H_6 in Figure 2-35). This broadening effect, which sometimes obscures the proton splitting pattern (making interpretation of the spectrum more difficult), occurs because the NMR time scale is not fast enough to truly freeze the pyramidal nitrogen atom in time. The rate at which the pyramidal nitrogen inverts can be slowed by decreasing the pH of the sample to shift the equilibrium toward the protonated species.

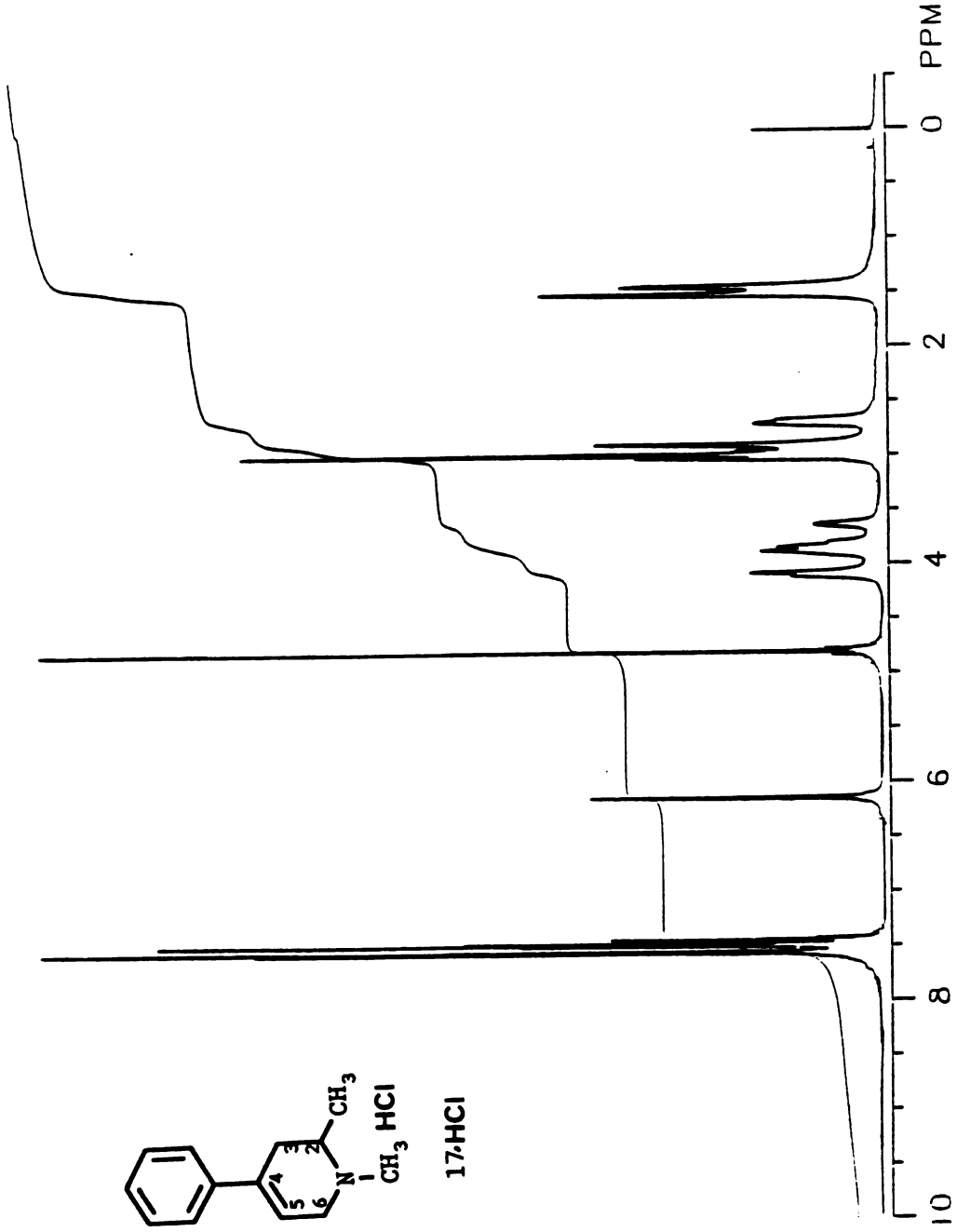

Figure 2-35. 500-MHz ^1H NMR (D_2O) spectrum of pure **17**·HCl with broad signals due to nitrogen inversion.

After addition of a trace of DCl to **17**·HCl (in D_2O), the peaks corresponding to tetrahydropyridine ring protons (H_2-H_6) are considerably sharpened in the 500 MHz ^1H NMR spectrum shown in Figure 2-31.

The double irradiation experiments which led to the unambiguous assignments of the 500-MHz ^1H NMR signals for **17**·HCl and **18**·HCl are described in the following sections.

RESULTS OF DOUBLE IRRADIATION EXPERIMENTS WITH **17**·HCl

The intense doublet of doublets appearing at 1.45 ppm of the spectrum for **17**·HCl (Figure 2-31) was assigned to the C_2-CH_3 protons based on its integration (3 H) and its chemical shift. On irradiation of this signal, the only detectable change in the rest of the spectrum occured in the multiplet at 3.6 ppm (0.5 H) which resulted in assigment of the latter signal to the H_2 axial proton.

Irradiation of the multiplet (1H) at 2.65 ppm resulted in no change of either the C_2-CH_3 doublet (1.45 ppm) or any of the signals from 3.6 to 7.5 ppm. This result established that the proton giving rise to this signal was not coupled to the C_2-CH_3. It's chemical shift and integration dictated its assignment to the H_3 axial proton. Overlap of the decoupler band (~0.3 ppm) obscured possible effects in the signals at 2.95 and 3.0 ppm. Since the doublet at 2.95 ppm could be clearly

attributed to the N-CH_3 protons (split into a doublet due to the diastereotopic nature of the protonated nitrogen atom substituents), the signal at 3.0 ppm was assigned to the H_3 equatorial proton and this assignment was not disputed by the results of the rest of the double irradiation experiments.

On irradiation of the multiplet at 3.6 ppm (0.5 H), which had already tentatively been assigned to H_2 axial, the multiplets at 3.0 ppm and at 2.65 ppm, became a more intense singlet and a more intense symmetrical doublet, respectively. Most importantly, the pair of doublets at 1.45 ppm collapsed to a single doublet indicating that the proton giving the signal at 3.6 ppm was strongly coupled to the C_2-methyl protons and to two other protons which were beta to a nitrogen atom (H_3 axial and H_3 equatorial). These results firmly established the signal at 3.6 ppm as that of the H_2 axial proton.

Unfortunately, due to the band width of the decoupler (0.5 ppm), attempts to selectivly irradiate the multiplet at 3.85 ppm (1.5 H) were unsuccessful. Instead the entire area between 3.6 ppm and 4.1 ppm was irradiated with effects much the same as just described for irradiation at 3.6 ppm. In addition the signal at 6.1 ppm became a sharper, more intense singlet indicating that one of the allylic protons was observed within this group of signals. Thus the multiplet at 3.85 ppm (1.5 H)

was assigned jointly to the H_2 equatorial (0.5 protons) and to the H_6 axial (1.0 proton).

By centering the decoupler band downfield of the doublet at 4.1 ppm (1 H) it was possible to selectively irradiate this signal with only a slight overlap into the signal at 3.85 ppm. As a result the broad singlet at 6.1 sharpened and became more intense, but no signal upfield of 3.85 ppm was affected. The doublet at 4.1 ppm had already been tentatively assigned to the H_6 equatorial proton due to its chemical shift. This evidence that it was coupled to the olefinic proton confirmed the assignment. Theoretically, the H_6 equatorial proton should be geminally coupled to the H_6 axial proton (3.85 ppm) however overlap of the decoupler band caused the effect of irradiation at 4.1 ppm on the H_6 axial proton to be obscured. The geminal coupling of the H_6 axial proton with the H_6 equatorial proton was expected to be the largest coupling (approximately 30 hz) that the H_6 equatorial proton would experience and the likely reason for the doublet appearance of this multi-coupled proton signal.

Irradiation of the broad singlet at 6.1 ppm (1 H) caused the multiplet at 3.85 ppm and the doublet at 4.1 ppm to sharpen slightly but caused no perceptible simplification and no other effect in any of the signals.

Thus with the identity of the signal at 3.6 ppm firmly established as the axial proton coupled to the

newly introduced methyl group, its relative upfield chemical shift and integration (only 0.5 protons, consistant with the single H_2 proton which would be observed as 0.5 axial and 0.5 equatorial protons) indicated that this pure compound was indeed **17**·HCl.

RESULTS OF DOUBLE IRRADIATION EXPERIMENTS WITH **18**·HCl

The 500-MHz NMR spectrum of **18**·HCl is displayed in Figure 2-33. The first signal irradiated in this series of experiments gave the largest piece of evidence that this compound was indeed **18**·HCl. This came from irradiation of the pair of doublets 1.5 ppm (3 H) which been assigned to the C_6-methyl protons. By centering the decoupler band on the upfield side of this pair, the doublet at 1.45 ppm was selectively irradiated with the result that the broad singlet at 4.25 ppm (0.2 H) was both sharpened and intensified. By centering the decoupler band to the downfield side of this pair of doublets, the doublet at 1.55 ppm was selectively irradiated which caused the broad singlet at 4.0 ppm (0.8 H) to sharpen and intensify. These two experients identified the signals at 4.0 ppm and at 4.25 ppm as those due to the H_6 axial and equatorial protons, respectively, which are vicinally coupled to the C_6-methyl group. In contrast to the spectra observed with **17**·HCl where the H_2 proton was evenly split between the

axial and equatorial populations, with **18**·HCl the H_6 axial proton (4.0 ppm) was observed as 80% of the H_6 proton population while the H_6 equatorial proton (4.25 ppm) was observed as 20% of the H_6 proton population.

Irradiation of the multiplet at 2.8 ppm (2 H) caused changes in three other signals including; 1) simplification of the multiplet at 3.45 ppm to a doublet, 2) simplification of the multiplet at 3.55 ppm to a singlet and 3) simplification of the multiplet at 3.75 ppm to a doublet. In toto, the multiplets from 3.45 ppm to 3.75 ppm integrated for two protons. Thus the signal at 2.8 ppm which also integrated for two protons and which was clearly coupled to two other protons at a more downfield chemical shift was assigned to the H_3 axial and equatorial protons. Likewise, the signals at 3.45 to 3.75 ppm were assigned to the H_2 axial and equatorial protons.

Due to the width of the decoupler band (0.4 ppm) it was not possible to selectively irradiate each of the signals from 3.4 to 3.8 ppm. However, irradiation of the region between 3.4 to 3.8 ppm caused no identifiable change to signals outside of that region which would be consistant with the proton assignment discussed above.

Irradiation of the broad singlet at 4.0 ppm (0.8 H) caused collapse of the doublet at 1.55 ppm to a singlet, and intensification of the doublet at 6.1 ppm. This behavior on irradiation confirmed the identity of the

signal at 4.0 ppm as belonging to the H_6 axial proton of **18**·HCl which should be coupled to both the C_6 methyl protons and the H_5 olefinic proton. Likewise irradiation of the broad singlet at 4.25 ppm (0.2 H) caused collapse of the doublet at 1.45 ppm to a singlet but no discernable enhancement of the olefinic proton signal at 6.1 ppm. This evidence was consistant with the assignment of the broad singlets at 4.0 and 4.25 ppm as the H_6 axial and equatorial protons respectively. The low field position of this signals, (consistant with allylic character) and the fact that they are coupled to both the C_6 methyl protons and to the olefinic proton H_5 are fully consistant with the characterization of this compound as **18**·HCl.

SYNTHESIS OF 1,2-DIMETHYL-4-PHENYL-2,3-DIHYDROPYRIDINIUM PERCHLORATE, **15**

Dihydropyridine compounds are synthetically accessible by a variety of methods. A very interesting class, the 1,4-dihydropyridines substituted with electron withdrawing groups at the 3 and 5 positions, such as nifedipine, **68**, have shown pharmaceutical promise as calcium channel blockers and are sufficiently stable to be formulated and marketed.[145] In contrast, those dihydropyridines which do not contain electron withdrawing substituents are very unstable and are usually intermediates in the synthesis of pyridine

derivatives.[136] $MPDP^+$ is an example of a substituted 2,3-dihydropyridinium ion which has been isolated and purified as its perchlorate salt. Since $MPDP^+$ ClO_4^- is sufficiently stable to permit isolation, it was expected that the perchlorate salt of **15** would exhibit similar stability. Our interest in the potential role of $MPDP^+$ in the neurotoxic effects of MPTP prompted a desire to compare the biological properties of $MPDP^+$ with its methyl substituted analog **15**. Because of the steric effects of introduction of a methyl group on potential MAO-substrate interactions we had good reason to believe that the MAO substrate properties of the methyl-substituted tetrahydropyridines **17** and **18** would be significantly different from the parent compound MPTP. However we had little knowledge of the basis for the toxic effects of $MPDP^+$. Since $MPDP^+$ is a highly activated molecule, susceptible to oxidation, disproportionation and alkylation, its toxic effect might be quite structurally non-specific. If this is the case the additional methyl group in compound **15** would not be expected to interfere with these properties. However if the toxic effects of $MPDP^+$ were due to its interaction with enzyme systems, these, like MAO substrate activity, might be substantially altered by addition of the methyl group. Thus synthesis of **15**·ClO_4 would afford us the opportunity to begin to probe the structural specificity, and perhaps the basis for $MPDP^+$ toxicity.

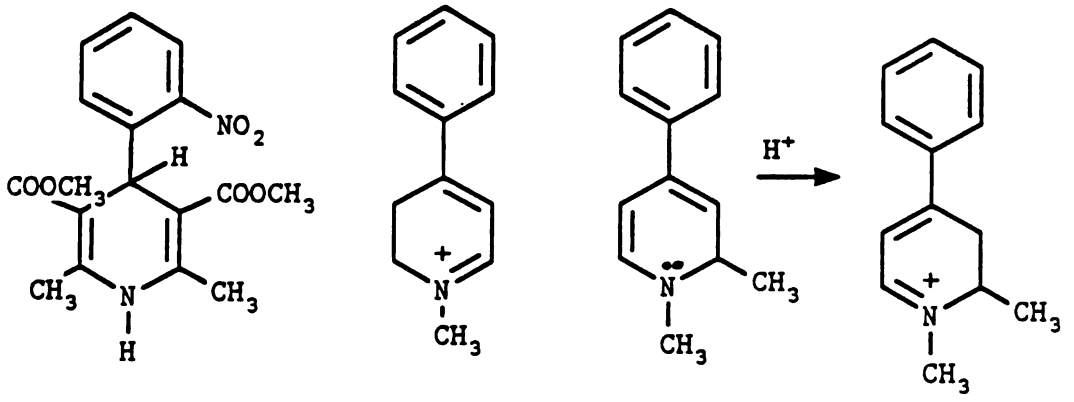

68 MPDP$^+$,5 14 15

Our experience with UV monitoring of the Grignard reaction of methylmagnesium bromide and MPP^+ had shown that the dihydropyridine product **14** could be rapidly protonated in aqueous HCl to give a solution of **15**·HCl which was stable to disproportionation. We observed disproportionation (Scheme 2-7) when the Grignard reaction mixture was slowly protonated allowing time for the interaction of **14** with **15** and **16**. Thus we felt the disproportionation was an event related to the speed of acid addition.

Our initial synthetic strategy to obtain **15**·ClO_4 involved the rapid addition of methanolic perchloric acid to the dihydropyridine **14**, formed by Grignard reaction of methylmagnesium bromide with MPP^+, which we expected to yield the stable salt of **15**. Use of methanol, which is miscible in ether, would avoid the biphasic reaction medium which was believed to promote disproportionation. A UV spectrum (Figure 2-36) of the products of this

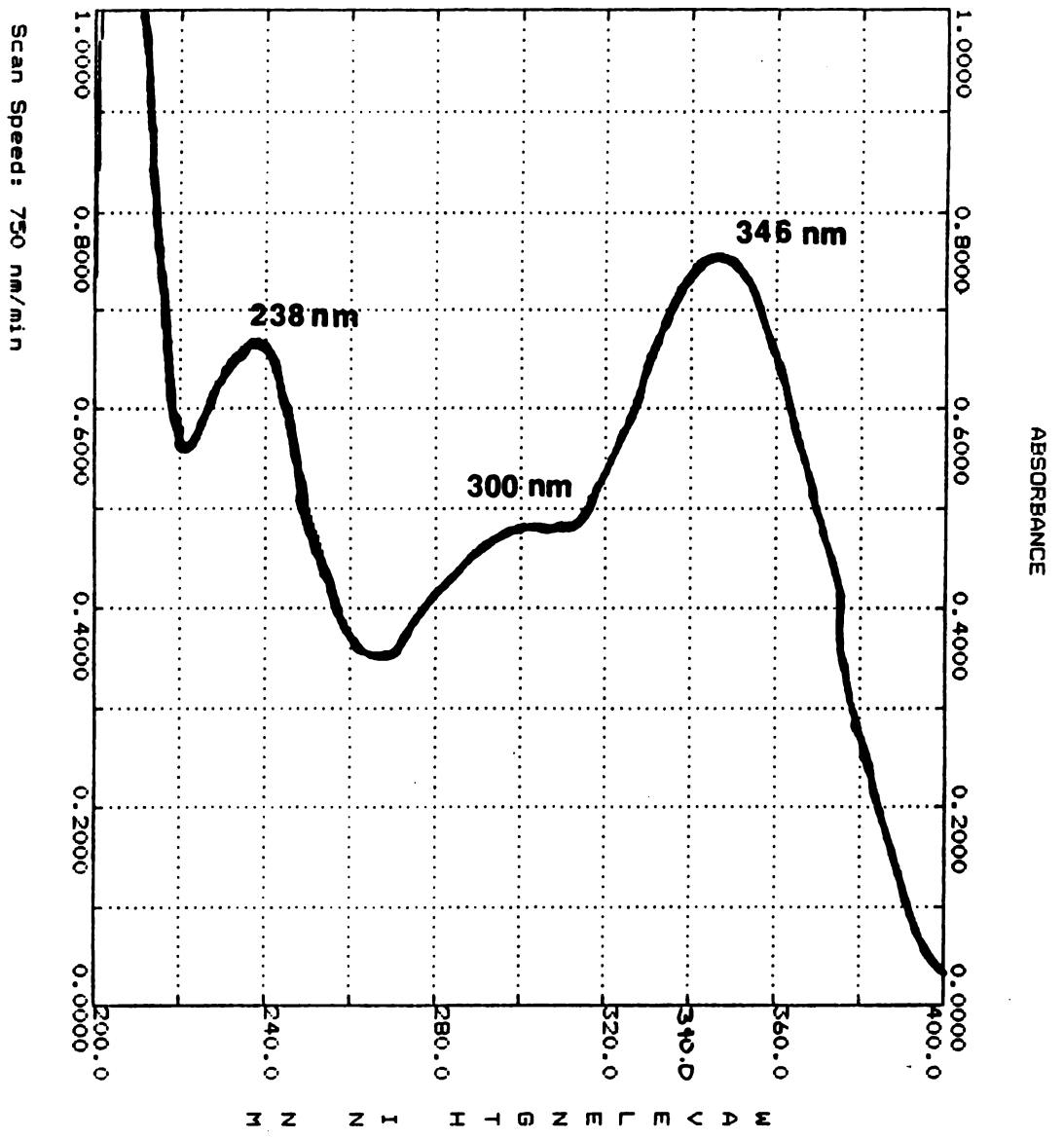

Figure 2-36. UV spectrum of the products of addition of methanolic perchloric acid to 1,2-dimethyl-4-phenyl-1,2-dihydropyridine (14)

sequence, however, showed the presence of tetrahydropyridine (UV max 240 nm) and pyridinium (UV max 285 nm) in addition to the desired dihydropyridinium product (UV max 340). Apparently, when the acid was added to the dihydopyridine, the disproportionation reaction proceeded too rapidly for quantitative recovery of dihydropyridinium salt **15**.

$MPDP^+$ has been synthesized via treatment of the cyano adduct **69** with perchloric acid which promotes the elimination of HCN and formation of the conjugate diene product. Thus another possible synthetic route to **15** involved the synthesis and purification of the corresponding cyano adduct **70**. When the crude dihydropyridine **14** was treated with aqueous perchloric acid followed by addition of potassium cyanide a mixture of products resulted. The 80 MHz ^1H NMR spectrum, (Figure 2-37), was interpreted as an indication of the presence of a mixture of cyanotetrahydropyridine compounds. In particular the presence of partially resolved doublets in the region 1.0-1.4 ppm was taken as evidence for the presence of diastereomeric compounds bearing a C_6 methyl substituent such as **70,71** and their respective diasteromers. The multiplet signal at 4.4 ppm was assigned to the H_6 proton, alpha to the cyano moiety.

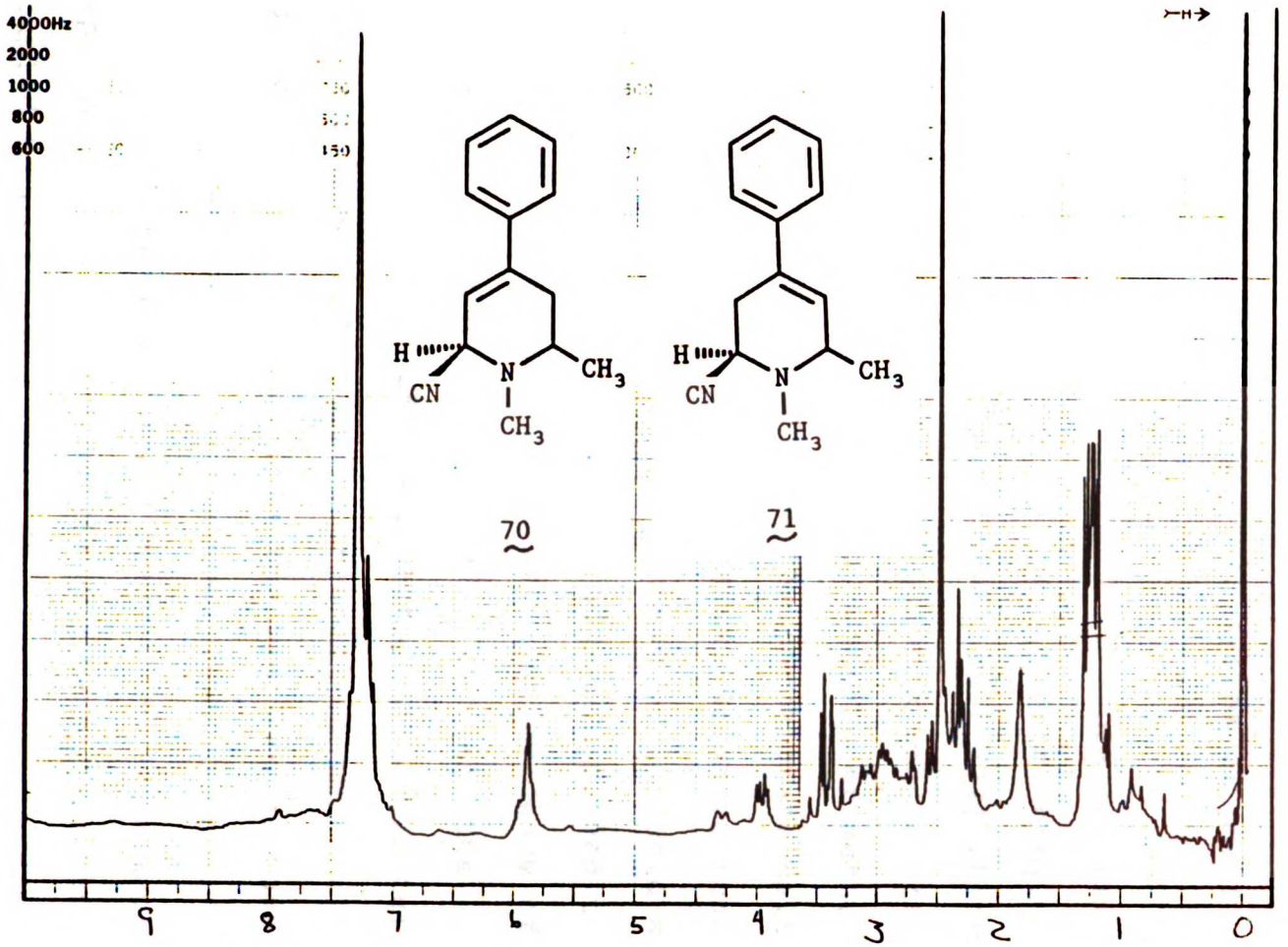

Figure 2-37. 80-MHz ^{1}H NMR (CD_3CN) spectrum of a mixture of cyano-adducts of **15** and **16**.

The UV spectrum of this mixture of products showed a single maximal absorption at 248 nm, consistant with the spectrum of the suspected products. Unfortunately the cyanotetrahydropyridines proved to be unstable to silica gel chromatography and no other system of purification was devised.

The report by Fry (1963[34]) of isolation and purification of the crystalline 1,4,5-trimethyl-2-benzyl-2,3-dihydropyridinium perchlorate salt (**72**) which is structurally related to **15** prompted a second effort to trap the product of a Grignard reaction of methyl magnesium bromide on MPP^+ as the perchlorate salt. In this instance however, the ethereal Grignard reaction mixture was added to a large excess of ice cold aqueous perchloric acid. The order of addition proved to be the key to the sucess of this effort. No evidence of disproportionation was observed. Instead, the perchlorate salt of **15** was isolated and characterized as a pale yellow, hygroscopic, crystalline material. Doublet signals arising from the olefinic protons H_5 and H_6 were a key feature in the spectrophotometric identification of **15**$\cdot ClO_4$ (Figure 2-38). Decoupling experiments indicated that the H_5 and H_6 protons were coupled to each other (Jvic 5Hz), as anticipated for the 2,3-dihydropyridinium structure. The UV spectrum of **15**$\cdot ClO_4$ displayed a maximal absorbance at 349 nm (extinction coefficient 15,600). In comparison, $MPDP^+$

has a maximal absorption at 345 nm (extinction coefficient 17,400).

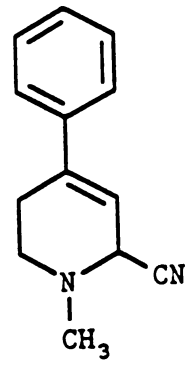

69

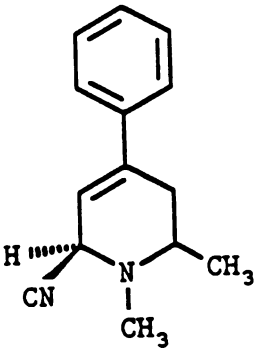

70

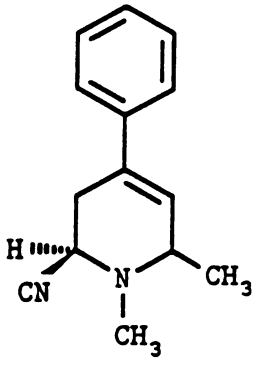

71

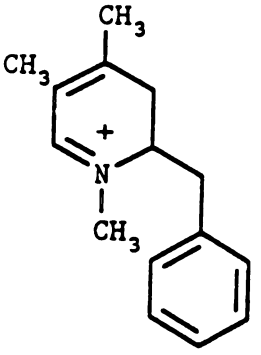

72

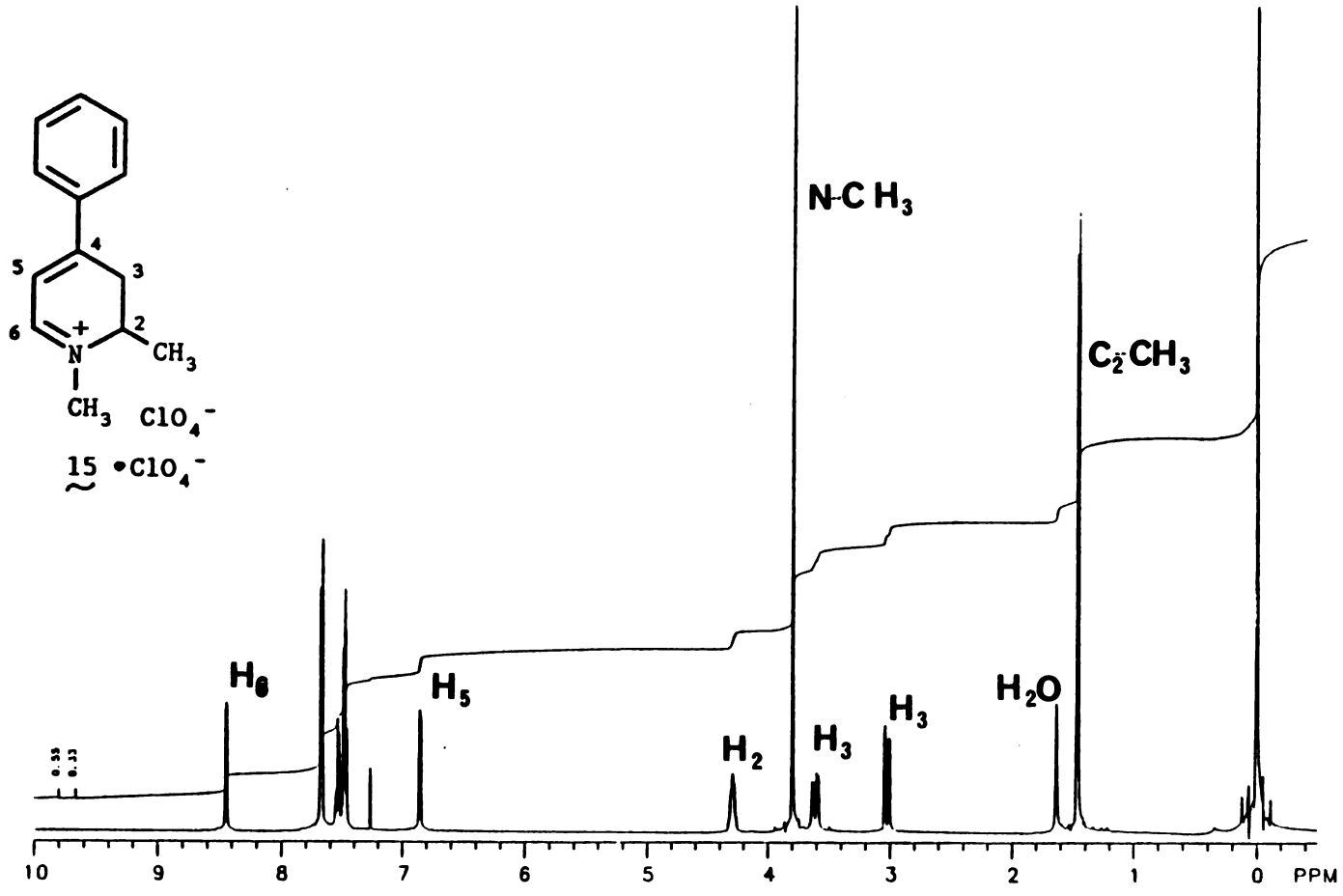

Figure 2-38. 500-MHz ^{1}H NMR ($CDCl_3$) spectrum of 1,2-dimethyl-4-phenyl-2,3-dihydropyridinium perchlorate (**15**·ClO_4^-)

BIOLOGICAL EVALUATION OF TETRAHYDROPYRIDINES 17, 18, AND ANALOG METABOLITES 15 AND 60

Long before the synthetic work described above was completed, the biological evaluation of **17** and **18** had begun. Unwittingly, the initial evaluation of the tetrahydropyridines was begun with a sample containing 85% **17** and 15% **18**. Initial efforts focused on the MAO B substrate activity of the sample. The mixture was then evaluated as a mouse dopaminergic neurotoxin in the mouse dopamine depletion model and as a cytotoxin in the rat isolated hepatocyte model. Not until the 500-MHz NMR spectra of this sample were obtained was it discovered that the sample was a mixture. This discovery spurred efforts to develop the separation techniques and synthetic routes described above. Subsequently, the biological assays performed on the mixture were repeated on the pure samples of **17** and **18**. The only exception was the mouse neurotoxicity data. In light of the data obtained with purified **17** and **18** with MAO, the original neurotoxicity results from the mixture of **17** and **18** were not expected to differ significantly from those of the pure compounds. In the interest of avoiding unnecessary animal sacrifice, the neurotoxicity experiments were not repeated with purified **17** and **18**.

PURIFICATION OF MAO B

In order to evaluate the interaction of new tetrahydropyridine compounds with MAO B, the enzyme was prepared from beef liver mitochondria by the method described by Salach.[36] Beef liver mitochondria were used because they supply the pure B form of the enzyme. The mitochondrial membranes were freed from intramitochondrial protein by lysis and washing and were digested with phospholipases A and C to liberate the MAO which is membrane bound. Differential centrifugation, followed by extraction into a detergent buffer served to separate undesired membrane proteins from the MAO B. The partially purified protein was then further purified by a polymer partitioning procedure which separates proteins roughly according to density. MAO B forms a solid interface between two layers of the polymer and is readily isolated. This method resulted in a 100-fold increase in specific activity from membranes (0.023 Units/mg protein to 2.05 Units/mg protein). During the purification, enzyme activity was monitored using the spectrophotometric MAO activity assay described by Tabor et al.[46] using benzylamine as substrate.

INTERACTION OF 17 AND 18 WITH MONOAMINE OXIDASES A AND B

Strong evidence was presented by Chiba et al.[4] that MPTP is metabolized by MAO B. The product of the 2 electron oxidation was first suggested and then proven by

Castagnoli et al. to be $MPDP^+$.[37] Conveniently, $MPDP^+$, with its long conjugated system of double bonds, absorbs strongly at 343 nm making it's spectrophotometric detection practical. This has formed the basis of the UV assay of MAO substrate activity assays for tetrahydropyridines. The possibility exists, however, that MPTP might be oxidized not at the allylic carbon (C_6 in MPTP) but at the other carbon atom alpha to nitrogen, C_2. In this instance oxidation of substrate would not be detected by the UV assay since the oxidation product, the 1-methyl-4-phenyl-2,5-dihydropyridinium ion (**54**), is likely to have the same UV spectrum as MPTP since it contains the same styrene type chromophore (UVmax 240 nm).

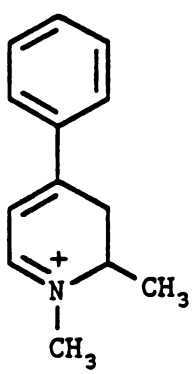

15

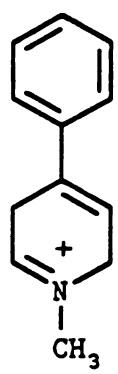

54

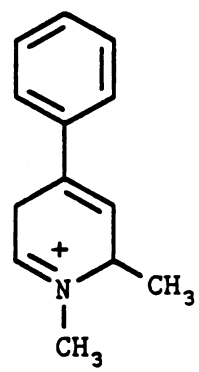

16

Although oxidation at the non-allylic carbon atom seems unlikely, the occurance can be detected by use of the Clark type oxygen electrode, since molecular oxygen is a required co-substrate of MAO. An assay of enzyme activity based on oxygen consumption is less sensitive

than the UV assay and requires the use of more enzyme so it is not used for routine screening. The oxygen consumption assay, however, can be used to explore further (and perhaps confirm) the lack of substrate activity in compounds identified as poor substrates by the UV assay.

The interaction of the 85:15 mixture of **17** and **18** with MAO B was evaluated using the UV assay, monitoring for an increase in absorbance at 343 nm and the mixture did not exhibit substrate activity. An additional experiment was performed in which the absorbance at 290 nm was monitored. Increase of absorbance at this wavelength would have indicated enzyme catalysed production of the 4 electron oxidation product the pyridinium species **60**. However again the results indicated no substrate activity.

Evidence of the mixed nature of the sample opened the possibility that the 15% contamination by **18** inhibited the enzyme, with the effect of masking potential substrate activity of **17**. Indeed the mixed sample displayed moderately potent competitive inhibitor properties (Ki 378 uM) when assayed against the MAO B catalysed oxidation of MPTP (0.2-3.2 mM) as shown in the plot in Figure 2-39.

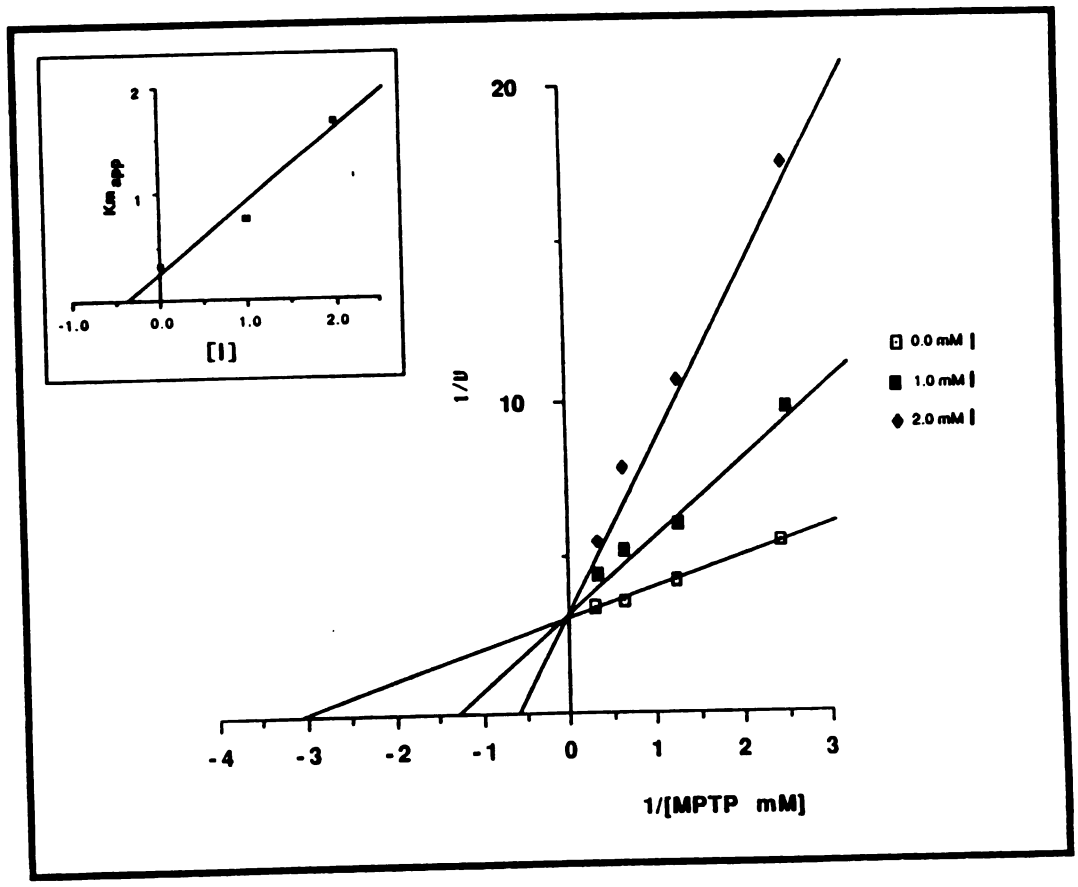

Figure 2-39. Competitive inhibition of MAO B catalyzed MPTP oxidation by a mixture of **17**·HCl and **18**·HCl (85:15), Ki 378 uM.

According to Michealis-Menton kinetics, competitive inhibition (where inhibitor competes with substrate for binding on the enzyme) will result in lines in a plot of 1/velocity versus 1/substrate concentration which intersect on the 1/velocity axis.[124] As the inhibitor concentration is increased, the apparent Km of substrate for enzyme is increased due to competition with the inhibitor. Thus in the presence of a given inhibitor concentration the 1/velocity versus 1/substrate line gives a new intersection with the x axis ($-1/Km_{apparent}$).[124] A plot of $Km_{apparent}$ versus inhibitor concentration (0-2.0 mM, inset in Figure 2-39) was used to calculate the Ki (identified as the negative reciprocal of the y intercept) for the tetrahydropyridine mixture.[124]

The Ki for a competetive inhibitor may be considered to be an affinity constant which indicates the binding affinity of the inhibitor molecule for the enzyme. While it does not indicate high potency, the Ki obtained for the mixed tetrahydropyridines (378 uM) does compare favorably with the reported Km of MPTP (330 uM)[5] as a substrate for MAO B. This indicates that the methyl substituted tetrahydropyridines gain access to the MAO B active site and bind nearly as tightly as does MPTP.

MPTP, a non-classical substrate of MAO B, was chosen as the substrate for this study because the chromophore of the oxidation product lacks significant absorbance at

240 nm. Normally inhibitor studies should be performed with the classical substrate of the enzyme of interest, which is benzylamine in the case of MAO B. Use of a standard substrate in inhibitor studies results in data which can be compared with reported values. However, use of benzylamine as substrate in inhibitor studies with tetrahydropyridines is technically difficult because the UV assay depends upon the detection of the oxidation product benzaldehyde (**42**) by monitoring the enzyme catalysed increase of absorbance at 250 nm. The candidate inhibitor tetrahydropyridines also absorb at this wavelength and since they must be present in the assay medium in micromolar to millimolar quantities, their absorbance interferes with detection of the increase of absorbance of benzaldehyde. It should be noted, however, that no such interferance exists with the use of benzylamine as a substrate in inhibitor studies of tetrahydropyridines conducted with the oxygen electrode.

The competetive nature of the inhibition observed with the tetrahydropyridine mixture indicated that **17** and/or **18** were able to gain access to the MAO B active site, although the enzyme was unable to catalyze their oxidation. The possible selective inhibition of the enzyme by **17** or **18** could be examined once the pure substances had been obtained. Table 2-4 lists the results obtained from assays of the substrate activities of compounds **17** and **18**. Compound **17** was assessed as a

substrate for both MAO A (kindly supplied by Dr. James I. Salach) and MAO B and was shown to be extremely slowly oxidized by each enzyme. In comparison with the turnover rates for the standard substrates of each enzyme (kynuramine for MAO A, and benzylamine for MAO B), the turnover rate of **17** is so slow that, in practicality, it must be termed a non-substrate of both forms of the enzyme. The assays performed with the oxygen electrode demonstrate that oxidation to a 2,5-dihydropyridinium species such as **16**, which would not have been detected by the UV assay but which is detectable by oxygen consumption measurments, does not occur with **17**. Compound **17** was tested as a substrate for MAO A because the A form of the enzyme is found in the striatal region of the brain which is susceptible to damage by MPTP.

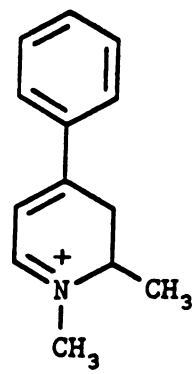

15

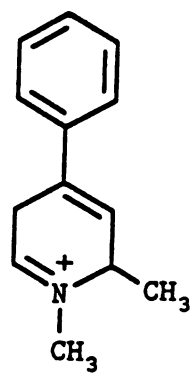

16

Table 2-4. MAO A and B substrate activity of **17** and **18**

Compound number	MAO isozyme	Assay type	Turnover
17	MAO A	UV	0.58
		O_2 consump.	0.44
17	MAO B	UV	1.7
		O_2 consump.	0.7
18	MAO B	UV	5.0
Kynuramine	MAO A	UV	120
Benzylamine	MAO B	UV	530
MPTP	MAO A	UV	14
	MAO B	UV	197

Turnover numbers are reported in units of moles product formed per mole enzyme per min. Turnover numbers were determined in the spectrophotometric assay using 41 picomoles MAO B; or in the oxygen consumption assay using 1.2 nmole MAO B or 0.66 nmole MAO A. All turnover determinations were made under saturating substrate conditions (5 mM).

Although MPTP is more rapidly oxidized by MAO B than by the A form, the contribution of the A form in production of toxic metabolites is not negligible. These results indicate, however, that a methyl group placed at C_2 of MPTP is detrimental to MAO substrate activity in both forms of the enzyme.

Although the turnover number is slightly higher for compound **18** in the presence of MAO B, the oxidation still occurs at less than 1% of the rate at which MPTP is oxidized by the same enzyme. Furthermore, although **18** is oxidized faster in the presence of MAO B than in the

absence, no linear dependence of oxidation rate on enzyme concentration could be demonstrated. A small but measurable rate of auto-oxidation of **18** (0.132 nmole per min), to form a product absorbing at 343 nm, was observed in the absence of protein. The auto-oxidation, which is concentration dependent, may account for at least 50% of the turnover of **18** to product observed in the presence of enzyme.

All of the studies described above were carried out under the standard conditions of MAO activity assays, at pH 7.2. As discussed above, introduction of an additional methyl group alpha to the nitrogen will affect the acidity of protons alpha to the nitrogen and will affect the basicity of the nitrogen lone pair as well as changing the steric characteristics of the molecule. In an effort to determine which of these effects were dominant in the loss of substrate activity on introduction of a methyl group into MPTP, an MAO B enzyme assay under more basic conditions (pH 9) was developed. At pH 9, MAO B retains 82% of the activity observed at pH 7.2, using benzylamine as substrate. According to the Henderson-Hasselbalch equation, the ratio of free base/protonated amine for any amine at pH 9 is 100 fold higher than at pH 7.[125] Thus the effect of the additional methyl group in **17** and **18** on the basicity of the tetrahydropyridine nitrogen atom and on the acidity of the protons alpha to the nitrogen atom should be much

less important. Only the steric effect of the methyl groups remains the same under both sets of pH conditions. Neither compound **17** or **18** showed any significant rate of oxidation in the presence of MAO B at pH 9. This result indicates the importance of the steric effect at the 2 and 6 positions on the MAO B catalysed oxidation of MPTP and related compounds. Increased steric bulk interferes with proper alignment of substrate and flavin cofactor in the active site of the enzyme. These results indicate that the enzyme active site experiences a very tight fit with MPTP allowing very little tolerance for increased size of the molecule near the nitrogen atom.

The results obtained earlier on the inhibitor properties of the C-methyl substituted tetrahydropyridines indicated that these compounds had access to the enzyme active site. When these studies were repeated with the purified tetrahydropyridine samples, inhibition was still observed as shown by Figures 2-40 and 2-41 (See Figure legends for more details). The intersection of the families of reciprocal plots lie to the right side of the 1/v axis for both compounds. The type of inhibition cannot therefore be characterized as purely competitive but instead is a mixed-type inhibition with some competitive character. With mixed-type inhibition, calculation of a Ki value is very complicated.

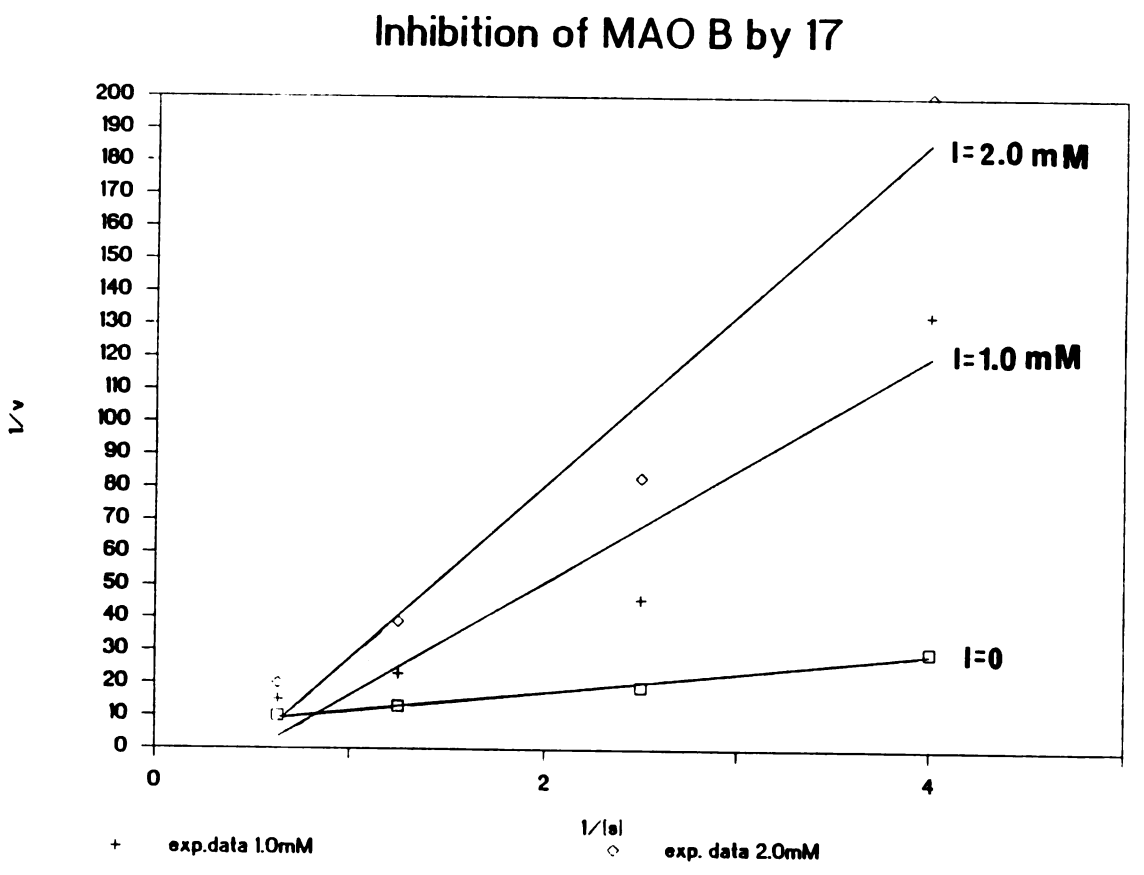

Figure 2-40. Inhibition of MAO B catalyzed MPTP (0.25-3.2 mM) oxidation by pure **17**·HCl (0.5-2.0 mM). Assays performed in triplicate.

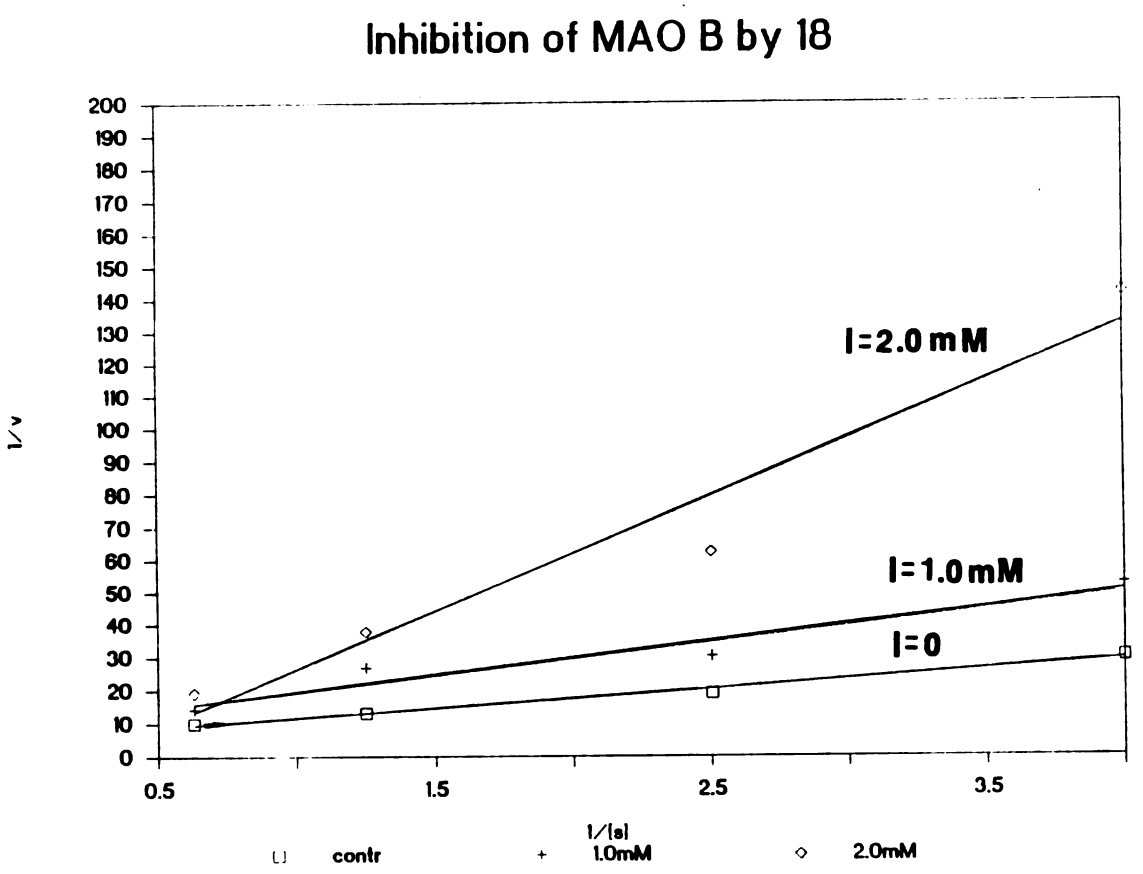

Figure 2-41. Inhibition of MAO B catalyzed MPTP (0.25-3.2 mM) oxidation by pure **18**·HCl (0.5-2.0 mM). Assays performed in triplicate.

Therefore, in order to compare the inhibitory potency of the mixed tetrahydropyridine sample which we had previously examined with the purified samples of **17** and **18**, we turned to IC_{50} calculations. Since the IC_{50} of an inhibitor is dependent on the concentration of substrate present, we compared the IC_{50} values calculated for each sample at a single saturating concentration of substrate (MPTP 3.2 mM) from data shown in Table 2-5

TABLE 2-5. Effect of **17**, **18** and mixed **17** + **18** (85:15) on the velocity of MAO B catalysed oxidation of MPTP

Inhibitor	[I]	velocity[c]	%Inhibition	IC_{50}
17+18 [a]	0 mM	0.296[c]	0%, control	
	1.0 mM	0.225	20 %	
	2.0 mM	0.183	40 %	2.53 mM
17 [b]	0 mM	0.100	0%,control	
	0.5 mM	0.090	10%	
	1.0 mM	0.070	30%	
	2.0 mM	0.060	40%	2.33 mM
18 [b]	0 mM	0.100	0%, control	
	0.5 mM	0.099	1%	
	1.0 mM	0.074	26%	
	2.0 mM	0.065	30%	2.62 mM

All assays used [S] = 3.2 mM MPTP
a) Mixed **17** and **18** were assayed using 0.053 units MAO B per determination
b) Pure **17** and pure **18** were assayed using 0.018 units MAO B per determination
c) velocity is reported as optical absorbance units per minute
d) IC_{50} calculation used least squares linear regression of velocity versus [I], solved for v=0.5(control v)

The IC_{50} values calculated for the pure samples of **17** and **18** are nearly equivalent at 2.33 mM and 2.64 mM, respectively. The IC_{50} value for the mixed sample of **17**

and **18** is essentially equivalent to the mathematical average of the values for pure **17** and pure **18** as might be expected. Of the three samples, the 2-methyl substituted tetrahydropyridine is the most potent inhibitor by a slight margin. However, none of the samples are particularly potent inhibitors.

These results indicate that placement of a methyl group alpha to the nitrogen atom essentially abolished the substrate activity of MPTP regardless of whether it is placed on the allylic or the non-allylic apha carbon atom. Since the Ki obtained for the mixed tetrahydropyridine sample compares favorably with the Km of MPTP we can conclude that the methyl substituent does not interfere with access to the enzyme active site. Thus reduced access is not the basis for abolition of substrate activity. Furthermore, our studies of enzyme activity at pH 9 indicated that the loss of substrate activity was not due to the influence of the additional methyl group on the pKa of protons alpha to the nitrogen group. We conclude that the effect of additional methyl groups may be to increase steric hindrance at the active site of the enzyme. Thus although the methyl-substituted tetrahydropyridine is able to gain access to the MAO B active site, the additional methyl group sterically inhibits proper alignment of essential enzyme functional goups with the FAD cofactor so that the enzyme is rendered catalytically incompetant.

INTERACTION OF **15**·ClO_4 WITH MAO B

$MPDP^+$ has been reported to be a substrate of both MAO A and MAO B.[61] In veiw of the effect of methylation on the substrate activity of tetrahydropyridines it was of interest to assess the activity of the methyl-substituted dihydropyridinium, **15**·ClO_4, as a substrate of MAO B. The incubation of **15**·ClO_4 0.56 mM with MAO B (26 picomole, 0.013 units) in sodium phosphate buffer was followed spectrophotomentrically for the formation of the expected oxidation product, **60**·ClO_4. Although a slow rate of oxidation was detected, less than 0.8 umole per minute, it was not different from the rate of oxidation of **15**·ClO_4 at the same concentration in the absence of protein. It was concluded from this study that **15**·ClO_4 is not a substrate of MAO B and that the slight oxidation observed is due to auto-oxidation or disproportionation. Apparently methyl-substitution has abolished substrate activity in this class of substrates as well as in the tetrahydropyridines.

NEUROTOXICITY OF **17** AND **18** IN THE C57 BLACK MOUSE

As discussed in the introduction to this dissertation, one of the most valuable, though tragic, discoveries connected with the MPTP story has been the developement of a human model of Parkinson's disease. The hope has arisen that through research on the

mechanism of MPTP induced Parkinsonism the cause and possible prevention of idiopathic Parkinson's disease may be discovered. The need for a suitable animal model of MPTP induced parkinsonism spurred efforts of many research groups. Langston et al. demonstrated the neurotoxic effect of MPTP in the production of a parkinsonian syndrome in the squirrel monkey which was accompanied by histochemical evidence of nerve cell loss restricted to the substantia nigra.[38] Markey et al. showed similar results in the rhesus monkey.[39] The primate provides an excellent mimic of the behavioral and biochemical effects of MPTP in human including a parkinsonian syndrome of ridigity, loss of facial expression as well as severely depressed striatal dopamine levels, effects observed after administration of as little as 2 mg per kg bodyweight (cumulative dose). MPTP is a very potent dopaminergic neurotoxin in the primate. Unfortunately the specialized care and expertise required for primate maintainance renders this model inaccessable to many research groups including our own. For this reason the behavioral and biochemical effects of MPTP have been investigated in other animal models including the beagle dog,[40] the medicinal leech,[41] guinea pig,[42] and several varieties of rat and mouse. While the rat is not susceptible to MPTP-induced dopaminergic neurotoxicity after peripheral administration, intranigral administration results in

specific dopaminergic neuronal destruction. [43,44] In contrast, Heikkila and others have shown that the mouse exhibits dopaminergic neurotoxicity in the form of a severe and long lasting depletion of striatal dopamine levels after intraperitoneal administration of MPTP.[48,49,50] Up to 40 days after treatment, striatal dopamine levels of treated mice remained as low as 10% of the control values. The depletion of dopamine in the striata of treated animals is thought to reflect dopamine neuronal destruction induced by MPTP. The long lasting nature of the effect distinguishes it from transient dopamine depletion observed after treatment with amphetamine, a catecholamine releasing agent which does not induce neuronal destruction, or resperpine, a reversible catecholamine depletor. Heikkila[159] has reported histochemical evidence of dopamine nerve terminal destruction, though other research groups have been unable to confirm this result.[160]

The dose of MPTP required to induce neurotoxicity in the mouse (60-150 mg/Kg body weight, total cumulative dose) is at least an order of magnitude greater than the dose required for the same effect in primate (2 mg/Kg). Recently, a correlation between species susceptibility to the toxic effects of MPTP and levels of MAO in brain microvessels has been proposed by Sayer et al.[51] The levels of monoamine oxidase and monoamine oxidase catalysed MPTP oxidation are very high in the rat brain

microvessel, the walls of the blood brain barrier. The rat's relative insusceptibility to the toxic effects of MPTP has been proposed to be related to the rapid oxidation of MPTP at the rat blood brain barrier. Conversion of MPTP to MPP^+, a highly polar compound with severely restricted diffusion capability, limits the exposure of rat striatum to the toxic compound. The microvessels of highly susceptible human brain have been shown to process MPTP to MPP^+ very inefficiently, allowing more of the toxic compound to reach the striatal tissue.[51] Mouse microvessels process the compound more efficiently than human but less than rat resulting in the intermediate susceptiblity of mouse to MPTP's neurotoxic effects.[51] MAO catalysed oxidation of MPTP located in the microvessels is proposed to act as a protective effect in mammals since MPP^+ and $MPDP^+$, the toxic metabolites, may be excreted into the blood for removal by the kidney.[51] The toxic effects of $MPDP^+$ and MPP^+ in the epitheleal cells of the microvessel may be the same as in the striatum but since epitheleal cells are reproduced, the long term effects are less damaging as epithelial cells killed by the toxin can be replaced.

We chose to examine the effects of the methyl substituted tetrahydropyridines in the more accessible C57 black mouse dopamine depletion model. These studies were performed as a collaborative effort with Ellen Wu, Ph.D and Kim Hoag, Ph.D of the Department of

Pharmacology, University of California, San Francisco. Initially, a protocol of 10 mg/Kg IV injection, via the mouse tail vein, twice daily for 3 days was attempted. One week after the last injection the mice were sacrificed, the cortex and neostriatum were harvested, and the levels of dopamine and norepinephrine assayed by reversed phase HPLC with electrochemical detection. With MPTP, this protocol produced a 91% depletion of striatal dopamine, compare to controls. Injection of 10 mg/Kg **17** and **18** (85:15), was lethal in the mouse. To reduce the acute toxicity and morbidity associated with the methyltetrahydropyridine treatment, the regimen was changed to an IV injection of 5 mg/Kg twice daily for 3 days with sacrifice 1 week after the last injection. The effects of this treatment on mouse striatal dopamine are summarized in Table 2-6. Under these conditions MPTP produced a significant depletion (81.5%) in the levels of striatal dopamine relative to the control values. The methyl-substituted tetrahydropyridine mixture produced a very small depletion of dopamine (8.3%).

Table 2-6. Effects of **17**, **18** (85:15) and MPTP on mouse striatal dopamine

Compound	Trial number	Dopamine ng/mg tiss.	Average Dopamine ±(SEM)	% Depleted
Control	1	13.79		
	2	16.29	15.04	
MPTP	3	2.68		
	4	3.16		
	5	2.49	2.78±(0.20)	81.5%
17,18	6	15.01		
	7	14.04		
	8	12.30	13.78±(0.76)	8.3%

Treatment with MPTP, as well as the mixture of **17** and **18**, also produced a slight increase in cortical norepinephrine levels, compared to the control animals. This increase, (MPTP, 32%; **17,18**, 26%), may be explained by the competition of tetrahydropyridines for monoamine oxidase active sites in the brain, reducing the rate of deamination of brain neurotransmitters such as norepinephrine.

Compounds **17** and **18** proved to be non-toxic to the mouse neostriatum as evidenced by the lack of a significant depletion of striatal dopamine. This result, together with the fact that the tetrahydropyridines had been shown to be non-substrates of MAO, was consistant with the theory that MPTP and other tetrahydropyridines must be biotransformed to the species which mediate the neurotoxic effect.

CYTOTOXICITY OF 17, 18 AND ANALOG METABOLITES 15 AND 60 IN THE FRESHLY ISOLATED RAT HEPATOCYTE PREPARATION

The availability of **17**, **18** and the corresponding methyl substituted metabolite analogs, dihydropyridinium **15** and pyridinium **60**, provided us the opportunity to compare the cytotoxicity of each species in the isolated rat hepatocyte preparation. This well characterized preparation has been used by Smith et al. to compare the cytotoxic characteristics of MPTP, $MPDP^+$ and MPP^+.[52] Rat hepatocytes are isolated by incubation of the liver tissue with collagenase to produce a suspension of viable cells. The cells are then exposed to candidate toxins, and the effects of the toxins on cell viability are assessed by exposure to trypan blue. Dead cells, which have lost the ability to exclude the dye, can be counted with an optical microscope and the toxic effect expressed quantitativly as a percentage of the control viability. This *in vitro* assay is especially advantageous in the study of pyridinium compounds which are very polar and cannot be studied with most *in vivo* techniques. The compounds can be placed directly into the cell suspension, eliminating most of the access barriers inherent in *in vivo* toxicity assays. In addition, easy quantitation allows the rank ordering of cytotoxic potency. Cytotoxicity observed in hepatocytes may have relevance to neurotoxic effects as the mechanism of cell

death may well be the same, regardless of the cell type studied. Figure 2-42 illustrates the effects of MPTP (1.5 mM), $MPDP^+$ (1.5 mM), and MPP^+ (1.5 mM) on hepatocyte viability as measured by trypan blue exclusion.[52] The loss of cell viability ultimately occured in 100% of hepatocytes after the addition of any of the three compounds but was most rapid after $MPDP^+$ exposure, and occured only after a relatively long lag period in the presence of MPP^+.[52]

Figure 2-43 illustrates the results of similar studies with **17**, **18**, **15**, and **60**, (each at 1.5 mM), performed in collaboration with Dr. Donato Dimonte, Department of Biomedical and Environmental Health Sciences, School of Public Health, University of California, Berkeley, CA. In these studies, the tetrahydropyridines **17** and **18** show no cytotoxic effect, cell viability being the same after 4 hours exposure as control. The methyl-substituted dihydropyridinium, **15**, rapidly produced a 100% cell kill, exhibiting a cytotoxic effect the same as $MPDP^+$. The methyl-substituted pyridinium compound, **60**, also exhibited a cytotoxic effect causing an 80% cell kill after 4 hours exposure. This effect was comparable to that of MPP^+. The lagtime prior to onset of toxicity observed with the pyridinium compounds is attributed to the poor access of the quaternized compounds to the interior of the cell, apparently the compounds eventually cross the cell

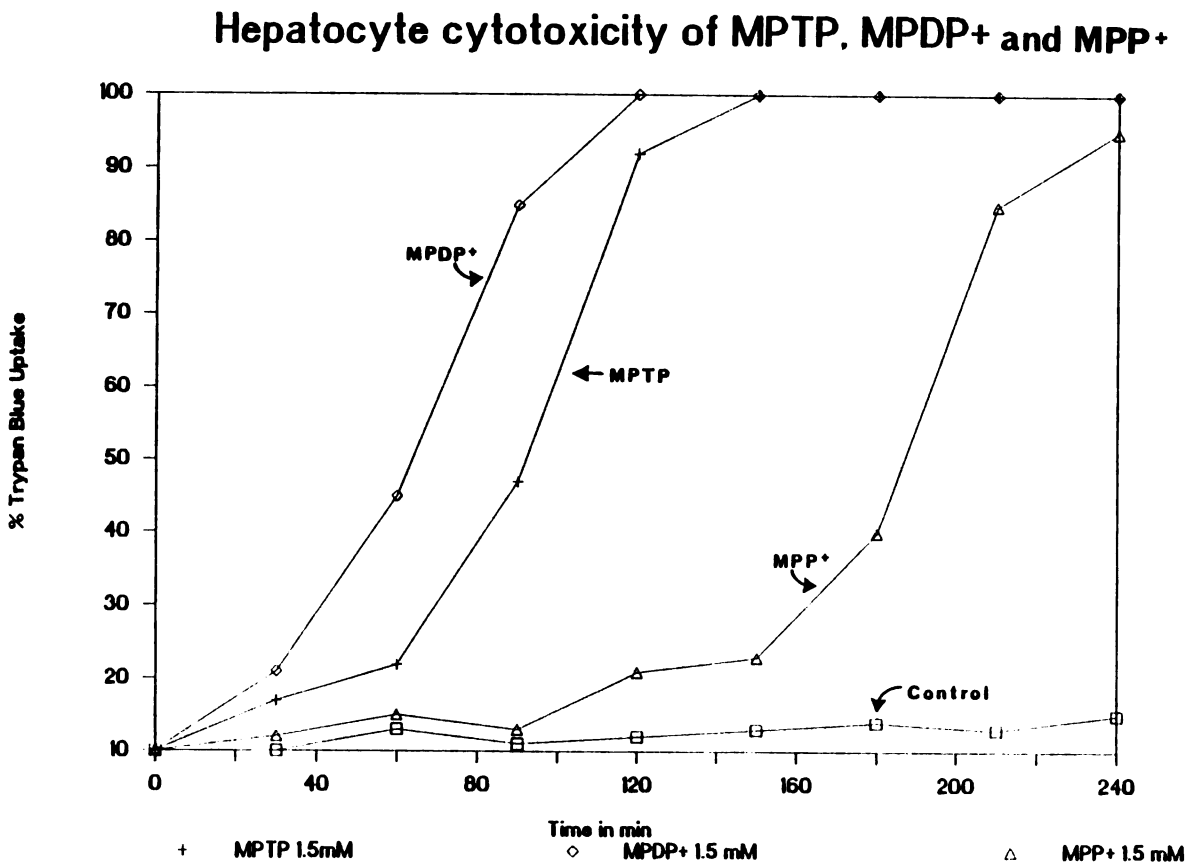

Figure 2-42. Toxic effects of MPTP, $MPDP^+$ and MPP^+ on freshly isolated rat hepatocytes, measured by trypan blue exclusion [52]

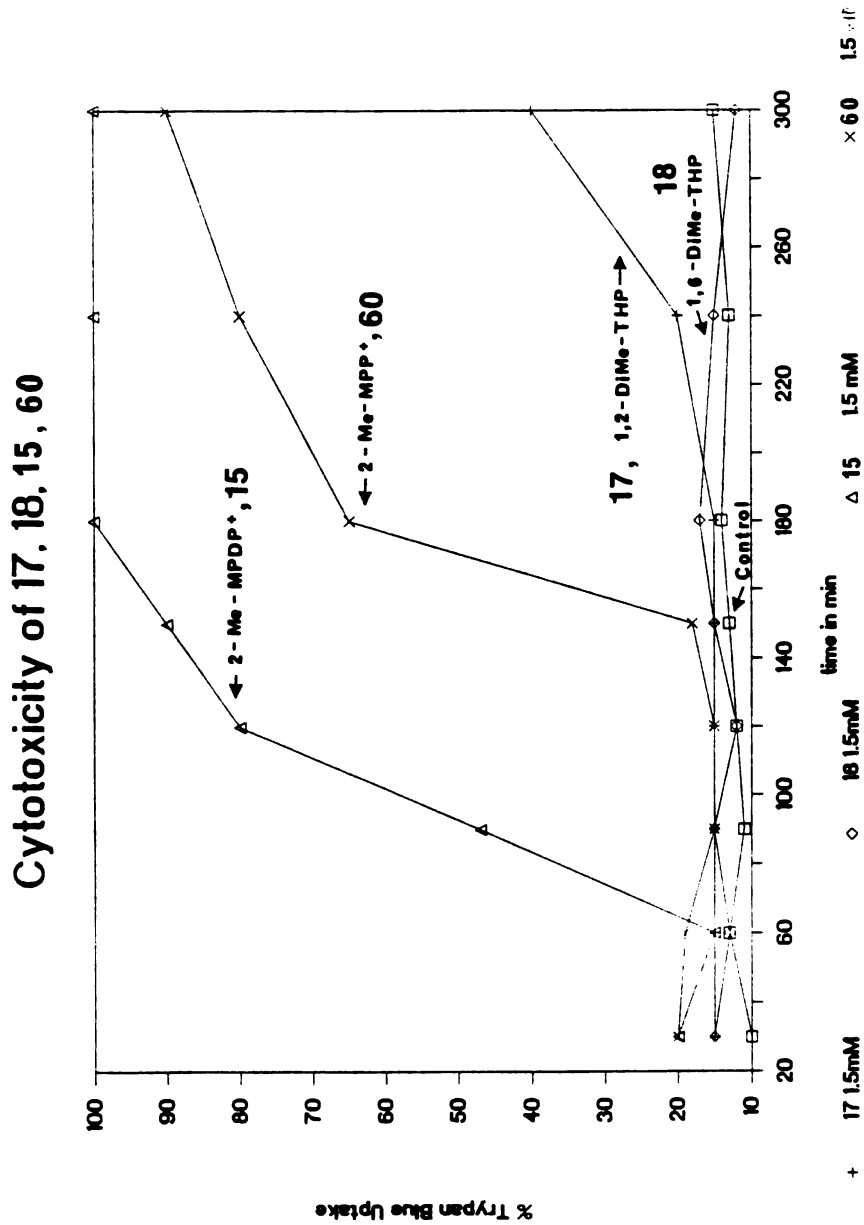

Figure 2-43. Toxic effects of tetrahydropyridines **17** and **18**, and metabolite analogs **15** and **60** on freshly isolated rat hepatocytes, measured by trypan blue exclusion

membrane but much more slowly than MPTP and $MPDP^+$ and their analogs which in their uncharged forms exhibit more rapid diffusion across lipid membranes.

These results indicated that although the methyl substitution of MPTP abolished MAO substrate activity, and with it, neurotoxicity and cytotoxicity, methyl substitution did not have the same effect on the toxic properties of the dihydropyridinium and pyridinium metabolites. The structure activity relationship for substrate activity with MAO is much more restrictive than that for the toxic properties of the metabolites. Chemical oxidation has accomplished the conversion of a non-toxic compound to a toxic one.

STUDY OF THE DOPAMINERGIC NEUROTOXICITY OF MPTP, $MPDP^+$, MPP^+ AND METHYL SUBSTITUTED ANALOGUES 17, 18, 15 AND 60 IN THE RAT CAUDATE. ELECTRON-MICROSCOPIC DETECTION OF NEUROTERMINAL DEGENERATION

While the isolated rat hepatocyte studies had indicated that the dihydropyridinium analog **15** and pyridinium analog **60** possessed cytotoxic activity similar or slightly more potent than $MPDP^+$ and MPP^+, a question as to the relavance of toxicity in this model to the neurotoxic effects of MPTP metabolites persists. To investigate the relavance of cytotoxicity observed with hepatocytes to a neuronal cell type, a study was performed in collaboration with Charles Meschul Ph.D,

Department of Neurology research, Veterans Administration Medical Center, Portland Oregon. In this study the candidate neurotoxins were injected intraventricularly in the female Wistar rat. The effects of drugs on neuroterminals in the rat caudate which forms part of the rat ventricle lining can be observed by electron microscopy. Dopamine neuroterminals are smaller than norepinephrine terminals and thus are identified on the basis of size. In a healthy terminal the synaptic vesicles containing stored neurotransmitter can be visualized as small spheres evenly distributed throughout the terminal body. The cytoplasmic background appears to be a light shade of gray. The synaptic junction is distinguished as a well defined dark band. Internal organells such as mitochondria and endoplasmic reticulum can be visualized in other healthy cells surrounding the neuroterminals. Previous studies by Dr. Meschul have shown that treatment with 10.5 mM $MPDP^+$ or MPP^+ in dimethylsulfoxide (5 uL, 56 nmole) results in dopamine neuroterminal degeneration. The degeneration is evidenced by a darkening of the cytoplasm, clumped synaptic vesicles and a less well defined synaptic junction in approximately 35% of the terminals visualized in the field. Dopamine neuroterminals constitute about 40% of the neuroterminals in the rat caudate, the balance being norepinephrine terminals. This effect is not induced by injection of the vehicle dimethylsulfoxide and

can be prevented by pretreatment with the dopamine uptake inhibitor Mazindol. The prevention of toxicity by pretreatment with a dopamine uptake inhibitor indicates that uptake of MPP^+ by the neuroterminal is likely required for expression of the MPP^+ toxic effect. This result is consistant with <u>in vivo</u> studies in mice where pretreatment with dopamine uptake inhibitors prevents the developement of MPTP induced dopamine depletion.[59,60] Furthermore, injection of 47.8 mM MPTP in DMSO (5 uL, 239 nmole) into the rat ventricle caused no damage to neuroterminals. The lack of effect by MPTP under these conditions is probably explained by the comparitively low levels of MAO present in rat caudate. In the study performed with Dr. Meschul it was found that injection of the purified methyl-subtituted tetrahydropyridines **17**·HCl and **18**·HCl, 48 mM in DMSO (5 uL, 240 nmoles), similar to MPTP, caused no degeneration of caudate neuroterminals. In contrast, injections of 11.7 mM **15**·ClO_4 and **60**·ClO_4, in DMSO (5 uL, 58 nmoles) caused the same type and extent of degeneration observed with MPP^+. An example of the electron micrographs which illustrate the neuroterminal degeneration observed with **60**·ClO_4 is shown in Figure 2-44. In this photograph, made from rat caudate tissue after treatment with **60**·ClO_4, normal terminals as well as degenerating terminals are marked.

Figure 2-44. Electron micrograph of rat caudate tissue after treatment with **60**·ClO_4^-. Two normal nerve terminals (**NT**) are making synaptic contact (arrowheads) with dendritic spines. Located within the terminals are round membrane bound synaptic vesicles. A degenerating terminal (**DT**) displays darkened cytoplasm and clumping of synaptic vesicles. Two other nerve terminals (**XX**) are in the initial stages of degeneration, with slightly darkened cytoplasm compared to the normal terminal. The density of degenerating terminals was similar to that seen with MPP^+. Magnification X 42,000.

Special care was taken in the experiment with the methyl-substituted dihydropyridinium **15**·CLO_4 to use the DMSO solution immediately after dilution since the disproportionation of **15**·CLO_4 seemed to be promoted by dissolution in DMSO. It could be demonstrated by cation exchange HPLC that the half-life for disproportionation of 5 mM **15**·ClO_4 in DMSO to form the pyridinium and tetrahydropyridine species was approximately 35 minutes. The disproportionation products were detectable, (but were not quantitated) after as little as five minutes in DMSO. In comparison the disproportionation rate of a solution of 0.56 mM **15**·ClO_4 in sodium phosphate 50mM buffer, pH 7.4, was less than 1 umole per minute. The insolubility of **15**·ClO_4 in sodium phosphate buffer precluded the study of the rate of disproportionation in more concentrated solutions. The basis for the acceleration of the disproportionation process by DMSO has not been definitively elucidated but may arise from the high concentration of the dihydropyridinium species that can be achieved in DMSO. Since a volume no larger than 5 uL could be injected in the rat ventricle, the high concentration could not be avoided. An alternative explanation involves the ability of the sulfoxide species to participate in Moffat type oxidation chemistry.

The neuroterminal degeneration observed in the rat caudate extended approximately 500 to 600 um from the ventricular surface, reflecting the slow diffusion of the

charged species from the ventricular space. Neuroterminal degeneration was not accompanied by nerve cell body destruction in the substantia nigra. It is most interesting that the dihydropyridinium species $MPDP^+$ and **15**·ClO_4 caused neuroterminal destruction as this indicates the neurotoxicity of dihydropyridinium species in contrast to the observations of Sayre et al.[55,56] Although compound **15** appears to possess intrinsic neurotoxicity as evidenced by neuroterminal degeneration, a possible alternative interpretation of these data stems from the increased rate of disproportionation observed with DMSO solutions of **15**. Possibly the toxicity observed with both $MPDP^+$ and with **15**·ClO_4 are due to the pyridinium species formed on disproportionation of the dihydropyridinium species in DMSO. A study that was not performed which might have answered this question would have required quantitation of the amounts of MPP^+ and **60** present in rat caudal tissue after injection of $MPDP^+$ and **15**·ClO_4.

CONCLUSIONS

The studies accomplished with the methyl substituted analogs of MPTP, $MPDP^+$ and MPP^+ have shown the following: **1**). Although 2- and 6-methyl-substitution of the tetrahydropyridine results in abolished MAO substrate activity, the compounds are still able to interact with the enzyme active site in some fashion since compounds **17**

and **18** are able to inhibit the oxidation of MPTP by MAO. The negative effect of the additional methyl moiety most probably involves steric hindrence which prevents the necessary alignment of the FAD cofactor with a potential substrate, since the loss of substrate activity is not pH dependent. This result is consistant with the work of Able and Brossi who have shown that methyl substitution at the 3 and 5 positions of MPTP similarly results in abolished substrate activity.[123] **2)** The loss of MAO substrate activity was accompanied by a loss of dopaminergic neurotoxicity in the mouse and cytotoxicity in freshly isolated hepatocytes, results consistant with the veiw that MPTP induced neurotoxicity is caused not by the parent compound, MPTP, but by its MAO derived metabolites. **3)** In contrast to the results of methyl-substitution on the activity associated with MPTP, methyl-substitution of the dihydropyridinium and pyridinium compounds had no ameliorating effect on their toxic activities as measured by rat hepatocyte cytotoxicity and dopaminergic neurotoxicity in the rat caudate. Our results with the methyl substituted $MPDP^+$ analog are not consistant with the evidence obtained by Sayre using a stabilized $MPDP^+$ analog, which imply a lack of $MPDP^+$ toxicity.

There are two possible explanations for this inconsistancy: First, our results which indicate the toxicity of a dihydropyridinium compound, may be

interpreted in terms of the effects of pyridinium **60** obtained by auto-oxidation and /or disproportionation of **15** during the biological assay. Alternatively, Sayre's results, which indicated that placement of the geminal dimethyl groups on the tetrahydropyridine ring to produce a stabilized $MPDP^+$ renders the analog nontoxic, may be due to even further steric hindrence produced by the second methyl group which is sufficient to interfere with the interaction of the dihydropyridine with its target causing an abolition of toxic activity. Perhaps a single methyl group placed at the 6 position in **15** is not sufficient to interfere with the toxic properties of the dihydropyridinium molecule.

This evidence of less stringent structural requirements for the toxicity of tetrahydropyridine metabolites provoked our desire to characterize further the structural requirements of pyridinium compounds as toxic agents. Chapters 3 and 4 of this dissertation describe our efforts to characterize the structure-activity relationships of pyridinium compounds in several biological systems which may have relevance to their neurotoxic effects.

CHAPTER 3. Effects of substituted pyridinium compounds on mitochondrial respiration and their in vivo dopaminergic neurotoxicity as measured by intracerebral microdialysis in rat brain

The ability of MPP^+ to inhibit the oxidation of NADH-linked substrates (e.g pyruvate and glutamate) in brain mitochondria was first demonstrated by Nicklas et al. who showed that pyruvate and glutamate oxidation were inhibited by millimolar quantities of MPP^+ whereas succinate oxidation was unaffected.[62] This important observation was interpreted as evidence that the mechanism of MPP^+ toxicity involved the inhibition of the cells ability to provide for its energy needs. Normal mitochondrial respiration or oxidative phosphorylation provides ATP, the cellular energy currency, which is required to power many of the metabolic functions of the cell such as maintainance of appropriate levels of sodium, potassium and calcium ions. Proper function of calcium homeostasis is particularly critical to maintainance of the cytoskeleton since calcium and its associated binding proteins play a pivotal role in regulating cytoskeletal structure and function.[63] Nicklas et al. found that the oxidation of glutamate and pyruvate are inhibited while the oxidation of succinate, which enters the oxidation scheme at a later site, is not inhibited. This indicates that mitochondrial respiration

is inhibited at the level of NADH oxidase (also called NADH dehydrogenase), a site early in the sequential chain of enzymes involved in ATP production.

These findings were confirmed and expanded upon by Ramsay et al. who demonstrated that the effect occured at low concentrations (0.5 mM) only in intact mitochondria. In inverted mitochondria or in mitochondrial membrane fragments [also called electron transport particles,(ETP)], the concentrations of MPP^+ required to achieve the same effect were much higher (7.2 mM). Based on these results Ramsay suggested that an energy dependent uptake of MPP^+ into the mitochondria, followed by inhibition of mitochondrial respiration by intramitochondrial MPP^+, might be operative.[64] Subsequently, Di Monte et al. demonstrated that MPP^+ produces a rapid intracellular depletion of ATP levels prior to the onset of cytotoxicity in isolated hepatocytes.[65]

Our interest in the mechanism of MPP^+ toxicity led us to examine the structural specificity exhibited by substituted pyridinium compounds as inhibitors of respiration in intact mitochondria and as inhibitors of NADH oxidase in membrane preparations. In order to assess the need for an aromatic lipophilic moiety in the 4 position of the pyridine ring, we chose to test compounds in which the 4-phenyl moiety of MPP^+ was exchanged for a methyl group (73), and a tert-butyl group

(74). In compounds **75** and **76** the phenyl group was exchanged for a 4-(3-cyclohexenyl) and a 4-cyclohexyl moiety, respectively, in order to give MPP^+ analogs with bulk and lipophilicity very similar to MPP^+ but lacking the aromatic character of the phenyl group. In compounds **77** and **78**, the attachment of the phenyl moiety was moved to the 3 and 2 positions, respectively. Compound **60** was included in the set to assess the effect of an additional methyl group in the 2 position. A portion of this work, a collaboration with Dr. Rona Ramsay, Department of Biochemistry and Biophysics, University of California, San Francisco, California, has recently been published.[66]

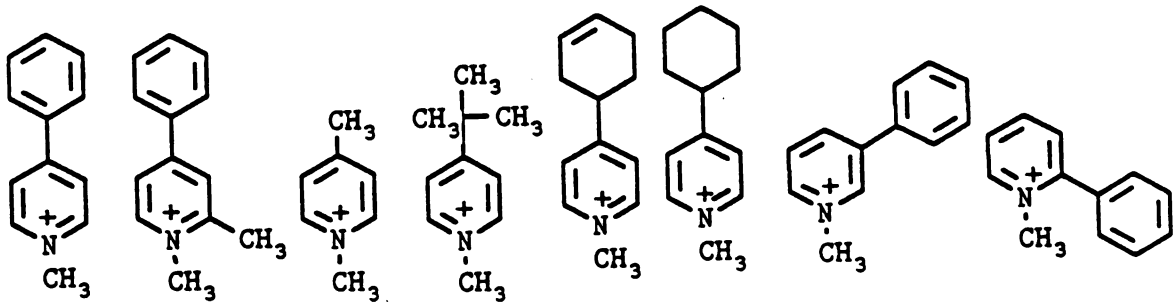

MPP^+ 60 73 74 75 76 77 78

SYNTHESIS OF THE TEST SET OF COMPOUNDS

Compounds **73**, **74**, **77** and **78** were synthesized according to previously published procedures.[67-70] Compound **75** was synthesised via methyl iodide alkylation of 4-(3-cyclohexenyl)pyridine (**79**). Catalytic hydrogenation of the isolated double bond in **79** afforded the fully saturated 4-cyclohexypyridine (**80**). After purification by distillation **80** was treated with methyl

iodide to give 76. An MPP^+ analog with the electron

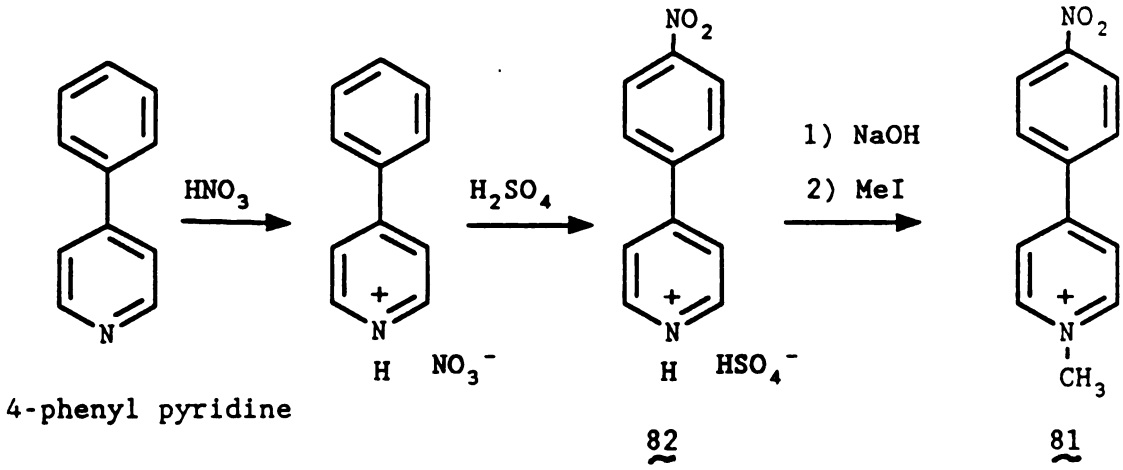

4-phenyl pyridine

82 81

Scheme 3-1. Attempted synthesis of 1-methyl-4(4'-nitro)phenyl pyridinium iodide (81)

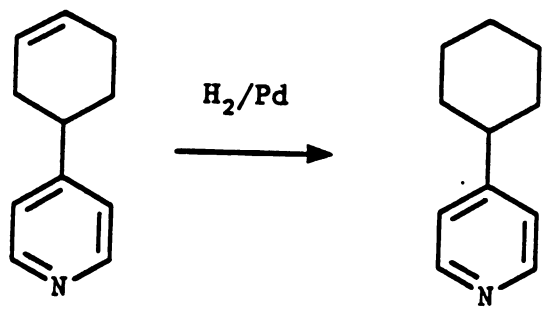

79 80

withdrawing 4'-nitro substituent, **81**, was desired for addition to this set. The synthesis of **81** was attempted as shown in Scheme 3-1. The sulfuric acid catalyzed electrophilic substitution of the nitrate salt of 4-phenyl pyridine gave **82**. However, once the 4'-nitro substituent was in place, alkylation of the pyridine nitrogen atom proved to be very difficult. Extended treatment of the free base of **82** with methyl iodide resulted in a very poor yield of a compound tentatively identified by 80 MHz ^{1}H NMR as **81**. The 80 ^{1}H NMR of **81** displayed a set of 4 doublets (8.1 ppm, 8.35 ppm, 8.45 ppm, and 8.8 ppm) which integrated for a total of 8 protons and which can be assigned to the aromatic protons of the phenyl and pyridine ring. Furthermore a singlet (3 H) at 4.4 ppm was assigned to the N-methyl protons of this pyridinium salt. However recrystalization did not result in a sample sufficiently pure for analysis so the compound was not included in the test set. The only other reported synthesis of **81** is found in a patent report on 4-arylpyridinium salts as herbicides.[161] In this case methyl flouromethylsulfonate was reacted with 4-(4'-nitro)-phenylpyridine in a sealed tube at 100 ^{o}C for 2 hours to give a low yield of **81** as the methylflourosulfate salt. Even under these very drastic conditions, the alkylation of 4-(4'-nitro)-phenylpyridine gives low yields which is probably related to the electron withdrawing effect of the nitro group which

leads to reduced nucleophilic attack by the pyridine nitrogen atom.

BIOLOGICAL EVALUATION

The most straight-forward way to test compounds for their ability to inhibit energy production and, hence, cause energy depletion of the cell involves measurement of mitochondrial respiration by measuring the oxygen consumption of treated mitochondria. The results of Ramsay et al.indicate, however, that MPP^+ (and possibly related compounds) must first be transported across the mitochondrial inner membrane before an inhibitory effect on NADH oxidase is expressed.[64] These workers have shown that an intramitochondrial MPP^+ concentration as high as 20 mM is reached starting from an extramitochondrial concentration of 0.5 mM MPP^+.[64] Thus, inhibition of respiration is the net result of the effects on two separate steps which may be differently affected by alterations in the structure of the inhibitor. In order to assess the effects of structural variation on each of these steps, the various pyridinium compounds were first screened for inhibition of mitochondrial respiration. In subsequent separate experiments, their effects on NADH dehydrogenase were studied and their capacity for uptake by mitochondria was estimated.

INHIBITION OF MITOCHONDRIAL RESPIRATION

Mitochondria can be prepared and observed in several different states. The state of most interest with respect to the inhibition of mitochondrial respiration is state 3 or the state in which mitochondria are actively phosphorylating adenosine diphosphate (ADP) to form adenosine triphosphate (ATP), the cellular energy carrier. The rate limiting factor controling the respiration of mitochondria in state 3 is the availability of ADP.[147] Therefore in the inhibition studies described here, the effects of inhibitors were examined in mitochondria which had been preincubated with inhibitor before exposure to a fresh supply of ADP. Following the addition of ADP, the respiration rate of mitochondria exposed to inhibitor were compared to that of control mitochondria (no inhibitor). Ramsay et al. had shown previously that the inhibition of mitochondrial respiration by MPP^+ is both concentration and time dependent due to the requirement for MPP^+ transport into the mitochondrial matrix.[64] Similar results were observed with the inhibitors investigated here. Figure 3-1 shows the time courses for the inhibition of mitochondrial respiration by MPP^+ at high concentration (0.5 mM), low concentration (0.05 mM) and the other pyridinium derivatives (0.5 mM). The inhibition is most rapid and complete with 0.5 mM MPP^+ and 0.5 mM **60**.

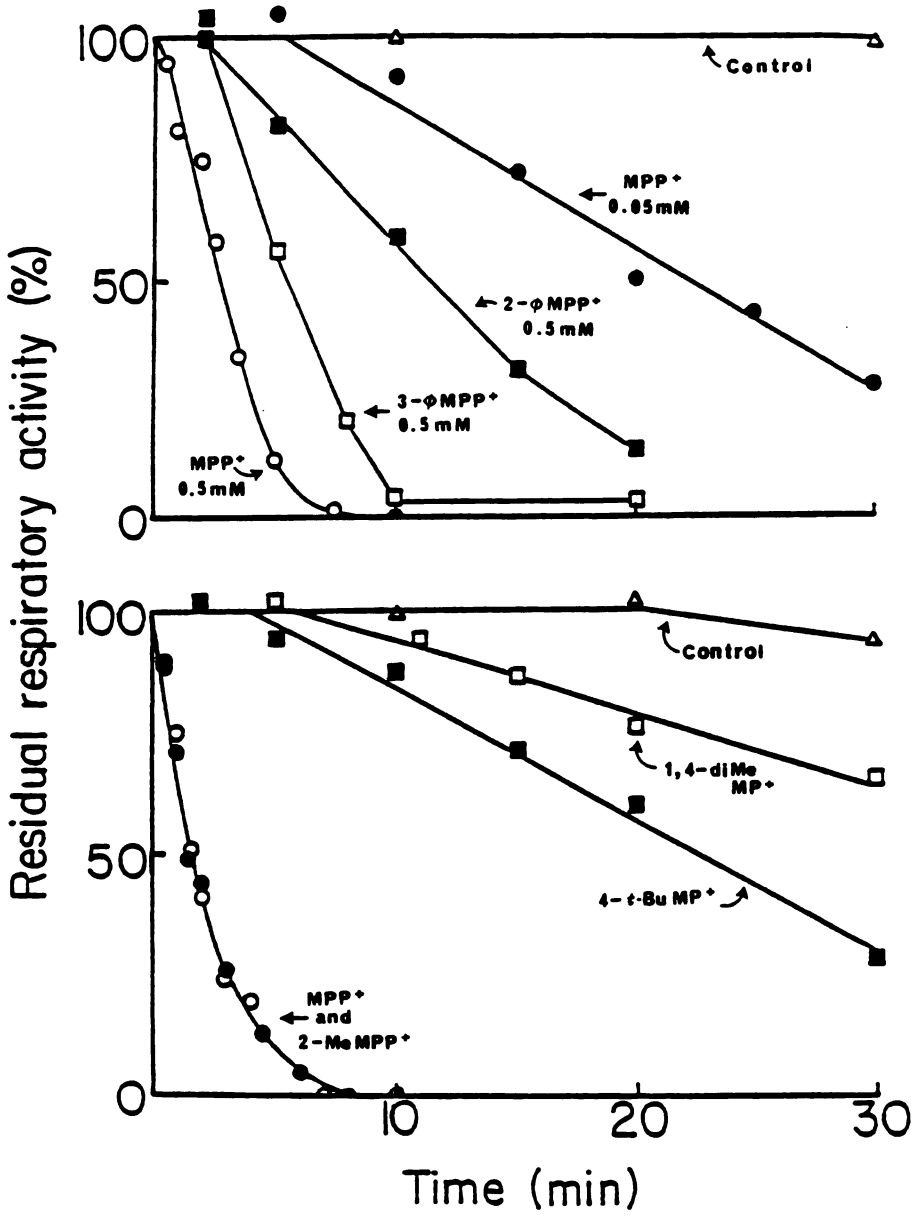

Figure 3-1. Inhibition of mitochondrial respiration by pyridinium derivatives.

A. Rat liver mitochondrial protein concentration was 1.9 mg/mL. The incubations contained no inhibitor (control,): 0.5 mM MPP^+ (o): 50 uM MPP^+ (●): 0.5 mM 1-methyl-3-phenylpyridinium, **77** (□): 0.5 mM 1-methyl-2-phenyl-pyridinium, **78** (■).

B. The protein concentration was 2.2 mg/mL. The incubations contained no inhibitor (control,) or 0.5 mM inhibitor: MPP^+ (o): 1,2-dimethyl-4-phenylpyridinium, **60** (●): 1,4-dimethylpyridinium, **73** (□): 1-methyl-4-t-butylpyridinium, **74** (■). The increase in respiratory activity induced by the addition of ADP was expressed as a percentage of the control value.

Incubation with 0.05 mM MPP^+ for 50 minutes also leads to complete inhibition of respiration. The relative efficacies of the derivatives tested in the inhibition of the oxidation of glutamate plus malate by rat liver mitochondria are as follows: MPP^+ equal to **60** > 1-methyl-3-phenylpyridinium (**77**) > 1-methyl-2-phenylpyridinium (**78**) > 1-methyl-4-tert-butylpyridinium (**74**) > 1,4-dimethylpyridinium (**73**). In a later experiment, (data not shown), the effects of the 4-cyclohexylpyridinium (**76**), and 4-(3-cyclohexenyl)pyridinium (**75**) salts were found to be approximately equal to those of MPP^+.

These data indicate that the position of the phenyl or large bulky moiety on the pyridine ring is of major importance in determining inhibitory activity with respect to mitochondrial respiration. Replacement of the phenyl group with the cyclohexyl and cyclohexenyl moieties which are non-aromatic but similar in lipophilicity and size to the phenyl group does not affect inhibitory character. Similarly, addition of a methyl group at the 2 position of the phenyl group does not reduce inhibitory activity. In contrast, substitution of the phenyl group with a slightly smaller tert-butyl or much smaller methyl group results in diminished inhibitory activity. Pyridinium ion inhibitory potency may be a function of more than the lipophilicity of the subsituent at the 4 position of the

pyridinium moiety since lipophilicity alone does not correlate well with potency. For example, the 4-tert-butyl substituent (pi = 1.98) has approximately the same lipophilicity as the 4-phenyl substituent (pi = 1.96) present in MPP^+, yet the potency of these two compounds as mitochondrial respiration inhibitors are considerably different. The potency of pyridinium ion inhibitors of mitochondrial respiration may correlate better with the size of the substituent (MR, molar refractivity) in the 4 position of the pyridinium ring as shown in Table 3-1.

Table 3-1. Correlation of 4-substituted pyridinium ion inhibitory potency in mitochondrial respiration with lipophilic, steric and electronic parameters.

Compound	Rank order	pi	MR	p sigma
MPP^+	1	1.96	25.36	-0.01
60	1	1.96	25.36	-0.01
75	1	2.51	26.69	-0.22
76	1	2.51	26.69	-0.22
77 3-substituted	2	parameters cannot be compared		
78 2-substituted	3	parameters cannot be compared		
74	4	1.98	19.62	-0.20
73	5	0.56	5.65	-0.17

Pi is a measure of lipophilicity, MR a steric parameter is a measure of size, p sigma an electronic parameter is a measure of electronegativity, values taken from Burger's Medicinal Chemistry [146]

AN ESTIMATE OF THE RELATIVE AFFINITY OF PYRIDINDIUM COMPOUNDS FOR THE MITOCHONDRIAL UPTAKE SYSTEM

The active accumulation of the compounds into the mitochondrial matrix is driven by the electrical gradient across the inner membrane[72] and can be measured directly

only if radiolabeled compounds are available. Since they were not, an estimate was made of the relative uptake of each compound by its inhibition of [^{3}H] MPP^+ uptake. The reliability of this procedure was tested by assessing the effectiveness of 2 mM unlabeled MPP^+. (Fig. 3-2, solid circles) on the uptake of 0.5 mM [^{3}H] MPP^+. Since the Km of the uptake system is 5 mM,[72] the net rate of total MPP^+ uptake increased, but the uptake of radiolabled MPP^+ was decreased by a factor of 0.73. This inhibition was that expected on the basis of competition for the carrier. In contrast, 2 mM 1-methyl-2-phenylpyridinium iodide (**78**) was ineffective and the 3-phenyl analog, **77**, (2 mM), was less effective than MPP^+. Compound **60** (6 mM) inhibited [^{3}H] MPP^+ uptake extensively, and may be as effective as MPP^+ (the relative potency of **60** with respect to MPP^+ can only be estimated since the two compounds were not tested at equal concentrations). This may explain the impressive inhibition of mitochondrial respiration by **60** despite its higher IC_{50} value for the inhibition of NADH oxidase (Table 3-2). The 4-tert-butyl and 4-methyl analogs were not tested as inhibitors of [^{3}H] MPP^+ uptake due to their lack of potency in mitochondrial respiration inhibition.

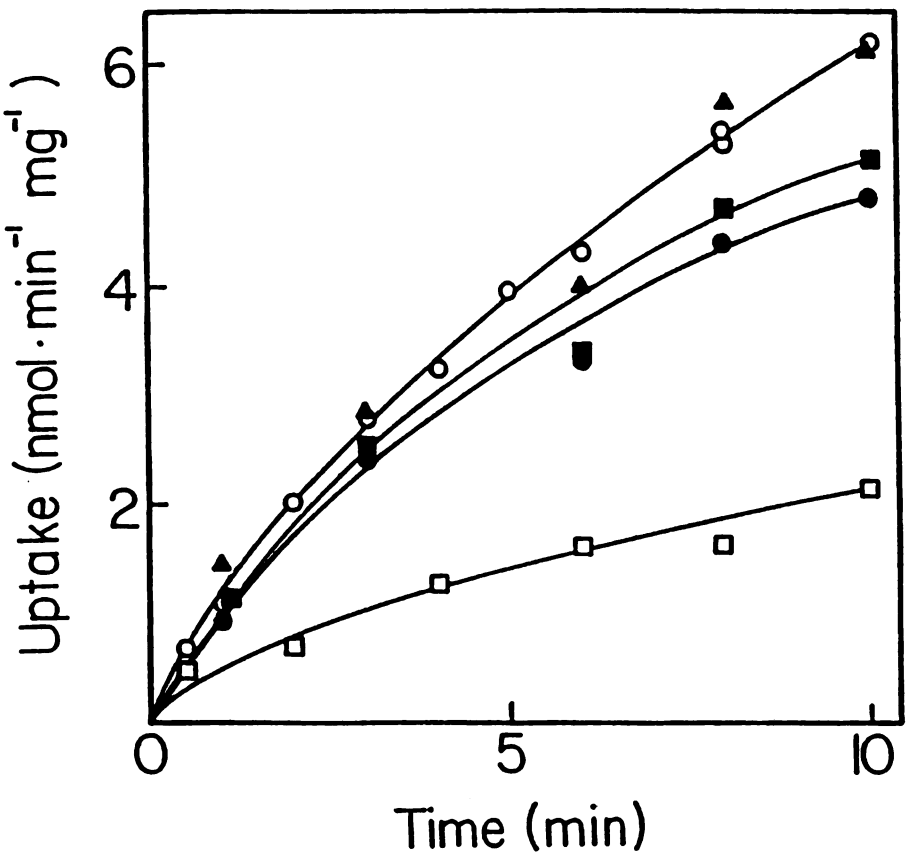

Figure 3-2. Inhibition of the active uptake of [^{3}H] MPP^+ into rat liver mitochondria by some pyridinium derivatives. Mitochondria (12.0 mg/ mL) were incubated with [^{3}H] MPP^+ 0.5 mM (0.2 Ci/mmol) in the absence or presence of antimycin (10 uM) and rotenone (10 ug/mL) to obtain the difference, representing the energy-dependent (active) uptake of [^{3}H] MPP^+. Non-radiolabeled derivatives added immediately before the [^{3}H] MPP^+ were: none (o); 2 mm MPP^+ (●): 2 mM 1-methyl-3-phenylpyridinium, **77** (■): 2 mM 1-methyl-2-phenylpyridinium, **78** (▲): or 6 mM 1,2-dimethyl-4-phenylpyridinium, **60** (□).

INHIBITION OF NADH OXIDASE

The effects of the pyridinium compounds on NADH oxidase activity in mitochondrial inner membrane preparations are summarized in Table 3-2 and in Figure 3-3.

Table 3-2. Inhibition of NADH oxidase activity in inner membrane preparations

Inhibitor	IC_{50} (mM)	Rank Order
1-methyl-4-phenylpyridinium (MPP^+)	7.2	#1
1-methyl-3-phenylpyridinium (**77**)	>20	#3
1-methyl-2-phenylpyridinium (**78**)	11	#2
1,2-dimethyl-4-phenylpyridinium (**60**)	11	#2
1,4-dimethylpyridinium (**73**)	not reached	#4
1-methyl-4-tert-butylpyridinium (**74**)	not reached	#4

NADH oxidase activity of beef heart electron transport particles was measured spectrophotometrically at 30 ^{o} C in 0.25 M sucrose-0.05M K phosphate, pH 7.6. IC_{50} is the concentration of inhibitor required to decrease the activity by 50 % immediately after addition of the inhibitor.

The energy-dependent uptake process has been shown to concentrate MPP^+ into the matrix by at least 40-fold.[72] It seems likely, therefore, that positively charged inhibitors similar to MPP^+ such as **60**, **77** and **78** can be accumulated in concentrations high enough to achieve the high IC_{50} values listed in Table 3-2. The

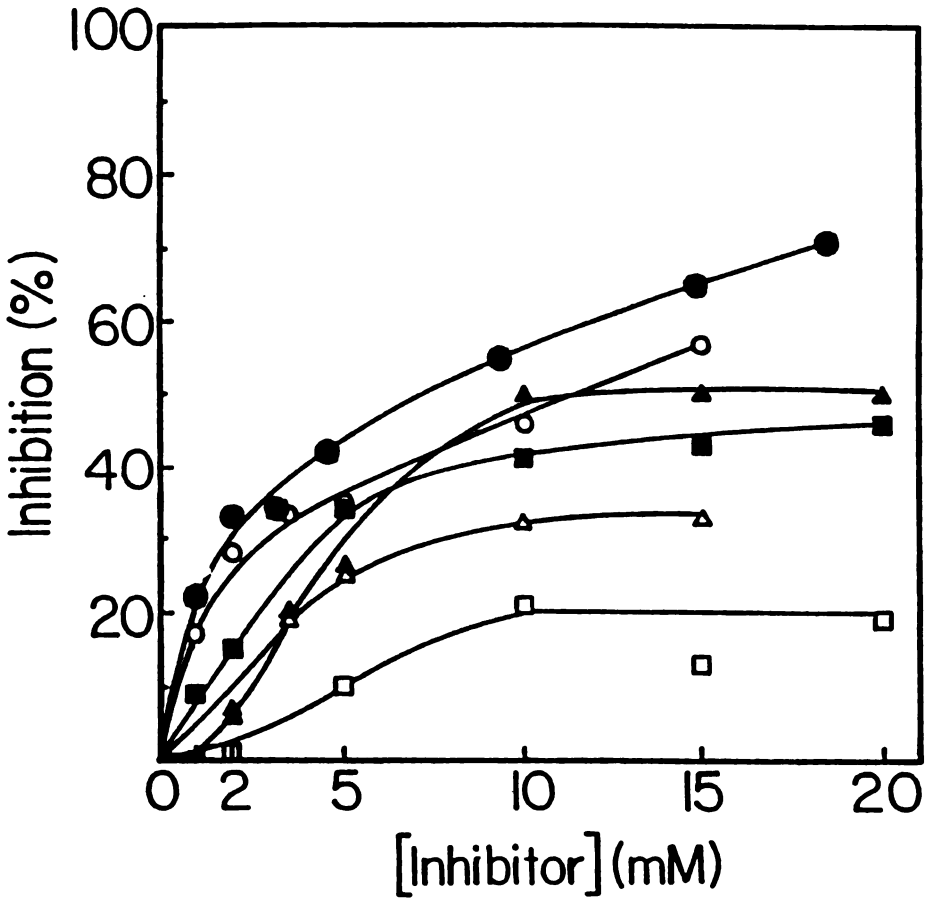

Figure 3-3. Inhibition of NADH oxidase activity by MPP^+ analogs. Electron transport particles (0.8 mg/mL) were incubated for 5 minutes at 25 °C in a final vol. of 0.2 mL 0.25 M sucrose, 50 mM potassium phosphate, pH 7.6, with or without inhibitor. A sample (25 uL) of the incubation mixture was assayed in the same buffer in the presence of 0.28 mM NADH and the same concentration of inhibitor as present in the incubation. The inhibitors were: MPP^+ (●): 1-methyl-3-phenylpyridinium, **77** (■): 2 mM 1-methyl-2-phenylpyridinium, **78** (▲): 1,2-dimethyl-4-phenylpyridinium, **60** (○): 1,4-dimethylpyridinium, **73** (□): 1-methyl-4-t-butylpyridinium, **74**, (△).

concentration dependence of the inhibition by these compounds is not a simple titration effect. Figure 3-3 shows that plateau values are reached above which no further inhibition is observed. Consistant with their low potency as inhibitors of respiration in intact mitochondria, compounds **73** and **74** are the least potent of the pyridinium derivatives tested as inhibitors of NADH oxidase. The trend for the phenyl-substituted analogs still shows that the 4 position of the phenyl ring (MPP^+) is optimal. Again the addition of the methyl group to the 2 position (**60**) does not cause a substantial loss of inhibitory activity.

In an effort to identify a carrier protein responsible for transport of MPP^+ across the mitochondrial inner membrane, Ramsay et al. have shown that the malate, glutamate and acylcarnitine carriers are not involved.[71,72] The latter finding was surprising since acyl-carnitine is the only quaternary ammonium compound known to be actively tranported across the mitochondrial inner membrane. Although the data presented here (as well as data subsequently obtained by Youngster et al.[71]) on pyridinium inhibition of MPP^+ uptake in mitochondria indicate structural specificity among pyridinium inhibitors and therefore imply that some specific protein interaction is involved, there is as yet no firm evidence for this proposal.

Regardless of the source,(specific protein interaction with NADH oxidase, with a protein carrier, or otherwise), a degree of structural specificity with regard to the effects of pyridinium ions on the respiration of mitochondria has been demonstrated by the studies described here. The rank order of potency of the compounds studied indicates that the position of the phenyl group or similar sized, large bulky moiety is the most important factor determining potency. Optimal inhibition of mitochondrial respiration is observed with such substituents in the 4 position, followed by the 3 then 2 positions of the pyridinium ring. Potency then decreases as the size of the 4 position substituent is decreased. These structural requirements may arise from formation of an inhibitor-protein complex formation such as the binding of an inhibitor to NADH oxidase. Alternatively, the interaction of pyridinium ions with mitochondria may be a less specific detergent effect. For example, lipophilic cationic molecules such as MPP^+ may lodge in the membranes of the mitochondrial matrix promoting dissipation of the electronic gradient which normally exists across the inner mitochondrial matrix. Dissipation of the electronic gradient may result in inhibition of mitochondrial respiration.

ASSESSMENT OF *IN VIVO* DOPAMINERGIC NEUROTOXICITY OF PYRIDINIUM COMPOUNDS WITH *IN VIVO* BRAIN DIALYSIS IN THE RAT

The arrival of Dr. Hans Rollema in our laboratory, for a sabbatical leave from the Department of Medicinal Chemistry of the State University of Groningen provided the opportunity to investigate the relevance of the structural specificity observed in mitochondrial respiration inhibition to *in vivo* dopaminergic neurotoxicity. The *in vivo* neurotoxicity of pyridinium compounds is difficult to assess by most methods of pharmacologic administration since the compounds are permanently positively charged and (in the absence of an active uptake process such as in the mitochondrion) cross membrane barriers very poorly. The intraventricular administration and electron microscopic assessment of toxicity discussed in Chapter 2 for compounds **17**, **18**, **60** and **15** were valuable but laborious and expensive procedures which were not practical for the analysis of large numbers of compounds. Dr. Rollema, however, has developed a method of assessment of *in vivo* neurotoxicity by microdialysis of the rat striatum which is quite practical for the study of numbers of pyridinium compounds. The results of a collaborative study with Dr. Rollema on the *in vivo* dopaminergic neurotoxicity of the same set of pyridinium compounds is presented here.

The microdialysis technique requires the surgical implantation of a bilateral cannula with an U-shaped dialysis membrane into both side of the striatum of an anethetized rat. After the animal has recovered from the surgery, the striatum of the conscious rat is perfused with a dialysis solution containing the pyridinium compound under investigation. The effects of the drug perfusion on dopamine and dopamine metabolite release by the striatum are measured by on-line HPLC analysis of the dialysate. In previous studies, perfusion of rat striatum with a solution of 10 mM MPP^+ for 15 minutes resulted in a massive release of dopamine (22,067 % of the basal level) with a concommitant decrease in the efflux of the metabolites homovanilic acid (HVA) and 3,4-dihydroxyphenylacetic acid (DOPAC).[73] This effect of MPP^+ could not be re-elicited one to several days later upon a second challenge with MPP^+. In addition, the metabolite levels were persistantly decreased to less than 20% of basal levels. Moreover, the MPP^+ effects on the output of DA and the metabolites closely resembled the effects of death of the rat during dialysis. It was concluded that 10 mM MPP^+, perfused for 15 minutes, causes irreversible damage of the dopaminergic nerve terminals.

The selectivity of the MPP^+ effect was established by infusion of a number of drugs (in 1-10 mM concentrations) which either share some pharmacological

properties with MPP^+ or are structurally related to this compound. MPP^+ has been shown to be a competitive inhibitor of MAO,[162] which could lead to an increase in detected release of DA since conversion to DA metabolites would be inhibited. To investigate the possible role of MAO inhibition in the massive DA release observed with MPP^+ MAO-inhibitors (pargyline, deprenyl, chlorgyline) were perfused in the rat striatum. MPP^+ has also been shown to inhibit DA-uptake.[75,76,78,79,80] To examine the possibility that DA uptake inhibition might explain the increase in detected DA release, other DA uptake inhibitors (GBR 12909, nomifensine) were perfused. Finally, a known DA-releaser [E(S)-amphetamine] and DA-depletor (reserpine) were examined in the rat striatal perfusion model. All of the pharmacologic congeners of MPP^+ examined induced an increase in the release of DA. However, the increase was never more than 10-20% of that induced by 10 mM MPP^+. Infusion with 1-methylpyridinium iodide induced only a 2-fold increase in the output of DA, without affecting metabolite levels. Similarly, paraquat (11) was completly without effect in this model (Rollema et al.)[73]

In the collaborative study with Dr. Rollema reported here the compounds were studied initially using a similar experimental paradigm. Each compound (10 mM) was perfused into the striatum of a conscious rat for 15 or 30 minutes and the effects on DA and DOPAC release were

measured. The following day a second perfusion of the compound was performed and the effects on DA and DOPAC measured. The effects of the 4-(3-cyclohexenyl) (**75**), 1,2-dimethyl (**60**), 3-phenyl (**77**), and 2-phenyl (**78**) derivatives were similar to those of MPP^+. As shown in Table 3-3, a 15 or 30 minute perfusion of these 4 compounds resulted in the initial release of extremely high amounts of dopamine while perfusion of the 4-tert-butyl (**74**) and 4-methyl (**73**) derivatives resulted in much more modest DA release even after perfusion for 30 minutes. Although the initial dopamine release by MPP^+, **75**, **77**, **78**, and **60** was very high in each case, in contrast to the effects of MPP^+, a second high release of DA still could be elicited from rats treated with the drugs by a reperfusion the next day. This result was interpreted as evidence that irreversible damage had not been caused by the 15 to 30 minute perfusion with these drugs. All of the drugs were initially classed as less potent neurotoxins than MPP^+, while **74** and **73** were initially labeled as unlikely to be neurotoxic. MPP^+ was considered the most potent since it gave a very high initial release followed by the lowest release on the second day. The cyclohexenyl derivative (**75**) was considered slightly less potent than MPP^+ since the first day release was very high but the second day release was not as depressed as with MPP^+. The 1,2-dimethyl (**60**) and the 3-phenyl (**77**) derivatives were classed as less potent

than MPP^+ because a 30 minute perfusion was required to elicity the massive initial dopamine release and the second day release was higher than that observed with MPP^+. The 2-phenyl derivative (**78**) was labled as less potent than or equipotent with **77** since a 15 minute perfusion of **78** resulted in an initial DA release of about half that seen with the 30 minute perfusion of **77**. The low second release observed with **78** (comparable to that with MPP^+) was the factor which argued for a rank order of potency equal to **60** and **77**. The tert-butyl (**74**) and 4-methyl (**73**) derivatives were the least potent or non-neurotoxic since 30 minute perfusions of these drugs caused a minimal initial release of DA (less than 1000% of basal levels). Thus a preliminary rank order of potency for this group of drugs in the rat striatal perfusion model was established (Table 3-3).

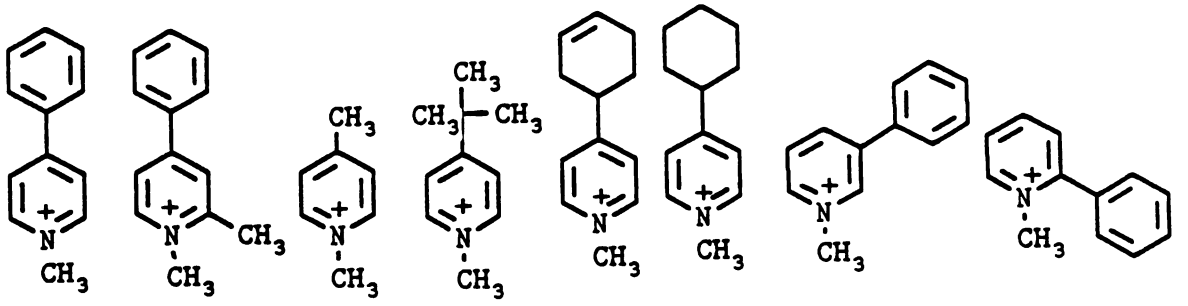

MPP^+ 60 73 74 75 76 77 78

Table 3-3.
Effects of striatal perfusion of substituted pyridinium derivatives on rat striatal Dopamine release

Compound	Perfusion time	Dopamine Release in % basal level (fmole/min)		Rank order of potency
		Day 1	Day 2	
MPP^+	15 min	22,067% (1,002)	285% (12.9)	#1
75	15 min	26,700% (1,016)	1,950% (74)	#1
60	30 min	19,200% (192)	1,750% (18)	#2
77	30 min	16,480% (2,537)	1,492% (230)	#2
78	15 min	9,995% (440)	300% (11)	#2 or 3
74	30 min	650%	NA	#4
73	30 min	290%	NA	#4

Each rat served as its own control. Basal DA output levels were determined for each animal prior to drug perfusion on day 1 and 2. NA means not assayed

The rank order indicated that a large bulky lipophilic moiety in the 4-position of the pyridinium ring gave optimal toxic activity. Placement of a methyl group at the 2 position or movement of the bulky moiety to the 3-position of the pyridinium ring gave a slight reduction of toxic potency. Movement of the bulky moiety to the 2-position gave a further reduction of toxicity while substitution with the smaller tert-butyl and methyl

groups resulted in a significant reduction in toxicity. These data represented single experiments with each drug so the rank order of potency was considered preliminary at best. Yet these results were very interesting in that they seemed to indicate a structure activity relationship for *in vivo* neurotoxicity which paralled that observed in the mitochondrial respiration inhibition studies. The results supported the conclusion that mitochondrial respiration inhibition was an important aspect of neurotoxicity.

In order to be able to compare the effects of all the drugs in a more standard manner, the experimental paradigm was changed to include a second day perfusion with MPP^+, rather than the test drug. The reasoning behind this change was that we were interested in whether the compounds tested were affecting the same neurons as MPP^+. If a very large dopamine release could be elicited with the MPP^+ challenge on the second day it could be determined that the initial drug treatment had either 1) affected a different set of neurons than those affected by MPP^+ or 2) caused a reversible release of DA but not permanent damage, a non-neurotoxic effect. In addition, the time of perfusion was changed in the new paradigm. We reasoned that less potent neurotoxins might require longer perfusion time since the amount of drug passing into the tissue was dependent both on the concentration of the dialysate and on the length of perfusion. It was

hoped that a rank order of potency for the test compounds could be better established by determining the length of perfusion time required to achieve a toxic end-point. The toxic end-point was defined as a massive DA release (10,000-20,000% of basal) on the first day followed by minimal DA release (less than 1,000 % of basal) elicited by MPP^+ perfusion on the second day and DOPAC levels that remained persistantly depressed. In the experiments that followed Dr. Rollema used perfusion times of 15 min and 1 hr. The results of all of these experiments are summarized in Table 3-4.

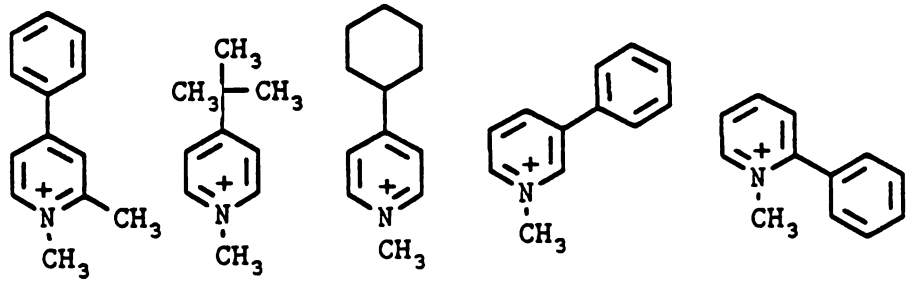

60 74 76 77 78

Table 3-4. Effects of Striatal perfusion of substituted pyridinium derivatives followed by MPP^+ challenge (on Day 2) on rat striatal dopamine release

Compound	Perfusion time in minutes	Dopamine Release in % basal level (fmole/min) DAY 1	DAY 2
MPP^+	15	22,067% (1,002)	285% (13)
60	15	12,222% (733)	16,389% (983)
	60	13,851% (737)	585% (29)
76 (cyclohexyl)	15	13,169% (1,067)	8,143% (659)
	60	22,913% (813)	1,116% (40)
77	15	16,500%	1,500%
	60	38,167%	2,272%
78	15	17,920%	10,200%
	60	20,901%	4,725
74	15	8,100%	28,000%
	60	8,230%	2,900%

Cannula implantation surgery was performed and rats were allowed to recover. Twenty four hours later (Day 1) the cannula was perfused with Ringer solution and perfusates assayed by online HPLC to obtain basal DA output. Drugs were then perfused as 10 mM solution for the specified period and DA output assayed. On Day 2, after determination of basal DA output, the cannula was perfused with 10 mM MPP^+ and subsequent DA output assayed.

None of the pyridinium derivatives other than MPP^+ gave a toxic effect after perfusion for 15 minutes. Thus MPP^+ was clearly established as the most toxic analog of those tested. Perfusion of the 1,2-dimethyl-4-phenyl

derivative (**60**) and the 4-cyclohexyl derivative (**76**) for 60 minutes resulted in a toxic effect, i.e. a massive DA release on Day 1 accompanied by a minimal release on Day 2. Perfusion of the 3-phenyl (**77**), the 2-phenyl (**78**) and the tert-butyl (**74**) derivatives resulted in effects which were less than clearly toxic. For example, although very high DA release was observed on Day 1 after 60 minutes of perfusion with each drug, significant DA release was also observed on Day 2 after MPP^+ challenge. As a group, **77**, **78**, and **74** were clearly less potent than MPP^+, **60** and **76**, but it was difficult to discriminate between **77**, **78** and **74** to assign individual rank orders of potency. Thus the overall rank order of potency was assigned as follows: MPP^+ > the 1,2-dimethyl derivative **60** > the 4-cyclohexyl derivative **76** > **77**, **78** and **74**.

In order to obtain a more discriminatory measure of the toxicity of these substituted pyridinium ions in rat striatum, their effects on lactate efflux, an index of mitochondrial respiration inhibition, were measured. Increased lactate production is observed when mitochondrial respiration has been inhibited and arises from the compensatory effort of the brain to maintain requisite ATP levels through increased anearobic glycolysis. In previous work [106] Dr. Rollema showed that the average basal level of lactic acid in rat striatal dialysates is approximately 1 mM and that MPP^+ perfusion causes a dose-dependent increase in lactate efflux when

applied in concentrations of 1 mM or higher. He also showed that paraquat (11) and N-methylpyridinium iodide had no effect on lactate efflux, establishing that there is some structural specificity for this effect on rat striatum.[106] For this study, each of the substituted pyridinium drugs was perfused (10 mM) for one minute. The short perfusion of pyridinium drug was used because the lactate assay depends on detection of a flourescent product, since the pyridinium ions are also flourescent under the same condition, only a short perfusion time that allowed wash-through of the drug before detection of lactate efflux could be used. The results of the study are summarized in Table 3-5.

Table 3-5. Effects of substituted pyridinium ions on lactate efflux from perfused rat striatum.

Compound	Maximal lactate output as % of basal output	Delay period till maximal output achieved	Rank Order
MPP^+	190%	23 min	#1
60	174%	18 min	#2
76	107%	no significant effect	#6
77	144%	24 min	#4
78	153%	16 min	#3
74	131%	18 min	#5
73	100%	no significant effect	#6

Each drug was perfused as a 10 mM solution for 1 min. Following perfusion, the brain dialysate was mixed on-line with a reagent solution (5 ug/mL lactate dehydrogenase and 0.5 mM NAD^+ in carbonate buffer, pH 9.5 at a flow rate of 100 uL/minute. Lactate was measured as generated NADH which was assayed flourimetrically with an Aminco flourimeter using an excitation wavelength of 340 nm and recording an emission above 450 nm.[106]

MPP^+ was clearly the most potent elicitor of lactate efflux followed by the 1,2-dimethyl-4-phenyl derivative (**60**). The remaining derivatives fell into a rank order as follows: MPP^+ > 1,2-dimethyl (**60**) > 2-phenyl (**78**) > 3-phenyl (**77**) > tert-butyl (**74**). Unlike the results with previous assays (mitochondrial respiration, NADH dehydrogenase), the cyclohexyl derivative (**76**) had no effect on lactate efflux. (This anomalous effect was reinvestigated by Dr. Rollema when he returned to The Netherlands, on repetion of the experiment **76** was found to induce lactate efflux.) The 1,4-dimethyl derivative (**73**) also had no effect on lactate efflux but this result conformed to results with other assays and thus was not unexpected.

CONCLUSIONS

The results of assays of pyridinium ion-induced DA and lactate efflux did not give exactly the same rank orders of potency in each case, so using a subjective correlation the pyridinium analogs tested were assigned an overall rank order of potency as neurotoxins in the rat striatal perfusion model as follows. MPP^+ is clearly the most potent followed by the 1,2-dimethyl-4-phenyl analog (**60**) > the cyclohexyl (**76**) and cyclohexenyl (**75**) > 3-phenyl (**77**) and 2-phenyl (**78**) > 4-tert-butyl (**74**) > 1,4-dimethyl (**73**) derivatives. This overall rank order was drawn from the correlation between the rank orders of

potency for the various pyridinium analogs tested in the assays discussed in this chapter, and summarized in Table 3-6.

Table 3-6. Rank orders of potency of substituted pyridinium analogs in various assays of biological activity.

Compound	Mitochondrial 1)Resp 2)Uptake		NADH oxidase	Rat Microdialysis 1)Drug plus Drug	MPP^+	2)Lactate Efflux
MPP^+	#1	#1	#1	#1	#1	#1
60	#1	#1	#2	#2	#2	#2
75	#1	NT	NT	#1	#3	#6
76	#1	NT	NT	NT	#3	#6
77	#2	#2	#3	#2	#4	#4
78	#3	#3	#2	#2/3	#4	#3
74	#4	NT	#4	#4	#4	#5
73	#5	NT	#4	#4	NT	#6

NT means not tested.

Thus the structural specificity exhibited by substituted pyridinium derivatives is similar for both inhibition of rat liver mitochondrial respiration and the induction of dopaminergic neurotoxicity as examined by <u>in vivo</u> perfusion of rat striatum. This is circumstantial evidence supporting the concept that inhibition of mitochondrial respiration is involved in the development of pyridinium ion-induced neurotoxicity. The molecular

basis for selectivity of the neurotoxic effect of MPP^+ and similar compounds on the dopaminergic neuron which has been a puzzle from the beginning was not addressed specifically by these experiments however. The selectivity, which has been proposed to arise from selective uptake of MPP^+ into the dopaminergic nerve terminal, was addressed by the experiments described in Chapter 4 of this dissertation.

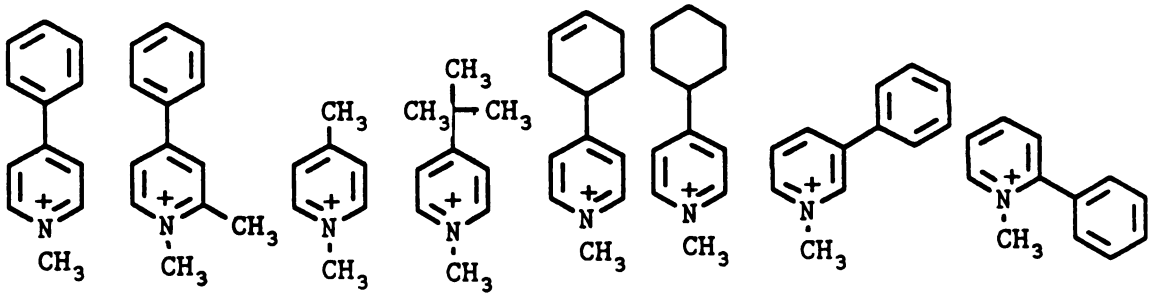

MPP^+ 60 73 74 75 76 77 78

Chapter 4. The effects of compounds structurally related to MPP^+ on the mouse striatal synaptosomal uptake of [^{3}H] Dopamine and [^{3}H] MPP^+

The basis for the selectivity of the toxic effect of MPTP with respect to dopaminergic neurons of the substantia nigra has been the focus of many research efforts. In order to account for this selectivity it was initially suggested that the conversion of MPTP to its toxic metabolites might be confined to the substantia nigra. MPTP's selective toxic effects could then be explained by the local production of toxic metabolites. However, Salach et al. showed that MPTP is much more efficiently processed to its toxic metabolites by MAO B than by MAO A.[5] Furthermore, using monoclonal antibodies specific for each of the forms of MAO, Westlund et al. have shown that MAO B is not concentrated in the dopaminergic areas affected most by MPTP but instead is located in the serotonergic cell groups including the nucleus raphe dorsalis and the nucleus centralis superior,[74] neurons which are not affected by MPTP. Thus the selectivity of the MPTP toxic effect could not be explained by localization of the bioactivating enzyme, MAO B. In a rapid communication Javitch and Snyder presented evidence of the active uptake of [^{3}H] MPP^+ by the dopamine uptake system in synaptosomes prepared from rat corpus striatum. They proposed that this phenomenon

formed the basis for the selectivity of MPTP neurotoxicity, specifically, that MPP^+ was formed by the MAO B-catalysed oxidation of MPTP at a site outside of the dopaminergic neuron. It was then transported into the dopaminergic neuron, accumulating to a concentration where toxicity was expressed.[75] Subsequently, Javitch et al. reported that kinetic parameters for striatal synpatosomal uptake of [^{3}H] MPP^+ (K_m 170 nM, V_{max} 2 nmol/gm tissue per min) were very similar to those for uptake of [^{3}H] dopamine (Km 150 nM, Vmax 2 nmol/gm tissue per min).[76] Furthermore these investigators showed that the uptake of [^{3}H] MPP^+ was saturable, as well as temperature dependent, phenomena which are usually associated with an enzyme or protein mediated event.[76] The close comparison of kinetic values reported for dopamine and MPP^+ uptake implied that large amounts of MPP^+ might be accumulated by the dopamine neuron as effectively as if it were the normal neurotransmitter.

The neuronal dopamine uptake system had been studied for many years prior to these discoveries and was well characterized as the major biochemical mechanism for termination of catecholamine neurotransmitter action.[85] Following the release of dopamine into the synaptic cleft, where it interacts with post-synaptic dopamine receptors, the uptake system terminates neurotransmitter activity by pumping dopamine back into the presynaptic neuron. There, it is repackaged into granuals to await

the next neuronal release. Other mechanisms of neurotransmitter inactivation include MAO-catalysed amine oxidation and the action of catechol-O-methyl-transferase (COMT). COMT is an enzyme which catalyses the methylation of the 3-position hydroxyl moiety of catechol neurotransmitters.[77] The protein which acts as the dopamine translocator in the process of dopamine reuptake is similar to a sodium-potassium ATPase in that it requires sodium ions and energy in order to execute the dopamine uptake event.[84] Like many enzymes, this protein exhibits saturable kinetics with increasing substrate concentration.[84] The protein is located in the nerve terminal membrane and thus can be semi-purified by the preparation of synaptosomes which are spherical vesicles formed from the pinched-off ends of nerve terminals.[82,83,84] The uptake of dopamine into synaptosomes results in an accumulation of material on the interior of the spherical vesicle. Experimentally, the measurement of an uptake process depends on measurement of radiolabled ligand which has become associated with the synaptosomal protein. However, dopamine receptors which are present on the exterior of the vesicle, can also bind dopamine. Thus the experimental measurement of dopamine uptake must be able to distinguish not only between bound and free radioactive ligand, but must also be able to distinguish between ligand bound to the exterior of the vesicle and

ligand that has been transported to the inside of the vesicle. To separate bound ligand from free ligand in solution, the protein vesicles are filtered from the incubation medium at the end of the incubation period. Excess ligand which remains loosely associated with the exterior of the vesicle or bound to exterior receptor is washed off the filter with excess buffer. After washing, the remaining bound radioactive ligand is quantified by liquid scintillation analysis. Bound radioactive ligand which can be detected on the filter is the sum of several components of binding. If the experiment has been properly designed, the largest component of bound radioactivity is that which has been transported to the interior of the vesicle. This component is also called specific binding, or in an uptake experiment, this is "active uptake". Two other components of the total bound radioactivity can be defined including filter binding and non-specific binding. Filter binding is defined as the number of dpm which bind to the filter in the absence of protein and is dependent on the chemical characteristics of the filter and the radioligand used. Non-specific binding occurs in the presence of protein but is not due to the active uptake of the radioligand into vesicles. Instead non-specific binding may be due to binding of the radioligand to surface receptors or other protein components which are not involved in synaptosomal uptake. Furthermore, passive diffusion of the radioligand into

the vesicle may be detected as non-specific binding. Non-specific binding is experimentally determined by addition of a known uptake inhibitor. Thus non-specific binding is the number of dpm bound to the filter in the presence of the uptake inhibitor plus protein. It should be noted that filter binding is usually less than non-specific binding and can be considered a component of non-specific binding. For a good signal to noise ratio, both filter binding and non-specific binding should be minimized by adjustment of the uptake assay protocol. Uptake can then be defined as that portion of the total accumulated radioactivity which is not accumulated in the presence of the uptake inhibitor. The uptake system for dopamine can be distinguished from that of norepinephrine as it is not potently inhibited by the tricyclic antidepressants such as desipramine, imipramine, and protriptyline.[86,87,88] Although potent inhibitors of dopamine uptake have been developed, including nomifensine, GBR 13098, and mazindol, it should be noted that these compounds are also potent inhibitors of norepinephrine uptake.[76,89,90] Nevertheless, mazindol has been used experimentally to help distinguish the active, specific, synaptosomal uptake of [^{3}H] dopamine from non-specific binding of dopamine to membranes in the synaptosomal preparation.[75,76,91] Since uptake is an energy dependent process unlike passive diffusion, an alternative definition of uptake, the difference between

accumulation observed at 37 ^{o}C and 0 ^{o}C, has been used by some investigators.[81]

Javitch and Snyder were not alone in their interest in the interactions of MPP^{+} with the dopamine uptake system, especially since Pileblad and Carlsson [60] and Melamed et al. [59] had recently reported that pretreatment of mice with dopamine uptake inhibitors prevented the expression of MPTP-induced neurotoxicity. Chiba et al., almost simultaneously, reported results very similar to those of Javitch with the additional information that synaptosomes prepared from the corpus striatum accumulated [^{3}H] MPP^{+} at a rate 5-10 fold higher than preparations from other brain regions.[78] Heikkila et al.[79], Gessner et al.[80], and Shen et al.[81] also reported, in quick succession, essentially the same results as Javitch, though the experimental methods and actual kinetic values were slightly different in each report.

It was clear in all of these reports that synaptosomal uptake of [^{3}H] MPP^{+} could be demonstrated. It was becoming rapidly accepted by researchers in the MPTP field that dopamine neuronal uptake of the MPTP metabolite, MPP^{+}, was involved in the development of neurotoxicity. We had observed a structural specificity in the effects of MPP^{+} analogs on mitochondrial respiration; i.e. no compound was more potent than MPP^{+} but analogs with a large lipophilic moiety in the 4-position of the pyridinium ring were more potent than

those with small substituents or with differently positioned large substituents. Furthermore, we had demonstrated that although a methyl group placed in the 2 or 6 position of the tetrahydropyridine ring abolished MAO substrate activity, the methyl group was not detrimental to the toxic activity associated with the metabolites. We had observed that the same structural specificity seemed to apply to the neurotoxic effects of pyridinium compounds as examined in the in vivo brain dialysis experiments. In veiw of these results, the next logical step was to investigate the structural requirements of the dopamine uptake system. We asked the following question: Are pyridinium species other than MPP^+ transported by the dopamine uptake system and if so, what structure-activity relationship might govern the interaction?

Sensitive measurement of the synaptosomal uptake of DA and MPP^+ depends on the use of high specific-activity radiolabeled substrates. The analogs, whose potential substrate activity we wished to measure, were not available in radiolabeled form. We considered undertaking the synthesis of the radiolabled compounds via alkylation of the parent pyridines with commercially available [^{3}H] methyl iodide but found that the costs to obtain the required level of specific activity (ca 85 Ci/mmol) were prohibitive. Thus, rather than measure the uptake of the MPP^+ analogs directly, we estimated the

relative affinities of the compounds for the uptake system by measuring their inhibition of the uptake of [^{3}H] MPP^+ and [^{3}H] DA. Due to the structural similarity of the test compounds with MPP^+, we anticipated that inhibition of [^{3}H] MPP^+ and [^{3}H] DA uptake would be competitive in nature. Thus the relative affinities of the MPP^+ analogs for the dopamine uptake system would be related to their potency as inhibitors of [^{3}H] MPP^+ and [^{3}H] DA uptake. To form a basis on which our studies could be compared to those of other laboratories, we intended first to demonstrate uptake of [^{3}H] MPP^+ and [^{3}H] DA, measure the kinetic characteristics of the uptake of each substrate, then look for the effects, if any, of our pyridinium analogs on uptake. We expected that competitive inhibition would be observed if the compounds were themselves uptake substrates.

Although one of the early studies (Chiba et al. [78]) had originated from our laboratory, the postdoctoral scholar who had performed the studies had subsequently returned to Japan. The expertise required for preparation of synaptosomes and performance of the dopamine uptake assay was therefore redeveloped in a collaborative effort with Ellen Wu, a fellow graduate student, in order to accomplish the presently reported study. Ms. Wu performed all of the brain dissections and was a dedicated partner in performing the uptake assays.

This study could not have been completed without her participation.

PURIFICATION OF [^{3}H] MPP$^+$

In order to measure the uptake of [^{3}H] MPP$^+$ we required radiolabled compound of very high specific activity. The incubation concentrations of [^{3}H] MPP$^+$ were to be very low (1 nM). Thus in order to detect the small amounts of compound taken up, the specific activity of the radioligand would have to be very high (85 Ci/mMole). One of the difficulties of working with radiolabled compounds of very high specific activity is the decomposition which these compounds undergo with time. Radiolabeled MPP$^+$ is very expensive ($1,000 per mCi) and therefore we wished to make use of the stock we had on hand, although this stock was more than 1 year old. HPLC analysis with radiochemical detection revealed that the stock [^{3}H] MPP$^+$ was about 90% pure and was contaminated with several decomposition products more polar than the original compound (Figure 4-1). The identity of the dominant peak in the HPLC chromatograph (retention time 7.5 min) was established as [^{3}H] MPP$^+$ by comparison to the UV detected chromatograph of a sample diluted with unlabeled MPP$^+$.

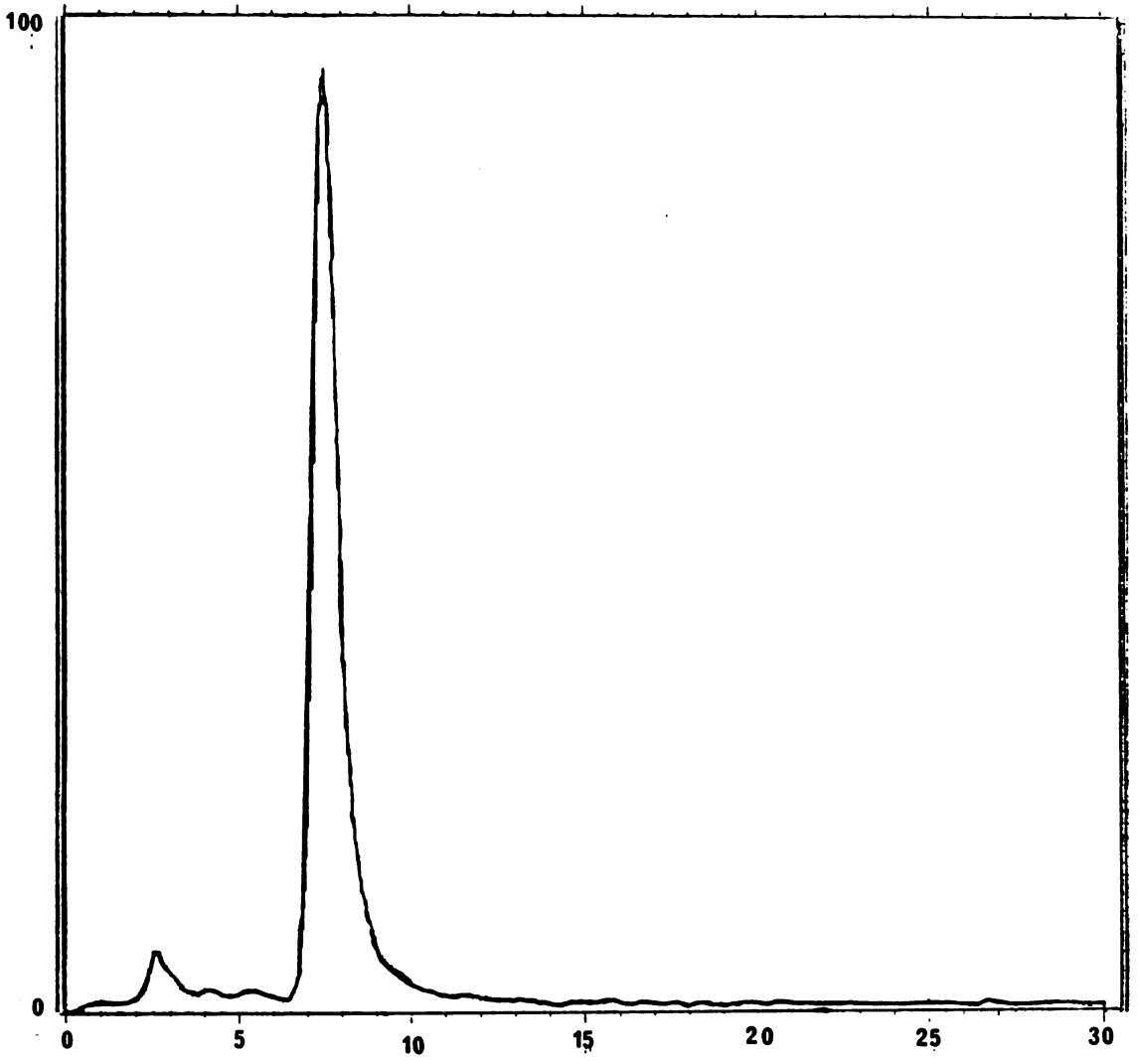

Figure 4-1. HPLC chromatograph of [^{3}H] MPP^+ prior to purification. Radiochemical detection showed unchanged [^{3}H] MPP^+ with retention time 7.5 min (89.8%) is the major component. The peaks at 2.6 min (5.9%), 4.1 min (1.8%) and 5.3 min (2.5%) arise from contaminants which are more polar than MPP^+ and thus elute earlier than the parent compound on the cation exchange column.

[^{3}H] MPP^+ was purified by chromatography on alumina TLC plates, which were developed with a solvent mixture of acetonitrile: dichloromethane (1:1). After the plates were dried and sectioned into 1 cm bands, each band of alumina was scraped from the plate and eluted with acetonitrile. The amount of [^{3}H] MPP^+ recovered in each eluate was quantified by liquid scintilation spectrometry. Most of the radioactivity was found in the eluates from the second and third bands, representing 43% and 37%, respectively, of the total recovered radioactivity (0.15 uCi, 7.5% of initial application to the plate). Scintillation spectrometry analysis of the eluted alumina indicated a large number of counts remained bound to the material. HPLC analysis revealed the eluates from the second and third bands contained pure [^{3}H] MPP^+ (Figure 4-2). The orginal specific activity was 85 Ci per mMol. Since we had not diluted the stock with unlabeled MPP^+, we assumed the specific activity of the purified [^{3}H] MPP^+ remained the same. The purified [^{3}H] MPP^+ was used in subsequent experiments. Analysis of the washed alumina indicated that a significant amount of radioactivity remained on the alumina even after the elution described above. The efficiency of this purification, though not high, was sufficient to provide pure [^{3}H] MPP^+ for an estimated 1800 incubations at 1 nM concentration.

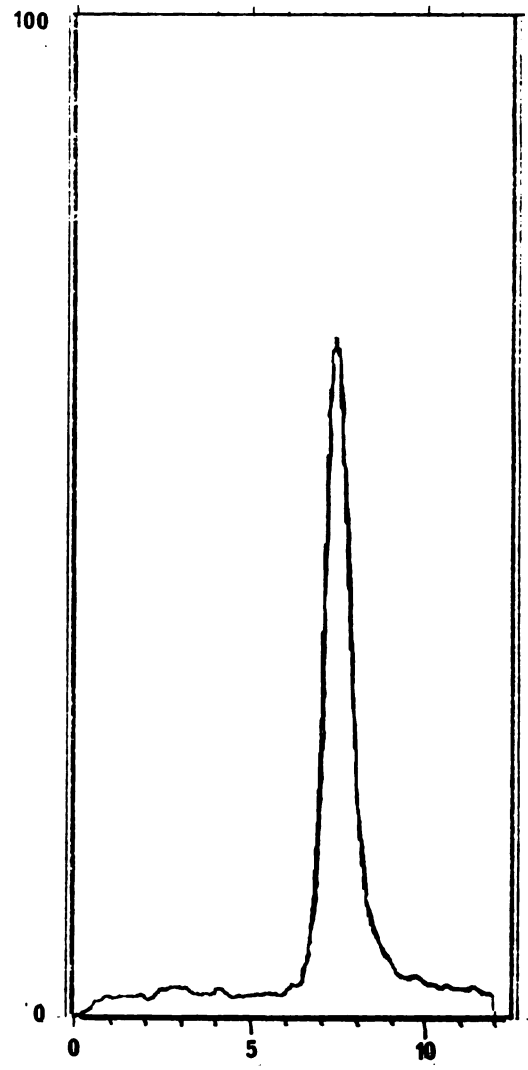

Figure 4-2. HPLC chromatogram of purified [^{3}H] MPP^+. Radiochemical detection shows a single peak with retention time 7.5 min corresponding to pure [^{3}H] MPP^+.

The [^{3}H] DA which we had on hand was contaminated with over 30% decomposition products. The catechol ring of dopamine is readily oxidized in solutions of pH greater than 7. Therefore no attempt was made to purify stocks of [^{3}H] DA. Instead, the much less expensive [^{3}H] DA was freshly purchased as needed, in small quantity. The pH 7 solutions of [^{3}H] DA required for uptake assays were prepared by dilution of the purchased stock (15 Ci/ mmol, a stable solution in ethanol/acetic acid, pH 4) with assay buffer immediatly prior to each use and not retained for more than 8 hours. Solutions were stored, protected from light, on ice to minimize oxidation of the [^{3}H] DA.

PREPARATION OF MOUSE STRIATAL SYNAPTOSOMES

The preparation of synaptosomes, vesicles formed from nerve terminal membranes, was first reported in depth by Gray and Whittaker, [82] who showed that the vesicles were formed on homogenization of neural tissue and could be separated from other cellular fragments such as nuclei, mitochondria and microsomes by centrifugation on a density gradient. The purity of this preparation was demonstrated by electron-micrographs. However, Gray's lengthy preparation scheme prevented synaptosomes from being widely used until Coyle and Snyder[83] demonstrated that density gradient centrifugation was not

necessary for isolation of a synaptosomal preparation sufficiently pure for dopamine uptake studies.

Our preparation scheme was essentially a modification of that reported by Javitch et al.[76] Briefly, C57 black mice were sacrificed with carbon dioxide, followed by decapitation. The striata were rapidly dissected on ice and homogenized in ice-cold 0.32 M sucrose. The homogenate was centrifuged at 1,000 x g for 15 minutes in a chilled microcentrifuge. The pellet, containing large cellular fragments, was discarded and the remaining supernatent centrifuged at 17,500 x g for 20 minutes. The resulting synaptosomal pellet was resuspended in 0.32 M sucrose and centrifuged again at 17,500 x g for 20 minutes. To "wash" the synaptosomes, the resulting pellet was resuspended again in 0.32 M sucrose and centrifuged a third time at 17,500 x g for 20 minutes. Eventually, the "wash" was omitted in order to save time and increase the protein yield. After the final centrifugation, the pellet containing synaptosomal protein was suspended in uptake buffer and kept on ice. A determination of synaptosomal protein was always made at this point in order to ensure accurate distribution of the protein at 0.3 mg per incubation. The fragile synaptosomal preparation was always freshly made and used immediately.

DEVELOPMENT OF UPTAKE ASSAY PROTOCOL

Much effort was expended to develop the uptake assay protocol to achieve maximum sensitivity and reproducibility of results. In early experiments we attempted to reproduce the kinetic values for [^{3}H] MPP^+ uptake that had been reported by others and to demonstrate that nonlabled dopamine inhibited the uptake of [^{3}H] MPP^+. We used a protocol which was modeled after that of Chiba et al.[78] Briefly, we prepared the synaptosomes, performed a protein determination, then used 0.3 mg protein per assay. All reagents and buffer were preincubated at 37 ^oC for five minutes to achieve temperature equilibration. The uptake reaction was initiated with addition of synaptosomal protein to the incubation mixture which was then maintained at 37 ^oC for an additional five minutes. The reaction was terminated by addition of iced uptake buffer, followed by rapid filtration of the synaptosomal protein over cellulose acetate/nitrate filters. After the filters had been rinsed twice with buffer, they were placed with 10 mL scintilation fluid in a vial for counting. Each vial was counted 3 times and the values averaged. Initially each assay was carried out in duplicate. Active uptake (see definition above) was defined according to the protocol of Javitch et al.[76] A selective inhibitor of dopamine uptake, 10 uM mazindol, was used in the control

experiments to correct for passive diffusion and adsorption to membranes and filters. Active uptake was calculated by subtracting from the total cpm (Total) the number of cpm accumulated in the presence of 10 uM mazindol (Non-specific) and was expressed as nmol per g of tissue per min. We used this protocol for the first uptake experiments with [^{3}H] MPP$^+$.

The data arising from the early experiments however made it clear that there were many problems with our assay protocol. The problems and their solutions are presented here in the approximate order in which they were encountered. It is important, however, that the reader understand that many of the solutions to the problems were not obvious. Intuition played a part in the development of the final successful assay protocol. Probably one of the most important factors in the final developement of a successful protocol was simple practice. We prepared the synaptosomes and performed assays over 22 times in the pursuit of reproducible data. In addition to improvements made in the assay protocol, we eventually developed a method for exact repetition of each operation required for the assay which undoubtably made an important contribution to the reproducibility of our data.

As discussed above, our initial goal was to assess the kinetic parameters for active uptake of [^{3}H] MPP$^+$. In our first experiment using cellulose acetate/nitrate

filters, we found a Km value of 332 nM and Vmax value of 2.78 nmol/gm min. We were encouraged by this result since our results were consistant with the Km values (180-480 nmol/gm.min) and Vmax values (2-7.35 nmol/gm.min) recently reported by others.[75,76,78,81]. In the subsequent experiment, however, we examined the effects of unlabeled dopamine on the uptake of [^{3}H] MPP^+. We could not demonstrate the concentration dependent inhibition of uptake which would be expected if dopamine and MPP^+ were competing for the same carrier system. Instead the data we obtained indicated an inhibition of [^{3}H] MPP^+ uptake at low dopamine concentration which diminished as the dopamine concentration increased to 50 nM but increased again as dopamine concentration reached 1 uM (Table 4-1).

Table 4-1. Effects of dopamine on mouse striatal synaptosomal [^{3}H] MPP^+ uptake, measured using cellulose acetate/nitrate filters.

[DA]	Total dpm	Nonspecific dpm (+ Mazindol)	Uptake dpm	% inhibition
0 nM	14,558	8,001	6,557	Control,0 %
1 nM	4,686	4,110	576	91.2%
10 nM	6,219	5,104	1,025	84.4%
50 nM	8,163	4,290	3,873	40.9%
100 nM	3,521	9,893	-6,372	?
300 nM	4,045	2,658	1,387	78.8%
600 nM	3,128	3,069	59	99.1%
1000 nM	1,810	1,818	-8	?

A typical assay containing 1 nM [^{3}H] MPP^+ (or 1 nM [^{3}H] MPP^+ plus 1 uM mazindol) and the specified concentration of DA was preincubated for 5 minutes, prior to the addition of 0.3 mg synaptosomal protein. A five min reaction period followed. Reactions were terminated by addition of iced buffer and filtration over cellulose acetate/nitrate filters. All assay conditions run in duplicate

We felt that such results were likely to be an artifact of some problem with the assay protocol. The clue to solving the problem was contained in other data from the same experiment where we examined the level of radioactivity that was bound to the filter in the absence of protein. This experiment revealed an unacceptably high level of radioactivity ([^{3}H] MPP^+) bound to the filter in the absence of protein (filter binding). The filter binding was as high as 90% of the total bound radioactivity (bound in the presence of protein) using the original cellulose acetate/nitrate (Millipore, 0.45 um) filters, which had been used by Chiba et al, in the work previously published.[78] The data are shown in Table 4-2.

Table 4-2. Filter binding in assays with 1 nM [^{3}H] MPP^+ and cellulose acetate/nitrate filters (Millipore, 0.45 um)

Filter	Mazindol	Total Bound dpm	Filter Bound dpm	Filter bound as percent of Total
Cellulose	-	6,750	6,603	97.3%
	+	11,045	10,481	94.9%

Assays performed in the presence (+) or absence (-) of 10 uM mazindol. Data source, expt.4

The results shown in Table 4-2 also showed that with Cellulose acetate/nitrate filters the non-specific binding (+ mazindol) was higher than total binding

(- mazindol) which, together with the high filter binding, indicated a severe problem with our assay.

The problem was solved when the cellulose acetate/nitrate filters were replaced with fiber glass filters (Whatman, GF/B). Ultimately, using the fiberglass filters, under optimized assay conditions (as described in the following pages), non-specific binding averaged 17% or 5% of the total bound radioactivity when [^{3}H] MPP^+ or [^{3}H] DA, respectively, were used. Furthermore, filter binding averaged 11.8% and 1.7% of total binding for [^{3}H] MPP^+ and [^{3}H] Da, respectively. See Table 4-3 for a summary of the raw data supporting these conclusions.

Table 4-3. Average and range values for total, non-specific and filter binding in assays of [^{3}H] MPP^+ and [^{3}H] Da uptake using fiberglass filters.

Substrate	Binding type	Average dpm	Range dpm
[^{3}H] MPP^{+A}	Total[C]	14,300	(19,530-8,817)
	Non-specific[D]	2,477	(3,148-1,547)
	Filter[E]	1,691	(3,747- 331)
[^{3}H] DA [B]	Total	71,448	(82,420-56,485)
	Non-specific	4,115	(4,720- 3,448)
	Filter	1,235	(1,459-1,081)

A Values obtained using 1 nM [^{3}H] MPP^+, expts, 13,14,21,22. B Values obtained using 10 nM [^{3}H] DA, expts.16,17,18,19,20. C Bound dpm obtained in presence of protein and uptake substrate. D Bound dpm obtained in presence of protein, mazindol and substrate. E Bound dpm obtained in presence of substrate only

We then further characterized the filter binding of [^{3}H] MPP^+ with fiber glass filters. The amount of

binding was temperature dependent. Using 1 nM [^{3}H] MPP^+ filter binding (absence of protein) was twice as high at 0 ^oC (1,009 dpm) as at 37 ^oC (582 dpm). This is consistant with the findings of many workers in the ligand binding science who have found that radioactive ligands may display higher affinity at 0 ^oC than at 37^o C. For example [^{3}H] imipramine dissociates rapidly from its binding site on the platelet membrane serotonin transport complex at 37^o C with a half-life of 5 minutes. In contrast, at 0 ^oC, [^{3}H] imipramine dissociates slowly from its binding site with a half-life of 61 minutes (Segonzac, 1987 [95]).

Furthermore, filters which had been presoaked in unlabeled MPP^+ 10 mM in uptake buffer exhibited a reduced level of filter binding. The MPP^+ presoaked filters attracted 530 dpm [^{3}H] MPP^+, while filters soaked in the standard uptake buffer adsorbed 959 dpm [^{3}H] MPP^+. Thus in the final experimental protocol, all filters were presoaked in 10 mM MPP^+ in uptake buffer and all controls were performed at 37 ^oC, to minimize filter binding and enhance sensitivity.

In the protocol of Javitch et al., 10 uM mazindol, a selective inhibitor of dopamine uptake, was used in the control experiments to correct for passive diffusion and adsorption to membranes and filters.[76] In their protocol, active uptake was calculated by subtracting from the total cpm the number of cpm accumulated in the

presence of 10 uM mazindol (nonspecific binding) and was expressed as nmol per g of tissue per min. We were uncomfortable with using such high levels of mazindol relative to the concentration of [^{3}H] substrate used (1 nM [^{3}H] MPP^+, 10 nM [^{3}H] DA). Therefore, the concentration dependence of the inhibition of uptake by mazindol was investigated and the results are presented in Table 4-4.

Table 4-4. Concentration dependence of Mazindol inhibition of synaptosomal [^{3}H] MPP^+ uptake.

[Mazindol]	Non-specific binding (+ Mazindol) in dpm	Non-specific as percent of total
0.1 uM	6,709	89.2
0.5 uM	4,572	60.8
1.0 uM	4,035	53.7
5.0 uM	2,447	32.6
10.0 uM	1,206	16.0

synaptosomal protein conc. 0.3 mg/mL, avg. total accumulation in absence of mazindol 7516 dpm (n=10). Fiberglass filters presoaked in 10 mM unlabeled MPP^+ in uptake buffer. Preincub. 5 min, assay incub. 5 min at 37 ^oC. [^{3}H] MPP^+ 1 nM in all incubations.

Maximum inhibition of MPP^+ uptake giving the lowest nonspecific binding (maximum sensitivity) was achieved with 10 uM mazindol, therefore we, like Javitch et al., used 10 uM mazindol in control incubations. Javitch et al had demonstrated that 10 uM mazindol was appropriate

for determination of non specific binding in DA uptake experiments[76] therefore in light of our results with MPP^+ uptake, we did not perform a similar study with [^{3}H] DA.

Following the example of Javitch et al.,[76] we adopted the following definition of "active uptake" in our final protocol: "Total control" samples were incubated under the conditions described in the experimental section to give total dpm accumulated. To correct for passive diffusion and adsorption to membranes and filters, "control nonspecific binding" samples were incubated in the presence of 10 uM mazindol. "Control active uptake" was calculated by subtracting from the "total control" dpm the number of dpm accumulated in the presence of 10 uM mazindol ("control nonspecific binding") and was expressed as nmol per g protein per min.

We found the "active" synaptosomal uptake of [^{3}H] MPP^+ was dependent on protein concentration as shown in Table 4-5.

Table 4-5. Protein concentration dependence of [^{3}H] MPP^+ uptake in mouse striatal synaptosomes.

Protein conc. mg/mL	Total dpm	Nonspecifc dpm	[^{3}H] MPP^+ uptake dpm
0.2	3,211	1,581	1,630
0.4	11,906	2,415	9,491
0.6	19,598	3,638	15,960

All assays performed in triplicate at 1 nM [^{3}H] MPP^+, nonspecific binding determined in the presence of 10 uM mazindol.

We desired to enhance inter-experimental reproducibility and allow the comparison of data obtained on separate days by using the same amount of synaptosomal protein for all assays. For this reason we performed a Lowry protein assay on every synaptosomal preparation so that we could add exactly the same amount of protein for each assay. We used 0.3 mg protein for all incubations since this amount of protein represented a good compromise between sensitivity and economy, giving sufficient activity to give good sensitivity, yet being a small enough amount of protein to give many samples per experiment.

Javitch et al. had reported that rat striatal synaptosomal [^{3}H] MPP^+ uptake is linear with time up to 8 minutes, after which time it begins to plateau.[76] In order to find the optimal incubation period for uptake with our mouse synaptosomes, we examined the variation of specific uptake with incubation periods of 5, 10, or 15 minutes. We did not examine shorter periods as we found it too difficult to manage all the pipetting operations required for large scale assays in shorter incubation periods. The results of this examination (Table 4-6), are somewhat difficult to interpret and are representative of the difficulties that we encountered throughout much of the work. If any trend of uptake dependence on incubation time is apparent in these data, it is that uptake with 0.4 mg protein is maximal at 5

minutes incubation time and declines with longer incubation periods. In our final assay protocol, we used a 5 minute incubation period in order to remain consistant with the uptake assay protocols published by others,[75,76,78,79,80,81]. This time period gave a reasonably large amount of uptake, and yet was conveniently short. A short incubation period was desireable since the incubations were performed in sets of eight. Thus for each set of eight tubes, all pipetting operations except addition of protein were completed, the tubes preincubated 5 minutes, the protein added, the tubes further incubated 5 minutes and the reactions stopped and filtered, before the next set of incubations were begun. Although this appears to be a tedious procedure, we felt it necessary to ensure that each incubation was performed under exactly the same conditions.

Table 4-6. Dependence of mouse synaptosomal [^{3}H] MPP^+ uptake on incubation time

Synaptosomal protein conc. mg/mL	Incub. period minutes	Total dpm	Nonspecific dpm	Uptake dpm
0.2	5	5,893	3,196	2,697
	10	3,211	1,581	1,630
	15	7,641	3,085	4,556
0.4	5	12,883	1,706	11,177
	10	11,906	2,415	9,491
	15	9,111	5,524	3,587
0.6	5	8,420	697	7,724
	10	19,598	3,638	15,960
	15	14,993	10,359	4,634

All assays performed in triplicate at 1 nM [^{3}H] MPP^+, nonspecific binding determined in the presence of 10 uM mazindol. Expt. #10

In early experiments the tissue specificity of the uptake phenomenon was investigated by incubating liver microsomal protein under the same conditions used for the synaptosomal uptake experiments. Table 4-7 displays the results of this study.

Table 4-7. Active uptake of [^{3}H] MPP^+ by mouse striatal synaptosomes and rat liver microsomes at 0 ^{o}C and at 37 ^{o}C

Protein	Temperature	Total dpm	Nonspecific dpm	Uptake dpm
mouse striatal synaptosomes	0 ^{o}C	870	816	54
	37 ^{o}C	7,516	1,206	6,310
Rat liver microsomes	0 ^{o}C	856	856	0
	37 ^{o}C	1,068	1,065	3

All assays performed in duplicate with 1 nM [^{3}H] MPP^+, nonspecific binding determined in the presence of 10 uM mazindol. All assays performed with 0.3 mg protein/assay

Negligible mazindol-inhibitable accumulation of [^{3}H] MPP^+ (the definition of active uptake) was observed with microsomal protein (3 dpm/5 min) while striatal synaptosomal uptake was significant (6310 dpm/5 min).

In the original assay protocol, each filter sample was added to the scintillation vial with 10 mL scintillation fluid and counted 3 times (five minute counts). The results of the counts were averaged to give the final data. In the course of the early experiments, we found that each successive count gave a higher dpm, possibly explained by slow release of protein-trapped tritium into solution where it came into contact with the scintillation-producing compounds in the fluid. For example, the controls in one of the experiments gave values of 840 and 900 dpm on first count. Sixteen hours later the same samples gave readings of 1114 and 1373 dpm, respectively. Twenty one hours after the first count, a third count gave 1178 and 1449 dpm. To remedy this time release effect and to ensure that all data for all experiments would be obtained under the same conditions we added a new aspect to the uptake assay protocol. After the addition of scintillation fluid to the filter, each sample was vortexed for 15 seconds, to release protein-trapped tritium into solution. The samples were analysed by liquid scintillation

spectrometry immediately after the conclusion of the incubations and only one reading was taken.

KINETICS OF MOUSE STRIATAL SYNAPTOSOMAL [^{3}H] MPP^+ UPTAKE

After the discovery of inappropriately high filter binding with the cellulose acetate/nitrate filter, it was necessary to reassess the kinetic values for [^{3}H] MPP^+ uptake using the new fiber glass filter. Uptake was measured at each of 5 concentrations of [^{3}H] MPP^+ (10-600 nM), in triplicate. The background binding (in presence of protein and 10 uM mazindol) and filter binding (absence of protein) were also measured at each concentration of [^{3}H] MPP^+, since these parameters increase linearly with increasing radiolabled ligand. The data obtained in this experiment are shown in Table 4-8 and graphically displayed in Figure 4-3.

Table 4-8. Mouse striatal synaptosomal uptake of [^{3}H] MPP^+

[^{3}H] MPP^+	Total dpm	Nonspecific dpm	Filter dpm	Uptake dpm	Uptake nmol/g per min
10 nM	82,991	22,147	8,040	60,845	0.22
50 nM	344,776	78,076	ND	266,700	1.19
100 nM	674,487	175,249	127,589	499,238	1.77
300 nM	1,378,557	349,322	ND	1,029,235	3.65
600 nM	1,338,530	731,865	530,068	606,665	2.15

Each assay performed in duplicate contained 0.3 mg synaptosomal protein plus the indicated concentration of [^{3}H] MPP^+, nonspecific binding was determined in the presence of 10 uM mazindol. ND = not determined, Expt. #7

A double reciprocal plot of these data (Figure 4-4) was used to determine kinetic parameters. Using the new filter, the Km value was 255 nM while the Vmax was 5.88 nmol/gm min. These values were still consistant with those reported by other groups in this field. It is interesting, however, that saturable kinetics and reasonable kinetic values were also obtained with the cellulose acetate/nitrate filters which exhibited such high filter binding. This indicates that saturable binding characteristics taken alone are not always a reliable indication that an uptake system is being accurately measured.

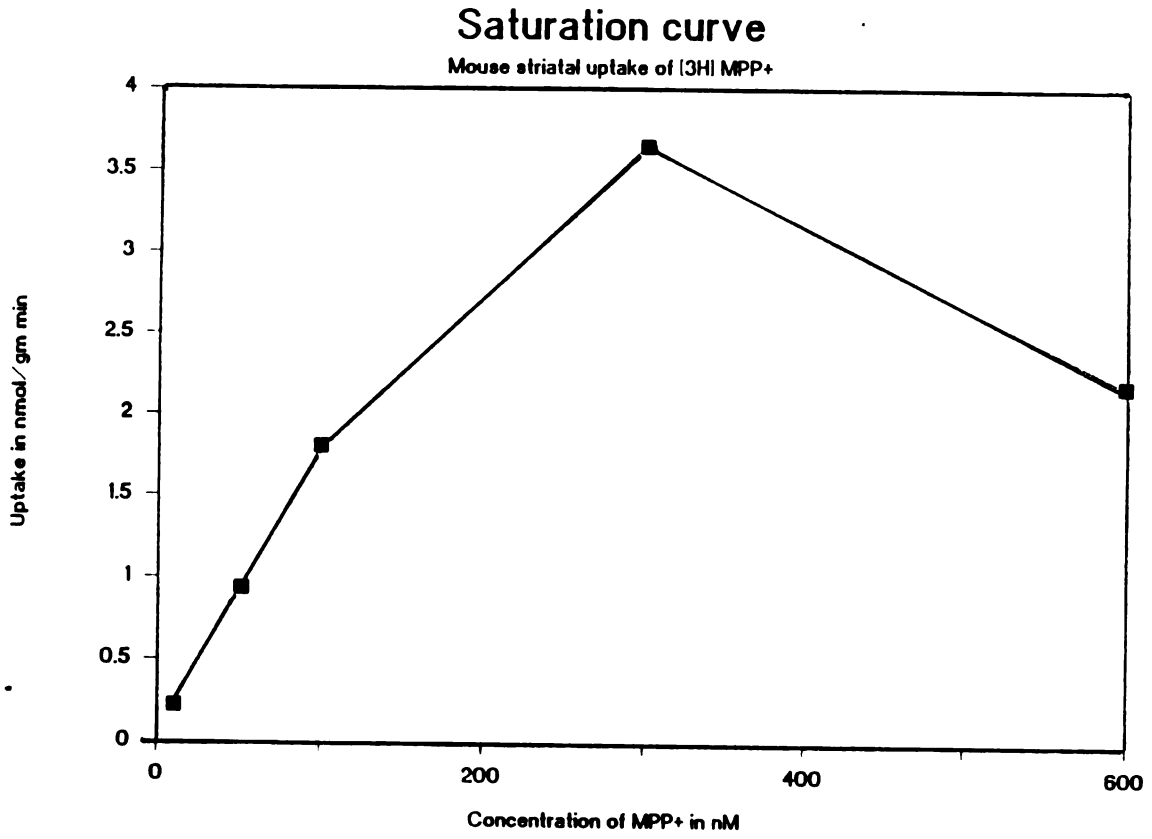

Figure 4-3. Saturation plot for mouse striatal synaptosomal uptake of [^{3}H] MPP^+. Data obtained from triplicate assays at each of 5 concentrations (10 nM-600nM [^{3}H] MPP^+). Nonspecific binding was determined using parallel triplicate incubations in the presence of 10 uM Mazindol.

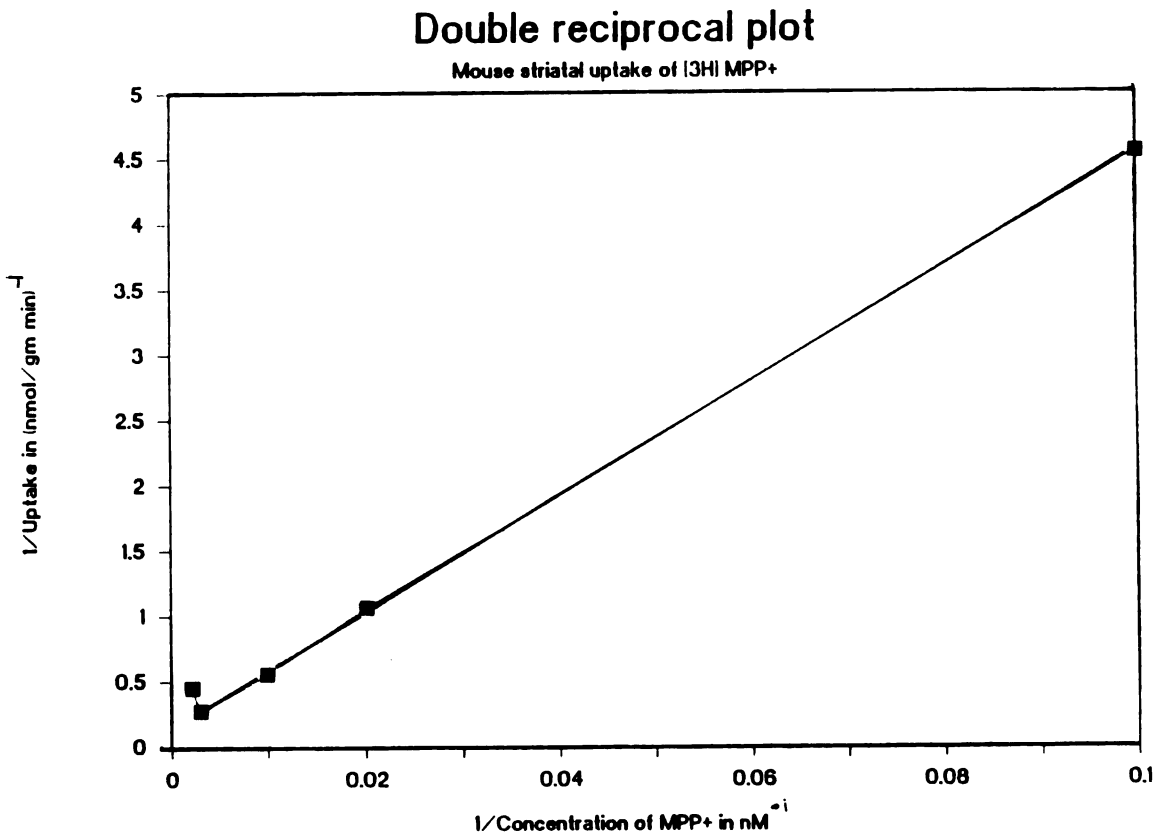

Figure 4-4. Double reciprocol plot of mouse striatal synaptosomal uptake of [^{3}H] MPP$^+$. Km (255 nM) and Vmax (5.88 nmol/g per min) were calculated by least squares linear regression.

DEVELOPEMENT OF PROTOCOL FOR COMPETITION EXPERIMENTS

However, the satisfactory new results obtained with the kinetic parameters for uptake of [^{3}H] MPP^+ led us to begin competition experiments. The first set of compounds tested as inhibitors of [^{3}H] MPP^+ included unlabled MPP^+, the 1,2-dimethyl MPP^+ analog **60**, the 2-phenyl analog **78**, the 3-phenyl analog **77**, the t-butyl compound **74** and the 4-cyclohexyl compound **76**. Each compound was tested at 4 concentrations (5 nM to 5 uM). Only one set of control incubations was performed at the beginning of the experiment. The level of nonspecific binding determined in control incubations with 10 uM mazindol at the beginning of the experiment was subtracted from the activity found with each inhibitor concentration to correct for passive diffusion and filter binding. The uptake activity in the presence of each inhibitor was expressed as a percentage of control uptake activity determined for that experiment. In the first competition experiments, we ran into difficulties when calculation of the uptake activity showed that uptake was actually more rapid in the presence of these putative inhibitors than in the controls. This data is summarized in Table 4-9.

Table 4-9. Effect of substituted pyridinium ions on mouse striatal synaptosomal uptake of [^{3}H] MPP^+

Compound	Concentration	Total bound dpm	Uptake# dpm	Percent Control
unlabled MPP^+	5 nM	10,258	8,050	143%
	50 nM	9,710	7,502	133%
	500 nM	7,761	5,553	98%
	5000 nM	3,252	1,044	19%
60	5 nM	7,059	4,851	86%
	50 nM	9,408	7,200	128%
	500 nM	11,341	9,133	162%
	5000 nM	7,481	5,273	94%
78	5 nM	9,191	6,983	124%
	50 nM	9,094	6,886	122%
	500 nM	8,358	6,150	109%
	5000 nM	6,829	4,621	82%
77	5 nM	7,144	4,936	88%
	50 nM	8,025	5,817	103%
	500 nM	8,390	6,182	110%
	5000 nM	7,413	5,205	92%
76	5 nM	14,078	11,870	210%
	50 nM	7,475	5,267	93%
	500 nM	8,180	5,972	106%
	5000 nM	8,378	6,170	109%
74	5 nM	15,336	13,128	233%
	50 nM	9,467	7,259	129%
	500 nM	9,543	7,335	130%
	5000 nM	13,449	11,241	199%

Uptake in the presence of a compound was determined as Total bound dpm minus control nonspecific binding. All assays were performed in duplicate with 1 nM [^{3}H] MPP^+. Control total binding 7850 dpm, control nonspecific binding 2208 dpm, control uptake 5,642 dpm. Expt. #8

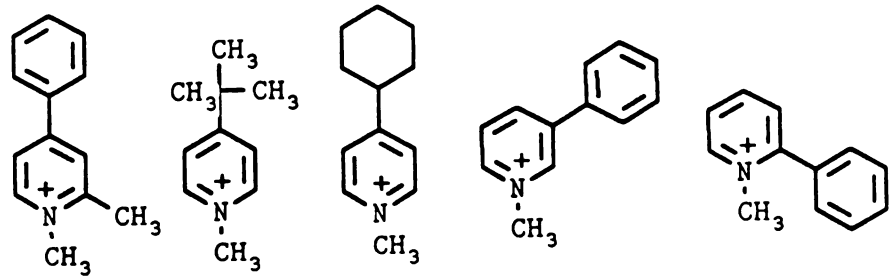

60 74 76 77 78

For example, the control uptake samples tubes 5 and 6 from the beginning of the experiment exhibited uptake of 7850 dpm and backgound binding of 2208 dpm, while the uptake in the presence of 5 uM 4-tert-butyl pyridinium iodide **74**, was 11,241 dpm or 199% of control. Of the compounds tested, only unlabled MPP^+ showed any inhibition of the uptake of $[^3H]$ MPP^+. We continued to work under the premise that MPP^+ analogs should inhibit the uptake of $[^3H]$ MPP^+ and interpreted the above data to mean that the activity of our synaptosomes had increased over the period of the experiment. Such an increase would remain undetected when only one set of controls is performed at the beginning of the experiment. One possible explaination was in the technique with which the synaptosomal protein was distributed to the incubation tubes. Since the incubations were performed in sets of eight, the protein had the opportunity to settle between sampling times. If the protein was not homogeneously suspended, early incubations might receive aliquots of

protein taken from the top of the vial which would be more dilute if protein had settled. Later incubations receive the more concentrated sample which would have more activity. To remedy this situation we adjusted the assay protocol to include a step in which the synaptosomal protein was vortexed to ensure resuspension prior to the removal of each sample. Furthermore the order in which protein was added to each set of eight tubes was varied to ensure that error introduced by protein sampling would be randomly distributed throughout the experiment.

After these improvements in the assay protocol had been implemented, the uptake activity of synaptosomes was again assessed in the presence of the same set of candidate inhibitors (5 nM to 5 uM). In this case three sets of controls were performed, at the beginning, middle, and end of the experiment. In contrast to the previous experiment, a decreasing trend of activity was observed in the controls starting with 7376 dpm to 6258 dpm to 5283 dpm. Since the synaptosomal preparation is a complex and fragile system, it had been anticipated that the activity of the uptake system might deteriorate over the 3 to 4 hour period required for completion of the incubations. We concluded that accurate determination of the effects of inhibitors on synaptosomal uptake required controls to be performed before each set of inhibitor incubations so that the effects of each inhibitor could

be related to a recent control. Inhibition of [^{3}H] MPP^+ uptake was observed in the presence of all of the compounds tested (Table 4-10). Although the inhibition observed with these compounds was not linearly dependent on concentration, IC_{50} values were calculated by linear regression in order to allow a preliminary rank order to be established. Unlabeled dopamine and MPP^+ were the most potent of the inhibitors followed by the cyclohexyl (**76**), the 2-phenyl (**78**), the 3-phenyl (**77**), the tert-butyl (**74**), and finally the 1,2-dimethyl analog (**60**).

Table 4-10. Preliminary results on the inhibition of synaptosomal [^{3}H] MPP^+ uptake by substituted pyridinium MPP^+ analogs

Compound	IC_{50}
DA	1.58 uM
MPP^+	2.59 uM
76	3.79 uM
78	4.22 uM
77	4.70 uM
74	11.85 uM
60	16.85 uM

IC 50s calculated using a linear regression of concentration I versus % control. Each assay performed in duplicate. Expt.#9

In the next experiment we attempted to repeat the determination of IC_{50}s for **78**, **60**, MPP^+ and **76** as inhibitors of [^{3}H] MPP^+ synaptosomal uptake using concentrations of 5nM to 5 uM. To improve the accuracy of the determination, each assay condition was now performed in triplicate and controls were performed before each set of inhibitor concentrations. In this

experiment, however, no inhibition of synaptosomal [^{3}H] MPP^+ uptake was observed. In contrast, the uptake activity appeared to increase in the presence of the candidate inhibitors. An increasing trend among the controls was also observed so that control activity at the beginning of the experiment (817 dpm) was only half the control observed at the end of the experiment (1819 dpm). This increase in control values had been observed in a previous experiment and had been attributed to inaccurate protein sampling technique. We had instituted a change in the assay procedure to remedy this problem by ensuring that the protein was resuspended before each sample was withdrawn however the problem resurfaced. To examine the possibility that we simply had not reached true inhibitory concentrations of the analog pyridinium compounds, we decided to assess the inhibitory properties of the compounds at much higher concentrations to see if the uptake system could be inhibited.

The 2-phenyl (**78**), 1,2-dimethyl (**60**), 4-cyclohexyl (**76**) analogs and unlabeled MPP^+ were again assayed as inhibitors, using concentrations of 0.5 uM to 500 uM. In this experiment, the controls showed more random variance, not a consistant pattern of increasing activity as indicated by the data in Table 4-11.

Table 4-11. Variation of control Total and Nonspecific binding and resultant Uptake values for mouse striatal synaptosomal uptake of [^{3}H] MPP^+ during the course of an early experiment.

Tube #	Total dpm	Nonspecific dpm	Uptake dpm
1-3 and 4-6	2,006	294	1,712
19-21 and 22-24	3,642	403	3,239
37-39 and 40-42	4,619	637	3,982
55-57 and 58-90	3,933	522	3,411

Each assay contained 1nM [^{3}H] MPP^+ and 0.3 mg synaptosomal protein. Nonspecific binding determined in the presence of 10 uM mazindol. Each total and nonspecific value listed is the average of triplicate determinations. Expt. #12

We could not be certain of the source of this variability but were beginning to wonder if this variance could be accounted for by simple variation of pipetting technique. Even very small differences in volume delivered would be significant using such high specific acitivity radioisotope. To counter the effects of this possible error, we made another change in the uptake assay protocol by averaging the control values obtained within each experiment. The effects of each inhibitor were then related to this averaged control.

[It should be noted, however, that the 2-fold range of variation of control values noted in Table 4-11 is wider than the range noted in later experiments. In the

later experiments from which the data for the ultimately reported IC_{50} values was derived, control values spanned a narrower range as shown in Table 4-12. Thus in the later experiments we felt comfortable with averaging the control total and nonspecific binding values within a given experiment so that an average control uptake value could be derived for each experiment. The effects of each pyridinium ion examined in a given experiment were then related to the average control for that experiment. However, the range of inter-experimental variation observed prevented us from averaging all the control values obtained over all experiments for a given uptake substrate.

Table 4-12. Range of control values for each experiment from which final inhibitory data was derived.

Expt.	Substrate	Total dpm	Nonspecific dpm	Uptake dpm
13	[^{3}H] MPP^+	20,249-18,040	3,621-2,549	17,248-14,419
14		20,141-18,851	3,398-2,190	17,951-15,686
60		11,241-6,918	1,966-1,152	9,275-5,766
22		10,912-7,700	3,148-1,568	7,764-6,134
17	[^{3}H] DA	92,400-80,002	3,824-5,889	86,511-76,178
18		67,493-43,710	4,625-2,493	62,868-41,217
19		80,062-56,586	5,119-3,685	74,943-52,901
20		98,620-59,975	4,891-3,516	93,729-56,459

In each experiment there was 1 set of controls performed in triplicate per inhibitor examined. Thus n=12-18 for each value of total and nonspecific binding.]

Using the protocol described above, in experiment 12, inhibition was examined for each of the 4 compounds tested and IC_{50} values were calculated by linear regression, although again the data were not well fitted to a line when plotted as percent control versus concentration of inhibitor. The results of this experiment (Table 4-13), however, bore little resemblance to those of the previous experiment in Table 4-10.

Table 4-13. Determinations of the inhibitory effects of substituted pyridinium salts on [^{3}H] MPP^+ uptake by mouse striatal synaptosomes

Compound	Expt. 12 IC_{50}
MPP^+	3.1 uM
76	118 uM
78	120 uM
60	242 uM

Each IC50 calculated by linear regression of %control versus concentration of inhibitor using triplicate determinations at each of 4 concentrations of inhibitor (0.5uM to 500 uM). Control total was 3,933 dpm, control nonspecific was 522 dpm to give an uptake of 3,411 dpm.

At this point in our studies we realized that a large effort might still be required to refine our assay conditions and data treatment protocol in order to obtain reproducible IC_{50} values. Experiments would have to be repeated several times in order to ensure reproducibility. We decided to concentrate our efforts on an examination of compounds in which we were particularly interested. For this reason we decided to exclude the tert-butyl (**74**) and the 1,4-dimethyl (**73**) derivatives from our test set since they had exhibited very low activity in the inhibition of mitochondrial respiration and in the <u>in vivo</u> rat microdialysis model and had given no indication of potency as uptake inhibitors. We also excluded the 3-phenyl (**77**) and the 2-phenyl derivatives (**78**) because preliminary studies had indicated very low potency as uptake inhibitors. We

retained the 1,2-dimethyl derivative (**60**) because it had already been characterized as a toxic compound. Unlabeled MPP^+ was retained in the test set for comparison. The 4-cyclohexyl compound (**76**) was also retained because of its relationship as a potential terminal metabolite of the 1-methyl-4-cyclohexyl-1,2,3,6-tetrahydropyridine for which Youngster had reported toxic activity.[148] Furthermore, a very interesting compound, a tricyclic $MPDP^+$ analog was added to the test set. This analog, 3,4-dihydro-2-methyl-9-H-indeno[2,1-c]pyridinium (**83**) had been synthesized by a fellow graduate student Raymond Booth and was of particular interest because it is a stabilized $MPDP^+$ analog.[151] In contrast to $MPDP^+$, the indeno analog exhibits a very slow rate of disproportionation and thus can be studied under physiological conditions.[151] Use of this analog allowed us to explore the possibility that dihydropyridinium ions might serve as uptake substrates. These 4 compounds were examined during the course of 2 further experminents using the updated assay protocol which incorporated the changes described above. The resulting data are summarized in Table 4-14.

Table 4-14. Effects of substituted pyridinium analogs of MPP^+ and $MPDP^+$ on synaptosomal [^{3}H] MPP^+ uptake.

Inhibitor in uM	Expt.	Total dpm	Uptake dpm	Percent Control	IC50
MPP^+	13				
500		1,033	--	0 %	
50		1,586	--	0 %	
5		4,990	1,942	11.8%	
0.5		16,988	13,940	84.6%	2.58 uM
MPP^+	14				
500		3,405	747	4.5%	
50		4,267	1,609	9.6%	
5		12,643	9,985	59.8%	
0.5		25,740	23,082	138.0%	159 uM
60	13				
500		3,795	747	4.5%	
50		9,665	6,617	40.1%	
5		18,352	15,304	92.8%	
0.5		18,360	15,312	92.9%	187.7 uM
60	14				
500		6,397	3,739	22.4%	
50		12,393	9,735	58.2%	
5		17,086	14,428	86.4%	
0.5		21,258	18,600	111.4%	238 uM
76	13				
500		1,374	--	0.0%	
50		4,456	1,408	8.5%	
5		13,798	10,750	65.2%	
0.5		18,652	15,604	94.7%	77.5 uM
76	14				
500		2,788	130	0.0%	
50		5,896	3,238	19.4%	
5		14,522	11,864	71.0%	
0.5		25,323	22,665	136.0%	179 uM

83	13				
500		3,530	482	2.9%	
50		12,278	9,230	56.0%	
5		18,674	15,626	94.8%	
0.5		19,017	15,969	96.9%	214 uM
83	14				
500		5,318	2,660	15.9%	
50		15,421	12,763	76.4%	
5		25,984	23,326	139.0%	
0.5		15,102	12,440	75.0%	319 uM

All assays perfomed in triplicate using 1 nM [^{3}H] MPP^+ with 0.3 mg protein. Nonspecific binding was determined in the presence of 10 uM mazindol. The synpatosomal protein was vortexed prior to removal of each sample to ensure sample uniformity. Fiberglass filters were presoaked in 10 mM MPP+ prior to filtration of the assay mixture. After filtration each sample filter was vortexed in scintillation fluid for 15 seconds and the resultant sample analyzed by liquid scintillation spectrometry. Values for control total and control nonspecific (n = 12) were averaged and effect of drug was then expressed as a percent of the average uptake. Average total and nonspecific binding was 19,530 dpm and 3,048 dpm for experiment 13. Average total and nonspecific was 19,359 dpm and 2,658 dpm for experiment 14. IC_{50} values were calculated from the linear regression of percent control versus inhibitor concentration.

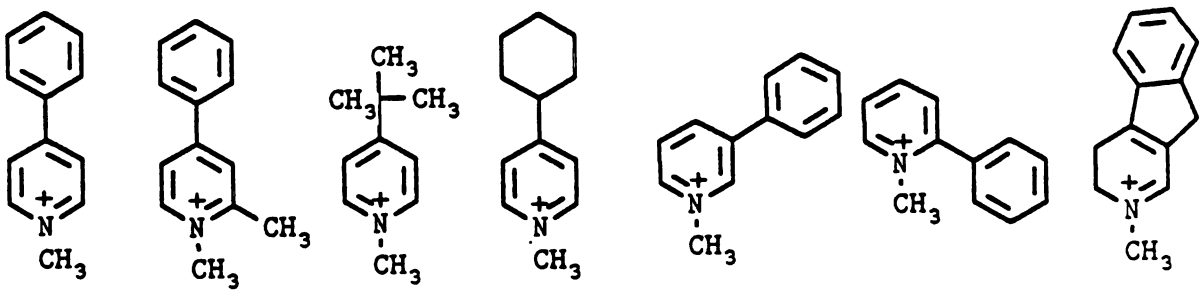

MPP^+ 60 74 76 77 78 83

At this point we were quite discouraged about the data that had been obtained since, in spite of multiple

assay improvements, we had not succeeded in obtaining reproducible IC_{50} values.

KINETICS OF MOUSE STRIATAL SYNAPTOSOMAL UPTAKE OF [^{3}H] DA

To give a means of assessing the validity of our experimental protocol, we decided to focus on the bonafide substrate for the system we had been studying and determine the kinetic parameters for uptake of [^{3}H] DA. Using [^{3}H] DA (15 Ci/mmol, Amersham) at 6 concentrations (10 nM-1000 nM) and our refined assay protocol, the kinetic parameters for [^{3}H] DA uptake were Km 264 nM and Vmax 61 nmol/gm protein·min. See Table 4-15 for the data, and Figures 4-5 and 4-6 for the plots, from which these parameters were derived.

Table 4-15. Mouse striatal synaptosomal uptake of [^{3}H] DA

[^{3}H] DA	Total dpm	Nonspecific dpm	Filter dpm	Uptake dpm	Uptake nmol/gm per min
10 nM	113,956	4,177	1,202	109,779	2.22
50 nM	602,033	22,896		579,137	11.7
100 nM	887,213	44,357		842,856	17.0
300 nM	1,535,650	85,858		1,449,792	29.3
600 nM	1,905,107	170,440		1,734,667	35.0
1000 nM	2,116,602	291,888		1,824,714	36.8

All assays in triplicate, nonspecific binding determined in the presence of 10 uM mazindol. Expt. #16

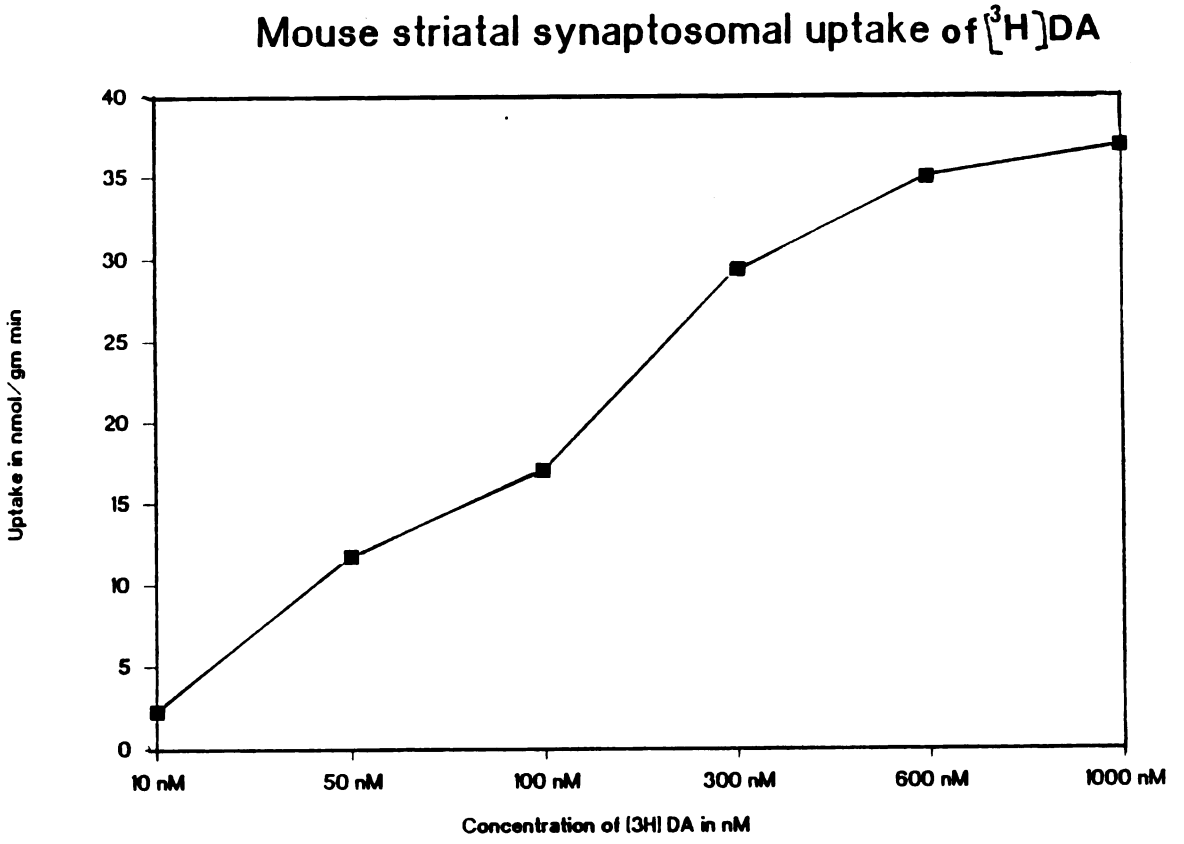

Figure 4-5. Saturation plot for mouse striatal synaptosomal uptake of [^{3}H] DA. Data obtained from triplicate assays at each of 6 concentrations (10nM-1000 nM [^{3}H] DA). Nonspecific binding was determined using parallel triplicate incubations in the presence of 10uM Mazindol.

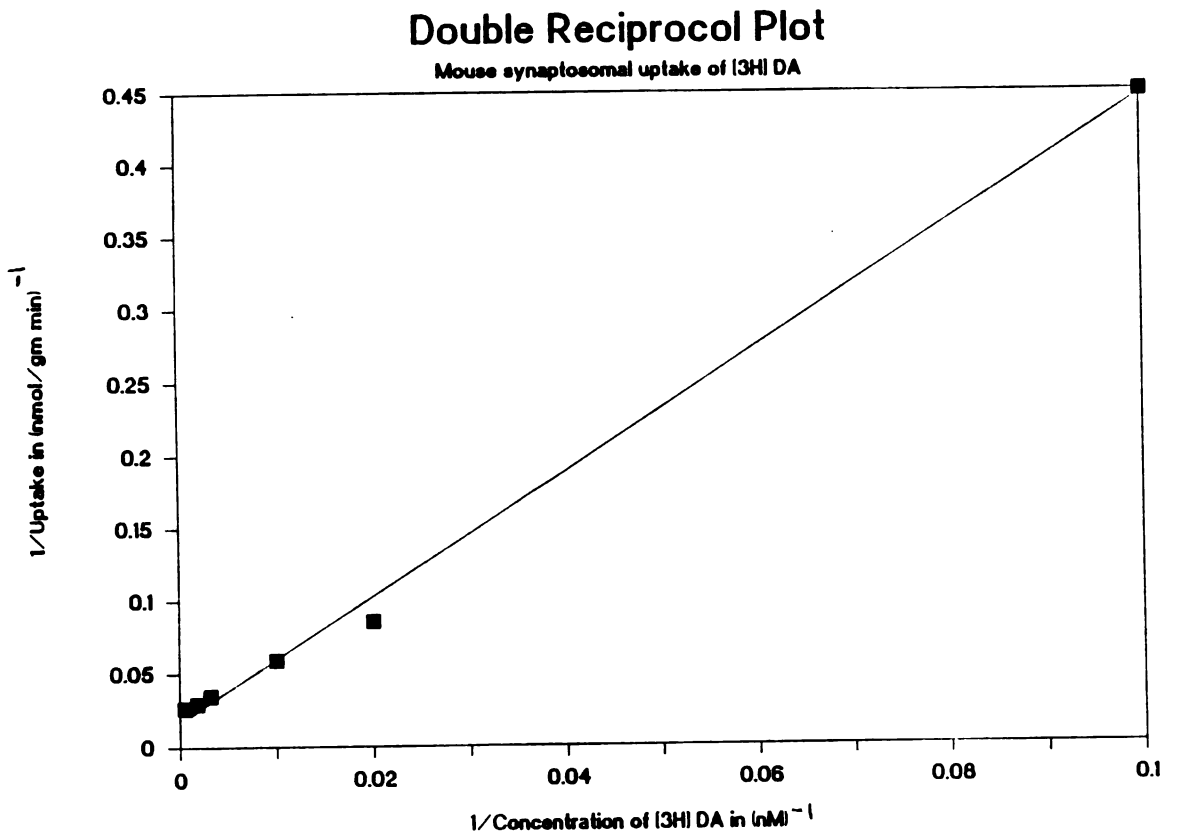

Figure 4-6. Double reciprocol plot for mouse striatal synaptosomal uptake of [^{3}H] DA. Km (264nM) and Vmax (61 nmol/g per min) were calculated from a least squares linear regression.

While our Km was well within the range reported (Km 150-490 nM and Vmax 2-42.8 nmol/gm protein · min) our Vmax was significantly higher than those in the range reported for rat synaptosomal uptake. A higher Vmax indicates a faster rate of transport of the labeled substrate. We reasoned that the difference in tissue source (mouse versus rat) might explain our observance of a higher Vmax value. As demonstrated by the data in Table 4-15, nonspecific binding and filter binding were consistantly lower for [^{3}H] DA than with [^{3}H] MPP^+, averaging 5% of the total radioactive ligand bound at low ligand concentrations. Furthermore, as indicated by the data in Table 4-16, the preliminary IC_{50} values for unlabeled MPP^+ and DA as competitive inhibitors of [^{3}H] DA uptake (assayed at 10 nM [^{3}H] DA) were determined to be 16.7 uM and 1.56 uM, respectively. The potency of MPP^+ and DA as competitive inhibitors was not as high as we had expected but was also not as poor as we had previously observed with inhibition of [^{3}H] MPP^+ uptake. We chose to examine the inhibition of 10 nM [^{3}H] DA uptake, as opposed to 1 nM [^{3}H] MPP^+ because of the lower specific activity of [^{3}H] DA. We wanted to have approximately the same number of dpm radioactive material added to each incubation for both [^{3}H] DA and [^{3}H] MPP^+ uptake. These concentrations were also chosen in order to make our studies consistant with and comparable to the

reported studies of Chiba et al.,[78] Heikkila et al.[79], Gessner et al.[80], and Shen et al.[81]

Table 4-16 Inhibition of mouse striatal synaptosomal uptake of [^{3}H] DA by unlabled MPP^+ and DA

Inhibitor	Total dpm	Uptake dpm	Percent Control	IC_{50}
DA				
500 uM	1,821--		0 %	
50 uM	3,281	--	0 %	
5 uM	9,110	5,450	6.1%	
0.5 uM	44,783	41,123	46.2%	16.7 uM
MPP+				
500 uM	3,017	--	0 %	
50 uM	6,143	2,483	3.4%	
5 uM	39,804	36,144	49.0%	
0.5 uM	81,958	78,298	106.0%	1.56 uM

Each assay performed in triplicate using 10 nM [3H]DA. Control Total dpm averaged 92,422, nonspecific dpm averaged 3,660 dpm and was determined in the presence of 10 uM mazindol. Average control uptake was 88,762 dpm. IC_{50} values were determined from a linear regression of percent control versus the concentration of inhibitor.

REFINEMENT OF COMPETITION ASSAY PROTOCOL AND DATA TREATMENT PROTOCOL

At this point we had successfully demonstrated uptake of [^{3}H] DA and [^{3}H] MPP^+ by our mouse striatal synaptosomes and found kinetic values consistant with those reported by others. Thus we were more encouraged about our experimental protocol for the measurement of uptake. However we were still disturbed by our apparent inability to obtain reproducible IC_{50} values for inhibition of [^{3}H] MPP^+ uptake. To attack this problem

we re-examined our data treatment protocol. Our original treatment was to plot percent control uptake obtained in the presence of a given concentration of inhibitor versus the concentration of inhibitor. This treatment gives plots such as the one in Figure 4-7.

It is evident from Figure 4-7 that such a plot gives hyperbolic curves rather than straight line segments. Thus our attempt to calculate an IC_{50} value from linear regressions of such data was likely to result in a high degree of error and probably contributed significantly to our inability to achieve reproducible IC_{50} values. Indeed when linear regression analysis was performed on the data from experiments 13 and 14 plotted as response versus concentration, the r coefficient which indicates the degree to which the actual data fits on the calculated line, was very poor ($r = 0.8$ or less). Although we were aware that this data treatment protocol presented a problem early in our studies, it was not until we had demonstrated satisfactory uptake kinetics for both substrates that we felt prepared to tackle the problem.

It is traditional among pharmacologists to present data as a log dose response curve for 2 reasons.[149] First, line segments rather than hyperbolic curves are obtained which are much easier to deal with in statistical analysis. Secondly, drugs that produce the same effect by the same mechanism but differ in potency

yield parallel line segments. Thus the appearance of a log dose-response plot gives a convenient method of comparison of drug effects.[149] When we replotted the data for inhibition of [^{3}H] MPP^+ uptake by substituted pyridinium ions (experiments 13 and 14) on a log dose-response plot (Figure 4-8) we indeed obtained line segments. Linear regression of these line segments resulted in a much better fit of the experimental data to the calculated line. Therefore the IC_{50} values generated from linear regression more accurately reflected the experimental data. We adopted this new method of data treatment. Table 4-17 compares the IC_{50} values obtained by linear regression of dose response curves with the IC_{50} values obtained by linear regression of log dose-response curves

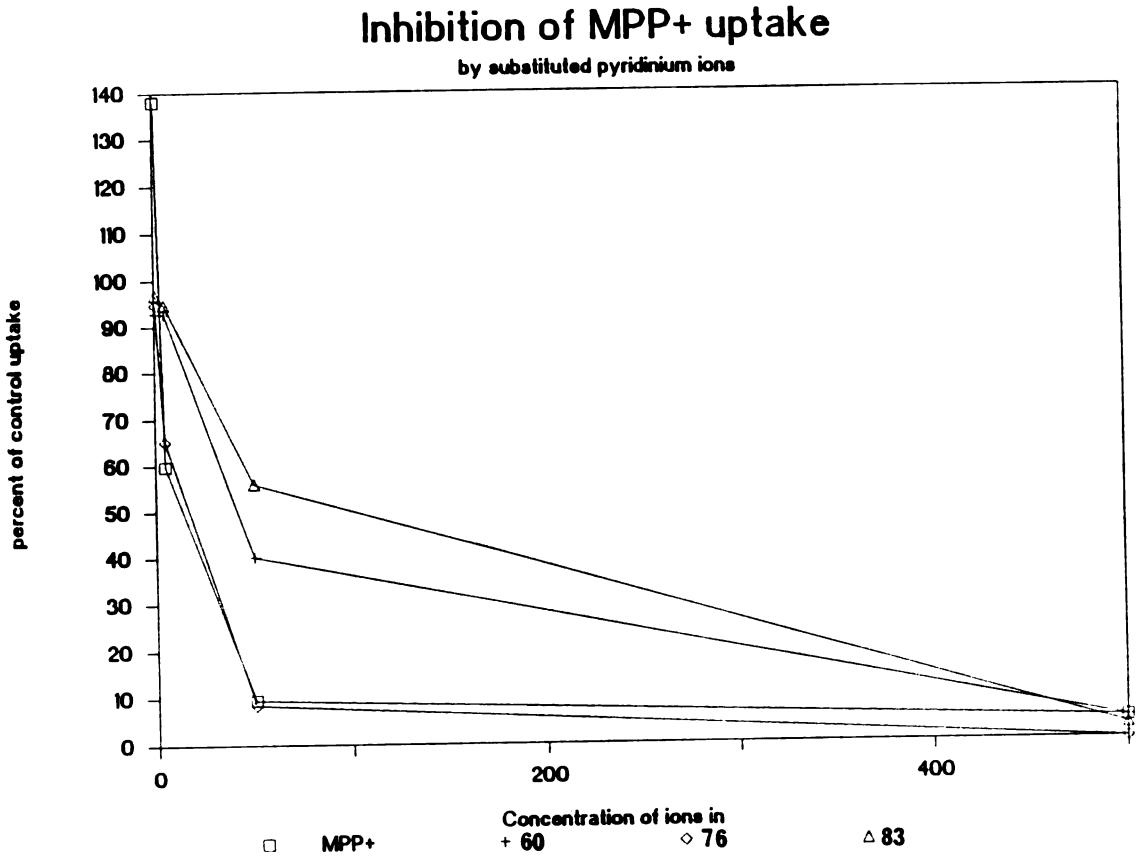

Figure 4-7. The effect of subsituted pyridinium ions on mouse striatal synaptosomal uptake plotted as percent control versus pyridinium ion concentration. This data treatment gives hyperbolic curves.

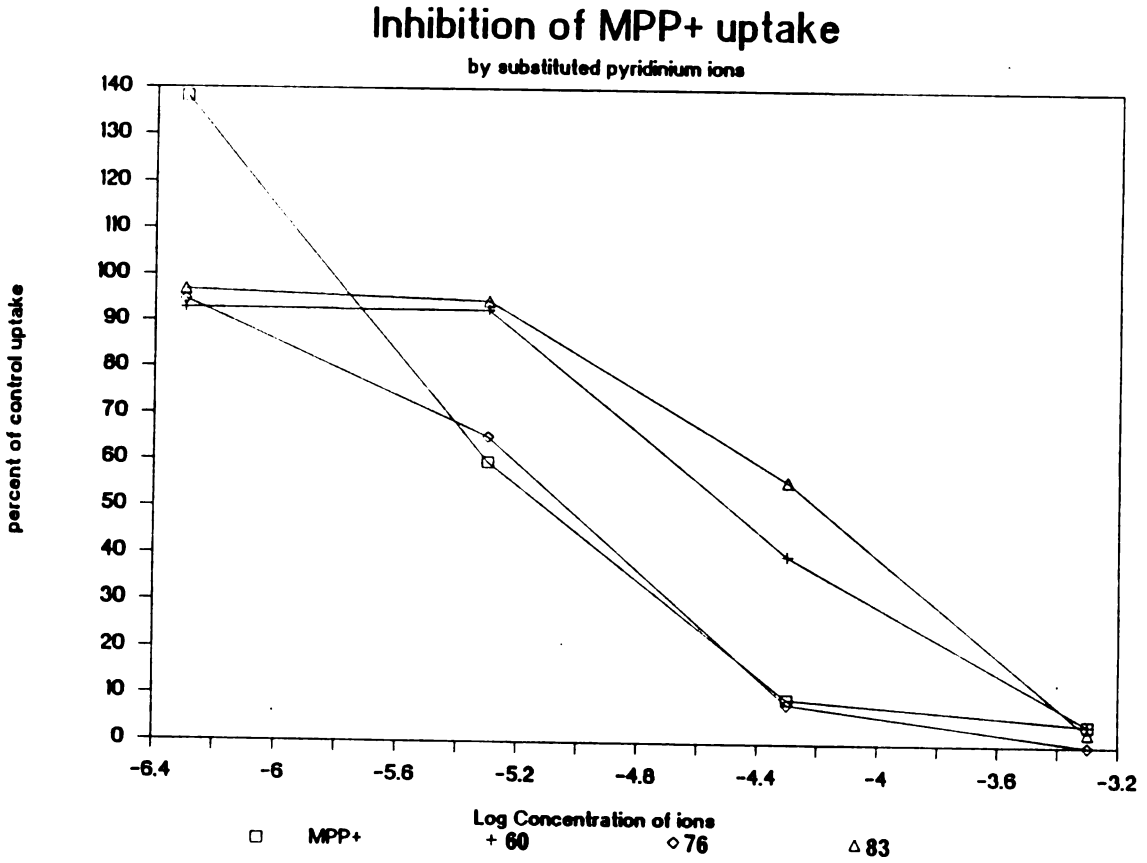

Figure 4-8. The effect of subsituted pyridinium ions on mouse striatal synaptosomal uptake plotted as percent control versus the log of pyridinium ion concentration. This data treatment gives straighter line segments.

Table 4-17. Comparison of IC_{50} values obtained for substituted pyridinium ion inhibition of [^{3}H] MPP^+ uptake caluculated by linear regression of dose-response curves versus linear regression of log dose-response curves

Compound	Expt.#	IC_{50} from Dose-response	IC_{50} from Log Dose-response
MPP+	13	2.58 uM	1.67 uM
	14	159.0 uM	18.5 uM
60	13	187.8 uM	27.4 uM
	14	238.0 uM	71.0 uM
76	13	77.5 uM	9.02 uM
	14	179.0 uM	22.2 uM
83	13	214.0 uM	39.2 uM
	14	319.0 uM	138.0 uM

IC_{50} values calculated from raw data presented in Table 4-14.

Inspection of Table 4-17 shows that the new method of data treatment (IC_{50} calculation by linear regression on log dose-response plots) had the effect of giving more potent IC_{50} values for all of the drugs tested. Furthermore, the inter-experimental variation (experiment 13 compared with experiment 14) was smaller with the improved data treatment. In effect, recalculation of the experimental data from experiments 13 and 14 with the improved data treatment protocol increased the reproducibility of our IC_{50} values with no change in experimental protocol.

With this knowledge in hand, our confidence was on the rise. We felt we were finally getting a good grasp of the techniques required to study uptake phenomena.

RESULTS OF [^{3}H] DA UPTAKE COMPETITION EXPERIMENTS

The new method of data treatment was coupled with our updated assay protocol for study of the effects of substituted pyridinium ions on uptake of [^{3}H] DA. With our renewed confidence we willingly took on the addition of two more interesting compounds to the test set. We added two rigid analogs of MPP^+, compounds **84** and **85**, which had been synthesized by our colleague Raymond G. Booth.[151] These compounds were of interest for several reasons. First they, like the stablized dihydropyridinium analog **83**, are locked into a conformation in which the phenyl group is coplanar with the nitrogen ring. This conformation is of interest as it approximates the conformation of dopamine which is preferred by the dopamine uptake site (Horn and Snyder, 1972 [92]; Miller et al., 1973 [93]; Horn, 1974 [94]). Compounds **84** and **85** are differentiated from each other by the character of the atom used to link the rings in rigid conformation. In compound **85**, the bridging atom is nitrogen, which confers a polar electron-withdrawing character to the bridge moiety. Such character is not shared by the carbon linked rigid analogs **83** and **84**. Compound **85**, besides being a rigid analog of MPP^+, is of special interest because it has been speculated to be an endogenous neurotoxin which might be responsible for the

development of idiopathic Parkinsonism (Collins et al,1985 [150])

In initial experiments inhibitor concentrations ranged from 0.5 to 500 uM. For later experiments the inhibitor concentrations were adjusted to give 10% to 90% of control uptake activity. This resulted in a better fit of the data to a line and more accurate IC_{50} determinations. The raw data from these experiments are listed in Table 4-18.

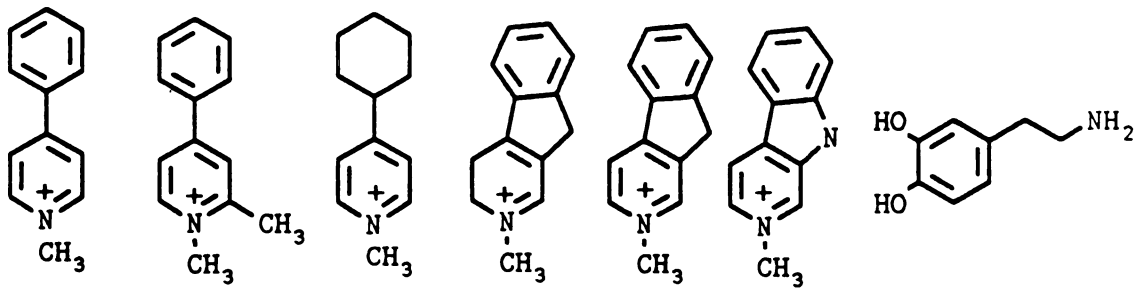

MPP+ 60 76 83 84 85 Dopamine

Table 4-18. Effects of substituted pyridinium analogs of MPP^+ and $MPDP^+$ on mouse striatal synaptosomal uptake of [^{3}H] DA

Compound in uM	Log [ ]	Expt.#	Total DPM	Uptake DPM	Percent Control
DA		17			
5.00 uM	-5.3		7,963	3,243	4.2
0.50	-6.3		32,292	27,572	35.5
0.05	-7.3		73,114	68,394	88.0
DA		18			
5.00 uM	-5.3		6,282	2,834	5.3
0.50	-6.3		19,112	15,664	29.5
0.05	-7.3		41,530	38,082	71.8
MPP^+		17			
50.00 uM	-4.3		5,433	713	0.9
5.00	-5.3		21,761	17,041	21.0
0.50	-6.3		71,353	66,633	88.8
MPP^+		18			
50.00 uM	-4.3		4,339	891	1.7
5.00	-5.3		16,564	13,116	24.7
0.50	-6.3		51,457	48,009	90.5
76		17			
500.00 uM	-3.3		4,278	0	0
50.00	-4.3		19,262	14,542	18.7
5.00	-5.3		68,210	63,490	81.7
0.50	-6.3		83,138	78,418	100.9
76		18			
500.00 uM	-3.3		2,976	0	0
50.00	-4.3		12,897	9,449	17.8
5.00	-5.3		46,620	43,172	81.4
0.50	-6.3		55,119	51,671	97.4
60		17			
500.00 uM	-3.3		14,580	9,860	12.7
50.00	-4.3		47,814	43,094	55.5
5.00	-5.3		69,977	65,257	84.0
0.50	-6.3		75,477	70,757	91.1
60		19			
500.00 uM	-3.3		10,103	5,876	9.4
50.00	-4.3		39,232	35,005	56.0
5.00	-5.3		53,458	49,231	78.8
0.50	-6.3		66,320	62,093	99.4

83		17			
500.00 uM	-3.3		21,970	17,250	22.2
50.00	-4.3		67,358	62,638	80.6
5.00	-5.3		72,962	83,242	87.8
0.50	-6.3		65,071	60,351	77.7
83		19			
1000.00 uM	-3.0		9,618	5,391	8.3
500.00	-3.3		21,242	17,015	27.2
100.00	-4.0		41,036	36,809	58.9
50.00	-4.3		52,990	48,763	78.0
5.00	-5.3		55,087	50,860	81.4
84		19			
500.00 uM	-3.3		10,663	06,436	10.3
50.00	-4.3		38,832	34,605	55.4
5.00	-5.3		53,901	49,674	79.5
0.50	-6.3		56,523	52,296	83.7
84		20			
500.00 uM	-3.3		17,200	13,134	17.3
50.00	-4.3		56,071	52,005	68.3
5.00	-5.3		66,950	62,884	82.6
0.50	-6.3		70,205	66,139	86.9
85		20, first trial			
500.00 uM	-3.3		16,358	12,292	16.2
50.00	-4.3		50,040	45,974	60.4
5.00	-5.3		63,221	59,155	77.7
0.50	-6.3		60,222	56,156	73.8
85		20, second trial			
500.00 uM	-3.3		12,876	8,810	11.6
50.00	-4.3		54,794	50,728	66.7
5.00	-5.3		77,768	73,702	96.8
0.50	-6.3		80,749	76,683	100.8

All assays performed in triplicate using 10 nM [^{3}H] DA with 0.3 mg protein. Nonspecific binding determined in the presence of 10 uM mazindol. The synaptosomal protein was vortexed prior to removal of each sample to ensure sample uniformity. Fiberglass filters were presoaked in assay buffer prior to filtration of the assay mixtures. After filtration each sample was vortexed in scintillation fluid for 15 seconds and the resultant sample analysed by liquid scintillation spectrometry. Values for control total and control nonspecific (n=12-15 for each experiment) were averaged for each individual experiement. Control nonspecific was subtracted from total dpm for each drug concentration and the effect of drug was then expressed as a percent of the control average uptake for the experiment.

Average total and		nonspecific binding was	
	82,420 dpm and	4,720 dpm	for expt #17
	56,485	3,448	#18
	66,781	4,227	#19
	80,169	4,066	#20

The IC_{50} values determined by linear regression of percent control versus log of dose are listed in Table 4-19.

Table 4-19. IC_{50} values determined for inhibition of synaptosomal [^{3}H] DA uptake by substituted pyridinium derivatives and unlabeled DA.

Compound	IC_{50} value			
	Expt. 17	Expt. 18	Expt. 19	Expt. 20
DA	332.0 nM	183.0 nM		
MPP^+	2.4 uM	2.8 uM		
76	15.9 uM	14.8 uM		
60	40.7 uM		37 uM	
85				36.3 uM and 68.7 uM
84			31 uM	65.5 uM
83	152 uM		164 uM	

Each compound was assayed against 10 nM [^{3}H] DA. IC_{50} values were derived from triplicate assays at each of at least 3 inhibitor concentrations. Percent control was calculated from averaged controls in each experiment. IC_{50} values were calculated from linear regressions of percent control versus log concentration of inhibitor.

As shown in Table 4-19, the changes made in uptake assay protocol and in data treatment, (as well as simple practice) had resulted in data that could be reproduced

within one order of magnitude. We now could veiw our data with some confidence and felt that we had developed sufficient expertise to re-examine [^{3}H] MPP^+ uptake.

RESULTS OF [^{3}H] MPP^+ UPTAKE COMPETITION EXPERIMENTS

The IC_{50} values from data on inhibition of [^{3}H] MPP^+ uptake obtained in experiments 13 and 14 had been recalculated using linear regressions of percent control activity versus log of inhibitor concentration (Table 4-17). The concentration range of inhibitor was then adjusted to give 10% to 90% control activity for some of the analogs which were reassessed in two additional experiments #21 and #22. The raw data from these experiments are listed in Table 4-20.

Table 4-20. Effects of substituted pyridinium analogs of MPP^+ and $MPDP^+$ on mouse striatal synaptosomal uptake of [3H] MPP+

Compound in uM	Log [ ]	Expt.#	Total DPM	Uptake DPM	Percent Control
DA		21			
5.00 uM	-5.3		2,538	991	13.6
0.50	-6.3		6,274	4,727	65.0
0.05	-7.3		7,375	5,828	80.2
0.005	-8.3		8,071	6,524	89.7
DA		22			
5.00 uM	-5.3		3,842	1,186	17.3
0.50	-6.3		8,238	5,582	81.6
0.05	-7.3		9,113	6,457	94.4
0.005	-8.3		9,328	6,672	87.6
MPP^+		21			
50.00 uM	-4.3		542	0	0
10.00	-5.0		1,133	0	0
3.00	-5.5		2,001	453	6.2
0.50	-6.3		5,963	4,416	60.7
MPP^+		22, first trial			
5.00 uM	-5.3		1,899	0	0
0.50	-6.3		5,367	2,711	39.7
0.05	-7.3		9,602	6,946	102.0
0.005	-8.3		8,840	6,184	90.4
MPP^+		22, second trial			
5.00 uM	-5.3		1,579	0	0
0.50	-6.3		5,778	3,122	45.7
0.05	-7.3		7,975	5,319	77.8
0.005	-8.3		10,187	7,531	110.0
76		21			
50.00 uM	-4.3		1,429	0	0
10.00	-5.0		3,164	1,617	22.0
3.00	-5.5		5,493	3,946	54.3
0.50	-6.3		7,487	5,940	81.7
60		21			
500.00 uM	-3.3		1,268	0	0
50.00	-4.3		3,935	2,388	32.8
5.00	-5.3		6,715	5,168	71.1
0.50	-6.3		8,590	7,043	96.9

84			21			
500.00	uM	-3.3		1,060	0	0
50.00		-4.3		3,133	1,586	21.8
5.00		-5.3		5,159	3,612	49.7
0.50		-6.3		6,509	4,962	68.2
84			22			
500.00	uM	-3.3		1,230	0	0
50.00		-4.3		3,831	1,175	17.2
5.00		-5.3		7,331	4,675	68.4
0.50		-6.3		9,301	6,645	97.2
85			22, first trial			
500.00	uM	-3.3		1,334	0	0
50.00		-4.3		3,976	1,320	19.3
5.00		-5.3		6,982	4,326	63.3
0.50		-6.3		9,575	6,919	102.0
85			22, second trial			
500.00	uM	-3.3		1,230	0	0
50.00		-4.3		3,831	1,175	17.2
5.00		-5.3		7,331	4,675	68.4
0.50		-6.3		9,301	6,645	97.2

All assays performed in triplicate using 1.0 nM [^{3}H] MPP^+ with 0.3 mg protein. Nonspecific binding determined in the presence of 10 uM mazindol. The synaptosomal protein was vortexed prior to removal of each sample to ensure sample uniformity. Fiberglass filters were presoaked in 10 mM MPP^+ in assay buffer prior to filtration of the assay mixtures. After filtration each sample was vortexed in scintillation fluid for 15 seconds and the resultant sample analysed by liquid scintillation spectrometry. Values for control total and control nonspecific (n=12-15 for each experiment) were averaged for each individual experiement. Control nonspecific was subtracted from total dpm for each drug concentration and the effect of drug was then expressed as a percent of the control average uptake for the experiment.

Average total and		nonspecific binding was		
8,817 dpm and		1,547 dpm	for expt	#21
9,494		2,656		#22

IC_{50} values were calculated from the linear regression of percent control versus log concentration for each drug. The accumulated IC_{50} values from these four experiments are listed in Table 4-21.

Table 4-21. IC_{50} values determined for inhibition of synaptosomal [^{3}H] MPP^+ uptake by substituted pyridinium derivatives and unlabeled DA.

Compound	IC_{50} value			
	Expt. 13	Expt. 14	Expt. 21	Expt. 22
DA			500 nM	1 uM
MPP^+	1.7 uM	18.5 uM	400 nM	275 nM and 269 nM
76	9.0 uM	22.2 uM	3.0 uM	
60	27.4 uM	71.0 uM	17 uM	
85				12.0 uM and 12.0 uM
84			4.0 uM	5.0 uM
83	39.2 uM	138 uM		

Each compound was assayed against 1 nM [^{3}H] MPP^+. IC_{50} values were derived from triplicate assays at each of at least 4 inhibitor concentrations. Percent control was calculated from averaged controls in each experiment. IC_{50} values were calculated from linear regressions of percent control versus log concentration of inhibitor.

FINAL RESULTS ON THE INHIBITION OF UPTAKE OF [^{3}H] DOPAMINE AND [^{3}H] MPP^+

To obtain the final IC_{50} values and standard error of mean values (SEM) which have subsequently been submitted for publication, the data giving the two closest IC_{50} values for each compound were treated in the following manner. The data were pooled to give six sets of determinations at each of 4 inhibitor concentrations. From this set, six IC_{50} values were calculated, each using data from the 4 concentration levels. The six IC_{50}

values were averaged and SEM values calculated. These final IC_{50} values are presented in Table 4-22.

Table 4-22. Average IC_{50} values for inhibition of synaptosomal [^{3}H] DA and [^{3}H] MPP^+ uptake by compounds structurally related to MPP^+.

	INHIBITION OF [^{3}H] DA UPTAKE	[^{3}H] MPP^+ UPTAKE
COMPOUND	Ave.IC_{50} ± SEM	Ave. IC_{50} ± SEM
Dopamine	0.27 ± 0.05 uM	1.23 ± 0.37 uM
MPP^+	2.70 ± 0.21 uM	0.28 ± 0.03 uM
76	14.5 ± 1.02 uM	6.00 ± 1.44 uM
60	39.3 ± 4.62 uM	20.7 ± 3.34 uM
84	51.5 ± 11.9 uM	4.33 ± 0.56 uM
85	52.0 ± 7.93 uM	12.2 ± 2.02 uM
83	144. ± 19.3 uM	178. ± 84.0 uM

Each IC_{50} value is an average of 6 values, each obtained by linear regression on plots of %control versus log concentration of inhibitor, using at least 4 concentrations of inhibitor for each line.

DISCUSSION

In order to assess the validity of our data on the inhibition of uptake of [^{3}H] DA and [^{3}H] MPP^+, we had included the corresponding unlabled compounds DA and MPP^+ in the test set. The IC_{50} values obtained for inhibition of uptake of each labeled substrate by the corresponding unlabeled substrate were compared with theoretically calculated IC_{50} values. A theoretical calculation of the IC_{50} value for inhibition of the uptake of a labeled

substrate by the unlabeled compound takes into account the dual effects of labeled substrate dilution. First, the addition of unlabled substrate to the incubation medium dilutes the specific activity of the tritiated compound. Theoretically, the labeled and unlabeled compounds compete for the same uptake site, the protein being unable to discriminate between them. This results in an apparant competitive inhibition of the uptake of the labeled compound. However the second effect of addition of unlabeled compound is to raise the overall concentration of uptake substrate in the medium, therefore increasing the rate of uptake if saturating conditions have not been reached. Since the Km values for [^{3}H] DA and [^{3}H] MPP^+uptake were 264 nM and 255 nM, respectively, and labled substrate concentrations in the competition experiments were 10 and 1 nM respectively, the uptake system was not saturated. The combined results of these competing effects of the addition of unlabled substate can be described by equation 1, derived from Michealis Menton kinetics (Segel, 1975[96]).

$$A = Vi/Vo = (Km + [S^*])/(Km + [S^*] + [S]) \qquad (1)$$

V_i is the velocity of uptake in the presence of unlabled plus labled substrate (the inhibited reaction). V_o is the velocity of uptake in the presence of labled substrate alone (the control reaction). The concentration of labeled substrate is signified by $[S^*]$,

while the concentration of unlabeled substrate is signified by [S]. Since the Km for the uptake of both substrates was determined and [S^*] is known, the theoretical IC_{50} ([S] required for apparent 50% inhibition) can be calculated by setting A equal to 0.5.

solving for A = 0.5,

$$0.5 = (K_m + [S^*])/(K_m + [S^*] + [S])$$

$$(K_m + [S^*] + [S]) = 2\ K_m + 2\ [S^*]$$

$$[S] = \text{theoretical } IC_{50} = K_m + [S^*]$$

For synaptosomal uptake of [^{3}H] DA a theoretical IC_{50} of 274 nM for cold DA was calculated. The actual IC_{50} determined from experimental data was 270 nM (SEM = 50 nM). In the case of [^{3}H] MPP^+ uptake, the theoretical IC_{50} value for inhibition by cold MPP^+ was 256 nM and the actual IC_{50} value was 280 nM (SEM = 30 nM). The good agreement of experimental data with theoretically predicted values implies that, in our hands, the synaptosomal uptake system obeys Michealis-Menten kinetics, and that competitive inhibition is observed as would be expected of an enzyme dependent uptake system. This has not been the case, however, with data recently reported on MPP^+ uptake by other laboratories. For example, Shen et al. (1985)[81] reported a K_m for MPP^+ uptake of 0.2 uM. Using [S*] of 0.5 nM, a theoretical IC_{50} for cold MPP^+ inhibition of [^{3}H] MPP^+ uptake can be calculated for their system as 0.2005 uM. However, their

reported IC_{50} was 0.02 uM-- an order of magnitude lower. In our case, the conformity of observed results with the predicted effects of isotope dilution led us to veiw the rest of our results with reasonable confidence.

Using the standard error of the mean (SEM) for each IC_{50} value (Table 4-22) as a guide of significant difference between values, rank orders for potency of inhibition of uptake by the other pyridinium analogs were assigned. For [^{3}H] DA uptake inhibition, unlabled dopamine was ranked as the most potent inhibitor followed by MPP^+ > the 4-cyclohexyl derivative (**76**). In fourth place, the 1,2-dimethylphenylpyridinium (**60**) was considered equipotent with the carbon-linked rigid analog, **84**, and the nitrogen-linked rigid analog **85**. The least potent inhibitor of [^{3}H] DA uptake was the rigid dihydropyridinium analog **83**. A slightly different rank order for the potency for inhibition of [^{3}H] MPP^+ uptake was observed. Unlabled MPP^+ was the most potent inhibitor followed by DA. In third place, the carbon-linked rigid analog, **84**, was considered equipotent with the cyclohexyl analog, **76**. The nitrogen-linked rigid analog **85** came in fourth place followed by the 1,2-dimethyl analog, **60**, in fifth place. Again the rigid dihydropyridinium analog **83** was the least potent of the compounds tested for inhibition of [^{3}H] MPP^+ uptake.

The rank orders of potency for inhibition of uptake of the two substrates are very similar but not identical.

Pharmacological characterization of a receptor traditionally depends upon the use of inhibitor profiles such as presented here. Since the rank orders of potency are non-identical for the two substrates, these results may be interpreted to indicate that although dopamine and MPP^+ may share the same uptake system, the two compounds likely bind to different sites on the uptake protein.

In order to compare the rank orders of potency more easily, a potency scale was constructed in which MPP^+ was arbitrarily assigned a potency of 100. This scale is shown in Table 4-23.

Table 4-23 Potency Scale for DA, MPP^+ and substituted pyridinium ions as inhibitors of [^{3}H] DA and [^{3}H] MPP^+ uptake

Compound	Inhibition of [^{3}H] DA	Inhibition of [^{3}H] MPP^+ uptake
DA	1,000	23
MPP^+	100	100
76	18.5	4.7
60	6.9	1.4
84	5.3	6.5
85	5.2	2.3
83	1.9	0.16

The scale was derived as follows: Each IC_{50} value was devided by the IC_{50} for MPP^+ in the appropriate assay to arrive at a factor, the reciprocal of this factor was then multiplied by 100 to give the scale.

Using the rank orders of potency for inhibition of the uptake substrates as a guide to the relative affinity of each pyridinium analog for the uptake site, some important information about the structural requirements for uptake of pyridinium compounds can be obtained. First, none of the compounds tested exhibited a higher affinity for the dopamine uptake site than dopamine. MPP^+ was about 10 fold less potent. The aromatic character of the substituent at the 4 position of the tetrahydropyridine ring appears to be important for binding since the 4-cyclohexyl analog retained only approximately one fiftieth of the affinity of dopamine. Additional steric bulk such as an alpha-substituted methyl group (**60**), or a methylene (**83** and **84**) or nitrogen (**85**) bridge at the beta position results in a more drastic reduction in the affinity for the dopamine uptake site since the IC_{50} values for the bulkier compounds were 150 to 200 fold greater than that for dopamine. Studies by Horn et al.[92], Miller et al. [93], and Horn [94] have shown that the planar conformation of dopamine is preferred at the dopamine uptake site, thus the reduced affinity of the rigid analogs observed in this study has been attributed to their increased steric bulk. All of the pyridinium compounds tested showed slightly better potency for displacement of MPP^+ than for DA, reinforcing the concept that the two compounds occupy distinct (but possibly overlapping) sites on the dopamine uptake

protein. If the two substrates were bound to different sites, then the structural constraints governing binding to each of the sites might be different. This concept is consistent with our observation that the cyclohexyl compound and the carbon bridged rigid analog show significantly greater affinity at the MPP^+ binding site than at the dopamine site. The rigid dihydropyridinium analog exhibited the poorest affinity of all the compounds tested for displacement at either of the uptake sites. Since this compound was significantly poorer than any of the other rigid analogs which would have similar steric characteristics, the drop in binding site affinity may be attributed to the oxidation state of this compound. The dihydropyridinium oxidation state allows this analog to deprotonate and adopt an uncharged form **86**.

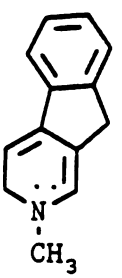

86

Possibly the permanent positive charge associated with the other pyridinium analogs is important for effective binding so that the ability to adopt an uncharged form is detrimental to binding. This finding has important implications, making it seem unlikely that $MPDP^+$, the

first MAO derived metabolite of MPTP, utitilizes the dopamine uptake system to gain access to the dopamine neuron. Of course the uncharged form of $MPDP^+$ may gain access to the dopamine neuron by passive diffusion thus this finding does not clear $MPDP^+$ of a role in the neurotoxicity associated with metabolites of MPTP.

The data obtained in our early studies with the 2-phenyl and 3-phenyl analogs of MPP^+ were not sufficiently reliable to allow quantitative assessment of the affinity of these compounds for the dopamine uptake site, however it is clear that these compounds do not posses higher affinity than MPP^+ or dopamine.

FINAL CONCLUSIONS

Table 4-24 shows the accummulated rank orders of potency for the pyridinium compounds tested as well as DA and MPP^+ in the vaious biological assays explored in Chapters 3 and 4 of this dissertation. Since not every compound was examined in each and every biological assay, our conclusions on the structural specificity associated with these measures of pyridinium ion induced toxicity must be limited to a few statements. First, some of the models of toxicity which were examined are much more structurally specific than others. For example, in the synaptosomal uptake assays the methyl substituted MPP^+ analog **60** is significantly less potent than MPP^+, while in the mitochondrial respiration assay, MPP^+ and **60** are

equipotent. In general, it appears that the structural requirements for optimal potency are similar across all of the biological assays examined. That is, MPP^+ is unique as the most potent of all of the pyridinium ions tested. Variation of the structure of MPP^+ by addition of a methyl group at the 2 position (**60**) does not reduce toxic potency in the less discriminating assays (mitochondrial respiration , mitochondrial uptake) but does reduce toxic potential in the more discriminatory assays (NADH oxidase, rat microdialysis) till a very significant reduction of potency is observed in the most discriminatory assays (mouse striatal synaptosomal uptake). Introduction of additional steric bulk in the form of a methylene bridge at the 3 position of MPP^+ (**85**) also compromised toxic potency. Displacement of the 4-phenyl moiety to the 3 or 2 position (compounds **77** and **78**, respectivly) or replacement with the smaller 4-tert-butyl (**74**) or 4-methyl (**73**) groups caused a more significant drop in toxic potency in all of the models in which these compounds were examined. The aromatic character of the phenyl moiety, however, is not essential to toxic potency, since, compounds **75** and **76** in which the phenyl moiety is replaced with a 4-(3-cyclohexenyl) or 4-cyclohexyl moiety retain a relatively high rank order of potency in most of the models examined.

The results of this dissertation effort show that some of the toxic characteristics of MPTP and its MAO-

derived metabolites $MPDP^+$ and MPP^+ are shared by their respective structural congeners. However, the potency differences between MPTP, $MPDP^+$ and MPP^+ and their structural analogs can be quite dramatic. This information has important implications for the pharmaceutical industry. Though tetrahydropyridine derivatives and their potential metabolites must be thoroughly scrutinized for toxic activity before widespread use as drugs or synthetic derivatives, these results show that it is likely that few tetrahydropyridines will be found to exhibit the tragic effects of MPTP.

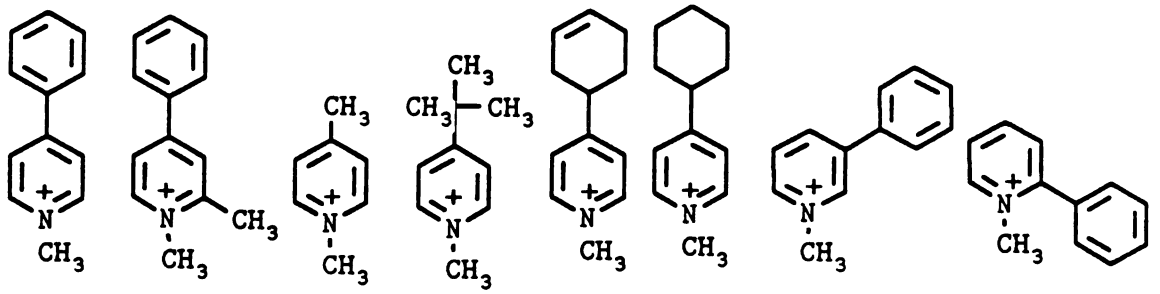

MPP^+ 60 73 74 75 76 77 78

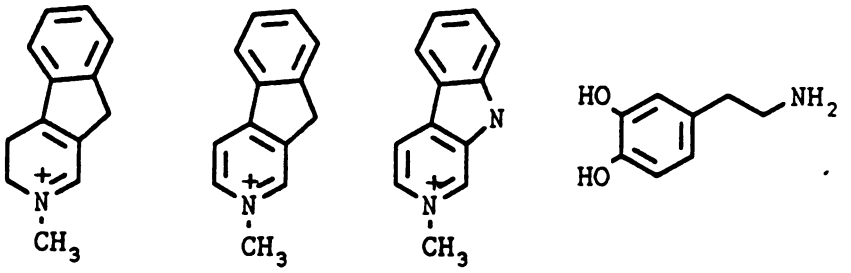

83 84 85 Dopamine

Table 4-24. Comparison of rank orders of potency of substituted pyridinium analogs in various assays of biological activity.

				Toxicity in Rat microdialysis				
	Inhib. of Mitochond.		Inhib. NADH Oxidase	DA release after Drug plus		Lactate Efflux	Inhibition of Mouse striatal synaptosomal	
Compound	Resp.	Uptake		Drug	or MPP+		[3H] DA uptake	[3H] MPP+ uptake
MPP+	#1	#1	#1	#1	#1	#1	#2	#1
DA	NT	NT	NT	NT	NT	NT	#1	#2
60	#1	#1	#2	#2	#2	#2	#4	#5
75	#1	NT	NT	#1	#3	#6	NT	NT
76	#1	NT	NT	NT	#3	#6	#3	#3
77	#2	#2	#3	#2	#4	#4	#6	NT
78	#3	#3	#2	#2or3	#4	#3	#6	NT
74	#4	NT	#4	#4	#4	#5	NT	NT
73	#5	NT	#4	#4	NT	#6	NT	NT
83	NT	NT	NT	NT	NT	NT	#5	#6
84	NT	NT	NT	NT	NT	NT	#4	#3
85	NT	NT	NT	NT	NT	NT	#4	#4

EXPERIMENTAL SECTION

SYNTHESIS

All synthetic reactions were carried out under a nitrogen atmosphere. All glassware including syringes and needles were dried 24 hours at 100°C then stored in a dessicator prior to use to maintain anhydrous conditions. Synthetic 1-methyl-4-phenylpyridinium iodide[35], 6-cyano-1-methyl-4-phenyl-1,2,3,6-tetrahydropyridine[10], 1-methyl-2-phenylpyridinium iodide [100], and 1-methyl-3-phenyl pyridinium iodide[101] were prepared as described previously. All other chemicals were reagent grade or, in the case of solvents HPLC grade. Proton NMR spectra were obtained at 80 MHz with the Varian FT-80; at 240 MHz with a custom-built instrument linked to a Nicolet 1180 computer; and at 500 MHz with a General Electric GN500 spectrometer. Chemical shifts are reported in parts per million (ppm) relative to tetramethylsilane (Me_4Si) in $CDCl_3$ or CD_3CN. For spectra obtained in D_2O, chemical shifts are reported relative to 3-(trimethylsilyl)-2,2,3,3-tetradeutero-propionic acid, a water soluble NMR standard. Spin multiplicity is given as (s) singlet, (d) doublet, (t) triplet, (q) quartet, or (m) multiplet. EI-mass spectra were obtained using a Kratos MS-25. LSI-mass spectra were obtained using a modified Kratos MS-50, fitted with a cesium ion gun in the ionization chamber, and thioglycerol as the sample diluent. UV spectra were

obtained using a Beckman DU-7 or Beckman DU-50 equipped with Beckman Data Capture and kinetics software. Melting points were obtained on a Thomas-Hoover melting point apparatus and are uncorrected. Microanalyses were performed by the Microanalytical Laboratory, University of California, Berkeley, CA. HPLC separations were achieved on a Beckman Model 330 liquid chromatographic system. Some studies were performed on the above system with an on-line diode array detector (Hewlett-packard Model 1040A) to monitor the concentrations of tetrahydropyridines (240 nm), pyridinium salts (285 nm), and dihydropyridinium salts (340 nm). Separation of the tetrahydropyridine isomers, **17** and **18**, was achieved using the above system with a 5 micron Altex ultrasphere-ODS reversed-phase column (4.6 mm x 25 cm), and a solvent system consisting of 80% acetonitrile, 20% buffer (0.05 M acetic acid, 0.3% triethylamine, adjusted to pH 5.6 with sodium hydroxide), at a flow rate of 1.5 mL per min. Separation of pyridinium salts from dihydropyridinium salts and tetrahydropyrdines was achieved using a 5 micron Altex ultrasil-cx cation exchange column (4.6mm x 25 cm), and a solvent system consisting of 15% acetonitrile, 85% buffer (0.1 M acetic acid, 0.05 M triethylamine hydrochloride, adjusted to pH 2.3 with formic acid), at a flow rate of 2 mL per min.

METHYL 3-METHYLAMINOPROPIONATE (24)

Methyl amine gas was condensed with a dewar condenser filled with dry ice and acetone into a 3 necked round bottom flask surrounded by a dry ice/acetone bath. The methyl amine (50 mL, 35 g, 1.13 mol) was stirred at -70 ^{o}C during the dropwise addition of methyl acrylate (25 mL, 24 g, 0.28 mol). After the 30 minute addition period, the reaction mixture was maintained at -70 ^{o}C for 6 hours. The mixture was then allowed to warm to 25 ^{o}C and stirred 40 hours to allow evolution of unreacted methyl amine. The mixture was transfered to a round bottomed flask and the residual exess methyl amine was evaporated at reduced pressure to yield 45.3 g of a pale yellow oil. Vacuum distillation at 3.5 mm Hg resulted in a fore-run of 8.5 g at 25 ^{o}C, followed by a fraction collected at 20-40 ^{o}C (1.6 g). The pure desired product distilled at 45-50 ^{o}C (3.9 g, 12%). After collection of the desired product, the pot temperature rapidly rose to 110 ^{o}C so the distillation was stopped leaving a pot residue of 24 g. GC chromatography of the fraction distilled at 45-50 ^{o}C gave a single peak with retention time 4.1 min (6 ft. packed column, OV-17 3%). The 80-MHz ^{1}H NMR (CD_3CN) spectrum exhibited the following signals as expected for the desired product, 1.34 ppm (s, 1 H, N-H), 2.31 ppm (s, 3 H, N-CH_3), 2.48 ppm (d, 2 H, -CH_2-N),

2.74 ppm (d, 2 H, $-CH_2-CO$), 3.61 ppm (s, 3 H, $-OCH_3$); GC-EIMS m/e 117 $(MH)^+$, m/e 44 $(M - CH_2-CO_2CH_3)^+$.

The pot residue was identified as the diadduct **32** by means of its 80-MHz ^1H NMR ($CDCl_3$) spectrum, 2.24 ppm (s, 3H, $N-CH_3$), 2.47-2.71 ppm (m, 8 H, $CO-CH_2-CH_2-N$), 3.67 ppm (s, 6H, $-OCH_3$); and GC-EIMS m/e 203 $(M)^+$, m/e 130 $(M - CH_2-CO_2CH_3)^+$.

METHYL 3-METHYL-2-BUTENOATE (25)

Using a teflon stoppered dropping funnel, 3-methyl-2-butenoic acid chloride (50 g, 0.42 mol, Aldrich) was added dropwise to anhydrous methanol (100 mL) in an ice-cooled 500 mL 3-necked round bottom flask fitted with a magnetic stirrer and condenser. The entire apparatus was protected from light by an aluminum foil jacket to prevent polymerization of the acrylic acid derivative. The addition was accompanied by vigourous reaction and heat evolution. After the addition was completed the mixture continued to stir at 25 ^oC for 24 hours. TLC on silica plates with methanol/ dichloromethane (1:9) followed by iodine staining was used to follow the progress of the reaction. Since the acid chloride decomposed on TLC, the corresponding acid 3,3-dimethyl acrylic acid (rf 0.67) was used as a reference in TLC. After 24 hours reaction time the TLC indicated no acid present but instead indicated a major product (rf 0.33) accompanied by a minor product (rf 0.06). Solvent was

removed at reduced pressure from the mixture to give a pale yellow, 2-phased oil. Distillation at atmospheric pressure gave 3 fractions (fraction 1, bp 47-52 ^{o}C, 8.6 g; fraction 2, bp 52-63 ^{o}C, 10.4 g; fraction 3, 63-65 ^{o}C, 5.5 g), each of which was also two phased. The 80-MHz ^{1}H NMR spectrum of fraction 2 indicated likely contamination by 3,3-dimethyl acrylic acid despite the previous TLC evidence to the contrary. This explained the low bp obtained for the fractions relative to the reported bp (135-138 ^{o}C at 760 mm Hg). [163] Fraction 2 was dissolved in diethyl ether (30 mL), extracted with saturated aqueous sodium carbonate (3 x 30 mL) to remove the contaminating acid, and the ether layer dried with anhydrous magnesium sulfate. The ether layer was evaporated at reduced pressure and the resulting oil was vacuum distilled (10 mm Hg, 24 ^{o}C, receiver packed in ice) to yield the desired ester as a clear colorless oil (7 g, 14%) 80-MHz ^{1}H NMR 1.88 ppm (s, 3H, vinylic-CH_3), 2.13 ppm (d, 3H, vinylic-CH_3), 3.61 ppm (s, 3H, O-CH_3), 5.67 ppm (pentup., 1H, vinylic H); GC-EIMS m/e 114 $(M)^{+}$, m/e 83 $(M- OCH_3)^{+}$.

SYNTHESIS OF 1,2-DIMETHYL-4-PHENYL-1,2,3,6-TETRAHYDROPYRIDINE (17), 1,6-DIMETHYL-4-PHENYL-1,2,3,6-TETRAHYDROPYRIDINE (18) AND 1,2-DIMETHYL-4-PHENYLPYRIDINIUM IODIDE (60) VIA THE DISPROPORTIONATION OF A GRIGNARD REACTION MIXTURE

A suspension of powdered $MPP^+ I^-$ (10.0 g, 34 mmol) in dry diethyl ether (500 g, 706 mL) was stirred at room temperature as a solution of methyl magnesium bromide 2.9 M (60 mL, 174 mmol, 5.1 equiv.) was added by syringe over a twenty min period. The mixture was slowly heated and stirred at reflux for one to two hours. After visible determination of dissolution of the starting material (usually two hours) the progress of the reaction was assessed by the anaerobic removal of a small aliquot which was diluted 1:1000 in 1M aqueous HCl. The UV spectrum of this diluted sample (ca. 56 $x10^{-6}$ M) gave a maximal absorption at 346 nm, o.d. =0.9 (theoretical 0.974) which corresponded to a 92% yield of dihydropyridine. Excess Grignard reagent was then quenched and the disproportionation reaction initiated by the slow addition of 1M aqueous HCl (8 x 20 mL) via syringe. After the vigorous reaction had subsided, the mixture was allowed to stir at 25 ^oC for 22 hours. The ether was then removed by aspiration. The resulting yellow gummy suspension (pH 2) was extracted with dichloromethane (8 x 200 mL). The resulting aqueous

layer was saturated with sodium chloride and further extracted with dichloromethane (3 x 200 mL). The organic extracts were combined and evaporated to give a paste containing **17**·HCl, **18**·HCl and **60**·I as well as a small amount of **15**·HCl. The content of the paste was confirmed by cation exchange HPLC (Figure 2-24). The hydrochloride salts of **17** and **18**, can be extracted with dichloromethane, a relatively polar organic solvent. The paste was diluted with water (200 mL), made alkaline (pH 9) with sodium hydroxide, and extracted with diethyl ether (4 x 200 mL). The basic aqueous layer was set aside for later isolation of **60**, see below. The organic extracts were combined, dried over calcium sulfate and evaporated to give 3.0 g (79% of theoretical yeild) of a mixture of **17** and **18** as their free bases as well as 4 minor contaminants. Chromatographic separation was achieved using the Chromatotron (silica gel plate, 4 micron thickness). Initial elution with dichloromethane (50 mL), allowed separation of 2 of the minor components of the mixture which were more polar than **17** and **18**. This was followed by elution with methanol/dichloromethane (5:95) to give 80 fractions of 5 mL volume. Every tenth fraction was assayed by reversed phase HPLC to ascertain its **17**:**18** ratio. This method allowed initial identification of the richest tetrahydropyridine fractions. Each of the rich fractions was then assayed individually by reversed phase HPLC to

ascertain its 17:18 ratio. The fractions containing pure compound 17 were then grouped and evaporated to a colorless oil (1.3 g, 43% recovery) whose purity was then reassessed by reversed phase HPLC. Compound 17 was obtained in 98% purity (reversed phase HPLC, Figure 2-29), and converted, by treatment with ethereal HCL, to a white solid. Recrystalization from ethanol/diethyl ether gave 227 mg (1 mmol, 6%) of pure white crystals: mp 191-192 ^{o}C; 500-MHz ^{1}H NMR (D_2O) 1.45 ppm (d o d, 3 H, C_2-CH_3), 2.65 ppm (m, 1 H, C_{3ax}), 2.95 ppm (d, 3H, N-CH_3 ax and eq), 3.0 ppm (m, 1 H, C_{3eq}), 3.6 ppm (m, 0.5 H, C_{2ax}), 3.85 ppm (m, 1.5 H, C_{6ax} and C_{2eq}), 4.1 ppm (d, 1H, C_{6eq}), 6.1 ppm (s, 1H, C_5), 7.5 ppm (m, 5 H, Ar H); EIMS m/e 187 $(MH)^+$, m/e 172 $(M - CH_3)^+$. Anal. Calcd for $C_{13}H_{17}N \cdot HCl$: C, 69.78; H, 8.11; N, 6.26. Found: C, 69.75; H, 8.07; N, 6.13.

ISOLATION OF PYRIDINIUM ION 60

The alkaline aqueous layer obtained above was made acidic with conc. HCl, saturated with sodium chloride, and exhaustively extracted with dichloromethane (4 x 200 mL). The extracts were combined and evaporated to give 3.3 g (crude yield 62%) of a yellow solid, which when recrystalized from acetonitrile gave 2 g (38%) fine yellow hygroscopic crystals: mp 187-189 ^{o}C; 240-MHz ^{1}H NMR ($CDCl_3$) 3.0 ppm (s, 3 H, C_2-CH_3), 4.5 ppm (s, 3 H, N^+-CH_3), 7.6 ppm (m, 3 H, $C_{3'}$, $C_{4'}$, $C_{5'}$), 7.75 ppm (m, 2

H, $C_{2'}$, $C_{6'}$), 8.1 ppm (m, 2 H, C_3 and C_5), 9.5 ppm (d, 1 H, C_6); L-SIMS (thioglycerol) m/e 184 $(M)^+$; UVmax 284 nm, ext. coeff 17,500. Anal. Calcd for $C_{13}H_{14}NI \cdot 1.7\ H_2O$: C, 45.68; H, 5.13; N, 4.10. Found: C, 45.67; H, 4.71; N, 4.03.

CONVERSION OF **60**·HALIDE TO **60**·PERCHLORATE

The iodide salt of **60** (371.4 mg, 1.2 mmol) was dissolved in deionized water (25 mL) with the aid of sonication. An aqueous solution of silver perchlorate (281.5 mg, 1.36 mmols, in 10 mL H_2O) was added to the pyridinium solution with the immediate formation of a fluffy yellow precipitate. The mixture was allowed to stand overnight at 25 °C, protected from light. The precipitate was then filtered and washed with water (3 x 20 mL). The colorless filtrate and washings were lyophylized to give a fluffy white solid (200 mg, crude yield 59%). Recrystalization from acetone gave 132.4 mg (0.5 mmol, 39%) of beautiful needles: mp 160-161 °C. Anal. Calcd for $C_{13}H_{14}N \cdot ClO_4$: C, 55.03; H, 4.97; N, 4.93. Found: C, 54.72; H, 4.86; N, 4.78.

1,6-DIMETHYL-4-PHENYL-1,2,3,6-TETRAHYDROPYRIDINE (18) VIA GRIGNARD REACTION ON 6-CYANO-1-METHYL-1,2,3,6-TETRAHYDROPYRIDINE (69)

Compound **69** (300 mg, 1.5 mmol) was dissolved in dry diethyl ether (40 mL) and cooled to 0 °C. Ethereal methylmagnesium bromide (2.9 M) (1.5 mL, 4.5 mmol, 3 equiv.) was added by syringe with the immediate formation of a white floculant precipitate. The mixture stirred for 2 hours while warming to 25 °C. After the addition of distilled water (35 mL), the mixture was extracted with dichloromethane (4 x 75 mL). The extracts were dried over sodium sulfate and evaporated to give a yellow oil which crystallized on standing at 5 °C. After storage for 12 hours at 5 °C, the oil became slightly orange. TLC on alumina plates with dichloromethane showed a slight amount of a very polar contaminant which was removed by filtration over alumina (eluent ethanol/chloroform 5:95). The eluent was concentrated and immediately treated with gaseous HCl to give the salt. Crystallization from ethanol/diethyl ether gave 185 mg (0.83 mmol, 55%) of pure product as white crystals (reversed phase HPLC, Figure 4b): mp 203-205 °C; 500-MHz ^{1}H NMR (D_2O) 1.5 ppm (d o d, 3 H, C_6-CH_3), 2.8 ppm (m, 2 H, C_{3ax} and C_{3eq}), 2.95 ppm (d, 3 H, N-CH_3), 3.4-3.8 ppm (m, 2 H, C_{2ax} and C_{2eq}), 4.0 ppm (bs, 0.8 H, C_{6ax}), 4.25 ppm (bs, 0.2 H, C_{6eq}), 6.1 ppm (d, 1 H, C_5), 7.4-7.6 ppm

(m, 5 H, Ar H); EIMS m/e 187 $(M)^+$, m/e 172 $(M - CH3)^+$. Anal. Calcd for $C_{13}H_{17}N \cdot HCl$: C, 69.78; H, 8.11; N, 6.26. Found: c, 69.74; H, 8.12; N, 6.14.

SODIUM BOROHYDRIDE REDUCTION OF 1,2-DIMETHYL-4-PHENYLPYRIDINIUM IODIDE TO FORM A MIXTURE OF TETRAHYDROPYRIDINES 17 AND 18

The pyridinium salt, 1,2-dimethyl-4-phenylpyridinium iodide **60** (120 mg, 0.38 mmol) was dissolved in methanol (5 mL) at room temperature, then cooled to 5 ^{o}C. Sodium borohydride (68 mg, 1.8 mmol) was added and the mixture allowed to stir for 15 minutes. TLC on silica plates with chloroform/acetonitrile (1:1) indicated most of the starting material still present after 15 minutes and again after 4 hours at 5 ^{o}C. Additional sodium borohydride (185 mg, 5 mmol) was added and the mixture allowed to stir at 25 ^{o}C protected from light for 59 hours. Distilled water (15 mL) was added, and the alkaline mixture (pH 9-10) was extracted with diethyl ether (5 x 20 mL). The extracts were dried over magnesium sulfate and evaporated to give a pale yellow oil (66.8 mg, 93%). The oil was immediately diluted with deuterated acetonitrile (0.5 mL) to obtain an 80-MHz ^{1}H NMR spectrum. The resulting spectrum exhibited two distinct sets of signals, appearing to arise from a mixture of tetrahydropyridine products. In particular two peaks were observed in the region around 6 ppm which

correspond to olefinic protons. The relative intensities of the peaks indicated a product ratio of approximately 4:1. In addition, two sets of doublet signals, approximately 4:1 in intensity, were observed in the region around 1.2 ppm which appeared to arise from two different alpha methyl groups (The C_2 and C_6 methyl groups). The 80-MHz ^1H (CD_3CN) spectrum (See figure 2-13) follows: 1.1 ppm (d, 3H of major component, C_2-CH_3), 1.14 ppm (d, 3H of minor component, C_6-CH_3), 2.21-2.45 ppm (m, 6H of major compound, H_{3ax}, H_{3eq}, H_2 and N-CH_3), 2.7 ppm (t, 1H of minor component, H_{3ax}), 3.0 ppm (q, 1H of major component, H_{6ax}), 3.2 ppm (pentuplet, 1H of major component, H_{6eq}), 3.4 ppm (pentuplet, 1H of minor component, H_2), 5.98 ppm (octet, 1H of minor component, H5), 6.08 ppm (octet, 1H of major component), 7.2-7.4 ppm (m, 5H of major and minor components), aromatic H). This data was consistant with the hypothesis that sodium borohydride reduction of pyridinium **60** had resulted in formation of a mixture of the tetrahydropyridines **17** and **18**. Two decoupling experiments were performed in which the sample was irradiated first at 1.19 ppm, to remove the coupling effect of the C_2-CH_3. This produced a change in the spectrum restricted to the signals in the region 2.33-2.5 ppm. The more downfield signals corresponding to aliphatic protons were not affected. Since such an irradiation should most affect the signal corresponding to the proton alpha to the methyl group,

and since the most obvious signal should correspond to the proton of the major component, this information indicated that the major component of the mixture was **17** whose H_2, alpha to the methyl group though non-allylic, would be expected to exhibit a signal which was upfield in chemical shift relative to the allylic protons of the molecule. In a second decoupling experiment, the sample was irradiated at the frequency of the olefinic protons (5.98 ppm). This process was designed to identify the signals corresponding to the allylic protons of the major component. Upon irradiation the multiplicity of 4 signals changed as follows:

component*	chem. shift	mult.	mult. after irrad.
minor	3.40 ppm	pentup.	quartet
major	3.20	pentup.	quartet
major	2.98	quartet	triplet
minor	2.73	triplet	unresolved

* assignment made on the basis of peak height

From this data, it was clear that the major component of the mixture contained at least 2 protons with signals at 3.2 ppm and at 2.98 ppm which were strongly coupled to the olefinic proton H_5. The previous decoupling experiment however had shown that these two protons were not coupled to the C_2 methyl group. This data again supported the hypothesis that compound **17** with two allylic C_6 protons was the major component of the

mixture. Additional evidence supporting the tetrahydropyridine character of the mixture came from the UV spectrum which exhibited a maximal absorption at 248 nm, similar to the spectrum of MPTP, another tetrahydropyridine.

ATTEMPT TO SYNTHESIZE **18** VIA pH CONTROLED REDUCTION OF PYRIDINIUM **60** WITH SODIUM CYANOBOROHYDRIDE UNDER ACIDIC CONDITIONS

The iodide salt of **60**, (300 mg,0.96 mmol) was dissolved in 1M HCL in methanol (25 mL) and cooled to 2 ^{o}C with an ice/brine bath. Sodium cyanoborohydride (374 mg, 5.96 mmol) was added to the pyridinium solution. After stirring for 30 minutes, TLC on silica plates with methanol/dichloromethane (15:85) showed the starting material unchanged. In this system the starting pyridinium salt traveled with an Rf of 0.22 while a reference sample of mixed **17/18** (85:15) obtained from disproportionation traveled with an Rf of 0.27. Additional sodium cyanoborohydride (614 mg, 9.8 mmole) was added to the reaction mixture and the mixture stirred at 25 ^{o}C for 36 hours. TLC again showed unchanged pyridinium with no desired product formed. The solvent was evaporated from the mixture to give a white powder. A small portion was disolved in ethanol for UV analysis. The maximal absorbance at 284 nm was characteristic for

the pyridinium structure and confirmed the recovery of starting material.

In a second attempt to generate the tetrahydropyridine **18** by pH controled reduction of **60** under acidic conditions, an indicator dye, methyl orange, with a pka of 3 was used to titrate the pH of the reaction mixture.

The pyridinium iodide **60** (502 mg, 1.6 mmol) was dissolved in methanol (25 mL). Three drops of a dilute solution of methyl orange in methanol were added to the pyridinium solution. A solution of 1M HCL in methanol was added dropwise to give a rose color (- 7 drops) indicating a pH of 3 in the reaction mixture. Sodium cyanoborohydride (672 mg, 10.7 mmol) was added all at once. The rose color (pH 3) was maintained by dropwise addition of 1 M HCl in methanol. After 30 minutes stirring, a 0.5 mL aliquot was removed and diluted into methanol (250 mL) for UV analysis which indicated a single UV max at 285 nm (UV max of **60**), indicating no detectable formation of the tetrahydropyridine reduction product which should exhibit a UV maximum at 243 nm. Additional sodium cyanoborohydride (711 mg, 11.3 mmol) was added to the mixture and stirring continued. After 1.5 hours reaction time the progress of the reaction was again checked by UV scan of a diluted aliquot. Still no reduction product had formed and the UV scan showed a

single maximum at 285 nm. A third portion of sodium cyanoborohydride (671 mg, 10.7 mmol) was added and the mixture heated to reflux. TLC after 4.5 hours reaction time showed still no product. After a total of 72 hours reaction time the mixture was poured into ice chips (300 mL), made alkaline with 50% aqueous sodium hydroxide, and extracted with dichloromethane (5 x 100 ml). The extracts were dehydrated over anhydrous sodium sulfate and evaporated to a white opaque oil. 80-MHz ^1H NMR ($CDCL_3$) of the oil indicated the characteristic singlets at 4.25 ppm and 2.8 ppm corresponding to the N-CH_3 and C_2-CH_3, respectively of pyridinium **60**. No peak at 6.05 ppm which would have indicated formation of tetrahydropyridine, corresponding to an olefinic H_5 proton appeared in the spectrum confirming recovery of unchanged pyridinium starting material.

ATTEMPT TO DEMONSTRATE CYANOBOROHYDRIDE REDUCTION OF PYRIDINIUM 60 UNDER NEUTRAL CONDITIONS

Pyridinium salt **60** (104 mg, 0.34 mmol) was dissolved in methanol (7 mL). Sodium cyanoborohydride (151 mg, 2.4 mmol) was added to the pyridinium solution and stirred at 25 ^oC. Progress of the reaction was monitored both by TLC on silica plates using methanol/chloroform (1:9) and using HPLC with diode array-UV detection. For HPLC an Altex Ultrasil Cx cation-exchange column (10 um partical x 250 mm x 4.6 mm) with a mobile phase of acetonitrile

15%:buffer 85% (0.1M acetic acid, 0.05 M triethylamine hydrochloride brought to pH 2.3 with formic acid) at a flow rate of 2 mL per minute was used. The diode array detector was set to monitor 3 wavelengths; 248 nm to detect tetrahydropyridine, 295 nm to detect pyridinium compounds, and 345 nm to detect potential dihydropyridinium intermediates of reduction. The relative percentages of compounds identified on HPLC were calculated using a correction factor which accounted for the molar absorptivity of each compound; ca. 12,000 for tetrahydropyridines, 18,000 for pyridiniums. Thus the percent of tetrahydropyridine formed was estimated as the ratio of area under the respective peaks for tetrahydropyridine (at 244 nm)/pyridinium (at 295 nm) multiplied by 1.5. HPLC standards for pure **60** and mixed **17/18** were used to identify the retention times for each compound as 6.0 minutes and 3.2 minutes respectively.

After 1 hour reaction time at 25 ^{o}C, HPLC indicated the reaction mixture contained 3% reduction product and 97% unchanged starting material. The mixture was warmed to 45 ^{o}C and stirred an additional 5 hours. TLC indicated the starting pyridinium was still the major component of the mixture. Additional sodium cyanoborohydride (1.64 g, 26 mmol) was added to the mixture and the mixture stirred for an additional 2 hours at 25 ^{o}C. HPLC indicated 12.6% of the reaction mixture was tetrahydropyridine. Further addition of sodium

cyanoborohydride (274 mg, 4.4 mmol) followed by 3.5 hours stirring resulted in no further change of the reaction mixture. A final HPLC analysis showed the mixture still contained only 12% tetrahydropyridine, while 88% of the starting material remained unchanged. It was concluded that sodium cyanoborohydride was too weak an agent to reduce the pyridinium ring.

1,2-DIMETHYL-4-PHENYL-2,3-DIHYDRO-PYRIDINIUM PERCHLORATE (15)

A suspension of $MPP^+ I^-$ (5.8 g, 19.4 mmol) in dry diethyl ether (500 mL) was stirred at 25 ^oC, while methylmagnesium bromide 2.9 M (17 mL, 49.3 mmol, 2.5 eq) was added slowly via syringe. After two hours, UV analysis (as described in disproportionation reaction above) indicated the reaction was complete. The mixture was poured, with vigourous stirring, into a solution of perchloric acid (100 mL of 70% $HClO_4$) in ice chips (400 mL) which was cooled with an external ice bath (very vigorous reaction!). The mixture was blanketed with an argon atmosphere and allowed to stand at 0 ^oC for 45 min. The pale yellow hygroscopic crystals which formed were filtered (2.7 g, 49% crude yield). Recrystallization by trituration with perchloric acid 2% in methanol gave 241.3 mg (0.85 mmol, 5%) pure lemon yellow crystals: mp 97-98 ^oC; 500-MHz ^1H NMR ($CDCl_3$) 1.5 ppm (d, 3 H, C_2-CH_3, J_{vic} 6 Hz), 3.04 (d o d, 1 H, C_{3ax}, J_{gem} 20 Hz, J_{vic} 2

Hz), 3.6 (d o d, 1 H, C_{3eq}, J_{gem} 20 Hz, J_{vic} 4 Hz), 3.8 (s, 3 H, N-CH_3), 4.3 (m, 1 H, C_2), 6.85 (d 0 d, 1 H, C_5, J_{vic} 5 Hz), 7.45-7.7 (m, 5 H, Ar H), 8.44 (d, 1 H, C_6, Jvic 5 Hz); UVmax 349 nm, ext. coeff. 15,600. Anal. Calcd for $C_{13}H_{16}N^{\cdot}ClO_4$: C, 54.64; H, 5.65; N, 4.90. Found: C, 54.32; H, 5.65; N, 4.82.

1,4-DIMETHYL-PYRIDINIUM IODIDE (73)

Methyl iodide (34.2 g, 241 mmol, 15 mL) was added dropwise to 4-methyl pyridine (18.6 g, 200 mmol, 19.5 mL) which had been dissolved in methanol (20 mL). Heat evolution accompanied the addition causing the solvent to reflux thus the reaction apparatus included a condenser and external ice bath for cooling. The progress of the reaction was monitored using TLC on silica plates with dichloromethane/acetonitrile (1:1). Under these very polar elution conditions the starting material gave an Rf of 0.51, while the product gave an Rf of 0.33. The reaction was nearly complete after 30 minutes, only a slight amount of unreacted pyridine remained. Additional methyl iodide (4.56 g, 32 mmol, 2 mL) was added and the reaction allowed to stir an additional 30 minutes at which time the reaction was complete (TLC). Yellow crystals formed as the reaction mixture cooled following completion of the methyl iodide addition. Diethyl ether (5 mL) was added to promote crystalization and the product filtered to give the crude product (18 g, 38% of

theoretical yeild). A second crop was harvested from the filtrate. Recrystalization from anhydrous ethanol gave pale yellow-white needles: mp 140-148 ^{o}C (lit. 153-153.8 ^{o}C)[98]. Anal. Calcd. $C_7H_{10}NI$: C, 35.76; H, 4.29; N, 5.96. Found: C, 35.66; H, 4.19; N, 5.96.

1-METHYL-4-tert-BUTYL-PYRIDINIUM IODIDE (74)

Methyl iodide (28.6 g, 0.2 mol, 12.5 mL) was added dropwise to a solution of 4-tert-butylpyridine (13.5 g, 0.1 mol, 14.8 mL) in methanol (100 mL). The solution stirred at 25 ^{o}C until the addition was complete then was warmed with an oil bath to stir at reflux for 17 hours. TLC on silica plates with dichloromethane/acetonitrile (1:1) indicated the reaction was complete. The mixture was cooled with an ice bath and diethyl ether (2 x 5 mL portions) was added to promote crystalization. The product, however, did not precipitate. Solvent was removed in vacuo to yield an orange oil (27.8 g, 100 %). The oil was allowed to stand 4 days at 25 ^{o}C in the dark while the product slowly crystalized. Two recrystalizations from acetone/diethyl ether gave the pure product (12.3 g, 44.4% of theoretical yield) as yellow needles: mp 115-119 ^{o}C, (lit. 124-125 ^{o}C)[99]; 80-MHz ^{1}H NMR ($CDCl_3$); 1.3 ppm (s, 9H, tert-butyl); 4.6 ppm, (s, 3H, N-CH_3); 8.0 ppm, (d, 2H, H_3 and H_5); 9.3 ppm, (d, 2H, H_2 and H_6). Anal. Calcd for $C_{10}H_{16}$ NI: C, 43.33; H, 5.82; N, 5.05. Found: C, 43.23; H, 5.89; N, 4.97.

1-METHYL-4-(3-CYCLOHEXENYL)PYRIDINIUM IODIDE (75)

The starting material for this reaction, 4-(3-cyclohexeny)pyridine **79** (generously donated by Reilly Tar and Chemical Company, Cleveland, Ohio) was purified by distillation to give a pure oil (bp 110 ^{o}C, 5 mm Hg; reported by Reilly Tar and Chem. Co. bp 226 ^{o}C, 760 mm Hg). The freshly distilled pyridine (16.3 g, 102 mmols, 16 mL) was dissolved in methanol (15 mL). Methyl iodide (57 g, 402 mmols, 25 mL) was added dropwise and the mixture allowed to stir at reflux for 3.5 hours. TLC on silica plates with ethyl acetate/hexane (1:1) indicated complete dissapearance of starting material, however the mixture was allowed to continue to stir at room temperature overnight. The solvent was evaporated to obtain a golden oil which crystalized at room temperature. The crystals were filtered, and washed with methanol/ether (1:4) and dried in vacuo to give pure yellow crystals: mp 119-121.5 ^{o}C; 500-MHz ^{1}H NMR ($CDCL_3$) 1.7-2.2 ppm (m, 6H, $H_{2'ax}$ and $_{eq}$., $H_{5'}$ $_{ax}$ and $_{eq.}$ and $H_{6'}$ $_{ax}$ and $_{eq}$.), 3.1 ppm (m, 1H, $H_{1'}$), 4.64 ppm (s, 3H, N-CH_3), 5.76 ppm (m, 2H, $H_{3'}$ and $H_{4'}$), 7.88 ppm (d, 2H, H_3 and H_5), 9.22 ppm (d, 2H, H_2 and H_6); UVmax 226 nm, ext. coeff 20,571; UV shoulder 254 nm, ext. coeff. 4,286. Anal. Calced for $C_{12}H_{16}NI$: C, 47.85; H, 5.36; N, 4.65. Found: C, 47.81; H, 5.45; N, 4.54.

This product proved to be hygroscopic and unstable to light, turning to a dark brown oil when stored for several weeks under normal flourescent light. An attempt to recover crystals from the brown oil by recrystalization was unsuccessful even after dessication of the solvent with $MgSO_4$. As a result of this discovery freshly prepared **75** was stored in a dessicator, in the dark.

SYNTHESIS OF 4-CYCLOHEXYL PYRIDINE (80) BY CATALYTIC REDUCTION OF 4-(3-CYCLOHEXENYL) PYRIDINE (79)

Palladium 10% on carbon (291 mg) was added to denatured ethanol (250 mL) and prereduced by exposure to H_2 gas (28 psi) for 25 minutes in a Parr Shaker hydrogenation apparatus (500 mL capacity bottle). Freshly distilled 4-(3-cyclohexenyl-pyridine (**79**) (16 g, 0.1 moles) was added to the catalyst/ethanol mixture. The hydrogenation bottle was then replaced into the Parr Shaker and the apparatus was charged with H_2 gas at 35 psi. Initially the H_2 pressure dropped rapidly (23 psi over 20 minutes), and H_2 pressure was recharged to 35 psi 3 times over the course of the first 3.5 hours reaction time. After 3.5 hours a sample was removed for ^1H NMR to check the progress of the reaction. Progress was monitored by following the disappearance of the resonance at 5.7 ppm which corresponded to the olefinic protons in the cyclohexenyl ring. After 3.5 hours hydrogenation,

the reaction was approximately 50% complete. The reaction was allowed to continue for a total of 7 hours 20 minutes, with a total H_2 uptake of approximately 60 psi. The catalyst was then removed by filtration over celite and the colorless filtrate stored under argon in the dark for 72 hours. Solvent was removed by evaporation at reduced pressure to give a colorless oil (16.1 g, 99%); 500-MHz ^1H NMR (CD_3CN) 1.0-2.0 ppm (m, 10H, $H_{2'}$,$H_{3'}$, $H_{4'}$, $H_{5'}$, $H_{6'}$), 2.2 ppm (m, 1H, $H_{1'}$), 7.2 ppm (d, 2H, H_3 and H_5), 8.48 ppm (d, 2H, H_2 and H_6). This oil was used without further purification in the synthesis of **76**.

1-METHYL-4-CYCLOHEXYL PYRIDINIUM IODIDE (76)

Methyl iodide (21.1 g, 0.15 mole) was added to a solution of 4-cyclohexylpyridine (**80**)(16.1 g, 0.1 mole) in methanol (20 mL). The mixture was allowed to stir at 25 ^oC. Progress of the reaction was monitored by TLC on silica plates with ethyl acetate/hexane (1:1), after 19 hours TLC indicated complete disappearance of the starting pyridine. The solvent was removed by evaporation under reduced pressure. The resulting oil (29.0 g, 96%) partially crystallized and was washed with diethyl ether. However, the bright yellow crystals were extremely hygroscopic and rapidly melted as they accumulated moisture. A yellow powder could be recovered by trituration with diethyl ether. The powder was

transferred under an argon atmosphere to vials for storage.

1-METHYL-4-CYCLOHEXYL-PYRIDINIUM (76) PERCHLORATE

In order to obtain a less hygroscopic salt for characterization, a portion of the yellow powder obtained above was converted to the perchlorate salt. The 4-cyclohexylpyridinium iodide (3.25 g, 11.1 mmol) was dissolved in distilled water (40 mL) and added to a solution of silver perchlorate (2.53 g, 12.2 mmol) in water (30 mL) with immediate formation of yellow silver iodide. The mixture was allowed to stir overnight at 25 ^{o}C, then filtered and the yellow inorganic iodide washed with distilled water (3 x 20 mL). The filtrate and washings were combined and frozen in a 1 liter round bottom flask then evaporated (lyophilized) to give a colorless waxy solid (3.3 g, 100%). No successful recrystalization system was found for the still very hygroscopic, waxy, low melting solid. HPLC analysis using a cation exchange column (Altex Ultrasil-Cx, 10 um particle, 4.2 mm x 25 cm) and a mobile phase of 16.5 % acetonitrile, 83.5% buffer (0.1 M acetic acid, 0.05 M triethylamine hydrochloride, adjusted to pH 2.3 with formic acid), at a flow rate of 2 mL per minute, indicated a single peak, with a retention time of 7.022 minutes. Using a Hewlett-Packard diode array UV detector, the UV spectrum of this peak was obtained and

exhibited a UVmax at 232 nm with a shoulder at 254 nm. After drying 4 hours at high vacuum, the white waxy solid gave a mp 75-78 ^{o}C; 500-MHZ ^{1}H NMR ($CDCL_3$) 1.2-2 ppm (m, 10H, $H_{2'}$-$H_{6'}$), 2.85 ppm (m, 1H, $H_{1'}$), 4.42 ppm (s, 3H, N-CH_3), 7.84 ppm (d, 2H, H_3 and H_5), 8.75 ppm (d, 2H, H_2 and H_6). Anal. calced for $C_{12}H_{12}N{\cdot}ClO_4 \cdot 0.75\ H_2O$: C, 49.82; H, 6.80; N, 4.84. Found: C, 50.01; H, 6.55; N, 4.64.

STUDIES WITH MONOAMINE OXIDASES

PREPARATION OF MAO B FROM BOVINE LIVER MITOCHONDRIA

Protein concentrations were determined by the Biuret method with the addition of 0.05 mL of 10% w/v deoxycholate per 3 mL, to solubilize lipids.[45] MAO activity was assayed spectrophotometrically by a modification of the method of Tabor et al.[46] One unit MAO activity is defined as the amount of enzyme required to oxidize 1 umol of benzylamime to benzaldehyde per minute at 30 ^{o}C at pH 7.2 in 50 mM sodium phosphate buffer. Phospholipases A and C were generously supplied by Dr. James Salach, Molecular Biology Division, Veterans Administration Hospital, San Francisco, CA. Beef liver mitochondria were prepared according to the method of Kearney et al.[47] Dextran 250, Ficol, and polyethylene glycol polymers were purchased from Sigma.

Beef liver mitochondria (270 mL, from 3.38 Kg beef liver) were stirred into cold distilled water (1 L) and homogenized with a teflon/glass homogenizer (0.25 mm, 0.010 in, 80 mL). The homogenate was added to cold distilled water to give a final volume of 2500 mL. Protein concentration and MAO activity were determined. The specific activity of the membranes was 0.023 units/mg protein.

The homogenate was centrifuged at 41,000 x g for 15 min. The resulting supernatent was discarded and the pellets were collected into triethanolamine (TEA) 0.1M buffer pH 7.2 (600 mL). This mixture was homogenized in a teflon/glass homogenizer. The volume of the mixture was increased to 1 L with TEA 0.1 M, mixed well and protein concentration and MAO activity again determined. The volume of the mixture was again increased to adjust the protein concentration to 30 mg/ mL with TEA 0.1 M.

The homogenate was then poured into a 2 liter beaker surrounded by a water bath at 30 ^{o}C. The reaction mixture was made 25 mM in $CaCl_2$ by the addition of a solution of 1 M $CaCl_2$. The pH of the mixture was adjusted to 7.3 with 2 N ammonium hydroxide. The quantities of phospholipase A and C to be added were calculated based on protein content of the mixture. For each 500 mg of protein, 1.66 mg phospholipase A and 1.0 mg phospholipase C were added. The pH of the mixture was monitored and maintained at 7.3 by the dropwise addition

of 2 N ammonium hydroxide for the duration of the 60 min incubation.

The incubation mixture was then centrifuged at 41,000 x g for 15 min. The supernatent was discarded and the pellet homogenized into TEA 0.1 M, pH 7.2 buffer (1 L). This homogenate was stored overnight, on ice, in a 4 ^{o}C refrigerator.

The protein concentration and MAO activity of the suspension were determined. Based on the protein concentration, Triton-x 100 20% w/v was added to give a final concentration of 1 mg triton per 3 mg protein. The mixture was homogenized for 20-30 seconds in a waring blender, then stirred for 25 minutes at 25 ^{o}C, to allow extraction of the lipophilic MAO enzyme. The mixture was centrifuged at 41,000 x g for 15 min. The supernatent was retained and the volume, protein concentration, and MAO activity determined. The quantities of each polymer to be used in the polymer partioning step were calculated based on the volume of the supernatent. For each 1 mL of supernatent, 0.110 g Dextran 250 (250,000 avg. m.w.), 0.120 g Ficol (400,000 avg. m.w.), and 0.080 g polyethylene glycol (6000 avg. m.w.) were measured and set aside. A volume of distilled water was calculated, for each 1 mL of supernatent, 0.019 mL distilled water was set aside. Finally, a volume of TEA 0.1 M buffer was calculated, which, when added to the supernatent, polymers, and water, calculated above, would give a final

concentration of 3 mg triton-x per mL. This volume of TEA 0.1 M was added to the polymers and water to give a homogenous mixture, then the polymer mixture was added with stirring to the supernatent. The mixture was stirred an additional 5 min at 25 ^{o}C. The mixture was then poured into centrifuge tubes fit for a swinging bucket rotor and allowed to sit at 25 ^{o}C for 1 hour to promote protein flocculation. The tubes were then centrifuged at 10,000 x g for 15 min at 20 ^{o}C. The polymer emulsion separated into 2 phases with a protein interface. The interfacial material was isolated by the careful decantation and aspiration of the polymer phases. The interfacial material was homogenized into cold TEA 0.1M buffer with a teflon/glass homogenizer and the protein and MAO activity determined. The protein concentration was adjusted to 10 mg/mL with cold TEA 0.1 M buffer. This mixture was centrifuged at 41,000 x g for 20 min . The supernatent was retained and stored on ice overnight in a refridgerator (4 ^{o}C).

The suspension was then centrifuged at 41,000 x g for 20 min. The supernatent was retained and its protein concentration and MAO B activity were determined. This supernatent was then centrifuged at 252,000 x g for 90 min. The pellet containing the MAO B was harvested into a buffer of 50% glycerol, 50 mM sodium phosphate, pH 7.2 (5 mL). The enzyme suspension was transferred to a brown vial and stored under argon at -20 ^{o}C. The final

preparation contained 330 units MAO B with a specific activity of 2.05 units/mg protein, 66 units per mL.

MAO A AND B SUBSTRATE ACTIVITY ASSAYS WITH 17 AND 18 AT pH 7.2

SPECTROPHOTOMETRIC ASSAYS

Spectrophotometric assays were performed using the Beckman DU-7 or DU-50 UV spectrometer equipped with Beckman Data-Capture and kinetics programs or with the Kontron Uvicon UV spectrometer. In the case of rapid oxidation rates, reaction rates were determined from the first 60 second period. In the case of very slow oxidation rates, reaction rates were determined from the first 5 or 30 minute period. The reaction was monitored by following the increase of absorbance at a wavelength appropriate to the product of oxidation; for benzylamine to benzaldehyde, 250 nm (molar extinction coeff. 12,000 L/mol·cm), for tetrahydropyridine oxidation to dihydropyridinium ions, 343 nm, (molar extinction coefficient 17,400 L/mol·cm). A typical assay mixture contained 5.0 mM candidate substrate in 50 mM sodium phosphate buffer, pH 7.2 at 30 ^{o}C. The reaction was initiated by addition of enzyme (0.02 units, 40 picomoles MAO B or 0.025 units, 200 picomoles MAO A). Assays were performed in triplicate. Kinetic constants (Km and Vmax) were determined using six concentrations of substrate (MPTP 0.25-5.0 mM). The inhibitory

characteristics of **17** and **18** with MAO B were determined using six concentrations of substrate (MPTP 0.25-5.0 mM) at each of three concentrations of inhibitor (**17** or **18**; 0.5-2.0 mM). For double reciprocal plots data was fitted to a line using standard linear regression.

AUTO-OXIDATION OF 18

The auto-oxidation of **18** was detected by following the increase in absorbance at 343 nm of a solution of **18**, 5.0 mM in sodium phosphate buffer 50 mM at pH 7.2, 30 ^{o}C. Under these conditions, oxidation occured at a rate of 132 nmoles per min while in the presence of MAO B (0.102 units), oxidation occured at a rate of 287 nmoles per min.

OXYGEN CONSUMPTION ASSAYS

The Clark-type oxygen electrode, fitted with a micro-stirring bar in a 1.5 mL incubation cell was equilibrated at 30 ^{o}C in sodium phosphate 50 mM, pH 7.2 for 4 hours prior to the start of assays. Calibration was accomplished by measuring the oxygen uptake due to excess dithionite. The oxygen content of buffer in the absence of dithionite, at 30 ^{o}C was assumed to be 0.234 micromole per mL. A typical substrate activity assay contained 1.0 mM or 5.0 mM candidate substrate in sodium phosphate 50 mM at pH 7.2, 30 ^{o}C. The reaction was initiated by addition of enzyme (MAO A, 0.082 units, 0.66

nmole; or MAO B, 0.56 units, 1.2 nmole). Reaction rates were determined from the initial 60 seconds for rapid oxidation, or 5 min for slow oxidation.

INTERACTION OF TETRAHYDROPYRIDINES 17 AND 18 WITH MAO B AT pH 9.0

Sodium phosphate buffer 50 mM at pH 9.0 was prepared and used for these studies. Enzyme activity was determined by monitoring the increase in absorbance at a wavelength appropriate to the product of oxidation; for benzylamine to benzaldehyde, 250 nm (molar extinction coeff. 12,000 L/mol·cm), for tetrahydropyridine oxidation to dihydropyridinium ions, 343 nm, (17,400 L/mol·cm). A typical assay mixture contained 3.0 mM benzylamine or 17 or 18. The reaction was initiated by addition of enzyme. Enzyme activity was first determined in sodium phosphate 50 mM at pH 7.2, (0.014 units enzyme or 28 picomoles enzyme), 30 ^{o}C, a turnover rate for benzylamine was determined to be 500 moles product formed per mole enzyme per minute. The turnover rate was then determined for benzylamine in sodium phosphate 50 mM at pH 9.0 at 30 ^{o}C, (0.014 units enzyme), and found to be 82% or 410 moles product formed per mole enzyme per minute. In order to maximize the chances for detection of enzyme catalyzed oxidation, the amount of enzyme added was increased for assays of 17 and 18 at pH 9. However, even using a higher amount of enzyme (0.043 units) in sodium phosphate

50 mM pH 9.0, the rates of reaction were undetectable for both **17** and **18**.

THE INTERACTION OF MAO B WITH **15**·ClO_4

The interaction of **15**·ClO_4 with MAO B was followed spectrophotometrically by monitoring the increase in absorbance at 284 nm, corresponding to formation of the expected 2 electron oxidation product **60**·ClO_4. The assay mixture consisted of **15**·ClO_4, 0.56 mM, in sodium phosphate buffer 50 mM, pH 7.2. The reaction was initiated by addition of MAO B (0.013 units, 26 picomoles). The duplicate assay mixtures were monitored every 30 seconds while incubating at 30 ^{o}C for 120 minutes. The results from the above incubations were compared to duplicate blanks consisting of **15**·ClO_4, 0.56 mM in buffer monitored under the same conditions.

DOPAMINERGIC NEUROTOXICITY OF A MIXTURE OF **17** AND **18** (85:15) IN THE C57 BLACK MOUSE, EXPERIMENTS PERFORMED IN COLLABORATION WITH KIM HOAG Ph.D AND ELLEN WU Ph.D

CHEMICALS AND REAGENTS

MPTP hydrochloride, 3,4-dihydroxy-benzylamine, ethanol and glycerol were purchased from Aldrich Chemical Co., Milwaukee, WI. The test sample of mixed **17** and **18** hydrochloride salts (85:15, reversed phase HPLC) was obtained from the disproportionation reaction described

above, mp 188.5-189.5 °C; Anal. ($C_{13}H_{17}N$.HCl) C, H, N. All other chemicals were of reagent grade or, in the case of solvents, HPLC grade. Aluminum oxide was activated by treatment in boiling 2 M HCl followed by washing with distilled water until the eluent reached a pH of 3.4. The treated aluminum oxide was dried at 100 °C for 12 hours then stored in a dessicator. HPLC analysis of catacholamines was performed using an Alltech C_{18} reversed-phase 5.0 um particle size column (4.6 mm x 25 cm). The column was protected with a hand packed pre-column containing Alltech C_{18} 10 um material. An electrochemical detector consisting of a glassy carbon electrode was referenced to a silver-silver chloride standard electrode. The mobile phase consisted of phosphoric acid 0.03 M, methanesulfonic acid 0.06 M, EDTA 0.05 M, adjusted to pH 3.5 with sodium hydroxide, at a flow rate of 1.5 mL/min.

PROCEDURES FOR BIOANALYSIS

Male C 57 black mice (7-9 months old) purchased from Jackson Laboratories, Bar Harbor, ME were treated intravenously with 5 mg/Kg MPTP HCl (n=6 animals) or mixed **17+18** (n=6 animals) dissolved in normal saline twice daily for three days. The animals were sacrificed 1 week after the last injection by carbon dioxide asphixiation and the brains removed rapidly and dissected on ice. The neostriata and cortex were frozen on dry ice

and weighed. The tissues of 2 animals were pooled for each determination to give n=3 data points for each drug treatment. Controls were obtained from untreated animals. The tissues were homogenized in cold perchloric acid 0.2 M. An internal standard, 3,4-dihydroxy-benzylamine (200 ng), (DHB), was added and the homogenate centrifuged at 15,000 x g for 5 min. One half of the supernatent was added to a tube containing activated aluminum oxide (20 mg), tris buffer 1.0 M pH 8.6 (1 mL) and the mixture was vortexed 5 sec. After a 15 min incubation to allow adsorption of catacholamines to the alumina, the alumina was allowed to settle and the supernatent removed. The alumina was washed with distilled water (1.5 mL), vortexed 10 sec and allowed to settle. The supernatent was removed from the alumina and catechols were eluted from the alumina with cold 0.1 M aqueous perchloric acid (1 mL). The catecholamine content of the supernatent was analysed by HPLC with electrochemical detection. Percent recovery was determined by comparison of internal standard peak heights with those in control samples spiked with a known amount of dopamine or norepinephrine. The average recovery of the internal standard, DHB, was 48%. The average recovery ratios for dopamine and norepinephrine were 1.29 and 0.995, respectively.

CYTOTOXICITY OF **17**, **18**, **15** AND **60** WITH FRESHLY ISOLATED RAT HEPATOCYTES, STUDIES PERFORMED IN COLLABORATION WITH DONATO Di MONTE Ph.D

Hepatocytes were isolated from male Sprague-Dawley rats (180-250 g) by incubation with collagenase according to the method of Moldeus et al.[58] Cell viability was assessed by trypan blue exclusion at various time points after incubation initiation. The number of viable cells in each incubation was estimated by counting a suspension that had been diluted 100 fold in of Krebs-Henseleit bufffer (pH 7.4) containing 0.5% trypan blue. Incubations were started immediately after isolation of the hepatocytes. A typical incubation contained 10 x 10^6 cells (1 x 10^6 per mL) and the candidate toxin (1.5 mM) in Krebs-Henseleit buffer (pH 7.4) containing 2% albumin. Incubations were carried out at 37 ^oC for 5 hours or until 100% cell kill was achieved.

ELECTRON MICROSCOPIC STUDY OF THE EFFECT OF TETRAHYDROPYRIDINES **17** AND **18** AND METABOLITE ANALOGS **15** AND **60**·ClO_4 ON DOPAMINERGIC TERMINALS IN THE RAT CAUDATE NUCLEUS, STUDIES PERFORMED IN COLLABORATION WITH CHARLES MESCHUL Ph.D

Female Wistar rats (200-220 g) were anesthetized with ketamine and placed in a Kopf rat stereotaxic holder. A solution of one of the following; **17**·HCl, **18**·HCl, **15**· ClO_4^-, **60**·ClO_4^- or MPP^+, 11.67 mM (5 uL, 58.4

nmoles), was injected into the right lateral ventricle, over a 5 minute period. The coordinates used for injection from Bregma were : 1.2 mm lateral, 0.5 mm posterior and 4.0 mm ventral. Two days following administration, the animals were perfused through the heart with 2.5% gluteraldehyde/ 3& parafomaldehyde in 0.1 M sodium Cacodylate buffer, pH 7.3, containing 0.03% $CaCl_2$. The caudate nucleus was removed in the area immediately surrounding the injections site. The ventricular lining of the caudate was preserved in order to determine the area most directly exposed to the drug. The tissue was washed in buffer, incubated in 1% osmium tetroxide/1.5% potassium ferricyanide for 1.5 hours. The tissue was then dehydrated with solutions of successively increasing ethanol content and embeded in plastic (Epon). Thin sections (800 angstroms) were cut on an RMC MT600 ultramicrotome and stained with 4% methanolic uranyl acetate and 0.075% aqueous lead citrate and veiwed on a Philips 301 Transmission electron microscope. Photographs were obtained at an initial magnification of 15,000 x and printed at a final magnification of 42,000 x.

INHIBITION OF MITOCHONDRIAL RESPIRATION, MITOCHONDRIAL MPP^+ UPTAKE, NADH OXIDASE INHIBITION, STUDIES PERFORMED IN COLLABORATION WITH RONA RAMSAY Ph.D

Rat liver mitochondria and electron transport particles (ETP) were prepared as previously published by Ramsay, et al.[102] [^{3}H] MPP^+ was purchased from New England Nuclear (Boston, Massachusetts, U.S.A.). NADH dehydrogenase (NADH oxidase was assayed using O_2 as the electron acceptor and monitoring either O_2 consumption (polarographic assay) or NADH disappearance (spectrophotometric assay) as reported by Singer.[103] Mitochondrial uptake of [^{3}H] MPP^+ was measured as before (Ramsay and Singer [104]). Mitochondrial respiration was measured polarographically in a 2.5 mL incubation cell with a Clark oxygen electrode at 25 oC. The mitochondria (2 mg protein/mL) were incubated in a final volume of 2 mL of respiration medium (90 mM KCl, 20 mM Tris HCl, 10 mM K phosphate, and 5 mM $MgCl_2$, pH 7.4 at 25oC, containing 5 mM glutamate and 2.5 mM malate, with or without inhibitor for 5 minutes prior to the addition of ADP (0.26 mM).

ASSESSMENT OF IN VIVO DOPAMINERGIC NEUROTOXICITY OF PYRIDINIUM COMPOUNDS WITH IN VIVO BRAIN DIALYSIS IN THE RAT

Dopamine hydrochloride (DA), dihydroxyphenylacetic acid (DOPAC), homovanillic acid (HVA), 5-hydroxyindoleacetic acid (5-HIAA), and chloral hydrate were purchased from the Sigma Chemical Company (St. Louis, MO). Heptanesulfonic acid was purchased from Eastman Kodak (Rochester, NY). All other chemicals were of reagent grade, or in the case of solvents, HPLC grade.

In vivo brain dialysis of rat striatum was performed as previously described (Westerink and Tuinte [105], Rollema et al., [106]). Male Sprague-Dawly rats (Bantin-Kingman, 220-240 g) were anesthetized with chloral hydrate (450 mg/kg, i.p.) and placed in a stereotaxic frame. A bilateral cannula with an U-shaped dialysis membrane was inserted into both striata and the rats were allowed to recover. Experiments were performed one day after surgery. The striatum was perfused with a Ringer solution (147 mM NaCl, 2.3 mM $CaCl_2$, 4 mM KCl adjusted to pH 7.0 with 0.05 N NaOH) at a flow rate of 3.5 uL/minute until a stable output of DA and the metabolites was obtained. Typically, 5-8 samples were collected to measure basal output. Drug solutions (10 mM) dissolved in Ringer were administered intrastriatally via the dialysis tube for 15 or 60 minutes; perfusion was then

continued using only Ringer solution for the remainder of the sample collection period. One day after drug treatment the basal output was measured (while perfusing with Ringer solution), followed by a 15 minute perfusion with 10 mM MPP+. The 15 minute perfusion with MPP^+ allowed assessment of the toxicity of the previous days treatment with test compounds.

Dialysate concentrations of DA and its metabolites DOPAC and HVA and of the 5-HT metabolite, 5-HIAA were measured by on-line HPLC, as described previously (Westerink and Tuinte [105]) using a BAS LC-3 Amperometric detector (set at +650 mV), a Beckman Ultrasphere 5 C18 column (250 x 4.6 mm) and an Altex 110A pump which delivered the mobile phase (2 mM heptanesulfonate and 10% methanol in 0.05 sodium acetate buffer, pH 3.7) at a flow rate of 1.0 mL/min. Dialysate amples were collected on-line in a 50 uL loop of a Rheodyne valve and injected every 20 min. Efflux of DA and the metabolites was calculated as fmoles/min, while effects of drugs were also given as percentages of basal release.

MOUSE NEOSTRIATAL SYNAPTOSOMAL UPTAKE OF [^{3}H] DOPAMINE AND [^{3}H] MPP^+

[^{3}H] Dopamine (15 Ci/mmol) was purchased from Amersham (Arlington Heights, IL); [^{3}H] MPP^+ was obtained from New England Nuclear (Boston, MA). In preliminary experiments [^{3}H] MPP^+ which had been purified by

chromatography on alumina TLC plates was used. Mazindol was obtained from Dr. C.E. Eden of Sandoz Pharmaceutical Company, (East Hanover, New Jersey).

Male C57Bl mice (Bantin-Kingman, 25-30 g) were anesthetized with carbon dioxide, then sacrificed by cervical dislocation and the brains rapidly removed. The neostriata were immediately dissected on ice according to the method of Glowinski and Iversen.[107] The striata from 25-36 mice were combined in sets of 5-6 and each set homogenized in 2 mL cold 0.32 M sucrose solution (pH 7.4 with a motor driven teflon pestle-glass homogenizer (0.15 mm clearance). Combined striatal homogenates were centrifuged at 4,000 x g for 8 minutes in a refrigerated Eppendorf microcentrifuge (Model 5415) at 4 ^{o}C. The supernatent was decanted and centrifuged at 14,000 x g for 22 minutes. The resulting pellet was washed by homogenization with 10 mL of 0.32 M sucrose solution (pH 7.4) followed by centrifugation at 14,000 x g for 22 minutes. The pellet thus obtained was suspended in 15 volumes (w/v) of a buffered medium ("Physiological Tris") containing 50 mM Tris-HCl (pH 7.4), 125 mM NaCl, 5 mM KCl, 1 mM $CaCl_2$, 1 mM $MgCl_2$, and 10 mM glucose. Protein was measured in each of the synaptosomal preparations by previously reported methods (Lowry et al.[108]) prior to the preparation of the uptake assay tubes.

A 1 mL incubation mixture containing radiolabeled compound (10 nM [^{3}H] dopamine or 1 nM [^{3}H] MPP^+) and

uptake buffer (0.2% ascorbic acid and 50 uM pargyline in "Physiological Tris") was preincubated in test tubes with or without the test compound at 37 ^{o}C for 5 minutes. The uptake of radiolabled ligand was initiated by the addition of freshly prepared synaptosomes (0.3 mg protein/ mL) followed by incubation of the mixture with shaking at 37 ^{o}C for 5 minutes. The uptake was terminated by placing the test tubes in ice water and adding 4 mL of ice-cold uptake buffer to each tube. Immediately after the addition, each diluted incubate was filtered through a presoaked fiberglass filter (Whatman GF/B 2.5 cm). After two consecutive 2.5 mL washes with ice-cold uptake buffer, the filters were placed into scintillation vials with 10 mL of Ecolite scintillation fluid (West Chem). Each vial was vigourously vortexed for 15 seconds to aid in dispersal of the bound radiolabled compounds. The radioactivity which had been collected on the filters was then measured by liquid scintillation spectrometry (Beckman model LS-7800) at a 40% average counting efficiency. "Total control" samples were incubated under the conditions above give the total accumulated dpm. To correct for passive diffusion and adsorption to membranes and filters, "control non-specific
binding" samples were incubated in the presence of 10 uM Mazindol, a specific dopamine uptake inhibitor. "Control active uptake" was calculated by subtracting from the

"total control" dpm the number of dpm accumulated in the presence of 10 uM Mazindol ("control non-specific binding") and was expressed as nmole per g protein per minute.

The kinetic parameters (Km and Vmax) of uptake were calculated from substrate saturation data using at least 5 concentrations (triplicate samples) of radiolabeled substrate. Separate incubations containing 10 uM mazindol were also run at each radioactive substrate concentration to determine the level of "non-specific binding" since this parameter increases linearly with the concentration of radioactive ligand.

In experiments in which IC_{50} values were to be calculated, at least four concentrations of test compound were chosen based on preliminary experiments to give between a 15% and 90% inhibition of uptake relative to controls. Incubations at each inhibitor concentration were run in triplicate in each of two separate experiments to give a total of n = 6 data points for a given inhibitor concentration. A set of controls ("total control binding" and "control non-specific binding") were run between each set of inhibitor concentrations. The values for "total control binding" and "control non-specific binding" (n = 15-18) obtained each day, were averaged for calculation of the day's results. The "control non-specific binding" was assumed to be independent of inhibitor concentrations so that uptake in

the presence of a given inhibitor could be calculated by subtracting the "control non-specific binding" in dpm (calculated for that particular experiment) from the total dpm accumulated in the presence of the inhibitor. Percent control values were calculated for each inhibitor concentration. These values were then plotted versus the log of the concentration of the inhibitor. The data was then fitted to a line by standard linear regression and IC_{50} values were calculated. The final average IC_{50} values and SEM values reported are from the averages of six independent IC_{50} values, each calculated from four inhibitor concentrations.

PURIFICATION OF [3H] MPP+ ON ALUMINA TLC PLATES

An initial assessment of the purity of a one year old lot of [^{3}H] MPP^+ (85 Ci/mmol, 1 mCi/mL, New England Nuclear) was made using HPLC with radiochemical detection. Using an Ultrasil-cx (10 um x 4.5 mm x 250 mm) cation exchange column with a mobile phase consisting of acetonitrile 10%/ buffer 90% (0.1 M acetic acid, 0.05 M triethylamine, adjusted to pH 2.3 with formic acid), at a flow rate of 2 mL per minute, a sample of [^{3}H] MPP^+ (ca. 2 nCi) gave 2 peaks. The major peak with a retention time of 6.5 minutes corresponded to 90% of the eluting radioactivity and was similar in retention time to unlabled MPP^+ (detected by UV detection). The minor peak which eluted more rapidly under these reversed-phase

HPLC conditions (retention time 2.6 minutes, 6% of the eluting radioactivity) was believed to represent a more polar contaminant. Using a TLC solvent system (acetonitrile/dichloromethane, 1:1) previously developed for detection of substituted pyridinium salts, the mobility of unlabeled MPP^+ on silica and alumina plates was compared. On silica plates, synthetic MPP^+ gave a large spot at Rf. 0.3 and a small highly flourescent spot at the origin. On alumina plates MPP^+ gave a single elongated spot extending from Rf. 0.42 to 0.22. Due to the ease with which the alumina chromatographic matrix could be removed from its glass support, alumina plates were chosen for the purification of [^{3}H] MPP^+.

The stock solution of [^{3}H] MPP^+ (2 uL, 2uCi, 4.4 x 10^6 dpm) was spotted on an alumina TLC plate (2.5 cm x 10 cm). The plate was developed with acetonitrile/dichloromethane (1:1) and solvent evaporated. The plate was then devided into 1 cm bands starting from the origin and running to the top of the plate. Each band was scraped into a labeled scintilation vial (20 mL) and eluted with acetonitrile (2 x 2 mL). An aliquot was removed from each eluent (0.5 mL) and mixed with scintillation fluid for counting (4.5 mL, ecolite).

Table E-1. Radioactivity in fractions obtained from chromatographic purification of [^{3}H] MPP^+

Fraction	dpm	percent of applied dpm
eluent, band 1	30,616	0.7%
eluent, band 2	181,240	4.1%
eluent, band 3	155,792	3.5%
eluent, band 4	3,544	0.08%
eluent, band 5	2,848	0.06%
eluent, band 6	1,912	0.04%
eluent, band 7	2,112	0.05%
eluent, band 8	1,408	0.03%

The amount of dpm listed for each fraction is the product of the result of scintillation count found for 0.5 mL aliquot multiplied by 8 since each eluent contained 4 mL.

The total radioactivity recovered by elution of the alumina bands was about 9% of the applied radioactivity. Most of the activity was concentrated in bands 2 and 3. HPLC with radiochemical detection idicated a single peak for yeach of fractions 2 and 3 with retention times of 7.4 minutes and 7.5 minutes, respectively. Again, these retention times were similar to those obtained with HPLC of synthetic MPP^+ using UV detection. The solvent was evaporated from fractions 2 and 3 under a nitrogen stream and the residues were dissolved in deionized water for use in the synaptosomal uptake studies. The final yield of purified MPP^+ (337,032 dpm, 0.153 uCi) was assumed to be the same specific activity as originally obtained from the manufacturer since no dilution with unlabeled material had been made.

REFERENCES

1. Marsden, C.D., Parkes, J.D. (1977), Success and problems of long-term levodopa therapy in Parkinson's disease. Lancet **1**, 345-349.

2. Langston, J.W. (1986) "MPTP-induced Parkinsonisma: How good a model is it?", in Recent developements in Parkinson's disease, (Fahn, S., Marsden, C.D., Jenner, P., Teychenne, P. eds) pp. 119-126, Raven Press, New York.

3. Burns, R.S., Chiueh, C.C., Markey, S.P., Ebert, M.H., Jacobowitz, D.M., and Kopin, I.J., (1983) A primate model of parkinsonism: selective destruction of dopaminergic neurons in the pars compacta of the substantia nigra by N-methyl-phenyl-1,2,3,6-tetrahydropyridine. Proc. Natl. Acad. Sci. U.S.A., **80**: 4546-4550.

4. Chiba, K, Trevor, A., and Castagnoli, N. Jr. (1984) Metabolism of the neurotoxic tertiary amine, MPTP, by brain monoamine oxidase. Biochem. Biophys. Res. Commun. **120**, 574-578.

5. Salach, J.I., Singer, T.P.,Castagnoli, N.Jr., and Trevor, A. (1984) Oxidation of the neurotoxic amine 1-methyl-4-phenyl-1,2,3,6-tetrahydropyridine (MPTP) by monoamine oxidases A and B and suicide inactivation of the enzymes by MPTP. Biochem. Biophys. Res. Commun. **125**, 831-835

6. Heikkila, R.E., Manzino, L. Cabbat. F.S., and Duvoisin, R.C. (1984) Protection against the dopaminergic neurotoxicity of 1-methyl-4-phenyl-1,2,5,6-tetrahydropyridine by monoamine oxidase inhibitors.Nature, **311**, 467-469

7. Langston, J.W., Irwin, I., Langston, E.B., and Forno, L.S., (1984) Pargyline prevents MPTP- induce parkinsonism in primates. Science. **225**. 1480-1482

8. Markey, S.P., Johannessen, J.N., Chiueh, C.C., Burns, R.S, and Herkenham, M.A., (1984) Intra-neuronal generation of a pyridinium metabolite may cause drug-induced parkinsonism. Nature, **311**, 464-467

9. Chiba, K., Peterson, L.A., Castagnoli, K.P., Trevor, A.J., and Castagnoli, N. Jr.,(1985) Studies on the molecular mechanism of bioactivation of the selective nigrostriatal toxin 1-methyl-4-phenyl-1,2,3,6-tetrahydropyridine. Drug Met. Disp. **13**, 343-347

10. Weissman, J., Trevor, A., Chiba, K., Peterson, L.A., Caldera, P., Castagnoli, N.Jr., and Baillie, T. (1985) Metabolism of the nigrostriatal toxin 1-methyl-4-phenyl-1,2,3,6-tetrahydropyridine by liver homogenate fractions. J. Med. Chem. **28**, 997-1001

11. Cashman, J.R. and Ziegler, D.M. (1986) Contribution of N-oxygenation to the metabolism of MPTP (1-methyl-4-phenyl-1,2,3,6-tetrahydropyridine) by various liver preparations. Mol. Pharmacol. **29**. 163-167

12. Caldera, P.S., Salach, J.I., Castagnoli, N.Jr., Trevor, A.J., and Singer, T.P., (1986) "Studies on the chemical and biochemical behavior of $MPDP^+$", in MPTP: a neurotoxin producing a parkinsonian syndrome (Markey, S.P., Castagnoli, N.Jr., Trevor, A.J., and Kopin, I.J., eds.) pp. 551-555. Academic Press, New York.

13. Ekstrom, G., DiMonte, D. Sandy, M.S., and Smith, M.T., (1987) Comparitive toxicity and antioxidant activity of 1-methyl-4-phenyl-1,2,3,6-tetrahydropyridine and its monoamine oxidase B-generated metabolites in isolated hepatocytes and liver microsomes. Arch Biochem. Biophys. **255**, 14-18.

14. Jonsson, G., Sundstrom, E., Nwanze, E., Hallman, H., and Luthman, J. (1986) in MPTP: A neurotoxin producing a parkinsonian syndrom (Markey, S.P., Castagnoli, N.Jr., Trevor, A.J., and Kopin, I.J., eds.) pp 253-272, Academic Press, New York

15. Ziering, A., Berger, L., Heineman, S.D., Lee, J., (1947) Piperidine derivatives, Part III. 4-arylpiperidines. J. Org. Chem. **12**, 894-

16. Janssen, P.A.J., U.S. patent 3030,372 (1962); Chem. Abstr., **59**, 2780 (1963)

16a. Langston, J.W., Ballard, P.A., (1983) Parkinson's disease in a chemist working with 1-methyl-4-phenyl-1,2,5,6-tetrahydropyridine N. Eng. J. Med. **309**, 310

17. Schmidle, C.J, and Mansfield, R.C., (1955) The aminomethylation of olefins. II. A new synthesis of 1-alkyl-4-piperidinols. J. Amer. Chem. Soc., **77**, 5698-5701

18. Walker,W.H, Kearney,E.B., Seng, R.L., and Singer, T.P., (1971) **TITLE** Eur. J. Biochem. **24**, 328-

19. Yu, P.H., (1981) Studies on the pargyline binding site of different types of monoamine oxidase. Can. J. Biochem. **59**, 30-36

20. Yasunobu, K.T., Watanabe, K., and Zeiden, H., (1979) "Monoamine oxidase: some new findings." in Monoamine oxidase, structure, function and altered functions, (Singer, T.P., Von Korff, R.W., and Murphy, D.L., eds.) pp.251-253, Academic Press, New York.

21. Cawthon, R.M., Pintar, J.E., Haseltine, F.P., and Breakefield, X.O., (1981), Differences in the structure of A and B forms of human monoamine oxidase J. Neurochem. **37**, 363-372

22. Silverman, R.B., Hoffman, S.J., Catus, W.B., (1980) A mechanism for mitochondrial monoamine oxidase catalyzed amine oxidation. J. Am. Chem. Soc. **102**, 7126-7128.

23. Heikkila, R.E., Hess, A., Duvoisin, R.C., (1985) Dopaminergic neurotoxicity of 1-methyl-4-phenyl-1,2,5,6-tetrahydropyridine (MPTP) in the mouse: relationships between monoamine oxidase, MPTP metabolism and neurotoxicity. Life Sci. **36**, 231-236

24. Gessner, W.P., Brossi, A., Fritz, R.R., Patel, N.T., and Abell, C.W., (1986) "Monoamine oxidase B inhibitory effects of MPTP analogs", in MPTP: a neurotoxin producing a parkinsonian syndrome (Markey, S.P., Castagnoli, N., Trevor, A.J., Kopin I.J., eds.) pp. 557-561, Academic Press, New York.

25. Silverman, R.B., (1984) Effect of alpha-methylation on inactivation of monoamine oxidase by N-cyclopropylamine. Biochem.**23**, 5206-5213

26. Lyle, R.E., Nelson, D.A., and Anderson, P.S., (1962) The mechanism of the reduction of pyridinium ions with sodium borohydride. Tet. Lett. 553-557.

27. Pirkle, W.H., Finn, J.M., Schreiner, J.L., and Hamper, B.C., (1981) A Widely useful chiral stationary phase for the high-performance liquid chromatography separation of enantiomers. J. Am. Chem. Soc. **103**, 3964-3966

28. Snyder, L.R., (1968) Principles of adsorption chromatography, chapter 7, Marcel Dekker, New York

Chromatography, (1967) E. Heffman, Ed., 2nd edition, pp. 54-57 Rheinhold, New York

29. Gessner, W., and Brossi, A., (1985) Reduction of phenyl-substituted pyridinium methiodides with sodium borohydride. Formation of amine-borane complexes in water. Synth. Commun. **15**, 911-916

30. Thiessen, L.M., Lepoivre, J.A., Alderweireldt, F.C., (1974) The preparation of 1,2,4-tri-alkyl or aryl substituted 1,2-dihydropyridines by grignard reagents. Tet. Lett, 59-62

31. Feliz, M., Bosch, J., Mauleon, D., Amat, M., and Domingo, A., (1982) Synthetic applications of 2-cyano-1,2,3,6-tetrahydropyridines. Improved synthesis of the fundamental tetracyclic framework of Dascycarpidone. J.Org. Chem. **47**, 2435-2440

32. Fischer, H., Summers, L.A., (1980) Synthesis, polarography and herbicidal activity of quaternary salts of 2-(4-pyridyl)-1,3,5-triazines, 5-(4-pyridyl)pyrimidines, 2-(4-pyridyl)pyrimidine and related compounds. Heterocyclic Chem. **17**, 333-336

Schwartzbeck, R.A., (1976) Proc. Br. Weed Control Conf.**12**, Vol. 2, 852

33. Abraham, R.J. and Loftus, P., (1981) Proton and carbon-13 NMR spectroscopy, an integrated approach. pp. 37-38, Heyden, Philadephia

34. Fry, E.M. (1963) Stereospecific tautaumerism in a 1,2-dihydropyridine. A beta-benzomorphan synthesis. J. Org. Chem. **28**, 1869-1874

35. Gessner, W., Brossi, A., Shen, R., Fritz, R., and Abell, C.W., (1984) Conversion of 1-methyl-4-phenyl-1,2,3,6-tetrahydropyridine and its 5-methyl analog into pyridinium salts. Helv. Chim. Acta **67**, 2038-2042

36. Salach, J.I. (1979) Monoamine oxidase from beef liver mitochondria: simplified isolation procedure, properties, and dtermination of its cysteinyl-flavin content. Arch. Biochem. Biophys. **192**, 128-137

37. Singer, T.P., Salach, J.I., Castagnoli, N. Jr., and Trevor, A. (1986) "Processing of MPTP to toxic metabolites by monoamine oxidases" in MPTP: a neurotoxin producing a parkinsonian syndrome.pp. 235-251, Academic Press, New York

38. Langston, J.W., Irwin,I., Langston, E.B., and Forno, L.S., (1984) Pargyline prevents MPTP-induced Parkinsonism in primates. Science **225**, 1480-1482

39. Burns,R.S., Chiueh, C.C., Markey, S.P., Ebert,M.H., Jacobowitz, D.M., and Kopin, I.J., (1983) A primate model of parkinspnism: selective destruction of dopaminergic neurons in the pars compacta of the substantia nigra by N-methyl-4-phenyl-1,2,3,6-tetrahydopyridine Proc. Natl. Acad. Sci. **80**, 4546-4550.

40. Parisi, J.E., and Burns, R.S., (1986) The neuropathology of MPTP-induced parkinsonism in man and experimental animals in MPTP: a neurotoxin producing a parkinsonian syndrome. pp. 141-148, Academic Press, New York

41. Lent, C.M. (1986) "MPTP depletes neuronal monamines and impairs the behavior of the medicinal leech", in MPTP: a neurotoxin producing a parkinsonian syndrome. pp.105-118, Academic Press, New York

42. Carvey, P.M., Kao, L.C., and Klawans, H.L., (1986) "Permanent postural effects of MPTP in the guinea pig", in MPTP: a neurotoxin producing a parkinsonian syndrome. pp. 407-412, Academic Press, New York

43. Chiueh, C.C., Markey, S.P., Burns, R.S., Johanessen, J.n., Pert, A., and Kopin, I.J., (1984) Neurochemical and behavioral effects of systemic and intranigal administration of N-methyl-4-phenyl-1,2,3,6-tetrahydropyridine in the rat. Eur. J. Pharmacol. **100**, 189-194.

44. Boyce, S., Kelly, E., Reavill, C., Jenner, P., and Marsden, C.D., (1984) Repeated administration of N-methyl-4-phenyl-1,2,3,6-tetrahydropyridine to rats is not toxic to straital dopamine neurons. Biochem. Pharmac. **23**, 1747-1752.

45. Gornal, Bardawill, and David (1949), Determination of serum proteins by means of the biuret reaction.J.Biol. Chem. **177**, 751

46. Tabor, C.W., Tabor, H., and Rosenthal, S.M., (1954) Purification of amine oxidase from beef plasma. J.Biol.Chem. **208**, 645

47. Kearney, E.B., Salach, J.I., Walker, W.H., Seng, R.L., Kenney, W., Zeszotek, E., and Singer, T.P., (1971) The covalently bound flavin of hepatic monoamine oxidase. European J. Biochem. **24**, 321

48. Heikkila, R.E., Hess, A., and Duvoisin, R.C., (1984) Dopaminergic neurotoxicity of 1-methyl-4-phenyl-1,2,5,6-tetrahydropyridine in mice. Science, **224**, 1451-1453

49. Heikkila, R.E., Hess, A., and Duvoisin, R.C., (1985) Dopaminergic neurotoxicity of 1-methyl-4-phenyl-1,2,5,6-tetrahydropyridine (MPTP) in the mouse: Relationships between monoamine oxidase, MPTP metabolism and neurotoxicity. Life Sci. **36**, 231-236

50. Hallman, H., Olson, L., and Jonsson, G., (1984) Neurotoxicity of the meperidine analogue N-methyl-4-phenyl-1,2,3,6-tetrahydropyridine on brain catecholamine neurons in the mouse. Eur. J. Pharmacol. **97**, 133-136

51. Riachi, N.J., Harik, S.I., Kalaria, R.N., and Sayer, L.M.,(1988) On the mechanisms underlying 1-methyl-4-phenyl-1,2,3,6-tetrahydropyridine neurotoxicity. II. Susceptibility among mammalian species correlates with the toxin's metabolic patterns in brain microvessels and liver. J.Pharm and Exp. Therap. **244**, 443-448

52. Ekstrom, G., Di Monte, D., Sandy, M.S., and Smith, M.T., (1987) Comparitive toxicity and antioxidant activity of 1-methyl-4-phenyl-1,2,3,6-tetrahydropyridine and its monoamine oxidase B-generated metabolites in isolated hepatocytes and liver microsomes. Arch. Biochem. Biophys. **255**, 14-18

53. Groutas, W.C., Essawi, M., and Portoghese, P.S., (1980) Alpha-cyanation of tertiary amines. Synth. Commun. 10, 495-502

54. Casey, A.F. and McEarlane, K.M.J., (1972) Diastereomeric esters of 1,2-dimethyl-4-phenylpiperidin-4-ol and related compounds. J. Chem. Soc. Perkin I, 726-731

55. Sayre, L.M., Arora, P.K., Feke, S.C., and Urbach, F.L. (1986) Mechanism of induction of Parkinson's disease by 1-methyl-4-phenyl-1,2,3,6-tetrahydropyridine (MPTP). Chemical and electrochemical characterization of a geminal-dimethyl-blocked analogue of a postulated toxic metabolite. J. Am. Chem. Soc. **108**, 2464-2466

56. Sayre, L.M., Arora, P.K., Iacofano, L.A., and Harik, S.I. (1986) Comparitive toxicity of MPTP, MPP^+ and 3,3-dimethyl-$MPDP^+$ to dopaminergic neurons of the rat substantia nigra. Euro. J. Pharmacol. **124**, 171-174

57. Castagnoli, N.Jr., Chiba, K., and Trevor, A.J., (1985) Potential bioactivation pathways for the neurotoxin 1-methyl-4-phenyl-1,2,3,6-tetrahydropyridine (MPTP). Life. Sci. **36**, 225-230

58. Moldeus, P., Hogborg, J., and Orrenius, S., (1978) Isolation and use of liver cells. Methods. Enzymol., **52**, 60-71

59. Melamed, E., Rosenthal, J., Cohen, O., Globus, M., and Ussan, A., (1985) Dopamine but not norepinephrin or serotonin uptake inhibitors protect mice against neurotoxicity of MPTP. Eur. J. Pharmacol. **116**, 179-181.

60. Pileblad, E., and Carlsson, A., (1985) Catecholamine -uptake inhibitors prevent the neurotoxicity of 1-methyl-4-phenyl-1,2,3,6-tetrahydropyridine (MPTP) in mouse brain. Neuropharmacol. **24**, 689-692

61. Singer, T.P., Salach, J.I., Castagnoli, N. Jr., and Trevor, A.J., (1986) Interactions of the neurotoxic amine 1-methyl-4-phenyl-1,2,3,6-tetrahydropyridine (MPTP) with monoamine oxidases. Biochem. J. **235**, 785-789

62. Nicklas, W.J., Vyas, I., and Heikkila, R.E., (1985) Inhibition of NADH-linked oxidation in brain mitochondria by 1-methyl-4-phenyl-pyridine, a metabolite of the neurotoxin 1-methyl-4-phenyl-1,2,3,6-tetrahydropyridine. Life Sci. **36**,2503-2508

63. Jewell, S.A., Bellomo, G., Thor,H., Orrenium, S., and Smith, M.T., (1982) Bleb formation in hepatocytes during drug metabolism is caused by disturbances in thiol and calcium homeostasis. Sci,. **217**, 1257-1259

64. Ramsay, R.R., Salach, J.I., and Singer, T.P., (1986) Uptake of the neurotoxin 1-methyl-4-phenyl-pyridine (MPP+) by mitochondria and its relation to the inhibition of the mitochondrial oxidation of NAD+-liked substrates by MPP+. Biochem. Biophys. Res. Commun. **134**, 743-748

65. Di Monte, D. Jewell, S.A., Ekstrom, G., Sandy, M.S., and Smith, M.T., (1986) 1-methyl-4-phenyl-1,2,3,6-tetrahydropyridine (MPTP) and 1-methyl-4-phenyl-pyridine (MPP^+) cause rapid ATP depletion in isolated hepatocytes. Biochem. Biophys. Res. Commun. **137**, 310-315

66. Ramsay, R.R., McKeown, K.A., Johnson, E.A., Booth, R.G., and Singer, T.P., (1987) Inhibition of NADH oxidation by pyridine derivatives Biochem. Biophys. Res. Commun. **146**. 53-60

67. Kosower, E.M., and Klinedienst, P.E. (1956) Additions to pyridinium ring. II. Charge-transfer complexes as intermediates J.Am.Chem.Soc. **78**, 3493-3495

68. Kosower, E.M., and Skorcz. J.A., (1960) Pyridinium complexes. III. Charge-transfer bands of poly alkyl pyridinium Iodides. J.Am.Chem.Soc. **82**, 2195-2198

69. Tomilenko, E.I., (1976) Kinetics of the reaction of quaternary salts of pyridine with potassium ferricyanide in an aqueous alkaline solution. Zh. Vses. Khim. O-Va. **21**,462-464

70. Abramovitch, R.A. and Adams, K.A.H. (1961) Tryptamines, carbolines and related compounds. Part IX. The cyclization of some nitro and azido-phenylpyridines. Pyrido[1,2-b] indazole. Can. J. Chem. **39**,2516-2528.

71. Youngster. S., Ramsay, R.R. personal communication

72. Ramsay, R.R., and Singer, T.P. (1986) Energy-dependent uptake of N-methyl-4-phenylpyridinium, the neurotoxic metabolite of 1-methyl-4-phenyl-1,2,3,6-tetrahydropyridine by mitochondria. J. Biol. Chem. **261**, 7585-7585

73. Rollema, H., Damsma, G., Horn, A.S., DeVries, H.B., and Westerink, B.H.C. (1986) Brains dialysis in concsious rats reveals an instantaneous massive release of striatal dopamine in response of MPP^+. Eur. J. Pharmacol. **126**, 345-346

74. Westlund, K.N., Denney, R.M., Kochersperger, L.M., Rose, R.M. and Abell, C.W. (1985) Distinct monoamine oxidase A and B populations in primate brain. Science **230**, 181-183

75. Javitch, J.A. and Snyder, S.H., (1985) Uptake of MPP^+ by dopamine neurons explains selectivity of parkinsonism-inducing neurotoxin MPTP. Eur. J. Pharmacol. **106**, 455-456

76. Javitch, J.A., D'Amato, R.J., Strittmatter, S.M., and Snyder, S.H. (1985) Parkinsonism-inducing neurotoxin, N-methyl-4-phenyl-1,2,3,6-tetrahydropyridine: Uptake of the metabolite N-methyl-4-phenylpyridine by dopamine neurons explains selective toxicity. Proc. Natl. Acad. Sci. USA, **82**, 2173-2177

77. Horn. A.S. (1979) "Characteristics of dopamine uptake" in The neurobiology of dopamine (A.S. Horn, J. Kur and B.H.C. Westerink eds.) pp 217-235 Academic Press, San Francisco.

78. Chiba, K., Trevor, A.J., and Castagnoli, N. Jr., (1985) Active uptake of MPP^+, a metabolite of MPTP by brain synaptosomes. Biochem. Biophys. Res. Commun. **128**, 1228-1232

79. Heikkila, R.E., Youngster, S.K., Manzino, L., Cabbat, F.S., and Duvoisin, R.C., (1985) Effects of 1-methyl-4-phenyl-1,2,5,6-tetrahydropyridine and related compounds on the uptake of [^{3}H] 3,4-dihydroxyphenylethylamine and [^{3}H] 5-hydroxytryptamine in neostriatal synaptosomal preparations. J. Neurochem. **44**, 310-313.

80. Gessner, W., Brossi, A., Shen, R., and Abell, C.W. (1985) Further insight into the mode of action of the neurotoxin 1-methyl-4-phenyl-1,2,3,6-tetrahydropyridine (MPTP) Fed. Exp. Biol. Sci. Letters. **183**, 345-348

81. Shen, R.S., Abell, C.W., and Brossi, A., (1985) Serotonergic conversion of MPTP and dopaminergic accumulation of MPP^+ Fed. Exp. Biol. Sci. Letters., **189**, 225-229

82. Gray, E.G. and Whittaker, V.P. (1962) The isolation of nerver endings from brain: an electron-microscopic study of cell fragments derived by homogenization and centrifugation. J.Anat. London, **96**, 79-88.

83. Coyle, J.T. and Snyder, S.H., (1969) Catecholamine uptake by synaptosomes in homogenates of rat brain: stereospecificity in different areas. J.Pharmacol. and Exp. Therap. **170**, 221-231

84. Holz, R.W., and Coyle, J.T. (1974) The effects of various salts, temperature and the alkaloids veratridine and batrachotoxin on the upatke of [^{3}H] dopamine into synaptosomes from rat striatum. Molec. Pharmacol. **10**, 746-748.

85. Iversen, L.L. (1975). In Handbook of Psychopharmacology, **vol 3** (Iversen, L.L., Iversen, S., and Snyder, S. eds) pp 381-442, Plenum Press, New York

86. Ross, S.B. and Renyi, A.L. (1967) Inhibtion of the uptake of tritiated catecholamines by antidepressant and related agents Eur. J. Pharmacol. **2**, 181-186

87. Hamberger, B. (1967) Reserpine-resistant uptake of catecholamines in isolated tissues of the rat. Acta Physiol. Scand. **71**, Suppl. 295

88. Jonason, J. and Rutledge, C.O. (1968) Metabolism of dapamine and noradrenaline in rabbit caudate nucleus <u>in vitro</u> Acta. Physiol. Scand. **73**, 411-417

89. Sugrue, M.F. and Mireylees, S.E. (1978) Effects of mazindol on rat brain synaptosomal monoamine uptake. Biochem. Pharmacol. **27**, 1843-1847

90. Koe, B.K. (1976) Molecular geometry of inhibitors of the uptake of catecholamines and serotonin in synaptosomal preparations of rat brain. J. Pharmacol. Exp. Therap. **199**, 649-661.

91. Sershen, H., Debler, E.A., and Lajtha, A., (1987) Effect of ascorbic acid on the synaptosomal uptake of [^{3}H] MPP^{+}, [^{3}H] Dopamine, and [^{14}C] GABA. J. Neurosci. Res. **17**, 298-301

92. Horn, A.S. and Snyder, S.H. (1972) Steric requirements for catecholamine uptake by rat brain synaptosomes: Studies with rigid analogs of amphetamine. J.Pharmacol. Exp. Therap. **180**, 523-530.

93. Miller, D.D., Fowble, J. and Patil, P.N. (1973) Inhibition of catecholamine uptake by conformationally restricted phenylethanolamine derivatives. J. Med. Chem. **16**, 177-737

95. Segonzac, A., Shoemaker, H. and Langer, S.Z. (1978) Temperature dependence of drug interactions with the platelet 5-hydroxytryptamine transporter: A clue to the imipramine selectivity paradox. J. Neurochem. **48**, 331-339

96. Segel, I.H. (1975)" Apparent competitive inhibition by carrier dilution" in Enzyme kinetics. Behavior and analysis of rapid equilibrium and steady state enzyme systems. pp 118-121. Wiley Interscience, New York

97. Lindsay, R.D. and Cheldelin, V.H. (1950) Pantothenic Acid studies. VII. N-methyl pantothenic acid. J. Am. Chem. Soc. **72**, 828-830.

98. Kosower, E.M. and Klinedinst. B.E. Jr. (1956) Additions to pyridinium ring. II. Charge-transfer complexes as intermediates. J. Am. Chem. Soc. **78**, 3493-3495

99. Kosower, E.M. and Skorcz, J.A. (1960) Pyridinium complexes. III. Charge-transfer bands of poly alkyl pyridinium Iodides. J. Am. Chem. Soc. **82**, 2195-2198

100. Abramovitch, R.A., and Adams, K.A.H. (1961) Tryptamines, carbolines and related compounds. Part IX. The cyclization of some nitro and azido-phenylpyridines. Pyrido[1,2-b] indazole. Can. J. Chem. **39**, 2516-28

101. Tomilenko, E.I. (1976) Kinetics of the reaction of quaternary salts of pyridine with potassium ferricyanide in an aqueous alkaline solution. Zh.vses. Khim. O-Va. **21**, 462-464

102. Ramsay, R.R., Salach, J.I. and Singer, T.P. (1986) Uptake of the neurotoxin 1-methyl-4-phenylpyridine (MPP^+) by mitochondria and its relation to the inhibition of the mitochondrial oxidation of NAD^+-linked substrates by MPP^+. Biochem. Biophys. Res. Commun. **134**, 743-748

103. Singer, T.P. (1974) Determination of the activity of succinate, NADH, Chline and alpha-glycerophosphate dehydrogenases. Methods. Biochem. Anal. **22**, 123-175

104. Ramsay, R.R., and Singer, T.P. (1986) Energy-dependent uptake of N-methyl-4-phenylpyridinium, the neurotoxic metabolite of 1-methyl-4-phenyl-1,2,3,6-tetrahydropyridine by mitochondria. J. Biol. Chem. **261**, 7585-7585

105. Westerink, B.H.C. and Tuinte, M.H.J. (1986) Chronic use of intracerebral dialysis for the invivo measurement of 3,4-dihydroxy phenylethylamine and its metabolite 3,4-dihydroxy phenylacetic acid. J. Neurochem., **46**, 181-185

106. Rollema, Hl, Kuhr, W.G., Kranenborg, G., DeVries, J.B. and Vandenberg, C. (1988) MPP^+ induced efflux of dopamine and lactate from rat striatum have similar time courses as shown by in-vivo brain dialysis. J. Pharmacol. Exp. Therap. in press.

107. Glowinski, J. and Iversen, L.L. (1966) Regional studies of catecholamines in the rat brain. The disposition of [^{3}H] Norepinephrine and [^{3}H] Dopamine and [^{3}H] DOPA in various regions of the brain. J.Neurochem. **13**, 655-669

108. Lowry, O.H., Rosebrough, N.J., Farr, A.L. and Randall, R.J., (1951) Protein measurement with the folin phenol reagent. J. Biol. Chem. **193**, 265-275

109. Erwin, V.G. and Hellerman, L.(1967) Mitochondrial monoamine oxidase I. Purification and characterization of the bovine kidney enzyme. J.Biol. Chem. **242**, 4230-4238

110. Schnaitman, C., Erwin, V.G., Greenwalt, J.W. (1967) The submitochondrial localization of monoamine oxidase. An enzymatic marker for the outer membrane of rat liver mitochondria. J. Cell Biol. **32**, 719-735

111. Blaschko, H. Richter, D., Schlossmann, H. (1937) The oxidation of adrenaline and other amines. Biochem. J. **31**, 2187-2196

112. Johnston, J.P.(1968) Some observations upon a new inhibitor of monoamine oxidase in brain tissue. Biochem. Pharmacol. **17**, 1285-1297

113. Yu. P.H., (1981) Studies on the pargyline binding site of different types of monamine oxidase. Can. J. Biochem. **59**, 30-37

114. Blaschko, H. (1974) The natural history of amine oxidases. Rev. Physiol. Biochem. Pharmacol. **70**, 84-148

115. Sandler, M. and Youdim, M.B.H. (1972) Multiple forms of monoamine oxidase: functional significance. Pharmacol. Rev. **24**, 331-348

116. Knoll, J. and Magyar, K. (1972) Some puzzling pharmacological effects of monoamine oxidase inhibitors. Adv. Biochem. Psychopharmacol. **5**, 393-408

117. Simpson, J.T., Krantz, A. Lewis, F.D. and Kokel, B. (1982) Photochemical and photophysical studies of amines with excited flavins. Relevance to the mechanism of action of the flavin dependent monoamine oxidase. J. Am. Chem. Soc. **104**, 7155-7161

118. Eberline, G. and Bruice, T.C. (1982) One and two-electron reduction of oxygen by 1,5dihydroflavins J. Am. Chem. Soc. **104**, 1449-1455

Eberline, G. and Bruice, T.C. (1983) The chemsitry of a 1,5-diblocked Favin. 2. Proton and electron transfer steps in the reaction of dihydroflavins with oxygen J. Am. Chem. Soc.**105**, 6684-6697

119. Silverman, R.B. (1984) Effect of alpha-methylation on inactivation of monoamine oxidase by N-cyclopropylbenzylamine. Biochemistry **23**, 5206-5213

120. Jones, J.R. (1973) The Ionization of carbon acids, P 29, Academic Press, London

121. Salach, J.I. (1979) Monoamine oxidase from beef liver mitochondria: simplified isolation procedure, properties, and dtermination of its cysteinyl-flavin content. Arch. Biochem. Biophys. **192**, 128-137 same as ref 36

122. Salach, J.I. and Detmer, K. (1979) "Chemical characterization of monoamine oxidase A from Human Placental mitochondria." In Monoamine Oxidase: structure, function and altered functions (Singer, T.P., VonKorf, R.W. and Murphy, D.L. eds.) pp 121. Academic Press, New York

123. Brossi, A., Gessner, W.P., Fritz, R.R., Benbenck, M.E. and Abell, C.W. (1986) Interactions of monoamine oxidase B with analogs of 1-methyl-4-phenyl-1,2,3,6-tetrahydropyridine derived from Prodine-type analgesics. J. Med. Chem. **29**, 444-445

124. Segel, I.H. (1975) "Reciprocol plot for competitive inhibition systems" in Enzyme kinetics. Behavior and analysis of rapid equilibrium and steady state enzyme systems. pp 107-109 Wiley Interscience, New York

125, Zimmerman, J.J. and Feldman, S. (1989) "Physical Chemical Properties and biologic activity" in Principles of Medicinal Chemistry (Foye, W.O. ed) pp 27, Lea and Febiger, Philadelphia

126. Singer, T.P., Salach, J.I., Castagnoli, N. Jr. and Trevor, A.J. (1986) Interactions of the neurotoxic amine 1-methyl-4-phenyl-1,2,3,6-tetrahydropyridine with monoamine oxidases. Biochem. J. **235**, 785-789

127. Silverman, R.B. and Hoffman, S.J. (1980) A mechanism for mitochondrial monoamine oxidase catalysed amine oxidation. J. Am. Chem. Soc. **102**, 7126-7128.

128. Aue, D.H., Webb, H.M., and Bowers, M.T. (1976) Quantitative proton affinities, ionization potentials, and hydrogen affinities of alkylamines J. Am. Chem. Soc. **98**, 311-317

129. Perrin, D.D., Dempsey, B. and Serjeant, E.P. (1982) pKa Prediction for Organic acids and bases. Chapman and Hall, London

130. Jackman, L.M. (1959) "The deshielding of alkyl protons by beta-substituents" in Applications of nuclear magnetic resonance spectroscopy in organic chemistry. pp 53, First edition, Pergamon Press, New York

131. Jackman, L.M. (1969) "Shielding by carbon-carbon single bonds and carbon-hydrogen bonds" in Applications of nuclear magnetic resonance spectroscopy in organic chemistry. Second edition. pp 78-80 Pergamon Press, New York

132. Schoolery, J.N. (1962) Recent applications of high resolution NMR to the determination of molecular structure. Disc. Farad. Soc. **34**, 104-114

133. Grewe, R. and Mondon, A., (1948) Synthesis in the phenanthrene series (VI) of morphinan. Chem. Ber. **81**, 279-287

134. Schnider, O. and Grosser, A. (1949) Synthese von Oxy-morphinan. Helv. Chim. Acta, **32**, 821-828

135. May, E.L. and Fry, E.M. (1957) Structures related to morphine. VIII Further synthesis in the benzomorphan series. J. Org. Chem. **22**, 1366-1372

136. Eisner, U. and Kuthan, J. (1972) The chemistry of dihydropyridines. Chem. Rev. **72**, 1-42

137. Meyers, A.I. and Singh, S. (1969) The chemistry of enaminoketones-V. Tetrahedron, **25**, 4161-4166

138. Peterson, L.A., Caldera, P.S., Trevor, A., Chiba, K. and Castagnoli, N. Jr. (1985) Studies on the 1-methyl-4-phenyl-2,3-dihydropyridinium species 2,3-MPDP$^+$. the monoamine oxidase catalysed oxidation product of the nigrostriatal toxin 1-methyl-4-phenyl-1,2,3,6-tetrahydropyridine (MPTP). J. Med. Chem. **28**, 1432-1436

139. Shinka, T., Castagnoli, N. Jr., Wu, E.Y., Hoag, M.K. and Trevor, A.J. (1987) Cation-exchange high performance liquid chromatography assay for the nigrostriatal toxicant 1-methyl-4-phenyl-1,2,3,6-tetrahydropyridine and its monamine oxidase B generated metabolites in brain tissues. J.Chromatography **398**, 279-287

140. Opitz, G. and Merz, W. (1962) Enamine VIII Salze von dien-aminen. Ann. Chem, **652**, 139-163.

141. Marshall, J.A., and Johnson, W.S. (1963) Reduction of steriodal enamines. J.Org. Chem., **28**, 421

142. Anderson, P.S. and Lyle, R.E. (1964) The mechanism of the reduction of pyridindium ions by sodium borohydride II. Tet. Lett. 153-158

143. Ingold, C.K. (1953) Structure and mechanism in organic chemistry. pp. 554-566, Cornell University Press, Ithaca, N.Y.

144. Silverstein, R.M., Bassler, G.C., and Morrill, T.C., (1981) Spectrophotometric identification of organic compounds, pp 206, Wiley Interscience, New York, New York.

145. Wehinger, E. and Gross, R. (1986) "Calcium Modulators" Annual Reports in Medicinal Chemistry **21**, 85-94

146. Wolf, M.E. (1980) Burger's Medicinal Chemistry pp 401-402, Wiley Interscience, New York, New York

147. Metzler, D.E. (1977) Biochemistry: The chemical reactions of living cells. pp 593-594, Academic Press, New York, New York

148. Youngster, S.K., Saari, W.S., and Heikkila, R.E., (1987). 1-methyl-4-cyclohexyl-1,2,3,6-tetrahydropyridine (MCTP): an alicyclic MPTP-like neurtoxin. Neurosci. Lett. 151-156

149. Goldstein, A., Aronow, L., and Kalman, S.M. (1974) Principles of drug action: The basis of pharmacology. pp 89, second edition, Wiley Interscience, New York, New York

150. Collins, M.A., Neafsey, E.J., Cheng, B.Y., Hurley, G.K., Ung, C.N., Pronger, D.A., Christensen, M.A., Hurley, G.I. (1987) Endogenous analogs of 1-methyl-4-phenyl-1,2,3,6-tetrahydropyridine: Indoleamine derived tetrahydro-beta-carbolines as potential causative factors in Parkinson's disease. Adv. Neurology. **45**, 179-182

151. Booth, R.G., Trevor, A., Singer, T.P., and Castagnoli, N. Jr. (1987) Synthesis and pharmacological activity of rigid MPTP analogs relating to Parkinson's Disease. The Japanese/United States Congress of pharmaceutical Sciences, Honolulu, Hawaii, Dec. 1987

152. Bianchine, J.R. (1985) "Drugs for Parkinson's disease, spasticity, and acute muscle spasms" in Goodman and Gilman's The Pharmacologic basis of therapeutics. (Goodman-Gilman, A., Goodman, L.S., Rall, T.W. and Murad, F., eds.) pp 473-490, Chapter 21, Seventh edition, Macmillan, New York, New York.

153. Suzuki, O., Katsumata, Y., Oya, M. (1979) "Characterization of some biogenic monoamines as substrates for type A and type B monoamine oxidase" in Monoamine Oxidase: Structure, function and altered functions (Singer, T.P., VonKorf, R.W., Murphy, D.L. eds.) pp 197-204, Academic Press, New York, New York

154. Silverman, R.B. (1983) Mechanism of inactivation of monoamine oxidase by trans-2-phenyl-cyclopropyl amine and the structure of the enzyme-inactivator adduct. J.Biol.Chem. **258**, 14766-14769

155. Silverman, R.B., and Hoffman, S.J. (1981) N-(1-methyl)cyclopropylbenzylamine: a novel inactivator of mitochondrial monoamine oxidase. Biochem. Biophys. Res. Commun. **101**, 1396-1401

156. Silverman, R.B., and Yamasaki, R.B. (1984) Mechanism-based inactivation of mitochondrial monoamine oxidase by N-(1-methylcyclopropyl)benzylamine. Biochemistry **23**, 1322-1332

157. Silverman, R.B. and Zieske, PlA. (1986) 1-Phenylcyclobutylamine, the first in a new class of monoamine oxidase inactivators. Further evidence for a radical intermediate. Biochemistry **25**, 341-346

158. Mann, C.K., Barnes, K.K. (1970) Electrochemical reactions in non-aqueous systems, Chapter 9, Marcel Dekker, New York, New York

Lindsay-Smith, J.R., Masheder, D.J., (1976) J. Chem. Soc. Perkin. Trans. **2**, 47

159. Heikkila, R.E., Hess, A., Duviosin, R.C., (1985) Dopaminergic neurotoxicity of 1-methyl-4-phenyl-1,2,5,6-tetrahydropyridine (MPTP) in the mouse: Relationships between monoamine oxidase, MPTP metabolism and neurotoxicity. Life Science **36**, 231-236

160. Hallman, H., Lange, J., Olsen, L., Stromberg, I., Jonsson, G., (1985) Neurochemical and histochemical characterization of neurotoxic effects of 1-methyl-4-phenyl-1,2,3,6-tetrahydropyridine on brain catecholamine neurons in the mouse. J. Neurochem. **44**, 117-127

161. Hedrich, L.W. (1971) Herbicidal 4-arylpyridinium salts. U.S. patent application 144,246 17 May. Chem Abst. vol78:84262h.

162. Youngster, S.K., McKeown, K.A., Jin, Y.E., Ramsay, R.R., Heikkila, R.E. and Singer, T.P. (1988) The oxidation of analogs of MPTP by monoamine oxidases A and B and the inhibition of monoamine oxidases by the oxidation product, manuscript submitted to J.Neurochem.

163. Halmos, M. and Mohacsi, T. (1960) J. Prakt. Chem. **12**, 50-58

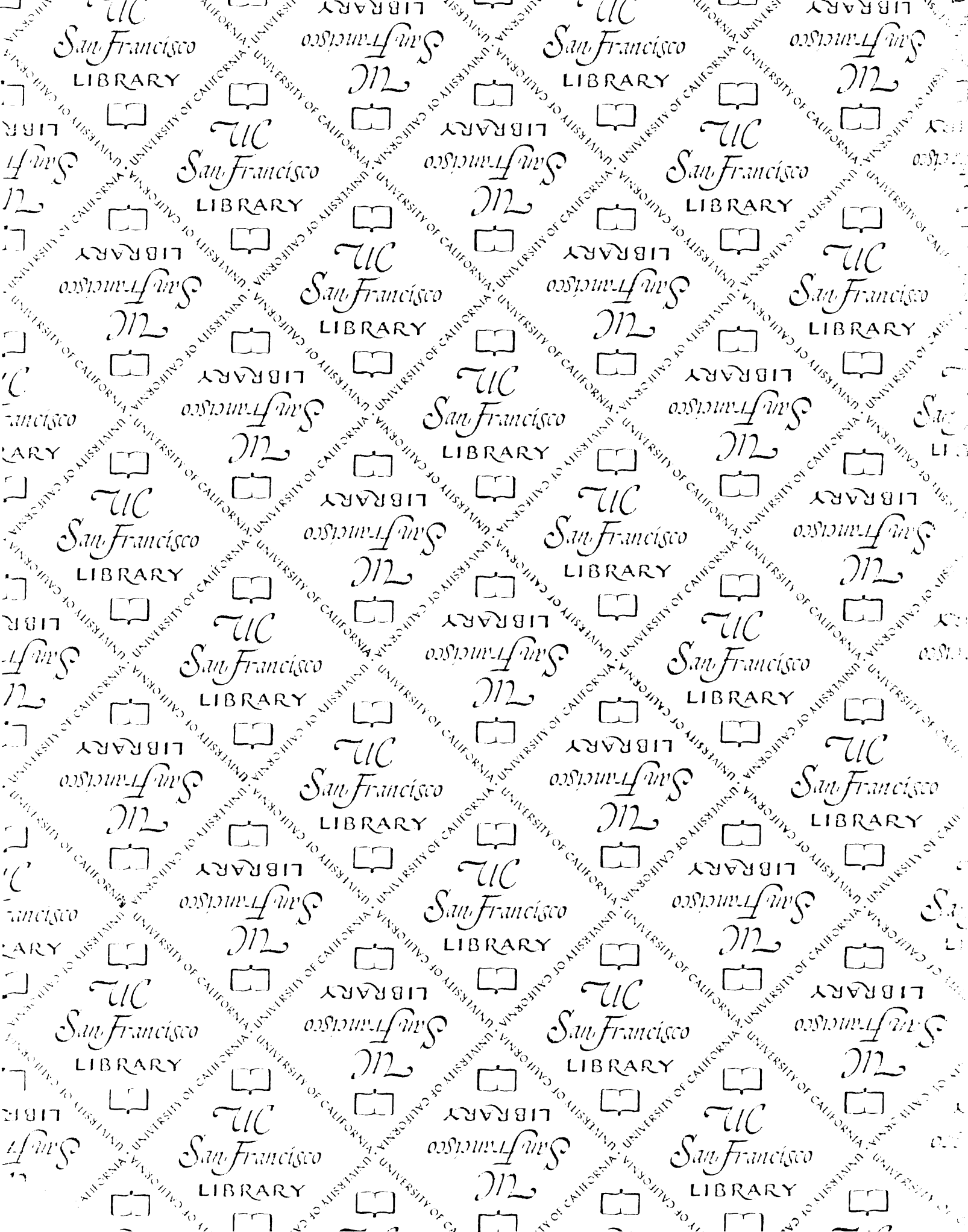
UC
San Francisco
LIBRARY
UNIVERSITY OF CALIFORNIA · UNIVERSITY OF CALIFORNIA

FOR REFERENCE

NOT TO BE TAKEN FROM THE ROOM

BRO DART CAT. NO. 23 012 PRINTED IN U.S.A.